Physics Lib.

SEP 1 3 1935

DO NOT TAKE FROM LIBRARY

Copy 2

THE PHYSICAL REVIEW

VOLUME 48 *Second Series* NUMBER 5

SEPTEMBER 1, 1935

Published for the

AMERICAN PHYSICAL SOCIETY

by the

AMERICAN INSTITUTE OF PHYSICS

Incorporated

LANCASTER, PA., AND NEW YORK, N. Y.

THE AMERICAN PHYSICAL SOCIETY

OFFICERS OF THE SOCIETY

R. W. WOOD, *President*
The Johns Hopkins University
Baltimore, Maryland

F. K. RICHTMYER, *Vice President*
Cornell University
Ithaca, New York

W. L. SEVERINGHAUS, *Secretary*
Columbia University
New York, New York

G. B. PEGRAM, *Treasurer*
Columbia University
New York, New York

JOHN T. TATE, *Editor*
University of Minnesota
Minneapolis, Minnesota

L. B. LOEB, *Local Secretary for the Pacific Coast*
University of California
Berkeley, California

THE PHYSICAL REVIEW

BOARD OF EDITORS

JOHN T. TATE, *Editor*

J. W. BUCHTA, *Assistant Editor*

Associate Editors

K. K. DARROW
J. C. HUBBARD
A. E. RUARK
A. ELLETT
L. A. TURNER
G. E. UHLENBECK
W. V. HOUSTON
R. S. MULLIKEN
I. I. RABI

THE PHYSICAL REVIEW, which was established in 1893, is a journal of experimental and theoretical physics. It is published for the American Physical Society by the American Institute of Physics Incorporated. There are two volumes annually with twelve issues in each volume.

Manuscripts for publication should be submitted to John T. Tate, University of Minnesota, Minneapolis, Minnesota.

Proof and all correspondence concerning papers in the process of publication, should be addressed to the Editorial Secretary, American Institute of Physics, 11 East 38th Street, New York, New York.

Subscription price: United States and Possessions and Canada, $15.00; Foreign, $16.50. Subscriptions and orders for back numbers should be addressed to Prince and Lemon Streets, Lancaster, Pennsylvania, or to the American Institute of Physics, 11 East 38th Street, New York, New York.

Advertising is not accepted for the *Physical Review* but attention is called to the *Review of Scientific Instruments with Physics News and Views*, a companion publication of the Institute, and a medium through which the field of physics can be reached most effectively. Rates and other information will be furnished on request to the Editorial Secretary.

Changes of address and complaints of failure to receive the *Physical Review*, in the case of members of the American Physical Society, should be addressed to the Treasurer; in the case of other subscribers, to the Editorial Secretary. New copies can be sent free in response to complaints of non-delivery only if notice of non-delivery is received within three months of date of issue.

The Physical Review is published semi-monthly at Prince and Lemon Streets, Lancaster, Pennsylvania.

Entered at the Post Office at Lancaster, Pennsylvania, as second class matter.

Acceptance for mailing at special rate of postage provided for in section 1103, Act of October 3, 1917, authorised September 6, 1926.

THE
PHYSICAL REVIEW
A Journal of Experimental and Theoretical Physics
VOL. 48, NO. 5 SEPTEMBER 1, 1935 SECOND SERIES

The Measurement of X-Ray Wavelengths by Large Ruled Gratings

J. A. BEARDEN, *Johns Hopkins University*
(Received June 19, 1935)

A plane ruled grating was placed between the crystals of a precision double crystal spectrometer for the determination of the diffraction angles and the absolute wavelengths of x-ray lines. This arrangement has two important advantages: (1) A large grating surface is employed and (2) the ionization chamber method for recording intensities permits an accurate location of the peak of the diffracted lines. The gratings were 75 mm long and were ruled with 100 and 300 lines per mm, respectively. The results on the copper $K\alpha$ line (1.54A) are in good agreement with previous ruled grating measurements. The differences between the ruled grating and crystal wavelengths as obtained by Backlin, Söderman and the writer have been recalculated using as the "true" value of the calcite grating constant $d=3.02810$A and the most recent determinations of the calcite diffraction angles. There is excellent agreement among the various observations and the difference between the grating and crystal values is independent of wavelength. The results of two independent methods of measuring x-ray wavelengths are included and these agree with the ruled grating values. Calculations of the "true" grating constant of calcite d, Avogadro's number N, the charge on the electron e, and Planck's constant h were made. Some of the difficulties encountered if these values of e and h are used are pointed out.

ONE objection to the previous use of ruled gratings for measuring x-ray wavelengths is that one actually uses only a very few lines of the grating. Slight errors in the spacing of the ruled lines could produce relatively large effects in the measured wavelength. No arrangement has previously been used to determine accurately the shape of the diffracted line and consequently the position of the point of maximum intensity. In the present arrangement these difficulties have been overcome by placing the grating between the crystals of a double crystal spectrometer.

METHOD

The principle of the present method is shown schematically in Fig. 1. The ruled grating was placed between the crystals of a double crystal spectrometer and the second crystal C_2 used to determine the angular directions of the rays from the grating. The vertical projection of the x-ray focal spot (2 mm$\times$2 mm) served as the first slit. This allowed both the α_1 and the α_2 lines to be reflected from the first crystal C_1 and to strike the grating at different angles of incidence θ (i.e., θ is the angle between the grating surface and the incident beam). Although the wavelength of the α_2 line is greater than that of α_1 this difference in the angle of incidence makes the diffracted α_2 line appear at a smaller angle from the direct beam than the α_1 line. Since the angle of incidence was only about 20′, a large part of the incident x-rays passed by the grating and were diffracted by the crystal C_2 in the usual (1+1) position. If C_2 were rotated counterclockwise, from the peak position of the α_1 line in the (1+1) position, through an angle (2θ) then the α_1 line reflected from the grating was diffracted by C_2. By continuing the rotation of

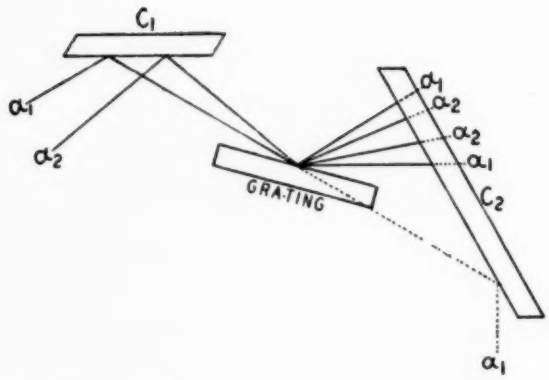

FIG. 1. The method used of placing the ruled grating between the crystals of a double crystal spectrometer.

C_2 the reflected α_2 was next recorded, then the α_2 which had been diffracted by the grating, and finally the diffracted α_1. A further rotation recorded the higher diffracted orders of the α_2 and the α_1 lines but in practice it was found that the intensity of the higher orders was so low that precise measurements were impossible.

Since an extended source of x-rays was used without any collimating slits, it is obvious that the entire length of the grating was effective in the x-ray diffraction. All the angles necessary for the calculation of the wavelengths were obtained from the precision divided circle on which C_2 rotated. The wavelengths were calculated from the usual grating formula which can be written in the following convenient form:

$$n\lambda = 2d\{\sin[(2\theta+\alpha)/2]\cdot\sin(\alpha/2)\}, \quad (1)$$

where λ is the wavelength, d the grating constant, θ the angle of incidence and α is the angle between the reflected and the diffracted lines.

The crystals C_1 and C_2 were placed in the (1+1) position (Fig. 1). From Eq. (1) it is obvious that the precision of the measured wavelength depends primarily on the accuracy with which the angle α can be determined. Therefore it was desirable to have the reflected and diffracted lines as narrow as possible so that their positions could be accurately determined. In the double crystal spectrometer a reflection from a surface between the crystals changes the effective positions from (1 ± 1) to (1 ∓ 1). By placing the crystals in the (1+1) as shown in Fig. 1, the width of the reflected line is that of the (1−1) width for the wavelength and the perfection of the crystals used (about 10″). The width of the diffracted line is the (1−1) width plus the width added by the dispersion of the grating (13″ to 16″ total). The width of the direct line is the usual (1+1) width.

Although this method makes use of a large grating the resolving power is not increased over that with a short grating. In the double crystal spectrometer a wide parallel bundle of rays is used but these rays originate at different points in the source. In order to increase the resolving power of a plane ruled grating by using a larger number of lines it is necessary that the wide bundle of rays originate from the same point. However, increased revolving power is not essential for x-ray measurements. It is more important to increase the number of lines per cm, but there are experimental limitations that prevent using finely ruled gratings.

APPARATUS AND ITS ADJUSTMENT

The double crystal spectrometer was built by the Société Genevoise. The second crystal C_2 was mounted on a table attached to a high precision circle. Four carefully calibrated microscopes were used to read the divided circle. The micrometer settings (read to 0.1″) were repeated three or four times and the average obtained. Since two lines, ten minutes apart, were read in each microscope, eight angular readings (or from 24 to 32 micrometer settings) were obtained for each individual setting of the circle. Two different parts of the circle were used in order to reduce any effects due to possible erratic rulings on the circle. The two parts of the circle used had proven to be particularly good when it was previously carefully calibrated.

The crystals C_1 and C_2 were accurately adjusted by the usual telescope and x-ray method. The surface of C_2 was not more than 0.01 mm from its axis of rotation. The surface of the ruled grating was placed accurately parallel to and on its axis of rotation by the use of a Michelson interferometer. This axis was then adjusted parallel to that of C_2 with the aid of two telescopes fitted with Gauss eyepieces. The accuracy of this adjustment was to within one minute of arc. The axis on which the ruled grating rotated was mounted on an adjustable horizontal slide so

its position could be altered. This allowed the grating to be placed in the most intense portion of the x-ray beam.

The source of high voltage and the vacuum tube method of measuring the ionization currents were the same as previously described.[1] The x-ray source was a water-cooled copper target tube with a line focus cathode. The effective size of the focal spot, as viewed from the ionization chamber was about 2 mm×2 mm.

The calcite crystals were split from a block of Iceland calcite. The crystals gave the theoretical width of 9.8″ for the (1−1) of the copper $K\alpha$ lines. The (1+1) width for the copper $K\alpha_1$ line was 39.5″.

Since the reflections of the various lines from C_2 occurred at slightly different points on the crystal surface it was necessary to know that the atomic planes of the crystal continued in a geometrical plane over the total region used. The maximum distance on the crystal between the direct α_1 and the diffracted α_1 was 10 mm. The planeness of C_2 was tested by adjusting C_1 to diffract both the copper α and β lines at the same time and in such a direction that the lines would strike C_2 (1−1) position on either side of the region of C_2 that was used when the grating was put in place. The ionization chamber was first set to receive the α lines only and the angular position of C_2 was carefully determined. The chamber was then adjusted to receive the β line only and the angular position of C_2 was again carefully determined. These angular positions agreed as closely as could be measured, which was within 0.1″ of arc. Thus between the places on C_2 where the α and β lines were reflected the crystal planes were parallel within the limits of measurement.

The lines of the grating were carefully ruled parallel to the edge of the grating blank (to within 1′ of arc) and this edge was then made parallel to the axis of rotation of the grating. The maximum error in the final value of λ due to this adjustment was less than one part in 10^5.

In making the angular measurements it was necessary that the temperature of both crystals remain constant during the entire time taken to make a complete determination of the wavelength. This time was about three hours. A thermometer was placed near each crystal and the temperature noted many times during the run. When the x-ray outfit was first started it required about two hours for the temperature of the crystals to reach an equilibrium temperature. Usually about three hours were allowed before an attempt was made to make measurements. After this time if no change were made in the x-ray load or no change in room temperature occurred, the temperature of the crystals remained constant to within 0.1°C.

Gratings

In choosing a suitable grating constant there are two important considerations. First the dispersion should be as large as possible; and second, the diffracted intensity must be easily measurable. One has to compromise in making a choice, for large dispersion and satisfactory intensity cannot be obtained simultaneously. From previous experience, grating constants were chosen corresponding to about 100 and 300 lines per mm.

Two gratings were ruled on the same optically flat blank which was 50 mm×75 mm. The actual ruled surfaces were each 18 mm×75 mm so that an unruled space existed between the rulings and also between each ruling and the edge of the blank. When the gratings were ruled the ruling engine was in very good condition, the Lyman ghost lines being less than 0.001 the intensity of the main line even for 6-inch gratings of 15,000 lines per inch. Optical examination of the gratings showed no detectable errors.

The grating constants were determined by directly measuring the distance between two lines from 10 mm to 40 mm apart and counting the number of spaces in the interval. Repeated measurements using different parts of the grating and different parts of the comparator disagreed in no case by more than one part in 50,000.

The gratings were sputtered with a layer of gold which reduced the intensity of transmitted light about 95 percent. This made it possible to use larger angles of incidence and also gave much greater intensity in the diffracted lines than could have been obtained with a glass surface.

[1] J. A. Bearden and C. H. Shaw, Phys. Rev. **48**, 18 (1935).

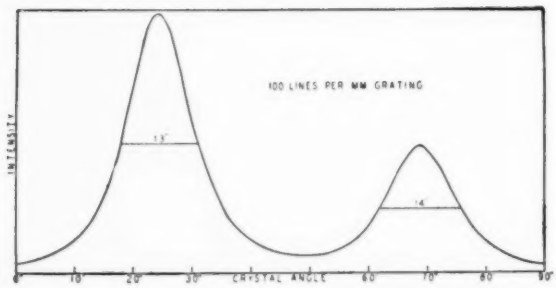

FIG. 2. The grating diffracted copper $K\alpha_1$, α_2 lines when using the 100 lines per mm grating.

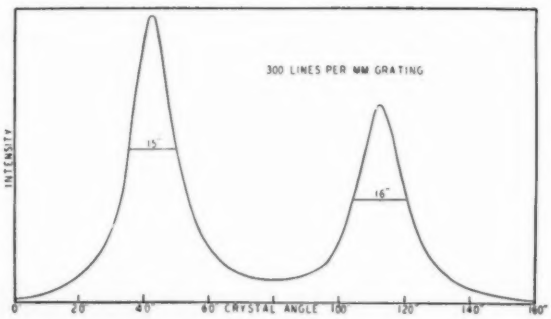

FIG. 3. The grating diffracted copper $K\alpha_1$, α_2 lines when using the 300 lines per mm grating.

RESULTS

A typical curve of the first order diffraction of the copper $K\alpha_{1,2}$ lines for each grating is shown in Fig. 2 and Fig. 3. Fig. 3 shows that the intensities of the α_1 and α_2 lines are not in the ratio of 2 to 1. The reason for this is not apparent but it is probably connected with the fact that the intensities of the diffracted lines are critically affected by variations in the angle of incidence. It is doubtful, however, that such effects could shift the peak of the line by a measurable amount. A further study of this is needed.

The method employed for determining the angles necessary for the calculation of the wavelengths was as follows: The position of the direct α_1 line was obtained, then the positions of the reflected and diffracted α_1 lines were recorded. The process was reversed and the diffracted, reflected and direct beams were recorded. This gave two determinations of each angle and the average was used as one independent value of α and θ. Sixteen circle readings or about 50 micrometer settings were contained in each angular determination.

A correction for the overlapping of the lines was made by using the classical equation[2] for the line shape as previously[3] described. In most cases this correction was negligible.

The second order was observed for both gratings and the third for the coarsely ruled grating. The intensity was very low in these cases and for this reason very accurate location of the lines could not be made. The second order from each grating was used and the resulting wavelengths agreed within 0.1 percent with those obtained when using the first order but since the results were much less accurate they have not been considered in the final average.

The results of 12 independent first order determinations of the wavelength of the copper $K\alpha_1$ line are shown in Table I. The first column gives the angle of incidence which is the measured angle divided by 2. The second column gives α the measured angle between the reflected and the diffracted beams. The third column gives the resulting wavelengths and the fourth the percent difference between these wavelengths and that obtained with calcite crystals. The maximum variation is about 0.04 percent and the probable error as calculated from consistency is 0.003 percent. It is possible that a constant error in the divided circle is present, but since six different angles and two entirely different parts of the circle have been used it is difficult to

TABLE I. *Twelve independent determinations of the wavelength of the copper $K\alpha_1$ line using two gratings.* The first six results were obtained using a grating with a constant of 2.03248×10^{-3} cm and the last six results with a grating whose constant was 0.67749×10^{-3} cm. The crystal value of λ was 1.53671A.

θ	α	λ_g	$(\lambda_g-\lambda_c)/\lambda_c$
15′ 10.43″	9′ 5.11″	1.5403A	0.234
15′ 10.30″	9′ 5.38″	1.5411	0.286
8′ 0.14″	12′ 32.85″	1.5403	0.234
7′ 59.91″	12′ 32.98″	1.5403	0.234
19′ 42.74″	7′ 37.10″	1.5405	0.247
19′ 43.75″	7′ 36.67″	1.5403	0.234
15′ 16.56″	20′ 53.64″	1.5405	0.247
15′ 16.57″	20′ 54.27″	1.5416	0.318
26′ 17.67″	15′ 44.19″	1.5409	0.273
26′ 18.14″	15′ 43.80″	1.5405	0.247
7′ 11.90″	26′ 22.06″	1.5404	0.241
7′ 11.79″	26′ 22.13″	1.5404	0.241
	Average	1.5406	0.253

[2] A. Hoyt, Phys. Rev. **40**, 477 (1932).
[3] J. A. Bearden and C. H. Shaw, Phys. Rev. **46**, 761 (1934).

TABLE II. *The percent difference between the ruled grating and calcite crystal values of x-ray lines.* The numbers in parentheses are the numbers of independent values that entered into the recorded value.

Observer	*Grating*	Cu $K\beta$	Cu $K\alpha$	Cr $K\beta$	Cr $K\alpha$	Al $K\alpha$
Backlin (1928)[4]						0.17(31)
Bearden (1929)[7]	a, b, c	0.24 (10)	0.25 (10)			
Bearden (1931)[8]	1, 3	.241(26)	.229(46)	0.239(16)	0.245(28)	
Bearden (1931)[8]	4	.234(4)	.250(11)	.250(15)	.255(27)	
Bearden (1931)[8]	4′	.264(30)	.257(49)	.253(3)	.254(5)	
Bearden (1931)[8]	5	.246(41)	.234(73)	.235(32)	.239(51)	
Bearden (1931)[8]	5′	.259(49)	.250(82)	.256(44)	.255(67)	
Bearden (1931)[8]	6	.239(11)	.244(16)	.240(3)	.240(4)	
Backlin (1935)[5]						.249(56)
Söderman (1935)[6]			Cu $K\alpha_1$			.255(9)
Bearden (1935)[11]	100		0.245 (6)			
Bearden (1935)[11]	300		.261 (6)			
Bearden (1935)[12]	Refr.	0.260(25)				
		Weighted average = 0.248 ± 0.0016%				

believe that an error of this type greater than 0.1″ to 0.2″ exists. The results are very consistent and agree excellently with previous photographic results. By using an entirely different grating technique for determining x-ray wavelengths we find again that the ruled grating measurements are correct.

COMPARISON OF PREVIOUS RESULTS

In Table II the differences between the ruled grating and crystal wavelengths as obtained by Backlin,[4, 5] Söderman,[6] and the writer[7, 8] have been recalculated using as the "true" value of the grating constant of calcite[9] $d = 3.02810$A and the most recent determinations of the calcite diffraction angles. In the case of the aluminum $K\alpha$ line a gypsum crystal was used for determining the crystal wavelength but since Larsson[10] has measured by x-rays the ratio of the grating constant of gypsum to that of calcite, the gypsum value can be easily converted to the calcite scale.

In Table II the numbers in parentheses are the numbers of independent measurements that entered into each recorded value. The weighted average was obtained by giving each value a weight equal to the number of measurements that entered into that value, except in the case of Backlin's 1928 value. This was given zero weight in view of the fact that his latter repetition of the experiment with improved technique gave a very much higher value. The probable error was calculated by the method of least squares giving each value equal weight.

It will be noted that, with the exception of Backlin's 1928 result,[4] all the results using different gratings and different methods are in exceptionally good agreement. The differences between the ruled grating and the crystal results apparently do not depend at all on the wavelength in the range from 1.4A to 8.3A. This gives strong evidence in favor of the correctness of the ruled grating measurements, especially since in both theory and experiment there appears to be nothing wrong with the idea of using ruled gratings for this wavelength region.

In Table II there is also included the results of two methods[11, 12] of determining x-ray wavelengths that are independent of the usual absolute ruled grating methods. In the first method Söderman[11] has used a 5 m concave grating to compare a high order of the aluminum $K\alpha$ line with a spark line of known wavelength. This essentially measures the x-ray line in terms of the red cadmium line which Michelson has measured in terms of the standard meter. In the second method[12] the wavelength of the copper $K\beta$ line has been measured by its refraction in a

[4] E. Backlin, Inaug. Diss. Uppsala (1928).
[5] E. Backlin, Zeits. f. Physik **93**, 450 (1935).
[6] M. Söderman, Nature **135**, 67 (1935).
[7] J. A. Bearden, Proc. Nat. Acad. Sci. **15**, 528 (1929).
[8] J. A. Bearden, Phys. Rev. **37**, 1210 (1931).
[9] J. A. Bearden, Phys. Rev. **38**, 2089 (1931).
[10] A. Larsson, Uppsala Univ. Arsskrift, 1929.
[11] J. A. Bearden, present paper.
[12] J. A. Bearden, Phys. Rev. **47**, 811 (1935).

diamond prism. Similar results have been obtained with a quartz prism by Shaw and the writer.[3] The good agreement between these and the other results of Table II also gives strong support to the conclusion that the ruled grating measurements are correct.

Calculation of the Constants d, N, e, and h

In view of the apparent correctness of the ruled grating wavelengths one should be justified in using these wavelengths together with the known calcite crystal diffraction angles to calculate the true grating constant of calcite. By using the weighted average of Table II and the value of $d_\infty = 3.02810$A which was used in the calculations for this table, one obtains for the true x-ray value of the grating constant

$$d_\infty = 3.02810 \times 1.00248 = 3.03560 \pm 0.00005\text{A}.$$

This value is independent of any theory of crystal imperfection.

Since the many tests made on crystals normally used in x-ray work have indicated no measurable mosaic structure it would appear that one should be able to use the x-ray data for calculating Avogadro's number N. This can be obtained from the usual crystallographic relation as

$$N = M/2\rho\varphi(\beta)d^3.$$

By using the following values of these constants

$M = 100.078$,[13]
$\rho =$ 2.71030 g/cm^3 at 20°C,[9]
$\varphi(\beta) =$ 1.09594 at 20°C,[9]
$d =$ 3.03566A at 20°C,

one obtains

$$N = 6.0221 \pm 0.0005 \times 10^{23} \text{ mole}^{-1}.$$

If one can assume that the apparent accuracy of the Faraday is correct then by using $F = 9648.9 \pm 0.7$ abs. e.m. units one obtains for the charge on the electron

$$e = 4.8036 \pm 0.0005 \times 10^{-10} \text{ e.s.u.}$$

In the case of Planck's constant h there are two possible values. The first is to use the values of d and e from above in the high frequency relationship $Ve = h\nu$ in which case by using Kirkpatrick and Ross's[14] result for V/ν we obtain

$$h = 6.607 \times 10^{-27} \text{ erg} \cdot \text{sec}.$$

In the second case if we assume there is some difficulty in calculating e from the x-ray data, that is, that there is something wrong in the value of the Faraday or that there is present some undetected crystal phenomena, then Millikan's oil drop value of e equal to 4.768×10^{-10} e.s.u. can be used. This together with d and V/ν from above gives

$$h = 6.558 \times 10^{-27} \text{ erg} \cdot \text{sec}.$$

which is the smallest value of h that can be obtained from x-ray data.

While the above methods of determining e and h are apparently correct the results obtained are difficult to reconcile with existing data obtained by other methods. One of the principal difficulties encountered concerns the Rydberg constant which may be written in the form

$$R = 2\pi^2 e^5/c^2 h^3 e/m.$$

If $e = 4.806 \times 10^{-10}$ e.s.u., $h = 6.607 \times 10^{-27}$ erg ·sec., $R = 109{,}737.4$ cm^{-1}, and $c = 2.99796 \times 10^{10}$ cm/sec. then $e/m = 1.774 \times 10^7$ e.m.u./g. This value is about 0.8 percent greater than the present accepted value. Other, but less serious, difficulties arise when one attempts to use the above high x-ray values in many of the interrelationships of the constants.

At the present time there appears to be no satisfactory explanation of this dilemma. If the accepted value of the Faraday were about 0.75 percent too high then the major difficulties would be removed. The difficulty of accurately determining F is well known but it would be very surprising if the error in its determination were 0.75 percent. In addition F enters into the x-ray refraction measurements and the use of a value of F 0.75 percent lower than the accepted value would raise the resulting x-ray wavelengths 0.50 percent above the average grating wavelengths. This seems impossible.

The writer is indebted to Professor R. W. Wood for his cooperation in allowing a modification of the ruling engine to be made so that the special gratings could be ruled on the best ruling engine.

[13] R. T. Birge, Rev. Mod. Phys. **1**, 1 (1929).

[14] Kirkpatrick and P. A. Ross, Phys. Rev. **45**, 454 (1934).

Energy Spectrum of the Beta-Rays of Radium E

F. A. Scott, *The Rice Institute*

(Received May 31, 1935)

The energy distribution curve for the beta-ray spectrum of radium E has been measured. The spectrum was found to have a maximum at 3.87×10^5 electron volts and an endpoint at $(15.34\pm0.28)\times10^5$ electron volts corresponding to an $H\rho$ of 6604 ± 98. The spectrum was obtained by the magnetic focusing method and the particles were counted by a Geiger counter. The absorption of the beta-rays in the counter window was determined and allowed for. The large number of very low energy beta-rays found by H. O. Richardson was not confirmed. The energy distribution found does not agree with that of Fermi's theory. The results obtained are compared with those of previous investigators.

A LARGE amount of work has been done on the distribution of the energy in the β-ray spectrum of radium E with some rather conflicting results. Several investigators find that the spectrum has an upper limit at about 10^6 electron volts corresponding to an $H\rho$ of about 5200. Among those finding this are Schmidt,[1] Gray and O'Leary,[2] Douglas,[3] Sargent,[4] Feather,[5] Madgwick,[6] Gray[7] and Champion.[8] Others have found that the spectrum extends beyond a million electron volts and does not have any definite upper limit but that the intensity falls to zero asymptotically. Danysz,[9] Curie and d'Espine,[10] Yovanovitch and d'Espine,[11] and Terroux[12] have found results of this kind. Very recently H. O. W. Richardson[13] has found that a low energy group of β-rays is emitted which was not observed in the previous work. The present investigation was undertaken to see if these low energy rays could be detected by the magnetic focusing method and to determine the energy distribution more accurately.

The β-ray spectrum of radium E was obtained by the magnetic focusing method and the particles were counted by a Geiger counter connected through a three-stage amplifier and thyratron to a mechanical impulse counter. The magnetic field was produced by a Weiss water-cooled electromagnet. The pole pieces of this magnet were cylindrical in shape and 10 cm in diameter. The current to the magnet was supplied from a 110-volt battery and was measured by means of a Weston standard ammeter which could be read to 0.5 percent. For an air gap of three centimeters it was found that the field increased nearly linearly with the current. Currents ranging from 0.100 to 6.50 amperes were used, the latter value producing a field of about 6000 gauss in the gap.

The strength of the magnetic field was determined by means of a fluxmeter and search coil. The fluxmeter was calibrated by means of a standard line-turn meter. This line-turn meter was first checked for accuracy by connecting it in series with the secondary of a standard mutual inductance. The value of the current through the primary of the mutual inductance was adjusted each time to such a value as to produce about the same flux when it was reversed as did the line-turn meter for a given deflection. The deflections produced by each on the fluxmeter agreed to within 0.5 percent. The fluxmeter was then calibrated using the line-turn meter. This was done by connecting the fluxmeter, line-turn meter, and snatch-coil of the fluxmeter in series and noting the deflections of the fluxmeter for definite values of the flux produced by the line-turn meter. The strength of the magnetic field was now determined for various values of the current. The direction of the current through the magnet was made such as to give the proper field direction for the magnetic focusing apparatus. The current was then increased to 6.50 amperes and reduced to zero so as to give the proper direction to the residual field of the magnet. The field strength was now determined by the snatch

[1] Schmidt, Physik. Zeits. **8**, 361 (1907).
[2] Gray and O'Leary, Nature **123**, 568 (1929).
[3] Douglas, Proc. Roy. Soc. Canada **16**, 113 (1922).
[4] Sargent, Proc. Camb. Phil. Soc. **25**, 514 (1929).
[5] Feather, Phys. Rev. **35**, 1559 (1930).
[6] Madgwick, Proc. Camb. Phil. Soc. **23**, 982 (1927).
[7] Gray, Proc. Roy. Soc. **A87**, 487 (1912).
[8] Champion, Proc. Roy. Soc. **A132**, 672 (1932).
[9] Danysz, Le radium **10**, 4 (1913).
[10] Curie and d'Espine, Comptes rendus **181**, 31 (1925).
[11] Yovanovitch and d'Espine, J. de physique **8**, 276 (1927).
[12] Terroux, Proc. Roy. Soc. **A131**, 90 (1930).
[13] Richardson, Proc. Roy. Soc. **A147**, 442 (1934).

coil. This was done by placing the coil in the field with its faces parallel to the pole pieces, removing it from the field and then reversing it and putting it back. From the area and number of turns on the snatch coil and the calibration of the fluxmeter the value of the field in the gap for each current was determined. The fluxmeter could be read to an accuracy of 0.5 percent with a hand magnifier. All the measuring instruments were kept sufficiently far from the magnet so that their magnetic fields were unaffected by it.

A diagram of the apparatus used for obtaining the spectrum of the β-rays is shown in Fig. 1. The lead block B fits tightly into the brass box F and is held in place by a peg at A. The source of the β-rays was placed at O and consisted of a nickel wire 0.452 mm in diameter which had been immersed for one hour in a solution of radium D from which the radium F had been completely removed. The wire extended along the axis of the aluminum cylinder L which fitted tightly into the lead block B. A vertical slit 3 mm wide was cut in the aluminum cylinder. A brass plate E_1E_2 extended from the center of the box to the side and had its upper edge in line with the radium E source. The slit S_2 in the brass plate E_1E_2 was 8×0.832 mm and was directly above the window in a Geiger counter C. A slit of the same dimensions as that in the plate was cut in the glass tube of the counter and was covered with cellophane of thickness 0.0254 mm. The cellophane was cemented to the glass with Dupont cement diluted with acetone. There was a similar slit in the copper cylinder of the counter directly under the cellophane window. D is an aluminum partition with a slit at S_1. This partition was removable. The box was lined with aluminum. The outside diameter of the brass box was 10 cm and the distance from O to S_2 was nearly four centimeters. The brass box containing the source was placed between the poles of the magnet and evacuated by means of a Hyvac pump which was kept running during the experiments. The Geiger counter was connected through a three-stage amplifier and thyratron to a mechanical impulse counter capable of counting 125 impulses per second. Counts were made for five-minute intervals for various values of the magnetic field.

The absorption of the cellophane window was measured by observing the counting rates in various fields with additional thicknesses of two and four layers of cellophane placed above the slit S_2. Table I shows the counting rate per minute for various thicknesses of cellophane. Curves were then plotted of the counting rate with a given field against the thickness of the cellophane. These curves were extrapolated to give the counting rates for zero thickness which are given in the last column of Table I. Plotting the percentage absorption for one layer against $H\rho$ gave a straight line over the region investigated and showed that the cellophane window had no appreciable effect when $H\rho$ was greater than about 2400. The results obtained with $H\rho$ less than 2400 were corrected for the absorption of the cellophane window.

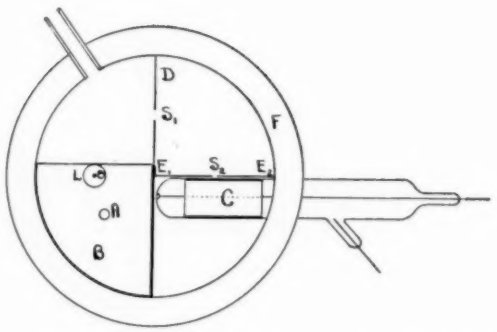

FIG. 1. Magnetic focusing apparatus for obtaining the beta-ray spectrum.

The amplifier, thyratron and mechanical impulse counter system was tested for accuracy in counting. This was done by first noting the residual count; then a small amount of radio thorium sealed in a glass tube was placed successively at three distances d_1, d_2 and d_3 in front of the counter. The radio-thorium increased the counting rate by 36, 61 and 77 counts per minute in the three positions. The radio-thorium

TABLE I. *Variation of counting rate with cellophane thickness.*

$H\rho$ ($\rho=1.975$) CM	ONE LAYER	THREE LAYERS	FIVE LAYERS	ZERO THICKNESS (CALCULATED)
439	5.1	2.4	—	7.4
573	13.3	7.2	—	19.0
737	25.5	17.0	9.8	35.0
914	44.2	30.0	21.6	58.0
1097	65.0	41.4	33.6	83.0
1274	82.5	60.9	53.0	101.0
1423	123.0	90.2	71.4	148.0
1619	197.3	146.0	113.3	227.0

was then removed and the counting rate obtained for the β-rays from the radium E spectrum for a given value of the magnetic field. The counting rates were also obtained when the radio-thorium was placed in each of the positions d_1, d_2 and d_3. The differences between the counting rates with and without the radio-thorium were found to be equal to the rates due to the radio-thorium alone within the limits of statistical error.

The equation for the motion of the β-rays along their paths in the magnetic field is

$$Hev = mv^2/\rho,$$

whence

$$H\rho = mv/e = m_0/e \cdot v/(1-v^2/c^2)^{\frac{1}{2}}.$$

The energy of such rays is obtained from these relations:

$$E = m_0c^2\{1/(1-v^2/c^2)^{\frac{1}{2}}-1\} \text{ ergs.}$$

$$= 299.8\{[(H\rho)^2+(cm_0/e)^2]^{\frac{1}{2}}-(cm_0/e)\}$$

electron volts

$$= 299.8\{[(H\rho)^2+(1703.41)^2]^{\frac{1}{2}}-1703.41\}.$$

If we put $H\rho = 1703.41 \tan\theta$, then it can be shown that

$$V = 510{,}682\{\sec\theta - 1\} \text{ electron volts.}$$

In Table II are shown three sets of data obtained for radium E showing the counting rates for various values of the magnetic field. The counting rates for each set of data have had the residual count subtracted. In column five is shown the average of the results for the three sets of data. In column six are the average values of the readings after they have been corrected for the absorption due to the cellophane window. For values of H greater than about 3300 the counting rate was not appreciably greater than the residual count. The curve of Fig. 2 represents the data of column six of Table II plotted against the values of the magnetic field H. The presence of the partition D in the brass box did not appreciably change the end point or tail of the curve. This seems to clearly indicate that the tail is not due to scattering. The curve of Fig. 3 shows a set of data obtained without the partition D in the box. The source used in obtaining these data was stronger than that previously used. The dotted curve was obtained with the partition. This dotted curve represents the data of Fig. 2 multiplied by a factor 1.64 such that the maxima of the two curves coincided. The two curves practically coincide for values of H above the value at the maximum. This shows that the screen had no effect on the end point and number for the higher energies, but reduced the number at the lower energies as was to be expected. The curve of Fig. 2 appears to indicate an upper limit at a value of H of about 3400 gauss. A more

TABLE II. *Counting rates for various values of H.*

H (GAUSS)	SET #1 COUNTS/ MIN.	SET #2 COUNTS/ MIN.	SET #3 COUNTS/ MIN.	AVE. (UNCORR.)	AVE. (CORR.)
222	1.2	1.0	0.9	1.02	1.4
373	7.0	4.3	3.3	4.9	6.7
555	23.0	16.8	15.7	18.5	23.6
720	47.0	40.0	38.3	41.8	50.2
901	100.0	77.7	80.7	86.1	96.5
1080	210.3	180.7	173.0	188.0	197.8
1255	267.0	260.3	249.0	258.8	258.8
1429	292.6	280.0	273.7	282.1	282.1
1610	280.0	270.7	257.7	269.5	269.5
1800	229.0	219.0	210.3	219.4	219.4
1966	187.0	170.7	159.0	172.2	172.2
2150	134.7	123.0	120.7	126.1	126.1
2330	85.3	71.7	70.3	75.8	75.8
2535	54.3	39.0	41.7	45.0	45.0
2685	33.5	20.0	18.0	23.8	23.8
2865	20.0	13.8	14.0	15.9	15.9
3042	11.0	6.3	5.0	7.4	7.4
3220	5.0	3.0	2.0	3.3	3.3
3304	—	—	—	—	0
3600	—	—	—	—	0

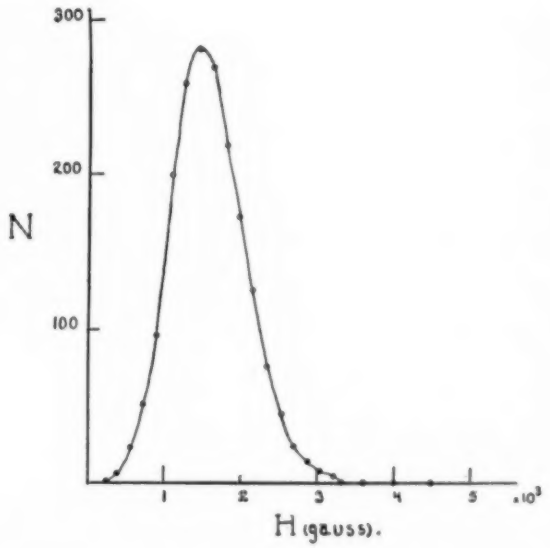

FIG. 2. Counting rates for various values of the magnetic field with the partition D in the brass box.

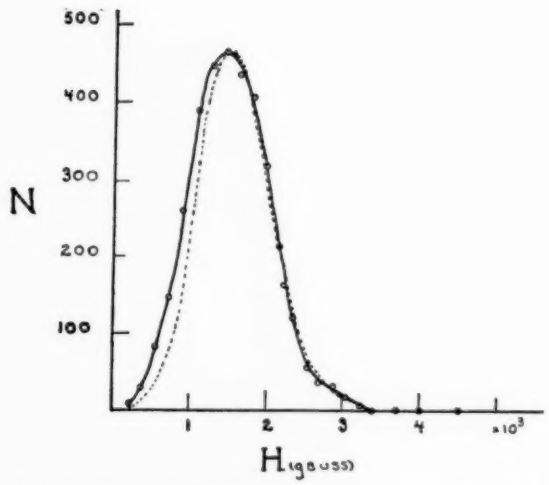

FIG. 3. Comparison of the counting rates for various values of the magnetic field without (solid curve) and with (dotted curve) the partition D in the box.

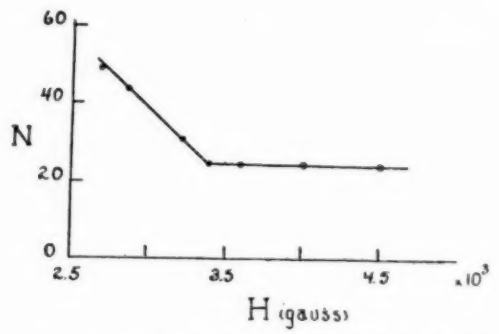

FIG. 4. Counting rates for various values of the magnetic field at the high energy end of the spectrum.

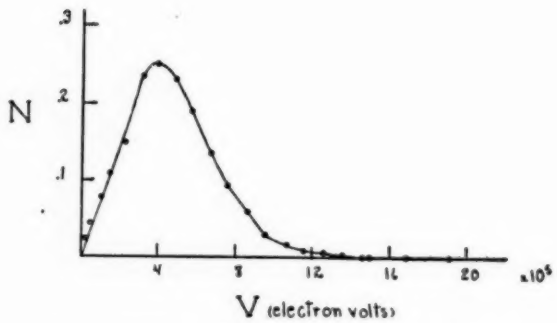

FIG. 5. Energy distribution curve of the beta-rays.

detailed study of this endpoint is shown in Fig. 4. This indicates an upper limit at $H\rho = 3380 \pm 50$ gauss. Readings were taken for values of the magnetic field as great as 4500 gauss and no increase in the counting rate above the residual value was found for any field strength above 3400 gauss. This upper limit represents an $H\rho = 6604 \pm 98$ corresponding to an energy of $(15.34 \pm 0.28) \times 10^5$ electron volts. The value of ρ used in computing the upper limit was one-half the distance from the side of the wire nearest S_2 to the edge of S_2 nearest the wire, which was 1.954 cm. In computing the energy distribution curve, however, the value used was one-half the distance from the side of the wire nearest S_2 to the center of S_2, a distance of 1.975 cm.

This value of the upper limit is higher than that obtained by such investigators as Madgwick, Sargent, Feather and Champion who obtained values for the endpoint from $H\rho = 5000$ to $H\rho = 5500$. On the other hand Terroux found there was no definite upper limit, while Curie and d'Espine and Yovanovitch found a band extending from $H\rho = 6000$ to $H\rho = 12{,}000$.

The ordinates of the curve of Fig. 2 were divided by H to give the distribution with respect to $H\rho$ and then divided by $\sin\theta$ to give the distribution with respect to the energy which is shown in Fig. 5. This curve has a maximum at 3.87×10^5 electron volts. The average value of the energy obtained from this curve by graphical means is 4.71×10^5 electron volts. Fig. 6 shows the experimental curve and the curve obtained from the Fermi theory. Both curves have been reduced to unit area and the abscissae are proportional to the energy instead of being actual energies. Since all the energy distribution curves of the simple type of the different radioactive substances are of the same general form, Fermi's theory should apply to all. He, however, points out that the present theory which he has thus far developed does not apply to radium E. The curve of Fig. 6 shows this to be the case.

The endpoint of the β-ray spectrum of radium E has been estimated from the effective range of the particles in various substances such as paper and aluminum and has been found to be between an $H\rho$ of 5000 and 5500 corresponding to an energy of 10.3 to 12.1×10^5 electron volts. This method was used by Schmidt, Gray, Douglas, Feather and Sargent. A kink always appears in the absorption curve which is taken to be the effective range of the fastest particles in the substance. From this it is possible to estimate the endpoint of the spectrum. It is quite often rather

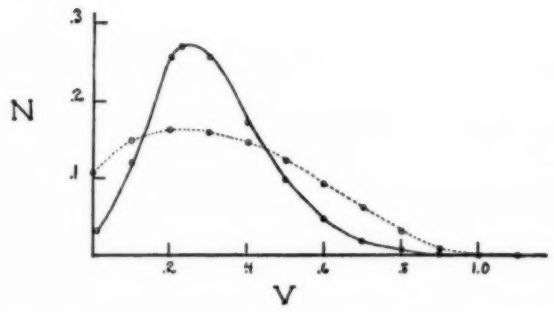

FIG. 6. Comparison of the experimentally determined energy distribution (solid curve) with that given by the Fermi theory (dotted curve).

difficult to detect this kink accurately in the presence of gamma-rays. Terroux points out that since the energy distribution spectrum has a sudden inflection at $H\rho = 5000$, one would also expect a kink in the absorption curve at this point. The kink does not then indicate complete absorption but only a sudden change in the absorption. If the right-hand side of the steep portion of the curve in Fig. 5 is extended to the axis it is found to cut the axis at about a million electron volts. This, however, neglects the tail which is definitely present.

Madgwick investigated the spectrum using the magnetic deflection method and an ionization chamber to detect the particles. He found an upper limit at about $H\rho = 5000$ which is considerably lower than the value found above. Champion measured the length of the β-ray tracks of radium E in a cloud chamber. From the tracks examined he concludes that the spectrum has an upper limit at $H\rho = 5500$ or about one million electron volts. Also Gray and O'Leary have estimated that less than one atom in 25,000 emits a β-ray with an $H\rho$ greater than 8000. Danysz, Curie and d'Espine, and Yovanovitch and d'Espine using photographic plates and magnetic focusing methods find a band extending from about 6000–12,000. Likewise Terroux, using the same method as Champion, obtains results which show that the spectrum does not end at $H\rho = 4900$–5500 but has a tail which extends beyond $H\rho = 12{,}000$. He also estimates that only about four percent of the total number of particles emitted have an $H\rho$ greater than 5000, which is in good agreement with the results of the present investigation.

The curves obtained by Henderson[14] in determining the endpoints of thorium C and thorium C″ spectra have a tail and definite endpoint similar to those observed for radium E in the present investigation. The curves obtained by Gurney[15] for radium C and radium C′ also have similar tails and endpoints.

In the previous work on radium E the various investigators who have placed the endpoint at values of $H\rho$ from 5000–5500 seem to have assumed that the tail, if present, was due to scattering and have neglected it. Since curves obtained both with and without the partition D in the brass box of the focusing apparatus in the present investigation indicate the same endpoint for the spectrum, the tail cannot be due to scattering. In the previous work the middle slit D was placed near the source and was wide. Such a slit does not define a beam with as small a range of ρ as a slit placed half-way along the path of the beta-particles. The few high speed particles observed by Terroux and others at values of $H\rho$ greater than 6700 may possibly have been due to contamination of the source.

Using a cloud chamber, H. O. Richardson has found a group of low energy β-rays for radium E extending from 0.10–0.65×10^5 electron volts. The numbers of β-rays for values of the energy in this region were greater than the number obtained at the maximum value of the energy distribution curve. The present experiments do not indicate the presence of such a large number of low energy β-rays. The curve in Fig. 5 only shows a number of β-rays of energy 0.40×10^5 electron volts equal to about 18 percent of the maximum number. This cannot be explained by the absorption of the cellophane as this has been allowed for. It is possible therefore that most of H. O. Richardson's low energy rays were secondary rays due to collisions of higher energy rays with atoms. This possibility was considered by Richardson but he thought that the number of low energy rays which he observed was probably too great to be explained in this way.

The writer wishes to express his indebtedness to Professor H. A. Wilson for suggesting the problem and for his interest and guidance during the progress of the work.

[14] Henderson, Proc. Roy. Soc. **A147**, 572 (1934).
[15] Gurney, Proc. Roy. Soc. **A109**, 540 (1925).

The Spectra of Argon in the Extreme Ultraviolet

J. C. BOYCE, *George Eastman Research Laboratory of Physics, Massachusetts Institute of Technology*

(Received June 28, 1935)

The term tables of A II, A III and A IV have been revised or extended upon the basis of new wavelength measurements in the extreme ultraviolet. A few lines of A I previously known have been remeasured. In the other stages the known lines have been remeasured and new lines added as follows: 23 in A II, 57 in A III, 23 (including some intersystem combinations) in A IV, and 10 in A V (where none were previously known). These results confirm the identification of the nebular lines λ4711.4 and λ4740.2 as due to "forbidden" transitions in A IV. The intervals in possible pairs of "forbidden" lines from A III and A V are discussed. Accurate ionization potentials are given, 15.69 volts for A I, 27.80 volts for A II and 40.78 volts for A III, while rough estimates yield 61 volts for A IV and 78 volts for A V.

THE spectra of argon in the extreme ultraviolet have been investigated by Lyman and Saunders,[1] Hertz and Abbink,[2] Saunders,[3] Hopfield and Dieke,[4] Dorgelo and Abbink,[5] Saunders,[6] Compton, Boyce and Russell,[7] Boyce and Compton,[8] and von Keussler.[9] Increased dispersion and resolving power have now been made possible by the two-meter normal incidence vacuum spectrograph[10] of the Carnegie Institution of Washington which is located in the Spectroscopy Laboratory of the Massachusetts Institute of Technology. Exposures made with an electrodeless discharge at different gas pressures distinguished between the spectra of the various stages of ionization. Traces of oxygen were present as an impurity and an examination of the group of lines of O II and O III near λ834 was a very convenient method of estimating the excitation of a particular exposure. The principal group of lines was already known for all of the spectra investigated except A V. The plates were measured by Dr. Carol A. Rieke and Mr. D. H. Clewell, both of whom it is a pleasure to thank for their careful work and for their assistance in the reduction of the measurements. The method of reduction has been given in the description of the instrument[10] and in the discussion of the results for neon.[11] The standards used have recently been published.[12] Wavelengths given to three decimal places are believed to be accurate to somewhat less than 0.01A. For those less certainly determined the error may be as great as 0.02A and such lines are given to two decimal places. Lines newly or differently identified in the present investigation are denoted by an asterisk.

A I

The electrodeless discharge is not particularly suitable for the excitation of first spectra. Only two lines were obtained with sufficient intensity to permit precise measurement. Four weak lines were also present. The lines are listed in Table I with term designations taken from the tables of Bacher and Goudsmit.[13] A few of the term values

TABLE I. *A I classified lines.*

λ(OBS.)	INT. SPARK	INT. ARC	ν	λ(CALC.)	CLASSIFICATION
1066.660	9	15	93750.0		$^1S_0-4s\ 2_1°$
1048.218	8	25	95400.0		$^1S_0-4s\ 4_1°$
894.30	1	4	111820	894.310	$^1S_0-3d\ 2_1°$
		3		879.949	$^1S_0-5s\ 2_1°$
876.06	2	4	114148	876.063	$^1S_0-3d\ 8_1°$
869.75	1	2	114975	869.754	$^1S_0-5s\ 4_1°$
866.80	3	4	115367	866.805	$^1S_0-3d\ 12_1°$
		2		842.808	$^1S_0-4d\ 2_1°$
		6		835.003	$^1S_0-6s\ 2_1°$
				834.397	$^1S_0-4d\ 8_1°$
		2		826.371	$^1S_0-4d\ 12_1°$
		1		825.348	$^1S_0-6s\ 4_1°$
		0		820.129	$^1S_0-5d\ 2_1°$
		4		816.466	$^1S_0-7s\ 2_1°$
				816.233	$^1S_0-5d\ 8_1°$
				809.933	$^1S_0-6d\ 2_1°$
				807.702	$^1S_0-5d\ 12_1°$
		2d		807.220	$^1S_0-8s\ 2_1°$ and $^1S_0-7s\ 4_1°$
				806.875	$^1S_0-6d\ 8_1°$

[1] T. Lyman and F. A. Saunders, Nature **116**, 358 (1925).
[2] G. Hertz and J. H. Abbink, Naturwiss. **14**, 648 (1926).
[3] F. A. Saunders, Proc. Nat. Acad. Sci. **12**, 556 (1926).
[4] J. J. Hopfield and G. H. Dieke, Phys. Rev. **27**, 638 (1926).
[5] H. B. Dorgelo and J. H. Abbink, Zeits. f. Physik **41**, 753 (1927).
[6] F. A. Saunders, Proc. Nat. Acad. Sci. **13**, 596 (1927).
[7] K. T. Compton, J. C. Boyce and H. N. Russell, Phys. Rev. **32**, 179 (1928).
[8] J. C. Boyce and K. T. Compton, Proc. Nat. Acad. Sci. **15**, 656 (1929).
[9] V. von Keussler, Zeits. f. Physik **84**, 42 (1933).
[10] K. T. Compton and J. C. Boyce, Rev. Sci. Inst. **5**, 218 (1934).
[11] J. C. Boyce, Phys. Rev. **46**, 378 (1934).
[12] J. C. Boyce and C. A. Rieke, Phys. Rev. **47**, 653 (1935).
[13] R. F. Bacher and S. Goudsmit, *Atomic Energy States*, (McGraw-Hill, 1932).

given by Bacher and Goudsmit have been revised by Meggers and Humphreys.[14] On the basis of the present results the lowest state, $(3s)^2(3p)^6\ ^1S_0$, should be revised to read 127,111 cm^{-1} as referred to the $(3s)^2(3p)^5\ ^2P_{1\frac{1}{2}}^\circ$ limit. The ionization potential remains 15.69 volts.

Discharges in mixtures with argon are frequently used in the excitation of molecular spectra. Since no accurate measurements were previously available it seemed worth while to compute the wavelengths for some additional lines. This has been done by using the ground state as here revised and for the upper states the values of Meggers and Humphreys.[14] Intensities designated "spark" represent those of the present electrodeless discharge. Those designated "arc" are taken from the earlier observations of Compton, Boyce and Russell[7] for excitation by controlled electron impact.[15]

A II

The second spectrum has been analyzed by de Bruin[16, 17] and by Compton, Boyce and Russell.[7] An extensive term table has been given by de Bruin.[17] The data from the extreme ultraviolet are with one exception very consistent with the values given by de Bruin for the even terms. Combinations between the ground state $(3s)^2(3p)^5\ ^2P_{1\frac{1}{2},\frac{1}{2}}^\circ$ and de Bruin's $(^1D)3d\ ^2P_{\frac{1}{2}}$ do not occur. There are two lines in the extreme ultraviolet indicating combination with a term 14 cm^{-1} deeper in the atom. De Bruin's $(^1D)3d\ ^2P_{\frac{1}{2}}$ term seems to depend on only two lines in the visible spectrum, of which one is a poor fit and the other comes from a high odd term the validity of which is about to be questioned. It therefore seems reasonable to reject de Bruin's identification of this term and tentatively to substitute the value indicated from the extreme ultraviolet, although it has not been possible to find definite combinations with higher odd terms among the lines of argon observed by Rosenthal.[18] Examination of the configuration assignments given by de Bruin revealed the fact that two groups of his term values were not consistent with any reasonable estimate of the relative positions of the ^3P, ^1D and ^1S states arising from the $(3s)^2(3p)^4$ electron configuration of A III. These states constitute the limits upon which the terms of A II are built. One of these inconsistent groups is the set of five ^2D terms marked by de Bruin $(^3P)3d$, $(^3P)4d$, $(^1D)4s$, $(^1D)5s$, $(^1S)3d$. A reassignment in a different order of these ^2D terms among the same electron configurations has been found which is satisfactory. Additional evidence in favor of the new assignment came from the intensities of the extreme ultraviolet lines associated with these terms, since in the present type of excitation second series members are expected to be considerably weakened. The $^2F^\circ$, $^2D^\circ$ and $^2P^\circ$ terms assigned by de Bruin to $(^1D)5p$ were questioned on the same grounds of incompatibility with their limit. It seems very likely that the first two of these terms came from the $(^3P)4f$ configuration and that the $^2P^\circ$ term may be a fragment of an associated quartet term or may be spurious. Some of the evidence in support of the reality of this $^2P^\circ$ term, apart from its exact designation, came from a visible combination with the $(^1D)3d\ ^2P_{\frac{1}{2}}$ term already questioned. The complete solution of these difficulties requires further investigation. The classified lines given in Table II locate the $(3s)^2(3p)^5\ ^2P_{1\frac{1}{2}}^\circ$ term at 224,755.5 on de Bruin's scale. In Table III term values are given with respect to this ground term as zero. Changes indicated in the discussion above have been made in the term identifications and in one case in the term value and the dubious high $^2P^\circ$ term has been omitted. Evaluation by a Ritz formula of the series limit of the $^4P_{2\frac{1}{2}}$ terms arising from $4s$, $5s$ and $6s$ electron places that limit, the $(3s)^2(3p)^4\ ^3P_2$ state of A III, at 225,168 cm^{-1} above the ground state of A II. This corresponds to an ionization potential of 27.80 ± 0.02 volts for A II.

A III

The first multiplet in the third spectrum was discovered by Hopfield and Dieke.[4] More recent work by von Keussler[9] and by de Bruin[19] have given three term systems, quintets and triplets

[14] W. F. Meggers and C. J. Humphreys, Bur. Standards J. Research **10**, 427 (1933); W. F. Meggers, ibid. **14**, 487 (1935).
[15] K. T. Compton and J. C. Boyce, J. Frank. Inst. **205**, 497 (1928).
[16] T. L. de Bruin, Zeits. f. Physik **48**, 62 (1928); **51**, 108 (1928).
[17] T. L. de Bruin, Zeits. f. Physik **61**, 307 (1930).
[18] A. H. Rosenthal, Ann. d. Physik (5) **4**, 49 (1930).
[19] T. L. de Bruin, Proc. Amst. Acad. **36**, 724 (1933).

TABLE II. *A II classified lines.*

λ	INT.	ν	CLASSIFICATION
*1973.48	1	50671.8	$s\,p^6\,{}^2S_{\frac{1}{2}} - ({}^3P)4p\,{}^2D_{1\frac{1}{2}}{}^\circ$
*1961.356	2	50985.1	$s\,p^6\,{}^2S_{\frac{1}{2}} - ({}^3P)4p\,{}^2P_{\frac{1}{2}}{}^\circ$
*1941.062	2	51518.2	$s\,p^6\,{}^2S_{\frac{1}{2}} - ({}^3P)4p\,{}^2P_{1\frac{1}{2}}{}^\circ$
*1909.58	1	52367.7	$s\,p^6\,{}^2S_{\frac{1}{2}} - ({}^3P)4p\,{}^2S_{\frac{1}{2}}{}^\circ$
*1574.985	4	63492.7	$s\,p^6\,{}^2S_{\frac{1}{2}} - ({}^1D)4p\,{}^2P_{1\frac{1}{2}}{}^\circ$
*1560.188	3	64094.8	$s\,p^6\,{}^2S_{\frac{1}{2}} - ({}^1D)4p\,{}^2P_{\frac{1}{2}}{}^\circ$
932.046	10	107291	$s^2p^5\,{}^2P_{\frac{1}{2}}{}^\circ - s\,p^6\,{}^2S_{\frac{1}{2}}$
919.78	15	108722	$s^2p^5\,{}^2P_{1\frac{1}{2}}{}^\circ - s\,p^6\,{}^2S_{\frac{1}{2}}$
762.192	2	131201	$s^2p^5\,{}^2P_{\frac{1}{2}}{}^\circ - ({}^3P)3d\,{}^4D_{1\frac{1}{2}}$
754.817	3	132482	$s^2p^5\,{}^2P_{1\frac{1}{2}}{}^\circ - ({}^3P)3d\,{}^4D_{2\frac{1}{2}}$
748.193	4	133655	$s^2p^5\,{}^2P_{\frac{1}{2}}{}^\circ - ({}^3P)4s\,{}^4P_{1\frac{1}{2}}$
*745.318	5	134171	$s^2p^5\,{}^2P_{\frac{1}{2}}{}^\circ - ({}^3P)4s\,{}^4P_{\frac{1}{2}}$
*744.920	5	134243	$s^2p^5\,{}^2P_{1\frac{1}{2}}{}^\circ - ({}^3P)4s\,{}^4P_{2\frac{1}{2}}$
740.263	12	135087	$s^2p^5\,{}^2P_{1\frac{1}{2}}{}^\circ - ({}^3P)4s\,{}^4P_{1\frac{1}{2}}$
*737.442	1	135604	$s^2p^5\,{}^2P_{1\frac{1}{2}}{}^\circ - ({}^3P)4s\,{}^4P_{\frac{1}{2}}$
730.929	8	136812	$s^2p^5\,{}^2P_{\frac{1}{2}}{}^\circ - ({}^3P)4s\,{}^2P_{1\frac{1}{2}}$
725.542	9	137828	$s^2p^5\,{}^2P_{\frac{1}{2}}{}^\circ - ({}^3P)4s\,{}^2P_{\frac{1}{2}}$
723.353	14	138245	$s^2p^5\,{}^2P_{1\frac{1}{2}}{}^\circ - ({}^3P)4s\,{}^2P_{1\frac{1}{2}}$
718.083	4	139260	$s^2p^5\,{}^2P_{\frac{1}{2}}{}^\circ - ({}^3P)4s\,{}^2P_{\frac{1}{2}}$
704.516	3	141941	$s^2p^5\,{}^2P_{\frac{1}{2}}{}^\circ - ({}^3P)3d\,{}^4F_{1\frac{1}{2}}$
698.760	4	143111	$s^2p^5\,{}^2P_{1\frac{1}{2}}{}^\circ - ({}^3P)3d\,{}^4F_{2\frac{1}{2}}$
697.944	1	143278	$s^2p^5\,{}^2P_{\frac{1}{2}}{}^\circ - ({}^3P)3d\,{}^2P_{\frac{1}{2}}$
697.484	2	143372	$s^2p^5\,{}^2P_{1\frac{1}{2}}{}^\circ - ({}^3P)3d\,{}^4F_{1\frac{1}{2}}$
693.295	2	144239	$s^2p^5\,{}^2P_{\frac{1}{2}}{}^\circ - ({}^3P)3d\,{}^2P_{1\frac{1}{2}}$
691.030	1	144711	$s^2p^5\,{}^2P_{1\frac{1}{2}}{}^\circ - ({}^3P)3d\,{}^2P_{\frac{1}{2}}$
686.50	1	145667	$s^2p^5\,{}^2P_{1\frac{1}{2}}{}^\circ - ({}^3P)3d\,{}^2P_{1\frac{1}{2}}$
*679.410	8	147186	$s^2p^5\,{}^2P_{\frac{1}{2}}{}^\circ - ({}^3P)3d\,{}^2D_{1\frac{1}{2}}$
*672.849	3	148622	$s^2p^5\,{}^2P_{1\frac{1}{2}}{}^\circ - ({}^3P)3d\,{}^2D_{1\frac{1}{2}}$
*671.854	10	148842	$s^2p^5\,{}^2P_{1\frac{1}{2}}{}^\circ - ({}^3P)3d\,{}^2D_{2\frac{1}{2}}$
*670.947	10	149043	$s^2p^5\,{}^2P_{\frac{1}{2}}{}^\circ - ({}^1D)4s\,{}^2D_{1\frac{1}{2}}$
666.014	10	150147	$s^2p^5\,{}^2P_{1\frac{1}{2}}{}^\circ - ({}^3P)3d\,{}^2F_{2\frac{1}{2}}$
*664.558	6	150476	$s^2p^5\,{}^2P_{1\frac{1}{2}}{}^\circ - ({}^1D)4s\,{}^2D_{1\frac{1}{2}}$
*661.868	15	151088	$s^2p^5\,{}^2P_{1\frac{1}{2}}{}^\circ - ({}^1D)4s\,{}^2D_{2\frac{1}{2}}$
602.854	4	165878	$s^2p^5\,{}^2P_{\frac{1}{2}}{}^\circ - ({}^1S)4s\,{}^2S_{\frac{1}{2}}$
597.695	5	167309	$s^2p^5\,{}^2P_{1\frac{1}{2}}{}^\circ - ({}^1S)4s\,{}^2S_{\frac{1}{2}}$
583.437	8	171398	$s^2p^5\,{}^2P_{\frac{1}{2}}{}^\circ - ({}^1D)3d\,{}^2D_{1\frac{1}{2}}$
580.261	8	172335	$s^2p^5\,{}^2P_{1\frac{1}{2}}{}^\circ - ({}^1D)3d\,{}^2D_{2\frac{1}{2}}$
578.605	4	172830	$s^2p^5\,{}^2P_{1\frac{1}{2}}{}^\circ - ({}^1D)3d\,{}^2D_{1\frac{1}{2}}$
578.107	4	172978	$s^2p^5\,{}^2P_{\frac{1}{2}}{}^\circ - ({}^1D)3d\,{}^2P_{1\frac{1}{2}}$
576.731	5	173391	$s^2p^5\,{}^2P_{\frac{1}{2}}{}^\circ - ({}^1D)3d\,{}^2P_{\frac{1}{2}}$
573.360	6	174411	$s^2p^5\,{}^2P_{1\frac{1}{2}}{}^\circ - ({}^1D)3d\,{}^2P_{1\frac{1}{2}}$
572.015	5	174820	$s^2p^5\,{}^2P_{1\frac{1}{2}}{}^\circ - ({}^1D)3d\,{}^2P_{\frac{1}{2}}$
560.224	7	178500	$s^2p^5\,{}^2P_{\frac{1}{2}}{}^\circ - a\,{}^2P_{\frac{1}{2}}$
556.813	6	179594	$s^2p^5\,{}^2P_{1\frac{1}{2}}{}^\circ - a\,{}^2P_{1\frac{1}{2}}$
*553.122	1	180791	$s^2p^5\,{}^2P_{\frac{1}{2}}{}^\circ - ({}^3P)5s\,{}^4P_{1\frac{1}{2}}$
*550.899	1	181521	$s^2p^5\,{}^2P_{\frac{1}{2}}{}^\circ - ({}^3P)5s\,{}^4P_{\frac{1}{2}}$
*550.475	2	181661	$s^2p^5\,{}^2P_{1\frac{1}{2}}{}^\circ - ({}^3P)5s\,{}^2P_{1\frac{1}{2}}$
548.779	4	182223	$s^2p^5\,{}^2P_{1\frac{1}{2}}{}^\circ - ({}^3P)5s\,{}^4P_{1\frac{1}{2}}$
*547.983	1	182487	$s^2p^5\,{}^2P_{\frac{1}{2}}{}^\circ - ({}^3P)5s\,{}^2P_{\frac{1}{2}}$
547.460	4	182662	$s^2p^5\,{}^2P_{\frac{1}{2}}{}^\circ - ({}^1D)3d\,{}^2S_{\frac{1}{2}}$
*547.164	3	182761	$s^2p^5\,{}^2P_{\frac{1}{2}}{}^\circ - ({}^3P)4d\,{}^4D_{\frac{1}{2}}$
546.176	4	183091	$s^2p^5\,{}^2P_{1\frac{1}{2}}{}^\circ - ({}^3P)5s\,{}^2P_{1\frac{1}{2}}$
543.727	3	183916	$s^2p^5\,{}^2P_{1\frac{1}{2}}{}^\circ - ({}^3P)5s\,{}^2P_{\frac{1}{2}}$
543.201	4	184094	$s^2p^5\,{}^2P_{1\frac{1}{2}}{}^\circ - ({}^1D)3d\,{}^2S_{\frac{1}{2}}$
*542.910	3	184193	$s^2p^5\,{}^2P_{1\frac{1}{2}}{}^\circ - ({}^3P)4d\,{}^4D_{\frac{1}{2}}$
541.304	1	184739	$s^2p^5\,{}^2P_{\frac{1}{2}}{}^\circ - ({}^3P)4d\,{}^4P_{\frac{1}{2}}$
537.13	3	186173	$s^2p^5\,{}^2P_{1\frac{1}{2}}{}^\circ - ({}^3P)4d\,{}^4P_{\frac{1}{2}}$
*535.035	1	186893	$s^2p^5\,{}^2P_{1\frac{1}{2}}{}^\circ - ({}^3P)4d\,{}^4P_{2\frac{1}{2}}$
530.489	4	188505	$s^2p^5\,{}^2P_{\frac{1}{2}}{}^\circ - ({}^1P)4d\,{}^2P_{\frac{1}{2}}$
*528.640	2	189165	$s^2p^5\,{}^2P_{\frac{1}{2}}{}^\circ - ({}^3P)4d\,{}^2P_{1\frac{1}{2}}$
526.495	3	189935	$s^2p^5\,{}^2P_{1\frac{1}{2}}{}^\circ - ({}^3P)4d\,{}^2P_{\frac{1}{2}}$
524.678	4	190593	$s^2p^5\,{}^2P_{1\frac{1}{2}}{}^\circ - ({}^3P)4d\,{}^2P_{1\frac{1}{2}}$
*522.791	4	191281	$s^2p^5\,{}^2P_{\frac{1}{2}}{}^\circ - ({}^1S)3d\,{}^2D_{1\frac{1}{2}}$
*519.326	6	192557	$s^2p^5\,{}^2P_{1\frac{1}{2}}{}^\circ - ({}^1S)3d\,{}^2D_{2\frac{1}{2}}$
*518.89	2	192718	$s^2p^5\,{}^2P_{1\frac{1}{2}}{}^\circ - ({}^1S)3d\,{}^2D_{1\frac{1}{2}}$
*514.301	2	194438	$s^2p^5\,{}^2P_{\frac{1}{2}}{}^\circ - ({}^1D)5s\,{}^2D_{1\frac{1}{2}}$
*510.550	3	195867	$s^2p^5\,{}^2P_{1\frac{1}{2}}{}^\circ - ({}^1D)5s\,{}^2D_{2\frac{1}{2},\,1\frac{1}{2}}$
*505.007	1	198017	$s^2p^5\,{}^2P_{\frac{1}{2}}{}^\circ - ({}^1D)4d\,{}^2P_{\frac{1}{2}}$
*504.80	1	198099	$s^2p^5\,{}^2P_{\frac{1}{2}}{}^\circ - ({}^1D)4d\,{}^2D_{1\frac{1}{2}}$
503.642	2	198554	$s^2p^5\,{}^2P_{\frac{1}{2}}{}^\circ - ({}^1D)4d\,{}^2P_{1\frac{1}{2}}$
502.164	2	199138	$s^2p^5\,{}^2P_{1\frac{1}{2}}{}^\circ - ({}^3P)6s\,{}^4P_{1\frac{1}{2}}$
502.01	1	199198	$s^2p^5\,{}^2P_{\frac{1}{2}}{}^\circ - ({}^1P)6s\,{}^2P_{\frac{1}{2}}$
*501.40	1	199442	$s^2p^5\,{}^2P_{1\frac{1}{2}}{}^\circ - ({}^1D)4d\,{}^2P_{\frac{1}{2}}$
*501.185	2	199527	$s^2p^5\,{}^2P_{1\frac{1}{2}}{}^\circ - ({}^1D)4d\,{}^2D_{1\frac{1}{2}}$
*500.800	1	199680	$s^2p^5\,{}^2P_{1\frac{1}{2}}{}^\circ - ({}^1D)4d\,{}^2D_{2\frac{1}{2}}$
*499.92	1	200032	$s^2p^5\,{}^2P_{1\frac{1}{2}}{}^\circ - ({}^3P)6s\,{}^2P_{1\frac{1}{2}}$
489.191	3	204419	$s^2p^5\,{}^2P_{1\frac{1}{2}}{}^\circ - ({}^3P)5d\,{}^2P_{1\frac{1}{2}}$
*488.95	1	204518	$s^2p^5\,{}^2P_{1\frac{1}{2}}{}^\circ - ({}^3P)5d\,{}^2P_{\frac{1}{2}}$
488.786	3	204588	$s^2p^5\,{}^2P_{1\frac{1}{2}}{}^\circ - ({}^3P)5d\,{}^2D_{2\frac{1}{2}}$
487.227	2	205243	$s^2p^5\,{}^2P_{1\frac{1}{2}}{}^\circ - ({}^1D)4d\,{}^2S_{\frac{1}{2}}$

based on the ($^4S^\circ$) state of A IV and triplets based on the ($^2D^\circ$) state of that ion. No quintet to triplet intercombinations were known and the connection between the two triplet systems rested on one group of lines in the region of λ512. In the present investigation the quintet system has been related to the ground triplet state by two multiplets and an additional connection between the two triplet systems has been found. All classified lines for A III are given in Table IV. The three term systems of de Bruin have been reduced to the common zero of Table V, the ground $(3s)^2(3p)^4\ {}^3P_2$ state of the atom, and the error between systems is believed to be less than 1 cm^{-1}. In the system of triplets based on ($^4S^\circ$) the $3d\ {}^3D^\circ$ has been added with certainty. Tentative identifications are given for $3d\ {}^3D^\circ$ and $3d\ {}^3P^\circ$ based on ($^2D^\circ$) and for $3d\ {}^3D^\circ$, $3d\ {}^3F^\circ$ and $3d\ {}^3P^\circ$ based on ($^2P^\circ$). These tentative identifications rest on extreme ultraviolet combinations with the ground state and have not yet been confirmed by combinations with higher even terms. They seem consistent with such isoelectronic data[20] as are available and with the position of the limits as known from A IV. Isoelectronic data and the limit assignments in A II as here revised suggest that the $(3s)^2(3p)^4$ term lies about 14,000 cm^{-1} above the ground $(3s)^2(3p)^4\ {}^3P$ term. Two strong single lines, of proper excitation for A III, are believed to be $(3s)^2(3p)^4\ {}^1D_2 - 3s(3p)^5\ {}^1P_1{}^\circ$ and $(3s)^2(3p)^4\ {}^1S_0 - 3s(3p)^5\ {}^1P_1{}^\circ$ combinations and fix two other singlet terms with reference to this assumed value for the $(3s)^2(3p)^4\ {}^1D_2$. Two additional terms are tentatively suggested, but the whole singlet system floats with an uncertainty of several hundred inverse centimeters until triplet singlet intercombinations can be found. The same information could be obtained if the "forbidden" pair $^3P_2 - {}^1D_2$, $^3P_1 - {}^1D_2$ could be found in nebular spectra. Bowen has estimated the approximate position of these lines[21] in the near infrared and their separation must be 1112.4±1.0 cm^{-1}. The line at λ508.615, not resolved in this investigation, was resolved by von Keussler[9] into two

[20] *S I.*: R. Frerichs, Zeits. f. Physik **80**, 150 (1933); J. E. Reudy, Phys. Rev. **44**, 757 (1933). *Cl II.*: I. S. Bowen, Phys. Rev. **31**, 34 (1928); K. Murakawa, Zeits. f. Physik **69**, 507 (1931). *K IV, Ca V.*: I. S. Bowen, Phys. Rev. **46**, 791 (1934).

[21] I. S. Bowen, Astrophys. J. **81**, 1 (1935).

TABLE III. *A II term values.*

$(3s)^2\,(3p)^5\,{}^2P^\circ_{1\frac{1}{2}}$ 0.0 $3s\,(3p)^6\,{}^2S_{\frac{1}{2}}$ 108722.5
${}^2P^\circ_{\frac{1}{2}}$ 1432.0

LIMITS IN A III $(3s)^2\,(3p)^4$								
			${}^3P_2$	0.0	${}^1D_2$	14000	${}^1S_0$	31863
			${}^3P_1$	1112.4				
			${}^3P_0$	1570.2				
3d	${}^4D_{3\frac{1}{2}}$	132328.22	${}^2D_{1\frac{1}{2}}$	148621.14	${}^2G$		${}^2D_{2\frac{1}{2}}$	192557.81
	${}^4D_{2\frac{1}{2}}$	132482.20	${}^2D_{2\frac{1}{2}}$	148843.49	${}^2G$		${}^2D_{1\frac{1}{2}}$	192712.93
	${}^4D_{1\frac{1}{2}}$	132631.82			${}^2F_{3\frac{1}{2}}$			
	${}^4D_{\frac{1}{2}}$	132738.85			${}^2F_{2\frac{1}{2}}$	171110.79		
	${}^4F_{4\frac{1}{2}}$	142187.42	${}^2F_{3\frac{1}{2}}$	149494.74?	${}^2D_{2\frac{1}{2}}$	172336.42		
	${}^4F_{3\frac{1}{2}}$	142718.01	${}^2F_{2\frac{1}{2}}$	150148.63	${}^2D_{1\frac{1}{2}}$	172830.97		
	${}^4F_{2\frac{1}{2}}$	143108.63			${}^2P_{1\frac{1}{2}}$	174410.84		
	${}^4F_{1\frac{1}{2}}$	143372.48			${}^2P_{\frac{1}{2}}$	174821?		
	${}^4P_{2\frac{1}{2}}$	144495.24	${}^2P_{\frac{1}{2}}$	144711.00	${}^2S_{\frac{1}{2}}$	184094.10		
	${}^4P_{1\frac{1}{2}}$	144986.79	${}^2P_{1\frac{1}{2}}$	145669.91				
	${}^4P_{\frac{1}{2}}$	145212.44						
4s	${}^4P_{2\frac{1}{2}}$	134242.62	${}^2P_{1\frac{1}{2}}$	138244.62	${}^2D_{1\frac{1}{2}}$	150475.92	${}^2S_{\frac{1}{2}}$	167308.66
	${}^4P_{1\frac{1}{2}}$	135087.02	${}^2P_{\frac{1}{2}}$	139259.36	${}^2D_{2\frac{1}{2}}$	151088.35		
	${}^4P_{\frac{1}{2}}$	135602.78						
4p	${}^4P^\circ_{2\frac{1}{2}}$	155044.37	${}^2P^\circ_{\frac{1}{2}}$	159707.52	${}^2F^\circ_{3\frac{1}{2}}$	170401.88	${}^2P^\circ_{1\frac{1}{2}}$	191975.16
	${}^4P^\circ_{1\frac{1}{2}}$	155352.12	${}^2P^\circ_{1\frac{1}{2}}$	160240.48	${}^2F^\circ_{2\frac{1}{2}}$	170531.29	${}^2P^\circ_{\frac{1}{2}}$	192334.09
	${}^4P^\circ_{\frac{1}{2}}$	155705.42			${}^2P^\circ_{1\frac{1}{2}}$	172214.80		
	${}^4D^\circ_{3\frac{1}{2}}$	157234.92	${}^2D^\circ_{2\frac{1}{2}}$	158731.22	${}^2P^\circ_{\frac{1}{2}}$	172817.30		
	${}^4D^\circ_{2\frac{1}{2}}$	157674.28	${}^2D^\circ_{1\frac{1}{2}}$	159394.31	${}^2D^\circ_{1\frac{1}{2}}$	173348.78		
	${}^4D^\circ_{1\frac{1}{2}}$	158168.85			${}^2D^\circ_{2\frac{1}{2}}$	173394.43		
	${}^4D^\circ_{\frac{1}{2}}$	158429.17						
	${}^4S^\circ_{1\frac{1}{2}}$	161049.90	${}^2S^\circ_{\frac{1}{2}}$	161090.42				
4d	${}^4D_{3\frac{1}{2}}$	183676.42	${}^2D_{2\frac{1}{2}}$	186728.50	${}^2G_{4\frac{1}{2}}$	198595.91	${}^2D$	
	${}^4D_{2\frac{1}{2}}$	183798.22	${}^2D_{1\frac{1}{2}}$	186751.14	${}^2G_{3\frac{1}{2}}$	198604.78	${}^2D$	
	${}^4D_{1\frac{1}{2}}$	183986.83			${}^2P_{\frac{1}{2}}$	199447.56		
	${}^4D_{\frac{1}{2}}$	184193.12			${}^2P_{1\frac{1}{2}}$	199982.96		
	${}^4F_{4\frac{1}{2}}$	185093.92	${}^2F_{3\frac{1}{2}}$	186817.12	${}^2D_{1\frac{1}{2}}$	199525.96		
	${}^4F_{3\frac{1}{2}}$	185625.47	${}^2F_{2\frac{1}{2}}$	187589.62	${}^2D_{2\frac{1}{2}}$	199680.58		
	${}^4F_{2\frac{1}{2}}$	186075.06			${}^2F_{3\frac{1}{2}}$	200139.84		
	${}^4F_{1\frac{1}{2}}$	186341.39			${}^2F_{2\frac{1}{2}}$	200235.70		
	${}^4P_{\frac{1}{2}}$	186172.32	${}^2P_{\frac{1}{2}}$	189935.62				
	${}^4P_{1\frac{1}{2}}$	186471.32	${}^2P_{1\frac{1}{2}}$	190593.62	${}^2S_{\frac{1}{2}}$	205213.96		
	${}^4P_{2\frac{1}{2}}$	186891.92						
4f	${}^4G^\circ$		${}^2G^\circ$		${}^2H^\circ$		${}^2F^\circ$	
	${}^4G^\circ$		${}^2G^\circ$		${}^2H^\circ$		${}^2F^\circ$	
	${}^4G^\circ$							
	${}^4G^\circ$				${}^2G^\circ$			
					${}^2G^\circ$			
	${}^4F^\circ$		${}^2F^\circ_{3\frac{1}{2}}$	194842.37?	${}^2F^\circ$			
	${}^4F^\circ$		${}^2F^\circ_{2\frac{1}{2}}$	194883.98?	${}^2F^\circ$			
	${}^4F^\circ$							
	${}^4F^\circ$				${}^2D^\circ$			
					${}^2D^\circ$			
	${}^4D^\circ$		${}^2D^\circ_{1\frac{1}{2}}$	196622.78				
	${}^4D^\circ$		${}^2D^\circ_{2\frac{1}{2}}$	196634.04	${}^2P^\circ$			
	${}^4D^\circ$				${}^2P^\circ$			
	${}^4D^\circ$							
5s	${}^4P_{2\frac{1}{2}}$	181595.12	${}^2P_{1\frac{1}{2}}$	183091.32	${}^2D_{2\frac{1}{2}}$	195865.61	${}^2S_{\frac{1}{2}}$	
	${}^4P_{1\frac{1}{2}}$	182222.88	${}^2P_{\frac{1}{2}}$	183915.32	${}^2D_{1\frac{1}{2}}$	195867.68		
	${}^4P_{\frac{1}{2}}$	182952.02						
5p	${}^4P^\circ_{2\frac{1}{2}}$	189160.21	${}^2P^\circ_{1\frac{1}{2}}$	190106.84	${}^2F^\circ$		${}^2P^\circ$	
	${}^4P^\circ_{1\frac{1}{2}}$	189411.40	${}^2P^\circ_{\frac{1}{2}}$	190196.80	${}^2F^\circ$		${}^2P^\circ$	
	${}^4P^\circ_{\frac{1}{2}}$	189700.30			${}^2D^\circ$			
					${}^2D^\circ$			
	${}^4D^\circ_{3\frac{1}{2}}$	189986.00	${}^2D^\circ_{2\frac{1}{2}}$					
	${}^4D^\circ_{2\frac{1}{2}}$	190369.07	${}^2D^\circ_{1\frac{1}{2}}$	190528.00	${}^2P^\circ$			
	${}^4D^\circ_{1\frac{1}{2}}$	190774.08			${}^2P^\circ$			
	${}^4D^\circ_{\frac{1}{2}}$	191264.06						
	${}^4S^\circ_{1\frac{1}{2}}$		${}^2S^\circ_{\frac{1}{2}}$	191708.46				
5d	${}^4D$		${}^2D_{2\frac{1}{2}}$	204586.40	${}^2G$		${}^2D$	
	${}^4D$		${}^2D_{1\frac{1}{2}}$		${}^2G$		${}^2D$	
	${}^4D$				${}^2F$			
	${}^4D$				${}^2F$			
	${}^4F$		${}^2F$		${}^2D$			
	${}^4F$		${}^2F$		${}^2D$			
	${}^4F$				${}^2P$			
	${}^4F$				${}^2P$			
	${}^4P$		${}^2P_{1\frac{1}{2}}$	204418.50				
	${}^4P$		${}^2P_{\frac{1}{2}}$	204515.81	${}^2S_{\frac{1}{2}}$			
	${}^4P$							
6s	${}^4P_{2\frac{1}{2}}$	198813.17	${}^2P_{1\frac{1}{2}}$	200032.65	${}^2D$		${}^2S_{\frac{1}{2}}$	
	${}^4P_{1\frac{1}{2}}$	199138.92	${}^2P_{\frac{1}{2}}$	200624.00	${}^2D$			
	${}^4P_{\frac{1}{2}}$	200111.16						

TABLE IV. *A III classified lines.*

λ	INT.	ν	CLASSIFICATION
1973.780	4	50664.2	$(^4S)4s\ ^3S_1^\circ - (^2D)4p\ ^3P_2$
1962.74	2	50949.3	$(^4S)4s\ ^3S_1^\circ - (^2D)4p\ ^3P_1$
1957.83	1	51076.9	$(^4S)4s\ ^3S_1^\circ - (^2D)4p\ ^3P_0$
*1919.515	4	52096.8	$(^4S)3d\ ^3D_1^\circ - (^4S)4p\ ^3P_1$
*1918.667	4	52119.5	$(^4S)3d\ ^3D_1^\circ - (^4S)4p\ ^3P_2$
*1918.06	1	52135.8	$(^4S)3d\ ^3D_1^\circ - (^4S)4p\ ^3P_0$
*1915.564	7	52203.9	$(^4S)3d\ ^3D_2^\circ - (^4S)4p\ ^3P_1$
*1914.653	3	52228.8	$(^4S)3d\ ^3D_2^\circ - (^4S)4p\ ^3P_2$
*1914.398	9	52235.7	$(^4S)3d\ ^3D_3^\circ - (^4S)4p\ ^3P_2$
1675.637	4	59678.8	$(^4S)3d\ ^5D_2^\circ - (^4S)4p\ ^5P_1$
1675.484	7	59684.2	$(^4S)3d\ ^5D_{0,1}^\circ - (^4S)4p\ ^5P_1$
1673.425	7	59757.7	$(^4S)3d\ ^5D_3^\circ - (^4S)4p\ ^5P_2$
1673.241	3	59764.2	$(^4S)3d\ ^5D_2^\circ - (^4S)4p\ ^5P_2$
1673.14	1	59767.9	$(^4S)3d\ ^5D_1^\circ - (^4S)4p\ ^5P_2$
1669.671	7	59892.0	$(^4S)3d\ ^5D_4^\circ - (^4S)4p\ ^5P_3$
1669.304	5	59905.2	$(^4S)3d\ ^5D_3^\circ - (^4S)4p\ ^5P_3$
1669.10	1	59912.6	$(^4S)3d\ ^5D_2^\circ - (^4S)4p\ ^5P_2$
*1468.006	2	68119.6	$(^4S)3d\ ^3D_1^\circ - (^2D)4p\ ^3D_2$
*1467.841	3	68127.3	$(^4S)3d\ ^3D_1^\circ - (^2D)4p\ ^3D_1$
*1465.712	3	68226.2	$(^4S)3d\ ^3D_2^\circ - (^2D)4p\ ^3D_2$
*1465.532	2	68234.6	$(^4S)3d\ ^3D_2^\circ - (^2D)4p\ ^3D_1$ $(^4S)3d\ ^3D_3^\circ - (^2D)4p\ ^3D_2$
*1460.234	2	68482.2	$(^4S)3d\ ^3D_2^\circ - (^2D)4p\ ^3D_3$
*1460.077	4	68489.5	$(^4S)3d\ ^3D_3^\circ - (^2D)4p\ ^3D_3$
887.404	10	112688.2	$s^2p^4\ ^3P_1 - sp^5\ ^3P_2^\circ$
883.179	9	113227.3	$s^2p^4\ ^3P_0 - sp^5\ ^3P_1^\circ$
879.622	8	113685.2	$s^2p^4\ ^3P_1 - sp^5\ ^3P_1^\circ$
878.728	12	113800.8	$s^2p^4\ ^3P_2 - sp^5\ ^3P_2^\circ$
875.534	9	114216.0	$s^2p^4\ ^3P_1 - sp^5\ ^3P_0^\circ$
871.099	10	114797.5	$s^2p^4\ ^3P_2 - sp^5\ ^3P_1^\circ$
*769.152	12	130013	$s^2p^4\ ^1S_0 - sp^5\ ^1P_1^\circ$
*697.74	2	143319	$s^2p^4\ ^3P_0 - (^1S)3d\ ^3D_1^\circ$
*695.537	6	143774	$s^2p^4\ ^3P_1 - (^4S)3d\ ^5D_{0,1,2}^\circ$
*690.170	8*d*	144892	$s^2p^4\ ^3P_2 - (^4S)3d\ ^5D_{1,2,3}^\circ$
*676.241	6	147876	$s^2p^4\ ^1D_2 - sp^5\ ^1P_1^\circ$
*643.256	9	155495	$s^2p^4\ ^3P_0 - (^4S)3d\ ^3D_1^\circ$
*641.808	12	155810	$s^2p^4\ ^3P_1 - (^4S)3d\ ^3D_2^\circ$
*641.364	5	155918	$s^2p^4\ ^3P_1 - (^4S)3d\ ^3D_1^\circ$
*637.282	20 bl	156916	$s^2p^4\ ^3P_2 - (^4S)3d\ ^3D_2^\circ$
*636.818	3	157031	$s^2p^4\ ^3P_2 - (^4S)3d\ ^3D_1^\circ$
*604.152	10	165521	$s^2p^4\ ^1D_2 - (^2D)3d\ ^1F_3^\circ$?
*577.153	3	173264	$s^2p^4\ ^3P_1 - (^4S)4s\ ^5S_2^\circ$
*573.468	4	174378	$s^2p^4\ ^3P_2 - (^4S)4s\ ^5S_2^\circ$
558.321	5	179109	$s^2p^4\ ^3P_0 - (^4S)4s\ ^3S_1^\circ$
556.893	6	179568	$s^2p^4\ ^3P_1 - (^4S)4s\ ^3S_1^\circ$
553.470	9	180678	$s^2p^4\ ^3P_2 - (^4S)4s\ ^3S_1^\circ$
*538.788	6	185602	$s^2p^4\ ^3P_0 - (^2D)3d\ ^3D_1^\circ$
*537.459	6	186061	$s^2p^4\ ^3P_1 - (^2D)3d\ ^3D_1^\circ$
*536.745	8	186308	$s^2p^4\ ^1D_2 - (^2D)4s\ ^1D_2^\circ$?
*535.580	7	186714	$s^2p^4\ ^3P_1 - (^2D)3d\ ^3D_2^\circ$
*534.26	1	187174	$s^2p^4\ ^3P_2 - (^2D)3d\ ^3D_1^\circ$
*532.413	7	187825	$s^2p^4\ ^3P_2 - (^2D)3d\ ^3D_2^\circ$
*529.900	9	188715	$s^2p^4\ ^3P_2 - (^2D)3d\ ^3D_3^\circ$
512.769	7	195020	$s^2p^4\ ^3P_0 - (^2D)4s\ ^3D_1^\circ$
511.565	7	195479	$s^2p^4\ ^3P_1 - (^2D)4s\ ^3D_1^\circ$
511.497	8	195504	$s^2p^4\ ^3P_1 - (^2D)4s\ ^3D_2^\circ$
508.615	6	196612	$s^2p^4\ ^3P_2 - (^2D)4s\ ^3D_{1,2}^\circ$
508.434	9	196682	$s^2p^4\ ^3P_2 - (^2D)4s\ ^3D_3^\circ$
*492.228	3	203158	$s^2p^4\ ^3P_0 - (^2P)3d\ ^3D_1^\circ$
*491.121	4	203620	$s^2p^4\ ^3P_1 - (^2P)3d\ ^3D_1^\circ$
*490.68	3	203799	$s^2p^4\ ^3P_1 - (^2P)3d\ ^3D_2^\circ$
*488.452	7	204728	$s^2p^4\ ^3P_2 - (^2P)3d\ ^3D_1^\circ$
*487.988	7	204923	$s^2p^4\ ^3P_2 - (^2P)3d\ ^3D_2^\circ$
*487.025	7	205331	$s^2p^4\ ^3P_2 - (^2D)3d\ ^3D_3^\circ$
*485.515	4	205967	$s^2p^4\ ^3P_0 - (^2D)3d\ ^3P_1^\circ$
*485.150	6	206122	$s^2p^4\ ^3P_1 - (^2D)3d\ ^3P_2^\circ$
*484.445	5	206422	$s^2p^4\ ^3P_1 - (^2D)3d\ ^3P_1^\circ$
*484.116	5	206562	$s^2p^4\ ^3P_1 - (^2D)3d\ ^3P_0^\circ$
*482.548	8	207233	$s^2p^4\ ^3P_2 - (^2D)3d\ ^3P_2^\circ$
*481.848	6	207534	$s^2p^4\ ^3P_2 - (^2D)3d\ ^3P_1^\circ$
*476.432	7	209894	$s^2p^4\ ^3P_1 - (^2P)3d\ ^3F_2^\circ$
*473.918	6	211011	$s^2p^4\ ^3P_2 - (^2P)3d\ ^3F_3^\circ$
*473.025	6	211405	$s^2p^4\ ^3P_2 - (^2P)3d\ ^3F_2^\circ$
*469.968	4	212780	$s^2p^4\ ^3P_0 - (^2P)3d\ ^3P_1^\circ$
*469.831	4	212842	$s^2p^4\ ^3P_1 - (^2P)3d\ ^3P_2^\circ$
*468.956	3	213240	$s^2p^4\ ^3P_1 - (^2P)3d\ ^3P_1^\circ$
*468.467	4	213462	$s^2p^4\ ^3P_1 - (^2P)3d\ ^3P_0^\circ$
*467.390	6	213945	$s^2p^4\ ^3P_2 - (^2P)3d\ ^3P_2^\circ$
*466.530	5	214349	$s^2p^4\ ^3P_2 - (^2P)3d\ ^3P_1^\circ$
*398.86	1	250714	$s^2p^4\ ^3P_2 - (^4S)5s\ ^5S_2^\circ$
*397.67	1	251466	$s^2p^4\ ^3P_1 - (^4S)5s\ ^3S_1^\circ$
*396.38	4	252288	$s^2p^4\ ^3P_2 - (^4S)4d\ ^3D_3^\circ$
*395.92	1	252576	$s^2p^4\ ^3P_2 - (^4S)5s\ ^3S_1^\circ$

TABLE V. *A III term values.* (Singlets based on assumed value 14,000 for $(3s)^2\ (3p)^4\ ^1D_2$.)

$(3s)^2\ (3p)^4\ ^3P_2$	0.0		$3s\ (3p)^5\ ^3P_2^\circ$	113800.7	
$^3P_1$	1112.4		$^3P_1^\circ$	114797.6	
$^3P_0$	1570.2		$^3P_0^\circ$	115328.4	
$(3s)^2\ (3p)^4\ ^1D_2$	14000		$3s\ (3p)^5\ ^1P_1^\circ$	161876	
$(3s)^2\ (3p)^4\ ^1S_0$	31863				

LIMITS IN *A* IV $(3s)^2\ (3p)^3$		$^4S_{1\frac{1}{2}}^\circ$ 0				
			$^2D_{1\frac{1}{2}}^\circ$ 21090		$^2P_{\frac{1}{2}}^\circ$ 34854	
			$^2D_{2\frac{1}{2}}^\circ$ 21219		$^2P_{1\frac{1}{2}}^\circ$ 35034	
3*d*	$^5D_0^\circ$		$^3F_4^\circ$	186404.45	$^3D_1^\circ$	204726
	$^5D_1^\circ$	144883.8	$^3F_3^\circ$	186660 50	$^3D_2^\circ$	204923
	$^5D_2^\circ$	144887.3	$^3F_2^\circ$	186905.35	$^3D_3^\circ$	205331
	$^5D_3^\circ$	144894.3	$^1F_3^\circ$	179521?	$^1D_2^\circ$	
	$^5D_4^\circ$	144907.8				
			$^3G^\circ$		$^3F_2^\circ$	211009
	$^3D_3^\circ$	156916	$^3G^\circ$		$^3F_3^\circ$	211405
	$^3D_2^\circ$	156923	$^3G^\circ$		$^3F_4^\circ$	
	$^3D_1^\circ$	157030				
			$^1G_4^\circ$		$^1F_3^\circ$	
			$^1D_1^\circ$	187173.42	$^3P_2^\circ$	213145
			$^3D_2^\circ$	187825.35	$^3P_1^\circ$	214350
			$^3D_3^\circ$	188716.35	$^3P_0^\circ$	214574
			$^1D_2^\circ$		$^1P_1^\circ$	
			$^3P_2^\circ$	207233		
			$^3P_1^\circ$	207534		
			$^3P_0^\circ$	207674		
			$^1P_1^\circ$			
4*s*	$^5S_2^\circ$	174375.00	$^3D_1^\circ$	196591.50	$^3P^\circ$	
	$^3S_1^\circ$	180679.00	$^3D_2^\circ$	196616.21	$^3P^\circ$	
			$^3D_3^\circ$	196682.10	$^3P^\circ$	
			$^1D_2^\circ$	200308?	$^1P_1^\circ$	
4*p*	$^5P_1$	204565.95	$^3D_2$	225150.23	^3D	
	$^5P_2$	204651.66	$^3D_1$	225157.48	^3D	
	$^5P_3$	204799.79	$^3D_3$	225404.89	^3D	
	$^3P_1$	209127.04	$^1D_2$		$^1D_2$	
	$^3P_2$	209151.82	$^3F_2$	226358.26	^3P	
	$^3P_0$	209166.35				
			$^3F_3$	226505.52	^3P	
			$^3F_4$	226648.36	^3P	
			$^1F_3$		$^1P_1$	
			$^3P_2$	231344.10	$^3S_1$	
			$^3P_1$	231628.59	$^1S_0$	
			$^3P_0$	231756.78		
			$^1P_1$			

LIMITS IN *A* IV $(3s)^2\ (3p)^3$		$^4S_{1\frac{1}{2}}^\circ$ 0				
			$^2D_{1\frac{1}{2}}^\circ$ 21090		$^2P_{\frac{1}{2}}^\circ$ 34824	
			$^2D_{2\frac{1}{2}}^\circ$ 21219		$^2P_{1\frac{1}{2}}^\circ$ 35034	
4*d*	$^5D_0^\circ$		$^3F_2^\circ$	266725.12	$^3F^\circ$	
	$^5D_1^\circ$	246029.76	$^3F_3^\circ$	266879.82	$^3F^\circ$	
	$^5D_2^\circ$	246033.79	$^3F_4^\circ$	267073.52	$^3F^\circ$	
	$^5D_3^\circ$	246036.64	$^1F_3^\circ$		$^1F_3^\circ$	
	$^5D_4^\circ$	246046.57				
			$^3G_3^\circ$	267784.40	$^3D^\circ$	
	$^3D_2^\circ$	252253.69	$^3G_4^\circ$	267835.50	$^3D^\circ$	
	$^3D_1^\circ$	252279.92	$^3G_5^\circ$	267898.12	$^3D^\circ$	
	$^3D_3^\circ$	252289.02				
			$^1G_4^\circ$		$^1D_2^\circ$	
			$^3D_1^\circ$	268981.10	$^3P^\circ$	
			$^3D_3^\circ$	269003.10	$^3P^\circ$	
			$^3D_2^\circ$	269015.10	$^3P^\circ$	
			$^1D_2^\circ$		$^1P_1^\circ$	
			$^3P_2^\circ$	271510.18		
			$^3P_1^\circ$	271674.38		
			$^3P_0^\circ$	271698.52		
			$^1P_1^\circ$			
			$^2S_1^\circ$	272070.75		
			$^1S_0^\circ$			
5*s*	$^5S_2^\circ$	250712.27	$^3D^\circ$	272130.12	$^3P^\circ$	
	$^3S_1^\circ$	252575.88	$^3D^\circ$	272190.46	$^3P^\circ$	
			$^3D^\circ$	272523.20	$^3P^\circ$	
			$^1D_2^\circ$		$^1P_1^\circ$	

components the wavelengths of which, when shifted slightly to fit the present scale, would be λ508.655 and λ508.595. Three lines given by von Keussler without identification at λ1843.19, λ1839.43 and λ1836.42 were also observed on the present plates and seem to be due to this stage of ionization of argon, but attempts to classify them have not been successful. Approximate estimates of series limits to the ($^4S°$) state of A IV can be made on the basis of two series of two members each, quintet and triplet terms from the 4*s* and 5*s* electronic states. These give 330,723 and 329,980, respectively. Pending the discovery of additional series members the value of 330,350 is adopted as a rounded mean. This corresponds to an ionization potential of 40.78±0.05 volts.

A IV

Table VI gives the classified lines of this spectrum. The large discrepancy in wavelength in the one multiplet discovered by Boyce and Compton[8] has been traced to a clerical error in the preparation of the manuscript of that earlier paper. Intersystem combinations have been located by comparison with the unpublished results of H. A. Robinson on P I. These provide the connection between the doublet and quartet systems, so that all terms given in Table VII are on a common scale. Additional members expected to be strong in the intersystem multiplets would nearly coincide with adjacent strong hydrogen lines and are not observable. These results confirm the identification by Swings and Edlén,[22] and independently by Boyce, Mrs. Payne-Gaposchkin and Menzel[23] of the nebular lines λ4711.4 and λ4740.2[24] as due to the "forbidden" $^4S_{1\frac{1}{2}}°-{}^2D_{2\frac{1}{2}}°$ and $^4S_{1\frac{1}{2}}°-{}^2D_{1\frac{1}{2}}°$ transitions in A IV. No series have been found but a rough estimate based on the isoelectronic sequence yields 61 volts for the ionization potential.

TABLE VI. *A IV classified lines.*

λ	INT.	ν	CLASSIFICATION
*1197.84	1	83484	$s^2p^2\,{}^2P_{1\frac{1}{2}}°-sp^4\,{}^4P_{1\frac{1}{2}}$
*1190.354	2	84009	$s^2p^2\,{}^2P_{1\frac{1}{2}}°-sp^4\,{}^4P_{\frac{1}{2}}$
*1187.80	1	84190	$s^2p^2\,{}^2P_{\frac{1}{2}}°-sp^4\,{}^4P_{\frac{1}{2}}$
*1037.931	1	96346	$s^2p^2\,{}^2D_{2\frac{1}{2}}°-sp^4\,{}^4P_{2\frac{1}{2}}$
*901.804	2	110889	$s^2p^2\,{}^2P_{1\frac{1}{2}}°-sp^4\,{}^2D_{1\frac{1}{2}}$
*901.168	9	110967	$s^2p^2\,{}^2P_{1\frac{1}{2}}°-sp^4\,{}^2D_{2\frac{1}{2}}$
*900.362	5	111066	$s^2p^2\,{}^2P_{\frac{1}{2}}°-sp^4\,{}^2D_{1\frac{1}{2}}$
850.602	25	117564	$s^2p^2\,{}^4S_{1\frac{1}{2}}°-sp^4\,{}^4P_{2\frac{1}{2}}$
843.772	20	118515	$s^2p^2\,{}^4S_{1\frac{1}{2}}°-sp^4\,{}^4P_{1\frac{1}{2}}$
840.029	15	119044	$s^2p^2\,{}^4S_{1\frac{1}{2}}°-sp^4\,{}^4P_{\frac{1}{2}}$
*801.913	5	124702	$s^2p^2\,{}^2D_{2\frac{1}{2}}°-sp^4\,{}^2D_{1\frac{1}{2}}$
*801.409	10	124780	$s^2p^2\,{}^2D_{2\frac{1}{2}}°-sp^4\,{}^2D_{2\frac{1}{2}}$
*801.086	10	124831	$s^2p^2\,{}^2D_{1\frac{1}{2}}°-sp^4\,{}^2D_{1\frac{1}{2}}$
*800.573	5	124911	$s^2p^2\,{}^2D_{1\frac{1}{2}}°-sp^4\,{}^2D_{2\frac{1}{2}}$
*761.470	5	131325	$s^2p^2\,{}^2P_{1\frac{1}{2}}°-sp^4\,{}^2P_{1\frac{1}{2}}$
*760.439	3	131503	$s^2p^2\,{}^2P_{\frac{1}{2}}°-sp^4\,{}^2P_{1\frac{1}{2}}$
*755.212	3	132415	$s^2p^2\,{}^2P_{1\frac{1}{2}}°-sp^4\,{}^2P_{\frac{1}{2}}$
*754.205	4	132590	$s^2p^2\,{}^2P_{\frac{1}{2}}°-sp^4\,{}^2P_{\frac{1}{2}}$
*700.277	8	142801	$s^2p^2\,{}^2P_{1\frac{1}{2}}°-sp^4\,{}^2S_{\frac{1}{2}}$
*699.408	6	142978	$s^2p^2\,{}^2P_{\frac{1}{2}}°-sp^4\,{}^2S_{\frac{1}{2}}$
*689.007	12 bl	145136	$s^2p^2\,{}^2D_{2\frac{1}{2}}°-sp^4\,{}^2P_{1\frac{1}{2}}$
*688.392	7	145266	$s^2p^2\,{}^2D_{1\frac{1}{2}}°-sp^4\,{}^2P_{1\frac{1}{2}}$
*683.278	10	146353	$s^2p^2\,{}^2D_{1\frac{1}{2}}°-sp^4\,{}^2P_{\frac{1}{2}}$
*399.634	3	250228	$s^2p^2\,{}^4S_{1\frac{1}{2}}°-(^3P)4s\,{}^4P_{\frac{1}{2}}$
*398.546	4	250912	$s^2p^2\,{}^4S_{1\frac{1}{2}}°-(^3P)4s\,{}^4P_{1\frac{1}{2}}$
*396.869	4	251972	$s^2p^2\,{}^4S_{1\frac{1}{2}}°-(^3P)4s\,{}^4P_{2\frac{1}{2}}$

TABLE VII. *A IV term values.*

$(3s)^2\,(3p)^3\,{}^4S_{1\frac{1}{2}}°$	0	$3s\,(3p)^4\,{}^2D_{1\frac{1}{2}}$	145921
		$^2D_{2\frac{1}{2}}$	146000
$(3s)^2\,(3p)^3\,{}^2D_{1\frac{1}{2}}°$	21090		
$^2D_{2\frac{1}{2}}°$	21219	$3s\,(3p)^4\,{}^2P_{1\frac{1}{2}}$	166356
		$^2P_{\frac{1}{2}}$	167444
$(3s)^2\,(3p)^3\,{}^2P_{\frac{1}{2}}°$	34854		
$^2P_{1\frac{1}{2}}°$	35035	$3s\,(3p)^4\,{}^2S_{\frac{1}{2}}$	177833
$3s\ (3p)^4\,{}^4P_{2\frac{1}{2}}$	117564	$(^3P)\,4s\ {}^4P_{\frac{1}{2}}$	250229
$^4P_{1\frac{1}{2}}$	118515	$^4P_{1\frac{1}{2}}$	250912
$^4P_{\frac{1}{2}}$	119044	$^4P_{2\frac{1}{2}}$	251972

A V

Two multiplets in this spectrum given in Table VIII have been identified among the fainter lines of high excitation. A number of these lines are unresolved or are blended with the ghosts of the strong oxygen group at λ834. The accuracy for the terms given in Table IX is therefore somewhat less than that for the other stages of ionization. Since this table gives the intervals within the ground $(3s)^2(3p)^2\,{}^3P$ state it is possible to predict the approximate interval between nebular "forbidden" lines due to A V. Bowen[21] has estimated the position where such a pair might be expected to be found, but observational data in the red and infrared are not yet extensive enough to test these predictions for

TABLE VIII. *A V classified lines.*

λ	INT.	ν	CLASSIFICATION
*836.13	2	119599	$s^2p^2\,{}^3P_2-sp^3\,{}^3D_1°$
*835.79	1	119647	$s^2p^2\,{}^3P_2-sp^3\,{}^3D_2°$
*834.88	4bl	119778	$s^2p^2\,{}^3P_2-sp^3\,{}^3D_3°$
*827.350	3	120868	$s^2p^2\,{}^3P_1-sp^3\,{}^3D_1°$
*827.052	5	120911	$s^2p^2\,{}^3P_1-sp^3\,{}^3D_2°$
*822.161	4	121631	$s^2p^2\,{}^3P_0-sp^3\,{}^3D_1°$
*715.65	3	139734	$s^2p^2\,{}^3P_2-sp^3\,{}^3P_2°$
*715.60	4	139743	$s^2p^2\,{}^3P_2-sp^3\,{}^3P_{1,0}°$
*709.197	5	141005	$s^2p^2\,{}^3P_1-sp^3\,{}^3P_{2,1,0}°$
*705.352	3	141773	$s^2p^2\,{}^3P_0-sp^3\,{}^3P_1°$

[22] P. Swings and B. Edlén, Comptes rendus **198**, 2071 (1934).

[23] J. C. Boyce, C. H. Payne-Gaposchkin and D. H. Menzel, Publ. Astron. Soc. Pacific **46**, 213 (1934).

[24] W. H. Wright, Publ. Lick Observatory **13**, 193 (1918).

TABLE IX. *A V term values.*

$(3s)^2\,(3p)^2\,{}^3P_0$	0	$3s\,(3p)^3\,{}^3D_1^\circ$	121630
${}^3P_1$	764	${}^3D_2^\circ$	121675
${}^3P_2$	2028	${}^3D_3^\circ$	121806
		$3s\,(3p)^3\,{}^3P_2^\circ$	141762
		${}^3P_{1,0}^\circ$	141771

A V or for A III.[25] As in the previous spectrum only a rough estimate of the ionization potential may be made, the result of which is 78 volts. An isoelectronic sequence makes possible the prediction of the location of the principal multiplet of A VI and it is definitely absent from these spectrograms.

The experimental part of this work and a portion of the technical assistance in measurement and reduction of the plates were made possible by a grant to Dr. K. T. Compton from the Carnegie Institution of Washington. The writer is much indebted to Professor I. S. Bowen for many helpful suggestions in the discussion of certain phases of this paper and for making available, in advance of publication, many of his own data concerning the various isoelectronic sequences.

[25] R. H. Stoy, Publ. Astron. Soc. Pacific **46**, 363 (1934).

Note added July 14, 1935: A recent publication by de Bruin[26] has just been received giving some extensions to his previous analysis of A III. The following terms are added: $(^2D)3d\,{}^3F^\circ$, $(^2D)3d\,{}^3D^\circ$, $(^2D)5s\,{}^3D^\circ$. Table V has been revised to include these results. The first of these new terms gives no observed combination with the ground term of the atom. The second new term was already here identified tentatively as such, upon the basis of a multiplet in the extreme ultraviolet. The combination found by de Bruin now fixes its value more accurately. The discovery of the $(^2D)3d\,{}^3F^\circ$ term by de Bruin may cast some doubt upon the tentative identification here given for its companion singlet term. De Bruin has discovered the $(^4S)4s\,{}^3S^\circ-(^2D)4p\,{}^3P$ combination and so connects the groups of triplet terms based on the (^4S) and (^2D) limits. The connections here given are believed to be more accurate and they give a better fit with the wavelengths obtained in this laboratory for this new multiplet. Using de Bruin's identification but taking values of the wavelengths from the plates here investigated, these lines have now been added to Table IV.

[26] T. L. de Bruin, *Pieter Zeeman Jubilee Volume* (Martinus Nijhoff, The Hague, 1935), p. 413.

SEPTEMBER 1, 1935 PHYSICAL REVIEW VOLUME 48

Collisions of Alpha-Particles in Hydrogen

E. POLLARD AND H. MARGENAU, *Sloane Physics Laboratory, Yale University*

(Received June 13, 1935)

Experiments on the projection of protons by alpha-particles from polonium are described. The variation of the yield of projected protons with alpha-particle velocity was determined and shows agreement with the Rutherford-Darwin law for low velocities, a smooth rise for higher velocities. No evidence of resonance effects was observed, although experiments were made with the aim of their detection. A discussion is given of the inhomogeneity of the alpha-particles from polonium sources and the limitation it imposes on the observable size of resonance effects.

THE first systematic investigation of the scattering of alpha-particles in hydrogen was undertaken by Chadwick and Bieler.[1] Aside from the angular distribution of the projected protons, they determined the yield of protons as a function of the speed of the incident alpha-particles and discovered the anomalous rise in the yield curve which is now regarded as the effect of the nuclear field. The minimum on the alpha-particle range scale, beyond which more profuse ejection of protons takes place, was determined by these investigations to occur at $R=2.0$ cm. For greater residual ranges of the alpha-particles

[1] Z. Chadwick and E. S. Bieler, Phil. Mag. **42**, 923 (1921).

they observe a fairly monotone increase in the proton yield. Later experiments[2] have essentially verified these findings.

On the other hand, Frank,[3] and Pose and Diebner,[4] have reported the existence of irregularities in the proton yield curves for higher alpha-particle velocities, and their data have been interpreted by Beck and Horsley[5] to supply evidence for resonance phenomena, the assumption being that, for particular velocities, the alpha-particles may pass through the proton barrier with greater ease. Pose and Diebner locate, in fact, two minima, one at about 1.3 cm and the other at about 2.3 cm alpha-particle range.

Recently[6] the present authors have found an irregularity in the scattering of alpha-particles in deuterium, due to the presumable existence of a semi-stable resonance level in the Li^6 nucleus. In that connection measurements were made on the yield of protons from hydrogen as well, but no minima were found aside from the one discovered by Chadwick and Bieler, which is to be accounted for by the finite height of the proton barrier, and not by resonance. In continuation of these experiments we have now looked more searchingly for evidence of resonance in hydrogen.

I. Experimental Arrangement and Results

The apparatus employed is the same as described in paper I, Fig. 1. The source, also, was the same, and consisted of polonium deposited on a silver disk. The target, B, was a thin layer of vaseline of stopping power less than one millimeter air equivalent spread over an aluminum foil, its shape was circular, and the exposed portion had a diameter of 0.8 cm. The distance from source to target, AB, was 4 cm, the distance from target to counter 3 cm. Thus the mean angular spread of the projected protons is seen to be about 10°, the extreme spread about 20°.

As long as the range of the protons is considerably greater than the distance between target and counter their angular spread introduces no error in the determination of their number. If, however, the range of the protons ejected forward is but slightly greater than this distance, the particles thrown forth at an angle will have smaller ranges and may not reach the counter. In our experiments with alpha-particles of ranges greater than 1.6 cm (Fig. 1 of this paper) the former condition was always realized, while with low energy alpha-particles (Fig. 2) the spread in angles required a slight correction which was considerably smaller, however, than the probable error of the counts.

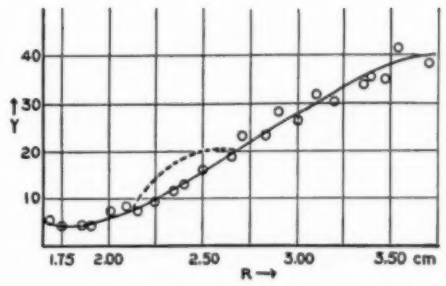

Fig. 1. Yield of protons *vs.* range (in cm air equivalent) of the incident alpha-particles. An irregularity of about half the amplitude of the dotted line could have been detected.

The experiment was performed in two parts. To obtain the number of protons projected by fast alpha-particles the vaseline was placed on the side of the aluminum foil B toward the source, and the stopping power of the foil was 2.2 cm. As previously, the range of the incident projectiles was varied by changing the (oxygen) pressure inside the source tube. In working with alpha-particles of small range the vaseline was spread on the face toward the counter of an aluminum foil of 1.8 cm stopping power. The absolute yields obtained in the two parts of the experiment are not equal because the vaseline targets, though of stopping power less than 1 mm in all cases, were not of equal thickness. The yield of protons from the disintegration of the aluminum was small compared to that from the vaseline.

All counts were recorded photographically, as described in I. The number of protons counted included the natural ones emitted by the source. In order to ascertain their number, observations were made at several pressures great enough to prevent the alpha-particles from reaching the

[2] E. A. W. Schmidt and G. Stetter, Zeits. f. Physik **55**, 467 (1929); C. Pawlowski, Ann. d. Physik [10] **16**, 150 (1931).
[3] E. Frank, Zeits. f. Physik **90**, 764 (1934).
[4] H. Pose and K. Diebner, Zeits. f. Physik **90**, 773 (1934).
[5] G. Beck and L. H. Horsley, Nature **135**, 431 (1935).
[6] E. Pollard and H. Margenau, Phys. Rev. **47**, 833 (1935), herein referred to as paper I.

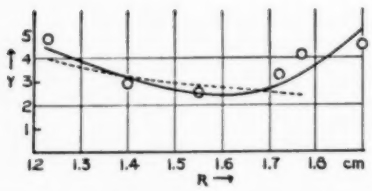

FIG. 2. Yield of protons *vs.* range (in cm air equivalent) of incident alpha-particles. Dotted curve represents the Rutherford-Darwin law.

target, and the number received by the counter at lower pressures was then deduced by extrapolation. In the experiments dealing with fast alpha-particles (cf. above) the number of naturals was a small fraction of the total number counted, while in the work with slow alpha-particles they constituted as much as half the total number.

The yield of projected protons per minute is plotted against range of the incident alpha-particles in Figs. 1 and 2. For the reasons just stated Fig. 1 is more accurate than Fig. 2. The dotted hump in Fig. 1 represents no experimental findings and will be explained in § III. For some of the points in Fig. 1 more than 1000 particles were counted. Although this figure exhibits a fairly uniform rise beyond the minimum at about 1.7 cm range, there were in some runs indications of a flattening at the maximum ranges attainable in this experiment. But we do not consider this as definitely established. The points plotted in Fig. 2 involve, beside the subtraction of the natural protons, a correction which will be discussed in the next section. The minimum is again clearly present, and the drop from 1.2 cm to 1.6 cm is in accord with the Rutherford-Darwin law (dotted curve) which expresses the scattering in a Coulomb field.

II. Range Spread of the Alpha-Particles from the Source

It is generally recognized that the detection of resonance effects and critical nuclear levels necessitates using small solid angles both for incident and counted particle. The reason for this is the spread caused by oblique passage through target and absorbing foils. It is also important, though this matter is not always fully discussed, to ensure that the particles from the source are homogeneous in velocity as far as possible and that if this cannot be secured, the essential limitation of the source must be recognized. Experience in the preparation and use of large polonium sources has shown that, when there is a definite blackening of the surface, inhomogeneity is to be expected and that strong sources deposited on small areas of silver, while helpful in securing small solid angles, develop an oxidized surface as time passes. The source used in the experiments on deuterium was tested for homogeneity and initially had a spread confined to three millimeters of range. For these later experiments it was found that a much greater spread was present. The curve showing the relation between numbers and range is shown in Fig. 3 and the differential curve derived from it is also given: it will be seen that a spread of over six millimeters was present. It is important to consider the effects of inhomogeneity as great as this on the results of the experiment. Firstly, the numbers counted at low energies need correction since the shorter range components will produce recoil protons which fall short of the counter. This correction was pointed out by Chadwick and Bieler and can be made directly from the distribution curve in Fig. 3. Secondly, it may render difficult or impossible the discovery of maxima and minima in the yield curve due to resonance. In the section which follows a quantitative treatment of this question is given.

III. The Effect of Alpha-Particle Straggling on the Detectability of Resonance Effects

If the alpha-particles impinging on the target were of perfectly homogeneous velocity the distribution curve (Fig. 3) would be a δ-function, and the yield curve would represent the true distribution in range of the projected protons.

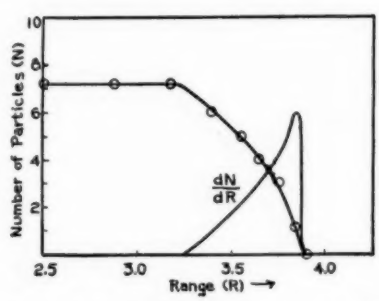

FIG. 3. Graphs of number (N) of alpha-particles of range R *vs.* R; and dN/dR *vs.* R.

The latter will be distorted, however, as a consequence of the real spread in the alpha-particle velocities. A maximum or a minimum in the true yield curve will in general suffer both a shift on the range scale and a reduction in amplitude. The first of these effects produces an error in the estimated position of the extremum, the second may render it undetectable.

To discuss these effects in a quantitative way let us assume a simple but fairly typical form for the resonance yield, and take it to be a drop and a rise given by

$$Y = A \cos x. \tag{1}$$

For the straggling function we will take a right triangle of base a, normalized to 1;

$$w(x) = (2/a^2)x \quad \text{if} \quad 0 < x \leqq a, \quad \text{otherwise } 0. \tag{2}$$

The distorted yield curve is then given by

$$U(R) = \int_{-\infty}^{\infty} w(x-R)\, Y(x)dx,$$

which, after substitution of (1) and (2), and integration, becomes

$$U(R) = (2A/a^2)[\cos (R+a) - \cos R + a \sin (R+a)]. \tag{3}$$

The maximum of U occurs at a value R' given by

$$\tan \rho = (a - \sin a)/(1 - \cos a), \tag{4}$$

where $\rho = R' + a$. For small values of ρ this equation is satisfied by $\rho = \frac{1}{3}a$, so that $R' = -\frac{2}{3}a$; this value is very nearly correct until a, the base of the straggling function, becomes greater than π, the base of the resonance hump. It is thus seen that the curve $U(R)$ has its maximum when the "center of mass" of $w(x)$ coincides with the maximum of γ. Hence, in locating the true maximum of the yield curve on the range scale, one must reckon the alpha-particle ranges not from the extreme range limit (3.89 cm for Po) but from the mean range of the distribution curve. In our experiment this correction amounted to 2 mm.

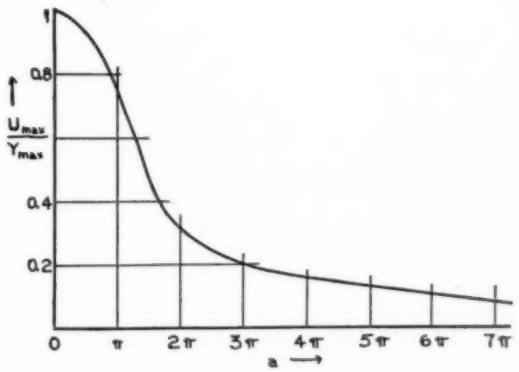

FIG. 4. Height of resonance maximum as function of the inhomogeneity of the source.

While the deductions above are fairly obvious and can be obtained without analysis, we have to make use of (3) and (4) to find the extent to which the resonance hump is reduced in magnitude. It is seen that

$$U_{\max.}/Y_{\max.} = (2/a^2)[(a - \sin a)^2 + (1 - \cos a)^2]^{\frac{1}{2}}.$$

Fig. 4 is a graph of this function. It shows that, if a is smaller than half the resonance region, 2π, the reduction is less than 75 percent, if it becomes greater, opportunity for detecting resonance decreases rapidly.

It is important, in the present experiments, to state how large a hump would have escaped detection. Let us assume its true width to be about 6 mm (cf. reference 4, Fig. 3). It would then have been observed if its maximum, after distortion, were greater than the spread of the points on our curves. On this basis we find that a hump the size of the dotted one in Fig. 1 could not have failed to be measured. But the anomaly to be expected, both from analogy with the deuterium case and from theory, is larger than this.

In conclusion we state that we have been unable to detect "resonance" effects in the collision of alpha-particles with protons.

We wish to express our thanks to Dr. L. R. Hafstad for preparation of the source and Dr. Burnam and Dr. West for supplying the radon tubes from which it was made.

Relative Intensities in the Principal Doublet of Thallium Under Arc and Fluorescence Excitation

L. N. MORSCHER, JR., *Ryerson Physical Laboratory, University of Chicago*

(Received May 23, 1935)

In harmony with theory, the components of the thallium resonance doublet ($6^2P_{1/2,\ 3/2}-7^2S_{1/2}$) were found to have approximately the same relative intensities under arc and fluorescence excitations. The average value found for the ratio is 0.92, the violet line being the stronger.

INTRODUCTION

EINSTEIN'S quantum analysis[1] of the radiation from excited atoms has been very generally accepted as valid. Since its formulation it has been a part of quantum theory, sometimes being viewed as an assumption, sometimes as derived.[2] A laboratory experiment which focuses sharply on this particular analysis seems hard to find and its experimental proof is not clearly distinguishable from the verification of a large body of quantum theory.

A direct consequence of Einstein's theory which seems adapted to a ready experimental proof is the well-known one that the relative intensities of lines with the same initial state should be independent of the conditions of excitation whenever forced transitions can be neglected. This rests directly on his assumption that the intensity due to spontaneous transitions is equal to the product of the number of atoms in the upper state (population) multiplied by a transition probability depending only on the states involved. Recently this consequence of the theory has been challenged on the basis of experimental evidence, notably by Christensen and Rollefson[3] and by Berry and Rollefson.[4] They conclude by indirect measurements that for excitation by fluorescence, the intensity ratio of the $2S-3P$ and $1S-3P$ unresolved sodium lines is about 2 : 1. This they compare with the value 25 : 1 found by Weiss[5] in a direct measurement of this ratio in a low voltage arc. In a theoretical paper, however, Prokofjew[6] estimates this ratio to be 2.1 : 1 and shows that Weiss' value of 25 : 1 clashes with the Thomas-Kuhn sum rules. Hence it seems quite possible that the disagreement with Einstein's assumption is due to an error in Weiss' measurements. The purpose of the present paper is to present the results of a more direct experimental test which is free from possible effects of fine structure.[7]

Pairs of spectral lines with a common upper state which are not too far apart nor too close together and which can be conveniently used in fluorescence work are difficult to find. A suitable pair is the principal doublet of thallium, which has been chosen for the experiments reported here. The relative intensities of the components have been directly measured for excitation by radiation (fluorescence) and by arc. However, even in this case we do not have a situation in which Einstein's assumption can be completely isolated from other assumptions of quantum theory. Self-absorption and forced transitions as well as splitting due to hyperfine structure and stray fields give rise to the chief departures from the idealized case. The influence of absorption is allowed for, that of forced transitions neglected as small. The effect of the multiplicity of states is treated theoretically in the next paragraph.

[1] A. Einstein, Verh. d. Deutsch. physik. Ges. **18**, 318 (1916); Physik. Zeits. **18**, 1921 (1917).

[2] An early formulation of Schrödinger which held the unusual position of running counter to this general scheme, was refuted by Gaviola, Nature **122**, 772 (1928). The scheme was first derived by P. A. M. Dirac, Proc. Roy. Soc. **A114**, 243 (1927). In earlier theories it was wholly or partly assumed.

[3] C. J. Christensen and G. K. Rollefson, Phys. Rev. **34**, 1157 (1929).

[4] N. E. Berry and G. K. Rollefson, Phys. Rev. **38**, 1599 (1931).

[5] C. Weiss, Ann. d. Physik **1**, 565 (1929).

[6] W. K. Prokofjew, Zeits. f. Physik **58**, 255 (1929).

[7] The writer is indebted to Professor Mulliken for calling his attention to papers by J. Kaplan which claim that there are intensity anomalies in band spectra indicating variably transition coefficients. See J. Kaplan, Phys. Rev. **36**, 778 (1930); **37**, 1406 (1931); **38**, 373 (1931); **38**, 582 (1931); **38**, 1079 (1931); **39**, 180 (1932); **41**, 114 (1932); **42**, 86 (1932). H. Schüler and J. E. Keyston, Zeits. f. Physik **71**, 413 (1931) report hyperfine structure intensity anomalies which challenge Einstein's theory.

On the basis of a quantum mechanical vector model of the atom, one may derive the usual sum rules for dipole transition probabilities.[8] In case of the principal thallium doublet, the hyperfine structure intervals are small compared with the fine structure intervals and we may expect the sum rules to hold rather well for those components of each line due to hyperfine structure and to stray field splittings. Consequently the probability of a transition from any particular component of $7^2S_{1/2}$ to the $6^2P_{1/2}$ levels should be the same as for any other component, likewise for the $7^2S_{1/2}$ to $6^2P_{3/2}$ transitions. Hence the relative doublet intensities should be practically independent of the way in which the population is partitioned among the $7^2S_{1/2}$ levels, and therefore independent of the type of excitation.[9] It ought to be clear that the results of the present experiment do not test just Einstein's scheme but rather a larger body of assumptions including that scheme.

Experimental Procedure and Results

The exciting source used in the fluorescence work consisted of a helium arc containing pieces of thallium in a Lavite constriction. Allowance for absorption in the thallium vapor was made on the assumption that the same absorption coefficient was good for all parts of a line.[10] The arc source, following Vonwiller,[11] consisted of an upper copper cathode and a lower lead-thallium anode.

Intensity measurements were made photographically[12] using a tungsten filament as the standard source. In the case of the three-hour exposures used in the fluorescence study, weakening was accomplished by the use of rocking screens[13] and a photographic step weakener; in putting the comparison strips on two minute exposure arc plates, both step weakener and varying slit methods were used, yielding substantially the same results. A glass filter was employed to render the blackenings of the two lines approximately equal. (A potassium ferrocyanide filter as used by Vonwiller[11] was tried but found to decompose.)

Measurements of five plates taken in the arc study gave 0.99, 0.86, 0.89, 0.96, 0.91 averaging 0.92 for the $P_{3/2}-S_{1/2}$ to $P_{1/2}-S_{1/2}$ intensity ratio. Three plates taken in the fluorescence work gave 0.98, 0.95, 0.84, averaging 0.92.

In appraising the above data it should be remembered that the determinations of this ratio in the arc and fluorescence cases were based upon the same calibrations and measuring methods and hence have a comparative significance apart from their absolute value. The intensity ratio of 0.92 diverges considerably from Vonwiller's arc value of 0.64.[11] The present experiment indicates, in conformity with theory, that arc and fluorescence excitation lead to approximately the same intensity ratio for the principal thallium doublet.

The writer wishes to thank Professor F. C. Hoyt for suggesting this problem and to thank him and Professor G. S. Monk for directing the research. The author is also indebted to Dr. F. P. Zscheile of the chemistry department, to Dr. A. E. Shaw of the physics department and to Mr. I. Kalberg.

[8] P. Güttinger and W. Pauli, Zeits. f. Physik **67**, 743 (1931); H. C. Brinkman, *Zur Quantenmechanik der Multipolestrahlung*, P. Noordhoff N.V. (1932).

[9] Since the above argument is applicable to each of the almost identical isotopes of thallium, the presence of several atomic species should not invalidate the conclusions.

[10] For details of procedure see reference 3. For criticism of method see reference 4.

[11] O. U. Vonwiller, Phys. Rev. **35**, 802 (1930).

[12] G. R. Harrison, J. Opt. Soc. Am. and Rev. Sci. Inst. **19**, 267 (1929).

[13] G. R. Harrison, J. Opt Soc. Am. and Rev. Sci. Inst. **18**, 492 (1929).

Total Scattering of Electrons in Helium

A. L. HUGHES* AND W. HARRIS, *Wayman Crow Laboratory of Physics, Washington University, St. Louis, Missouri*

(Received June 6, 1935)

The total electron scattering—defined as the sum of the elastically scattered electrons and all the inelastically scattered electrons—in helium has been measured for electron energies between 1000 and 200 volts. The results are compared with the theoretical values given by Morse's formula. According to the formula, the scattering in helium should be given by $(1/\mu^4)[Z^2(1-F)^2+Z(1-F^2)]$, where Z is the atomic number (here = 2), F the atom form factor, and $\mu = \sin(\theta/2)/\lambda$ in which θ is the angle of scattering and λ the wavelength of the associated electron waves. Theory and experiment agree well at 1000 and 700 volts. At 500 volts, there is a slight discrepancy which increases as we go down to 200 volts.

THE inelastic scattering of electrons by gas atoms has received much less attention than the elastic scattering. This is no doubt due to the fact that the inelastic scattering is more difficult to investigate experimentally and theoretically than the elastic scattering. Whereas in the latter one has to study only the angular distribution of those electrons which have lost no energy, a complete picture of the inelastic scattering calls for measurements of all the angular distributions of electrons which have lost all possible amounts of energy corresponding to various types of excitation or ionization of the atom. Morse[1] has shown, however, how to calculate the angular distribution of *all* scattered electrons regardless of how much energy they retain after collision. The angular distribution so defined may be conveniently termed the "total scattering coefficient." His formula—in the form applicable to hydrogen and helium—gives the total scattering coefficient $\alpha_t(\mu)$, which is the sum of the elastic scattering coefficient $\alpha_e(\mu)$ and the inelastic scattering coefficient $\alpha_i(\mu)$ (integrated over all possible energy losses) as a function of Z, the atomic number of the scattering atom, $F(\mu)$ its atom form factor[2] and a parameter μ which is equal to $\sin(\theta/2)/\lambda$ or $mv\sin(\theta/2)/h$. Here θ is the angle through which the electron is scattered, m and v are the mass and velocity of the impacting electron, and λ is the wavelength of the associated electron wave. Morse's formula for the total scattering is

$$\alpha_t(\mu) = (m^2e^4/4h^4)\{Z^2(1-F)^2+Z(1-F^2)\}\mu^{-4} \quad (1)$$

in which $\alpha_t(\mu)$ is the sum of the elastic scattering, $\alpha_e(\mu) = (m^2e^4/4h^4)Z^2(1-F)^2\mu^{-4}$, and the inelastic scattering $\alpha_i(\mu) = (m^2e^4/4h^4)Z(1-F^2)\mu^{-4}$.

METHOD

The apparatus consists essentially of two parts, a collision chamber and an analyzing chamber. As the collision chamber is substantially the same as that described in a previous paper[3] it is sufficient to say that it is a cylindrical brass vessel in which a beam of electrons from an electron gun can be rotated at will so that electrons scattered at any desired angle into the analyzing chamber can be investigated. The analyzing chamber contains several slits so arranged that, by applying a retarding voltage between a pair of them, only those electrons having energies greater than a value corresponding to this voltage can pass on to the collecting cylinder. This retarding voltage method has been used by several investigators of electron scattering[4] and so will not be described in detail. Four slits S_1, S_2, S_3 and S_4 separated by distances of 15 mm, 3 mm and 5 mm, respectively, were used in the analyzer. The first two, each 0.5×4.0 mm, defined the beam of scattered electrons passing from the collision chamber into the analyzer. Between S_2 and S_3 (S_3, 1.5×6.0 mm) a field of 45 volts was applied to turn back positive ions coming into the analyzer from the collision center. The retarding field to turn back the slower electrons, while allowing the faster

* The senior author was aided in part by a grant from the Rockefeller Foundation to Washington University for research in science.

[1] P. M. Morse, Physik. Zeits. **33**, 443 (1932); Rev. Mod. Phys. **4**, 610 (1932).

[2] The atom form factor used here is $1/Z$ times the value given in James and Brindley's tables (Phil. Mag. **12**, 81 (1931)).

[3] A. L. Hughes and J. H. McMillen, Phys. Rev. **39**, 585 (1932).

[4] F. L. Arnot, Proc. Roy. Soc. **A130**, 657 (1931); **A140**, 335 (1933); E. C. Bullard and H. S. W. Massey, Proc. Roy. Soc. **A133**, 637 (1931); J. T. Tate and R. R. Palmer, Phys. Rev. **40**, 731 (1932); E. B. Jordan and R. B. Brode, Phys. Rev. **43**, 112 (1933).

ones to pass into the collecting cylinder beyond S_4 (2×6 mm), was applied between S_2 and S_4. Helium was allowed to leak into the collision chamber through a fine capillary while the pumps were operating, thus securing a constant pressure between 0.01 and 0.02 mm of mercury. The gas was purified by passing it through outgassed charcoal which was contained in traps immersed in liquid air. The earth's magnetic field was neutralized by means of a current through a pair of Helmholtz coils.

The working of the analyzer was tested by directing a beam of 500-volt electrons from the electron gun down the axis of the analyzer, there being no gas in the apparatus, and measuring the current to the collector as a function of the retarding voltage. For all values of the retarding voltage between zero and 498 volts, the current was the same to within less than one percent; at a small fraction of a volt above 498 volts, it fell abruptly to zero. A second test was made by studying the angular distribution of elastically scattered 700-volt electrons. This was done by adjusting the retarding voltage so that only those electrons retaining the full 700 volts energy were permitted to enter the collector. The angular distribution so obtained agreed accurately with that found by Hughes, McMillen and Webb[5] with a totally different type of analyzer. We may, therefore, infer that the results obtained in the present investigation are free from error peculiar to the particular analyzer used.

Experimental Results

When an atom is ionized by an electron, two electrons leave the atom, the original electron and an ejected electron. It is usual to regard the slower of the two as the ejected electron. In the calculation of $\alpha_t(\mu)$ as given in Eq. (1), the original electrons only are counted; the ejected electrons are not considered. Hence, to get $\alpha_t(\mu)$ experimentally, it is necessary to set the retarding voltage in the analyzer at such a value as to prevent the ejected electrons from reaching the collector. Since the ejected electron and the original electron share the energy left over after ionization of the atom, the retarding voltage should have a value $(1/2)(V-V_0)$, where V is the original energy of the impacting electron and V_0 the energy necessary for ionization. When moderately high energy electrons are used ($V>200$ volts) it is sufficient to set the retarding voltage at $(1/2)V$. Additional justification is afforded by the fact that the current retarding voltage curves are at their flattest in the neighborhood of $(1/2)V$.

The experimental values of $\alpha_t(V,\theta)$, which we now use in preference to $\alpha_t(\mu)$ since the actual variables in a measurement are the energy V and the angle θ, were obtained as follows: A voltage V was applied between the filament and the body of the electron gun to give electrons the desired energy. Then readings of the electron current scattered into the analyzer were taken at a number of angles between about 5° and 150°. To obtain the scattering coefficient $\alpha_t(V,\theta)$, these readings were, as usual, multiplied by $\sin\theta$ to correct for the change in scattering volume with angle. In most of the measurements, V was held constant at one or the other of several selected values and $\alpha_t(V,\theta)$ measured as a function of θ. A few measurements were carried out with θ set at some selected angle (12°, 22°, 32°, or 42°) and $\alpha_t(V,\theta)$ measured as a function of V. It was thus possible to construct Table I, in which the values are in terms of the same unit regardless of the column in which they are listed. In view of the fact that a very slight error in setting the gun at small angles will make a big difference in the scattered electron current, we do not have much confidence in the values at 4°, a view which is perhaps justified by their lack of consistency.

The results are plotted in Figs. 1*a*–1*e*. The ex-

Table I. *Experimental values of* $\alpha_t(V,\theta)$.

θ \ V	200 volts	300 volts	500 volts	700 volts	1000 volts
4°	(2490)	(4210)	(2840)	(4570)	
8.5°	1402	1362	1022	1083	705
12°	994	734	550	571	303
22°	340	215	134.7	110.1	79.5
32°	141.0	91.2	47.2	32.0	18.25
42°	63.9	42.3	19.4	13.9	7.21
52°	41.2	22.5	10.73	6.98	3.64
62°	25.4	15.6	6.65	4.03	1.92
72°	18.15	10.2	4.22	2.33	1.43
82°	13.28	6.99	2.84	1.62	.905
92°	10.60	5.66	2.17	1.11	.641
102°	8.86	4.68	1.67	.80	.501
112°	7.40	3.80	1.41	.74	.406
122°	6.59	3.16	1.156	.64	.301
132°	5.70	2.94	.871	.60	.286
152°	4.68	2.56	.856	.55	.304

[5] A. L. Hughes, J. H. McMillen and G. M. Webb, Phys. Rev. **41**, 154 (1932).

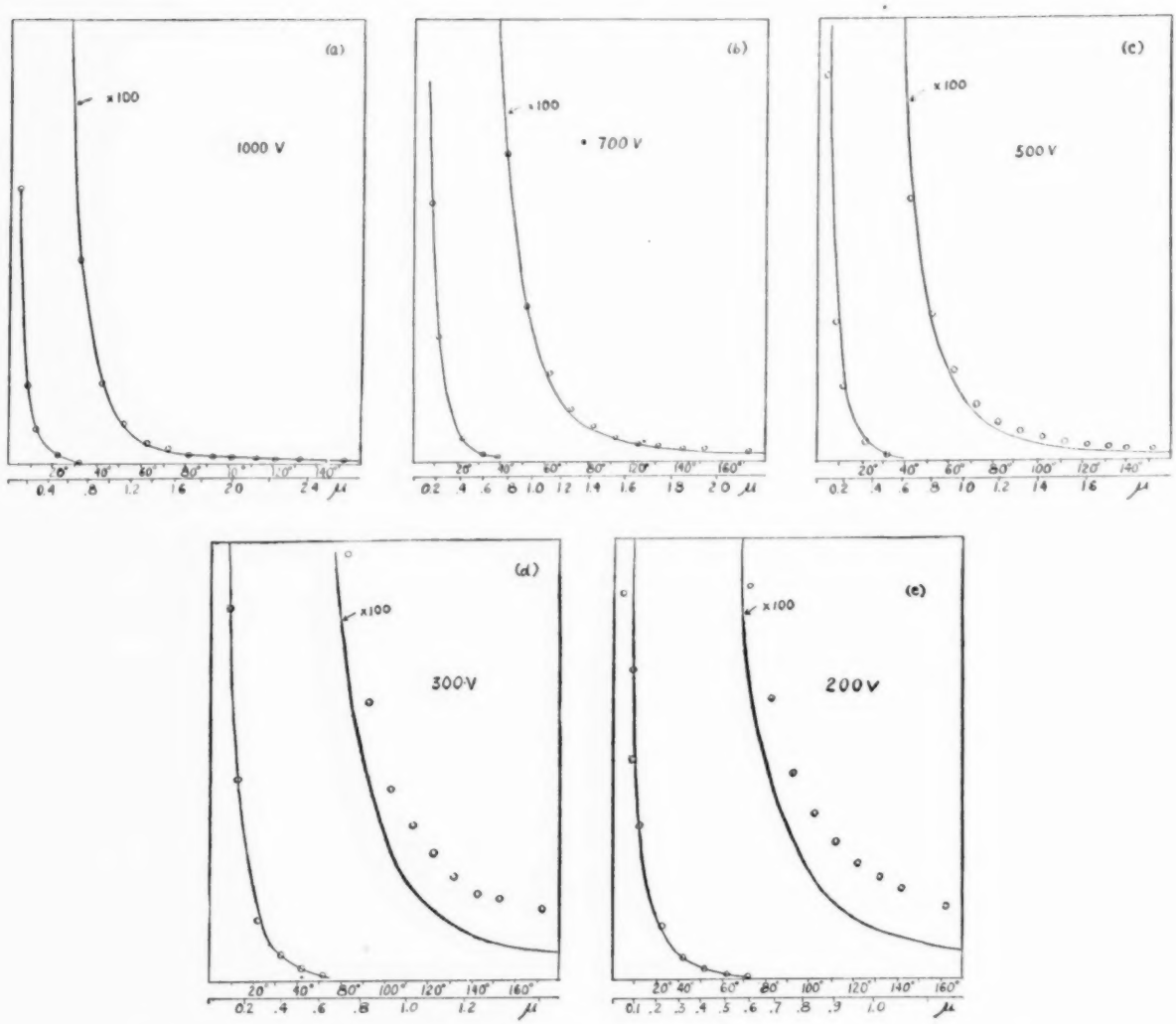

FIGS. 1*a*—1*e*. Total scattering for electrons of various energies; *full lines*, theoretical curves; *circles*, experimental points.

perimental curves are adjusted so that they all coincide with the corresponding theoretical curves at some selected angle between 22° and 30°. This way of plotting was chosen because it gives a very direct comparison between the *shapes* of the theoretical and experimental curves. It does not, however, reveal the gradually increasing disparity between the actual *magnitudes* of the experimental and theoretical values if we fit them together at 1000 volts, and then go down to lower energies. This feature is clearly shown in Table II. Here we have tabulated the ratios of the experimental values of $\alpha_l(V,\theta)$, as given in Table I, to the theoretical values given by Morse's expression. It will be noticed that while certain trends are clearly obvious, a considerable degree of irregularity is superposed on these trends.

TABLE II. *Ratio* $\dfrac{\alpha_l(V,\theta)\ experimental}{\alpha_l(V,\theta)\ theoretical}$.

θ	200 volts	300 volts	500 volts	700 volts	1000 volts
8.5°		0.61	0.81	0.99	0.91
12°	0.55	.51	.70	.95	.82
22°	.55	.61	.67	1.02	1.02
32°	.51	.65	.73	.89	.91
42°	.53	.65	.68	.96	.99
52°	.65	.65	.84	1.03	1.06
62°	.67	.84	.95	1.09	1.07
72°	.75	.91	1.00	1.10	1.28
82°	.86	.96	1.08	1.15	1.14
92°	.95	1.09	1.14	1.02	1.20
102°	1.08	1.21	1.16	.92	*1.47*
112°	1.14	1.42	1.33	.97	*1.62*
122°	1.24	1.32	1.31	1.08	*1.50*
132°	1.27	1.42	1.16	*1.29*	*1.53*
152°	1.30	1.42	1.20	*1.89*	*1.68*

This method of comparing results with theory is, of course, far more drastic in revealing experimental error than the method of plotting experimental and theoretical values side by side as was done in Figs. 1*a*–1*e*. (The values in italics in Table II are less reliable than the rest, for they are derived from measurements of extremely small electron currents.)

Discussion

We draw the conclusion that Morse's expression for the total scattering coefficient of electrons in helium is in agreement with experiment when the electron energies are 700 and 1000 volts. A slight but definite discrepancy between experiment and theory is to be noticed for 500-volt electrons, and this increases progressively as we go down to 200-volt electrons.

The relative contributions, according to the formula, of the elastic and inelastic scattering to the total scattering are shown in Fig. 2 in which $\mu^4\alpha(\mu)$ is plotted against μ. It is clear that for μ less than 0.43 inelastic scattering predominates, while for μ greater than 0.43, elastic scattering predominates. We have indicated the μ values in Figs. 1*a*–1*e* so that one may infer which part of any curve is determined chiefly by the elastic scattering and which part by the inelastic scattering.

In the work of Hughes, McMillen and Webb[5] on the elastic scattering in helium, it was found that the Mott theory was adequate to describe the experimental results down to 500 volts, while here it is true to the same extent only as far down as 700 volts. This points to the conclusion that the approximations made in Morse's theory for the inelastic scattering do not hold down to as low electron energy values as those made in Mott's theory of the elastic scattering. There is no compelling reason why one should expect them to be equally good over the same range for they are not based on identical assumptions.

According to Table II there is a marked tendency for the ratio of the experimental to the theoretical values, to increase as one goes to large angles. This is of little significance for the lower voltages when the shapes of the experimental and theoretical curves do not agree at all, but it is noteworthy that the same tendency is to be observed at the two highest voltages. This may be explained in part perhaps by the fact that at large angles the scattering is chiefly elastic, and that the Born-Mott formula for elastic scattering, even for high speed electrons, is less accurate at large angles than for small and moderate angles. According to Mott and Massey[6] the theoretical formula gives values which are somewhat too small at large angles.

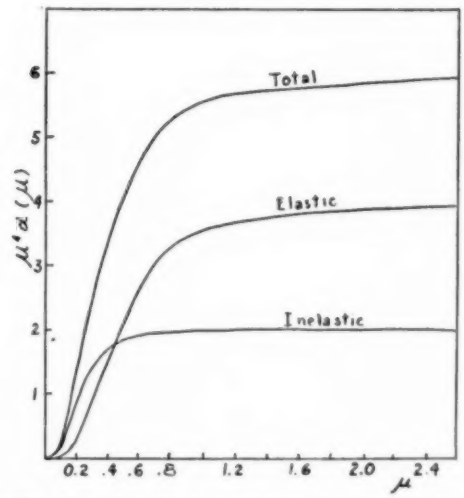

FIG. 2. Showing the relative contributions of the inelastic and elastic scattering to the total scattering.

Another, and more stringent, test of the formula would be to measure the ratio of the total inelastic scattering to the elastic scattering at different angles and for various voltages, and to examine whether or not it agreed with the theoretical value, *viz.*, $(1/Z)(1-F)/(1+F)$, derived from Eq. (1). A systematic investigation of the problem from this aspect has not yet been made, but a few random results show that under certain conditions, theory and experiment are in fair accord, but for large angles, there is considerable discrepancy. However, before drawing conclusions from such results, it will be necessary to examine more carefully whether or not there is any distortion in the retarding voltage curves, for widely different voltages.

[6] N. F. Mott and H. S. W. Massey, *The Theory of Atomic Collisions* (Oxford University Press, 1933), p. 130.

Velocity Distributions for Elastically Colliding Electrons

PHILIP M. MORSE, W. P. ALLIS AND E. S. LAMAR, *Massachusetts Institute of Technology*

(Received June 24, 1935)

The form of the function giving the distribution in velocity of electrons in a gas is determined by a pair of equations which correspond to the detailed balancing of energy and momentum, and take into account the variation of collision cross section with velocity. The kinetic energy ϵ of the electrons is supposed to be larger than that of the gas atoms, yet small enough so that the majority of the energy lost is by elastic collisions with the atoms. The equations are solved in detail for two cases. One case is that of electrons in a uniform electric field, where the distribution is independent of position. The distribution function is found to be proportional to $\exp(-\epsilon^2/a^2)$, instead of to $\exp(-\epsilon/a)$, as is the case for the Maxwell distribution, when the electrons are in temperature equilibrium with the gas atoms. The average energy of the electrons, the drift current, etc., are computed as a function of the field strength. The other case considered is that of a homogeneous beam of electrons of energy ϵ_0, shot into a field free space, where they lose energy to the gas atoms by collisions. The distribution function depends on z, the distance along the beam in mean free paths, and on t, the average number of collisions the electron has had before its energy decreases from ϵ_0 to ϵ. This distribution is also not Maxwellian, but depends on a solution of an equation in z and t having the form of the heat flow equation. The solution has been tested experimentally, and a quantitative check is obtained.

INTRODUCTION

IN all problems involving the motions of free electrons among the atoms of a gas, it has been customary to make one of two simplifying assumptions: either that the electrons lose no energy on collision with the atoms, so that at any point all the electrons have the same energy; or that the electronic velocities have a Maxwellian distribution whose density and temperature can vary from point to point in the gas. These two assumptions represent, in a sense, two opposite limiting conditions, and neither assumption is valid for intermediate cases.

The first assumption is only valid when the mean free path of the electrons is longer than the dimensions of the apparatus, for the electrons lose energy, even in an elastic collision, due to the recoil of the atom. This loss is small per collision, but unless the mean free path is very long, there will be enough impacts to give a noticeable "spread" to the energy distribution of the electrons.

The Maxwellian distribution, on the other hand, is only valid when the electrons are in temperature equilibrium with the gas, or when there is available some mechanism for transferring energy directly from electron to electron. These requirements are not fulfilled when there is an applied electric field, or when high energy electrons are shot into the gas from outside; unless, possibly, when the electron density is quite large. When the gas pressure is relatively large and the electronic density relatively low, one must expect a velocity distribution which is neither as "sharp" as the first assumption would demand, nor as "spread" as the second assumption would require.

It is possible to derive this intermediate distribution by balancing the electron's gain of energy, due to the applied field and to diffusion, with its loss, due to collisions with the gas atoms. In this paper only "elastically controlled" distributions will be studied, i.e. those cases where the average electronic energy is small enough so that, on the average, more energy is lost by elastic collisions than by inelastic ones. The method outlined below can be extended to cases where the inelastic collisions are more important, but the elastically controlled case is the simplest, and must be studied first.

ELASTIC COLLISIONS

The probability that an electron of velocity v will collide elastically with an atom and be scattered at an angle Θ to its primary direction is determined by the *angle scattering function* $\sigma(v, \Theta)$. The resultant probability of elastic collision for any direction of scattering can be expressed in terms of the *elastic collision cross section*

$$q(v) = 2\pi \int_0^\pi \sigma(v, \Theta) \sin \Theta d\Theta. \qquad (1)$$

If it is desired to find the loss of momentum of

the electron in the collision, the *momentum transfer cross section* is needed,[1]

$$Q(v)=2\pi\int_0^\pi\sigma(v,\Theta)(1-\cos\Theta)\sin\Theta d\Theta. \quad (2)$$

The two cross sections differ appreciably only if the angle scattering curve has a pronounced excess in the forward or backward direction. Both cross sections vary markedly with the electronic velocity, in most cases.

When an electron of mass m and energy $\epsilon=\frac{1}{2}mv^2$ collides elastically with an atom of mass M and is scattered at an angle Θ, it loses a certain fraction of its energy to the recoiling atom. We shall be interested in electrons whose energy although lower than the atomic excitation potentials is considerably higher than the thermal energy of the atoms, so that the atoms can be considered as being at rest. With this approximation, and neglecting the squares of the small quantity (m/M), the fraction of energy lost per collision is

$$(\Delta\epsilon/\epsilon)=(2\Delta v/v)=2(m/M)(1-\cos\Theta). \quad (3)$$

It can be seen that the expression for the average loss of energy per collision will involve the cross section Q.

Detailed Balancing

Let the number of electrons in the volume element $d\tau=dxdydz$, whose velocities fall in the range $d\gamma=d\xi d\eta d\zeta=v^2\sin\omega dvd\omega d\varphi$ be $f(x,y,z;\xi,\eta,\zeta)d\tau d\gamma$. This defines the *distribution function* f. For reasons of simplicity we shall usually discuss distributions which are homogeneous and isotropic in the yz plane so that f is a function only of x, v and ξ (or x, v and ω). It is possible to generalize the argument to three dimensional cases, however.

The distribution function f will be determined by a method similar to that given by Lorentz,[2] but extended to include the variation of the cross section with the velocity and the loss of energy at collisions. With Lorentz we assume that f can be expanded in a series of Legendre functions of $\cos\omega=(\xi/v)$,

$$\begin{aligned}f(x,v,\omega)&=f_0(x,v)+P_1(\cos\omega)f_1(x,v)\\&\quad+P_2(\cos\omega)f_2(x,v)+\cdots\\&=f_0(x,v)+(\xi/v)f_1(x,v)+\cdots. \quad (4)\end{aligned}$$

The function f_0 determines the random distribution in velocity, and f_1 determines the electron drift. The higher terms in the series are nearly always very small and do not correspond to any simple physical property of the distribution, but serve simply to improve the form of the distribution function. Consequently, we shall neglect all except the first two terms of series (4), and expect that the result will give very nearly correct values for the random and drift velocities, even though the function f thus calculated does, in some cases, actually become negative for certain values of the parameters.

The fundamental formula determining f is obtained by fixing the attention on an element $d\tau d\gamma$ of phase space. The number of electrons leaving this element due to the applied field E and to diffusion is

$$cd\tau d\gamma=\left(\frac{eE}{m}\frac{\partial f}{\partial\xi}+\xi\frac{\partial f}{\partial x}\right)d\tau d\gamma.$$

When the first two terms of series (4) are substituted in this expression, two terms in ξ^2 appear. Since we are neglecting spherical harmonics of order higher than the first, ξ^2 must be replaced by its average value $(v^2/3)$. To this approximation, then,

$$\begin{aligned}cd\tau d\gamma=\Big[&\frac{eE}{m}\cos\omega\frac{\partial f_0}{\partial v}+\frac{eE}{m}\frac{1}{3v^2}\frac{\partial(v^2f_1)}{\partial v}\\&+v\cos\omega\frac{\partial f_0}{\partial x}+\frac{v}{3}\frac{\partial f_1}{\partial x}\Big]d\tau d\gamma. \quad (5)\end{aligned}$$

The number leaving the element of phase space due to collisions is

$$ad\tau d\gamma=Nvf2\pi f\sigma\sin\Theta d\Theta d\tau d\gamma=Nqvfd\tau d\gamma, \quad (6)$$

where N is the number of gas atoms per cc.

So far, all is in accord with Lorentz; the difference comes in the discussion of the number scattered into the element $d\tau d\gamma$. These electrons had, before the collision, velocities in velocity element $d\gamma'$ (Fig. 1). Their initial velocity $v'=v+(mv/M)(1-\cos\Theta)$ is larger than the final

[1] Houston, Zeits. f. Physik **48**, 449 (1928).
[2] Lorentz, *Theory of Electrons* (Stechert), p. 267.

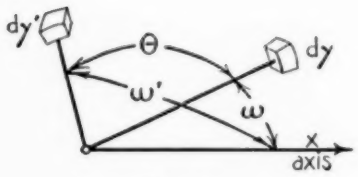

FIG. 1.

velocity as is seen from Eq. (3), and it can be shown from the same equation that the size of $d\gamma'$ is given by $d\gamma'=(v'/v)^3 d\gamma$. Hence, the total number of electrons scattered into the element $d\tau d\gamma$ per second is

$$bd\tau d\gamma = Nv\int_0^\pi 2\pi f(v', \omega')\sigma(v', \Theta) \times \sin\Theta d\Theta (v'/v)^4 d\tau d\gamma,$$

and hence the net number coming into the element $d\tau d\gamma$ by collisions is

$$(b-a)d\tau d\gamma = (2\pi N/v^3)\int_0^\pi [v'^4 f(v', \omega')\sigma(v', \Theta) - v^4 f(v, \omega)\sigma(v, \Theta)] \sin\Theta d\Theta d\tau d\gamma.$$

As v' differs little from v, the integrand may be written

$$v^4[f(v, \omega')-f(v, \omega)]\sigma(v) + \Delta v(\partial/\partial v)[v^4 f(v, \omega')]\sigma(v, \Theta).$$

The first term is that obtained by Lorentz, and gives on integration $-NQvf_1(v, \omega)\cos\omega$. The second term follows from the inclusion of the energy loss, and is small due to the factor (m/M) in Δv. Consequently, in it f can be replaced by f_0, and $(b-a)$ becomes finally

$$(b-a)d\tau d\gamma = \left[-NQvf_1\cos\omega + \frac{m}{M}\frac{N}{v^2}\frac{\partial}{\partial v}(v^4 Q f_0)\right] d\tau d\gamma. \quad (6a)$$

The condition for a steady state is now given by equating c to $(b-a)$. Equating separately the terms in $\cos\omega$ and those which do not contain $\cos\omega$ gives two equations:

$$eE\partial f_0/\partial v + mv\partial f_0/\partial x = -NQmvf_1, \quad (7)$$

$$\frac{eE}{2v}\frac{\partial}{\partial v}(v^2 f_1) + \tfrac{1}{2}mv^2\frac{\partial f_1}{\partial x} = \frac{m^2}{M}\frac{3N}{2v}\frac{\partial}{\partial v}(v^4 Q f_0). \quad (8)$$

The first of these equations is the one obtained by Lorentz, and represents the balance between the gain of momentum, due to diffusion and drift down the field, and the loss of momentum, due to collisions. The quantity $(1/NQ)$ is of course the electronic mean free path (for momentum transfer). The second equation represents the balance between the gain of energy, because of diffusion and drift down the field, and the loss of energy by collisions.

Since Lorentz had only Eq. (7), he had to assume the form of f_0 to be Maxwellian and then to find f_1 in terms of it. Pidduck[3] introduced an average balance of energy by determining the temperature of the Maxwell distribution in such a way that the total energy gained by drift and diffusion was equal to the total energy lost by collisions. As will be noted later, such a distribution predicts entirely too many fast electrons to agree with the experimental facts. The correct distribution must have less "spread" than the Maxwell distribution.

The addition of Eq. (8) secures a detailed balance of energy in each velocity range, and not merely a balance of the totals; and enables one to solve for both f_0 and f_1 without any further assumptions. In the present paper these two functions will be obtained for two special cases.

HOMOGENEOUS DISTRIBUTION

When f is independent of x, Eq. (8) integrates immediately to

$$eE\epsilon f_1 = 6(m/M)NQ\epsilon^2 f_0 - B \quad (9)$$

or, on multiplication by $(8\pi/3m^2)d\epsilon$,

$$\frac{8\pi eE}{3m^2}\epsilon f_1 d\epsilon - \frac{16\pi NQ}{m^2}\frac{m}{M}\epsilon^2 f_0 d\epsilon = -jd\epsilon, \quad (10)$$

where the constant B, or j, is a constant of integration. Eq. (10) gives the balance of energy, for the current carried by electrons having energies between ϵ and $\epsilon+d\epsilon$ (i.e., in the velocity element $d\gamma=(4\pi/m)vd\epsilon$) is $dJ=\overline{e\xi}fd\gamma=(ev/3)f_1 d\gamma$, and the energy taken from the field per sec. per cc is $EdJ=(8\pi eE/3m^2)\epsilon f_1 d\epsilon$. This is the first term of Eq. (10). The second term is the energy lost by collisions. If these energies are to balance, the constant B, or j, must be zero. On the other hand, if these energies do not balance and, say, the energy gained is less than that lost, then the

[3] Pidduck, Proc. Roy. Soc. **A88**, 296 (1913).

electrons are losing energy and j is a measure of that loss. In fact, j will be seen to be equal to the number of electrons per cc per sec. losing energy and passing through the energy value ϵ from higher energies to lower energies. Suppose electrons of high energy to be introduced into the system and allowed to lose energy by collisions, then j will equal the number of electrons so introduced per cc per sec. having energies higher than ϵ. If, on the other hand, high energy electrons are suffering inelastic impacts, and are thus being removed from the high energy range and replaced with a low energy, $(-j)$ will equal the number per cc per sec., originally having energies larger than ϵ, which are being stopped by an inelastic collision, and which must subsequently gain energy until they make another inelastic collision. This will be treated more fully in a later part of the paper.

At present, we will consider B, or j, to be zero. Substituting Eq. (9) into Eq. (7) when f is independent of x, and when Q is considered to be constant, one obtains

$$f_0 = Ae^{-h^4\epsilon^4} = A \exp\left[-\frac{3m}{M}\left(\frac{NQ\epsilon}{eE}\right)^2\right], \quad (11)$$

where $h^4 = (3m/M)(NQm/2eE)^2$ and the constant $A = [nh^3/\pi\Gamma(\frac{3}{4})]$. The number n is the density of electrons per cc.

The natural units of energy and velocity for this case are the energy $\epsilon_e = (eE/NQ)$ and velocity $v_e = (2eE/mNQ)^{\frac{1}{2}}$ gained by an electron in falling, from rest, down the field for a mean free path. In terms of these units the average kinetic energy and mean drift velocity of the electrons are

$$\bar{\epsilon} = \frac{\Gamma(5/4)}{\Gamma(3/4)}\left(\frac{M}{3m}\right)^{\frac{1}{2}}\epsilon_e = 0.4270\left(\frac{M}{m}\right)^{\frac{1}{2}}\epsilon_e, \quad (12)$$

$$u = \frac{\pi^{\frac{1}{2}}}{3\Gamma(3/4)}\left(\frac{3m}{M}\right)^{\frac{1}{2}}v_e = 0.6345\left(\frac{m}{M}\right)^{\frac{1}{2}}v_e. \quad (13)$$

It is seen that the mean energy increases as (M/m) increases, because the heavier the gas atoms are, the less energy can be lost per collision. On the other hand, the average drift velocity decreases as (M/m) increases. The average speed, $(2\bar{\epsilon}/m)^{\frac{1}{2}}$, bears to u the fixed ratio $1.03(M/m)^{\frac{1}{2}}$, which is as large as 63 even for hydrogen gas.

The relative size of f_1 and f_0 at the mean energy is obtained from Eq. (9), $f_1/f_0 = 2.56(m/M)^{\frac{1}{2}}$. Since this ratio is never larger than 0.07, it is seen that for the range of energy which is important, f_1 is only a small correction to the spherically symmetric term f_0. For electronic energies larger than the mean energy, f_1 becomes relatively more important, but the exponential in Eq. (11) renders the whole distribution function negligibly small before f_1 can be the same size as f_0.

It is of interest to compare the results of this distribution with those obtained by Pidduck.[3] If one neglects Eq. (8), sets $f_0 = Be^{-\epsilon/kT}$, and requires an average energy balance, it turns out that $kT = (M/3m)^{\frac{1}{2}}(\epsilon_e/2)$. The average kinetic energy is $0.4320\ (M/m)^{\frac{1}{2}}\epsilon_e$, only 1.014 times the average given in Eq. (12). The average drift velocity is $0.9900\ (m/M)^{\frac{1}{2}}v_e$, greater than the average given in Eq. (13) by a factor of 1.560. Hence average values are not much different for the two distributions. However, the number of fast electrons is markedly less for the new distribution, and quantities which depend only on fast electrons, such as rates of excitation and ionization, will be considerably less for the new than for the Maxwell distribution. This is in better accord with experiment, for the Maxwell distribution predicts several times more ionization than is measured by Townsend.[4] The difference between the two functions is shown in Fig. 2.

The distribution given in Eq. (11) is valid only if the momentum transfer cross section is nearly independent of velocity. If it cannot be assumed that Q is constant, then the distribution function must be written

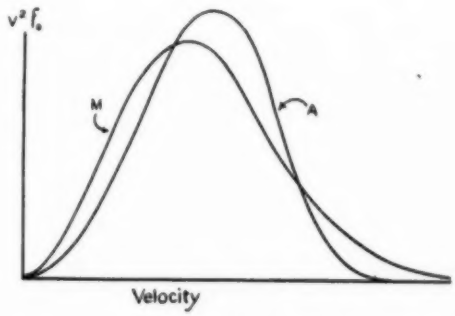

FIG. 2. Distribution in random velocity of electrons under the influence of an electric field (A), compared to a Maxwell distribution for the same average energy (M).

[4] Townsend, *Electricity in Gases*, p. 295.

$$f_0 = A \exp\left[-\left(\frac{6m}{M}\right)\int^{\epsilon}\left(\frac{NQ\epsilon}{eE}\right)d\epsilon\right],$$
$$f_1 = \frac{6m}{M}\frac{NQ}{eE}\epsilon f_0. \tag{14}$$

The general effect of a variable cross section is easily seen. The cross section Q can be considered as a scale factor for the variable ϵ, so that where the cross section is small the curve is flatter, where it is large the curve is steeper, than it otherwise would be. The change is small except when the cross section exhibits a Ramsauer effect, in which case the derived mobility, rate of ionization, etc., may be considerably affected.

Homogeneous Distribution without Field

The distribution discussed in the last section is maintained by the electric field E and will not hold if E falls low enough for the mean kinetic energy of the electrons to be comparable to that of the atoms. It is possible, however, to maintain a distribution without a supporting field by continuously introducing electrons of high energy ϵ_0, as, for instance, by ionizing the gas by x-rays. These electrons gradually lose energy by collisions and thus drift down the energy scale to end up in a large accumulation of electrons of low energy.

The stationary distribution must be such that the number of electrons falling in unit time below any energy level is equal to the rate j at which they are introduced. But the electrons crossing the energy level ϵ are just those in the range $\Delta v = vm/M$ above ϵ which have collisions. Thus, $j = NQvf \cdot 4\pi v^2(m/M)v$, or

$$f = f_0 = (M/m)(jm^2/16\pi NQ\epsilon^2). \tag{15}$$

This is, of course, the solution of Eq. (10) with E set equal to zero. The distribution is isotropic unless j varies with x. The distribution f goes to infinity as ϵ approaches zero, but Eq. (15) is no longer valid for electronic energies less than the temperature energy of the gas molecules.

Inhomogeneous Distribution

Imagine electrons of energy ϵ_0 to be liberated in a limited region of a gas, and to diffuse away from this region, at the same time losing energy due to collisions. The function giving the distribution both in space and in energy will be a solution of Eqs. (7) and (8) with $E=0$. When Q can be considered constant, it is convenient to introduce new variables, defined as follows:

$$z = NQx, \quad t = (M/2m)\ln(\epsilon_0/\epsilon),$$
$$R = 4\pi v^4 f = R_0 + \cos\omega R_1. \tag{16}$$

The variable z is the distance measured in mean free paths, and the relation $d\epsilon = -(2m/M)\epsilon dt = \overline{\Delta\epsilon} dt$ shows that in order to lose the energy $d\epsilon$ the electron must make, on the average, dt collisions. Hence, t measures the average number of collisions the electron has suffered since it started.

Making all these changes, Eqs. (7) and (8) reduce to

$$R_1 = -\partial R_0/\partial z, \quad 3\partial R_0/\partial t = \partial^2 R_0/\partial z^2. \tag{17}$$

By generalizing Eqs. (7) and (8), it can be shown that the three dimensional variation of R is governed by the equation

$$\nabla^2 R_0 = 3(\partial/\partial t)R_0, \tag{18}$$

where the unit of length is again a mean free path. In this case, the drift current due to electrons in the velocity range dv is the vector

$$\boldsymbol{dJ} = -(1/3v)\ \text{grad}\ (R_0)dv.$$

Eq. (18) or the second Eq. (17) is formally the same as the heat flow equation, R_0 corresponding to the temperature and t to the time; it shows that the electrons spread out in space as their energy decreases exactly as heat spreads out with time.

A solution of the one dimensional equation is the Green's function

$$R_0 = (M/2NQm)(3/\pi t)^{\frac{1}{2}} e^{-3z^2/4t},$$

which is here normalized to correspond to the introduction of one electron, with the energy ϵ_0, per second at the point $z=0$. The singularity in the solution at $t=0$ corresponds to the highest energy in the distribution, ϵ_0.

The problem to which we wish to apply this theory, and which has been studied experimentally, is the following: a beam of electrons is projected with kinetic energy ϵ_0 into a region free from electric fields, it is desired to find the

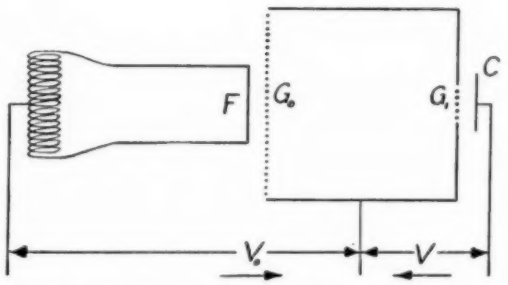

FIG. 3. Schematic diagram of apparatus.

distribution in velocity of the electrons at various points inside the region.

A schematic diagram of the experimental apparatus used is given in Fig. 3. Electrons from a filament F are accelerated by a potential V_0 to the entrance grid G_0 through which they enter into a field-free region surrounded by a metal cylinder. Samples of the distribution are taken through the exit grid G_1, L cm from G_0, by varying the retarding potential V to the collector C and by measuring the resulting collector current.

The electrons in any cc of the field-free region can be classified in two groups: those in the primary beam having the energy ϵ_0, and those, having suffered one or more collisions since their entrance into the region, which therefore have energies less than ϵ_0. Because of collisions with gas atoms, the primary current will decrease exponentially, its value at a distance x from the entrance grid being $I=I_0e^{-z}$, $z=NQx$. The steady state distribution of electrons of lower energy is maintained by the electrons scattered out of the primary beam, of which there are NQI per sec. per cc. According to the discussion above, this distribution is given in terms of a function R_0, a solution of the heat flow Eq. (18) which satisfies the boundary conditions at the surface of the region considered, and which satisfies the "initial condition" that at $t=0$ (i.e., at $\epsilon=\epsilon_0$) R_0 is equal to $(M/m)I$. The "initial value" of R_0 is obtained from Eq. (15) with j set equal to NQI.

The exit grid samples only the central part of the beam and if the diameter of the metal cylinder is greater than two or three mean free paths, so that we can neglect the boundaries at the sides, the problem may be treated as a one dimensional one. In this case the function R_0 is given in terms of the Green's function of Eq. (19).

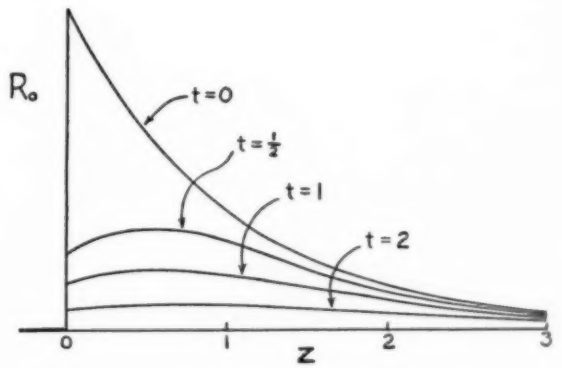

FIG. 4. Curves of $R_0=4\pi v^4 f_0$, for a beam of electrons entering a field-free space, as function of z the distance from entry in mean free paths, for different values of t the average number of collisions since entry.

$$R_0=(M/2m)I_0(3/\pi t)^{\frac{1}{2}}\int_0^{z_1}e^{-\lambda}e^{-3(z-\lambda)^2/4t}d\lambda$$

$$=I_0\frac{M}{2m}e^{-z+(t/3)}\left\{\Phi\left[\left(\frac{3}{t}\right)^{\frac{1}{2}}\left(\frac{t}{3}+\frac{z_1-z}{2}\right)\right]\right.$$

$$\left.-\Phi\left[\left(\frac{3}{t}\right)^{\frac{1}{2}}\left(\frac{t}{3}-\frac{z}{2}\right)\right]\right\}, \quad (19)$$

where $z_1=NQL$, and $\Phi(x)$ is the error integral $(4/\pi)^{\frac{1}{2}}\int_0^x e^{-u^2}du$. This function has been plotted for several values of t in Fig. 4 for the case $z_1=\infty$. It is seen that the curves smooth out after very few collisions, so that low velocity electrons predominate everywhere except within a mean free path of the entrance grid.

To find, from this expression, the current which will reach the collector through the exit grid, against a retarding potential V, requires some further assumptions. The random current is given by

$$2\pi\int_0^{r_0}v^2dv\int_0^{\pi/2}\xi f\sin\omega d\omega$$

$$=(m/2M)\int_0^\infty dt\int_0^{\pi/2}R\cos\omega\sin\omega d\omega.$$

However, the exit grid does not allow electrons to pass whose velocity makes a large angle ω with the axis of the tube, so that the integral over ω extends only up to a limiting angle ω_1. Since R_1 is small compared to R_0 everywhere except at the entrance grid, we can write for the random current passing the exit grid

$$(m/4M)\sin^2\omega_1\int_0^\infty R_0(z_1)dt.$$

The retarding potential does not allow all

electrons passing the grid to reach the collector, but only those whose normal velocity is great enough to overcome the retarding potential eV. The correct integration here would be difficult, but if the angle ω_1 is not large, no great error is made if we simply integrate over all energies ϵ greater than eV. The current to the collector is then

$$J_c = I + (m/4M)\sin^2\omega_1 \int_0^T R_0(z_1)dt$$

$$= I_0 e^{-z_1} + CI_0\left\{T^{\frac{1}{2}}(e^{-3z_1^2/4T} - e^{-z_1}) + \tfrac{1}{2}(3\pi)^{\frac{1}{2}}(1-z_1)\left[1-\Phi\left(\frac{z_1}{2}\left(\frac{3}{T}\right)^{\frac{1}{2}}\right)\right]\right.$$

$$\left. + \tfrac{1}{2}(3\pi)^{\frac{1}{2}} e^{-z_1+(T/3)}\left[\Phi\left(\left(\frac{T}{3}\right)^{\frac{1}{2}}\right) - \Phi\left(\left(\frac{T}{3}\right)^{\frac{1}{2}} - \frac{z_1}{2}\left(\frac{3}{T}\right)^{\frac{1}{2}}\right)\right]\right\},$$

where $C=(3/16\pi)^{\frac{1}{2}}\sin^2\omega_1$, and $T=(M/2m)\times\ln(V_0/V)$. Due to the factor $(M/2m)$, T becomes quite large as soon as the collector voltage V is made somewhat smaller than the accelerating voltage V_0, so that over most of the range of V the asymptotic form for J_c can be used:

$$J_c \rightarrow I_0 e^{-z_1} + I_0 A[\ln(V_0/V)]^{\frac{1}{2}}(1-e^{-z_1}). \quad (20)$$

The constant A is left in this expression to be determined by experiment. There are several factors whose effects cannot be exactly calculated, as the electron beam is not infinitely wide and the exact influence of the walls of the tube and of the grids is unknown. If these effects do not depend too markedly on the velocity, they should be taken care of by adjusting A.

An Experimental Check

The experimental tube was built to correspond to Fig. 3. It contained a nickel cylinder, a filament, and a plate collector. The cylinder was five cm long and five cm in diameter. The end of the cylinder nearest the filament was covered by the gauze grid G_0, and the other end with sheet nickel, except for a central circular window one cm in diameter, covered with nickel gauze, the grid G_1. The filament was ten-mil tungsten two cm long, situated five mm from the grid G_0. The plate C was a disk of sheet nickel and was five mm from the grid G_1. This was done to eliminate, as far as possible, collisions between electrons and gas atoms everywhere except in the field-free space between the grids.

The filament was heated by alternating current obtained from a low voltage transformer. Since the ends of the filament were cooled by conduction along the leads, only its central portion contributed to the emission current. An examination of the energy distribution of the electrons emitted by the filament showed a total spread which did not exceed one volt.

For a fixed accelerating voltage V_0 between filament and entrance grid, the current to the plate C was measured as a function of the retarding potential V between collector and exit grid. The first tests in high vacuum showed a wide-spread distribution in normal components of energy of the electrons reaching C. It was decided that this spread resulted from reflection of the electrons by the grids and from the walls of the cylinder. The tube was taken apart, therefore, and the cylinder, grids and collector were covered with amorphous carbon to reduce electron reflection. The energy distribution subsequently obtained in high vacuum was extremely flat over most of the range, and showed only a small residue of the previously observed effect.

After having made the run in high vacuum, runs were made with helium gas in the tube over a range of pressures such as to allow from one to ten mean free paths between the grids. Helium was chosen because its effective cross section varies least with velocity, and an accelerating potential of only 18.5 volts was used to insure that the number of inelastic collisions would be negligible.

The experimental results are shown as circles in Fig. 5. The solid curves are plots of Eq. (20). I_0 was taken as the value of the current when the tube was evacuated, and was 0.478 microampere, or 143 mm galvanometer deflection.

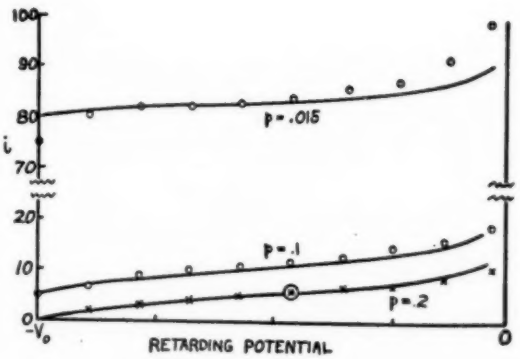

FIG. 5. Comparison of experimental results (circles and crosses) with calculated curves for the apparatus shown in Fig. 3, for different pressures of helium, in mm of mercury. Accelerating voltage V_0 is 18.5 v, and collector current i for vacuum is 143 mm galvanometer deflection. The single arbitrary constant is adjusted to make the curves fit the point indicated by the heavy circle.

The value of NQ, the number of collisions per cm path at 18.5 volts, is obtained from Normand's measurements of the cross section of helium.[5] It is 8 collisions per cm per mm gas pressure. Since the distance between grids, L, is 5 cm, the quantity z_1 is $40p$, where p is the gas pressure in mm of mercury. The only unknown parameter is A, and it was determined by fitting the single point indicated by the heavy circle in the figure. The agreement for all three curves is quite satisfactory.

FURTHER APPLICATIONS

The Green's function method can also be applied to the lateral diffusion from a narrow beam of electrons in a field-free space. For instance, the distribution function for a beam defined by a slit whose width is a mean free paths is given in terms of the function

$$R_0=\left(\frac{M}{4m}\right)I_0e^{-z+(t/3)}\left[1-\Phi\left(\frac{3}{t}\right)^{\frac{1}{2}}\left(\frac{t}{3}-\frac{z}{2}\right)\right]$$

$$\times\left[\Phi\left(\frac{a+2x}{4}\left(\frac{3}{t}\right)^{\frac{1}{2}}\right)+\Phi\left(\frac{a-2x}{4}\left(\frac{3}{t}\right)^{\frac{1}{2}}\right)\right], \quad (21)$$

where z is the distance, in mean free paths, along the beam, and x is the distance at right angles to the beam. Fig. 6 shows R_0 as a function of x for different values of z and of t. As the electrons have more than 0.997 of their initial energy when $t=3$, it is seen how rapidly the beam loses definition as the electrons lose energy.

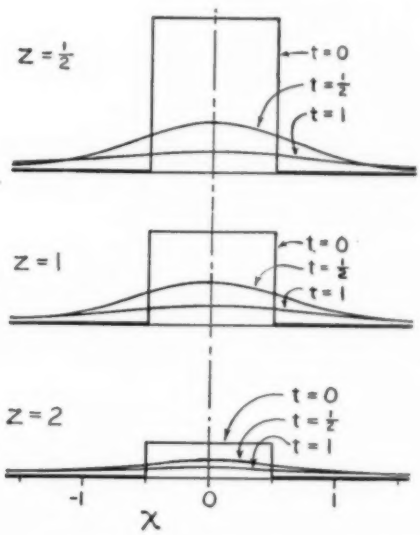

FIG. 6. Dispersion of a narrow beam of electrons by passage through a gas. Curves give values of $R_0=4\pi v^4 f_0$, as function of x the distance across the beam in mean free paths, for different values of z the distance from entry, and of t the average number of collisions since entry.

Although the discussion above was based on the assumption that the cross section Q was practically independent of the electronic velocity, it is possible to obtain a solution when Q cannot be considered constant. We set $S=4\pi v^4 NQf$, and Eq. (7), for $E=0$, becomes $S_1=-(1/NQ)(\partial S_0/\partial x)$. Choosing a new variable

$$\mu=(M/m)\int_v^{v_0}[dv/(NQ)^2v],$$

Eq. (8) becomes $(\partial^2 S_0/\partial x^2)=3(\partial S_0/\partial\mu)$, which is similar to Eq. (17). S can therefore be obtained by the methods discussed above. However, since the relation between μ and v is a complicated one if Q varies markedly with v, average values of current, etc., must be obtained by numerical integration.

The foregoing investigation originated from a suggestion, made by Dr. K. T. Compton in connection with a problem of sputtering, that the effects due to particles which had suffered several collisions would be as important as those due the primary beam. We are indebted to him and to Dr. Irving Langmuir for several helpful discussions.

[5] Normand, Phys. Rev. **35**, 1217 (1930).

The Ionization of Neon and Argon by Singly Charged Magnesium Ions

J. C. MOUZON AND N. H. SMITH,* *Duke University*

(Received May 10, 1935)

The efficiency of ionization (the number of electrons ejected per initial positive ion per cm path per mm pressure) by singly charged magnesium ions is compared with that by singly charged sodium ions to obtain further information on the parts played by mass and electron configuration in the ionization process. The efficiency of the magnesium ions is about 60 percent of that of the sodium ions in both gases. Data on the mean free path of magnesium and sodium ions in the two gases must be had before a quantitative comparison of the results can be made. If one assumes the mean free path of magnesium ions to be greater than that of sodium ions, the results indicate that the chance of ionization on a single impact may be approximately the same for both ions.

PREVIOUS work on the ionization of gases by slow positive ion bombardment has shown that the relative masses of the positive ion and gas atom involved play an important role in the ionization process. In order to investigate this question further, singly charged magnesium ions have been used to ionize neon and argon and the results are compared with those of singly charged sodium ions. Here the masses of the bombarding positive ions are approximately the same while the electron configuration is different.

Fig. 1 shows a cross section of the apparatus used. The ion source was similar to one used by Dempster[1] in determinations of the magnesium isotopes. A cylindrical iron shell M 2.5 cm long and 1.2 cm in diameter contained the magnesium which was the source of ions. This source was then mounted in such a way that it could be adjusted vertically and horizontally in order to place the 1 mm hole in the iron cylinder directly above the channel S_1 and slit S_2. Approximately 2 mm beneath the cylinder and directly in line with the hole in the cylinder and the slits was a horizontal 0.0085-inch thoriated tungsten filament F. The Armco iron cylinder L served as a magnetic shield. In the bottom of this shield was a 1×6-mm channel S_1. The shield rested on three glass beads which insulated it from the copper plate A.

When the source was in use the magnesium was kept at a dull red temperature. Electrons from the filament F were accelerated to the hot magnesium in cylinder M. Magnesium ions created by electron impact were accelerated toward the filament and magnetic shield, which were at the same potential, and passed through slits S_1 and S_2 into the magnetic field. The remainder of the apparatus and the method of taking the measurements are essentially the same as described previously by one of the authors.[2]

Fig. 2 is a diagram of the electrical connections. The vacuum tube T was a type 47 tube operated at saturation to maintain a steady current between the filament and magnesium. This current was only about 5 ma. After passing through the magnetic field the ions were again accelerated between plates A and B by voltage supplied

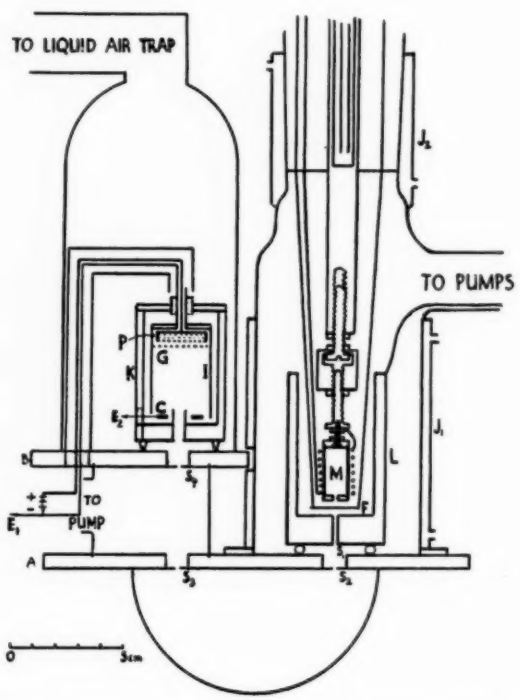

FIG. 1. Arrangement of source and ionization chamber.

* Based on a dissertation presented for the degree of Doctor of Philosophy at Duke University.

[1] A. J. Dempster, Phys. Rev. **18**, 417 (1921).

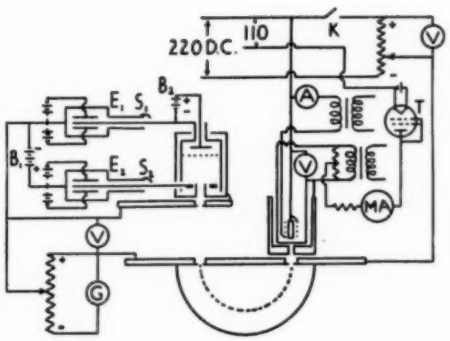

FIG. 2. Electrical connections.

from a 1000-volt generator G. If the voltage drop between the magnesium and plate A is added to that between A and B, the sum is the total accelerating potential for the ions. Measurement of the retarding potential necessary to stop the ions indicated, in agreement with Dempster,[1] that the ions fell through the total potential applied between M and plate B.

The neon was specified to be 99½ percent neon and ½ percent helium; the argon was specified to be 99½ percent argon and ½ percent nitrogen. The gas flowed through a capillary to a tube which passed through a mixture of CO_2 snow and alcohol and then through plate B to the bell jar. By adjusting the gas reservoir, the pressure under the bell jar could be regulated while the pumps were operating. A McLeod gauge was connected to the region containing the ionization chamber. Pressure could be read to 10^{-5} mm Hg with the gauge as it was ordinarily used.

In order to calibrate the magnetic field and in order to see whether the apparatus was properly assembled, a source of sodium ions was placed in the source chamber instead of the source described above. It was found that, if the current in the magnetic field coil were 2 amperes, singly charged sodium ions falling through a potential of 100 volts passed through the slits to the ionization chamber. The efficiency of ionization of neon by 950-volt sodium ions was measured and found to be 1.5 percent higher than the value obtained by one of the authors[2] at that voltage. Measurements at 500 volts gave a value approximately 9 percent lower than that of Beeck[3] at the same voltage. The magnesium source was then put into the apparatus and the magnetic yoke was demagnetized before the magnetic field current was increased to 2 amperes. The heater coil current was increased until ions could be observed. Several peaks appeared at first and the pressure in the source chamber increased because of the rise in temperature. After about a half-hour had elapsed, all of the peaks except two had disappeared. One of these peaks was found at an accelerating potential of 96 volts while the other appeared at 175 volts. Upon subsequent heatings the two peaks appeared suddenly as the temperature of the magnesium reached a certain value. The peak at 96 volts was definitely shown to be Mg^+. It is worth noting that this peak disappeared when the potential between the filament and the magnesium was less than about 8 volts. The first ionization potential of magnesium is 7.75 volts.

At one time sources of lithium, sodium and potassium were placed in the source chamber to calibrate the magnetic field and to see whether or not the product of the mass of the ion and the accelerating potential for a given magnetic field was constant. This product was found to increase somewhat with increase in mass but was constant within the resolving power of the apparatus. Mg^{++} has an effective mass of 12 and hence it seems logical to believe that the 175-volt peak was doubly ionized magnesium. Other evidence for this is that the energy necessary to remove two electrons from magnesium is 22 volts, and it was observed that the peak at 175 volts disappeared when the potential between F and M was less than about 24 volts.

Results of the measurements of the ionization of neon and argon by singly charged magnesium ions are given in Fig. 3. The efficiency of ioniza-

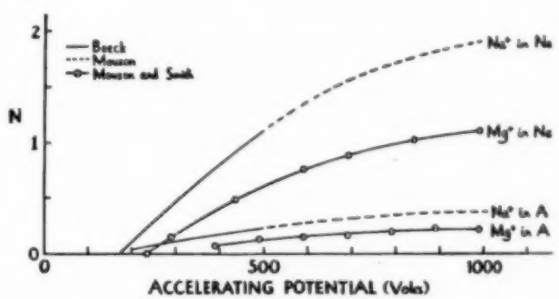

FIG. 3. Efficiency of ionization in neon and argon.

[2] J. C. Mouzon, Phys. Rev. **41**, 605 (1932); Phys. Rev. **44**, 688 (1933).
[3] O. Beeck, Ann. d. Physik **6**, 1001 (1930).

tion N (the number of electrons liberated from the gas per initial positive ion per cm path per mm pressure at 0°C) is plotted against the accelerating potential in volts. The efficiency curves obtained by Beeck[3] and Mouzon[2] for positive ions of sodium in neon and argon are given for comparison. In both gases the efficiency of Mg^+ is approximately 60 percent of that of Na^+. No attempt was made to measure accurately the insetting potential of ionization.

If the mean free path of Mg^+ is the same as that of Na^+ in neon and argon, and if the ionization is due to the energy given up in a partially inelastic collision, then the efficiency of ionization in neon should be slightly less than that of Na^+ and the efficiency in argon should be slightly greater than that of Na^+. In the first case the atomic weight of magnesium is more nearly equal to that of neon, while in the second case it is more nearly equal to that of argon.

At the present time there are no experimental data on the mean free path of Mg^+ in any gas. In order to get a rough idea of this mean free path as compared to that of Na^+ one might consider the cross section of the Mg^+ ion as being due principally to the core, neglecting the effect of the extra electron on collisions. From the classical model of the atom this consideration leads one to the conclusion that the mean free path of Na^+ in neon is 87 percent of that of Mg^+. If this is true, the efficiency of ionization of Mg^+ in neon should be 87 percent of that of Na^+, assuming that the chance of the ejection of an electron on a single collision is the same for Mg^+ as for Na^+. Approximately the same conclusion is reached if the relative cross sections are computed from the atomic volumes of the two elements. Following the same argument Mg^+ should be about 89 percent as efficient as Na^+ in ionizing argon.

Another point that may bear mention is that the extra electron of Mg^+ spends most of its period at a considerable distance from its core. If the core of the Mg^+ ion comes very close to the neon atom when a collision resulting in ionization takes place, it may be that the electron has to escape an effective charge of between two and three times the charge on an electron instead of a charge of just twice that of an electron. If such is the case, the efficiency for Mg^+ should be less than might be expected from other considerations.

The above are suggestions of the processes which may account for the lower efficiency of ionization of Mg^+ in neon and argon. Another matter which may complicate the recorded results is the possibility of the bombarding magnesium ion being ionized a second time by striking the gas atom. The conditions appear to be favorable for this to occur since the second ionization potential of magnesium is 15 volts while the first ionization potential of neon is 21.5 volts and the first ionization potential of argon is 15.7 volts. It does not appear to occur, however, since the insetting potential of ionization is higher than one would expect if Mg^+ were ionized a second time.

The following interpretation of the results may be suggested: The chance of ionization per collision by Mg^+ is approximately the same as that of Na^+ in neon and argon. This conclusion is reached on either of two assumptions: (a) The actual mean free path of Na^+ is somewhat less than that of Mg^+ as computed above. (b) The ratio of the mean free path of Na^+ and Mg^+ is the same as computed above, but the electron ejected from the struck atom has to escape a positive charge equal to more than that of two electrons to get away from the pseudo-molecule formed by the incident ion and gas atom.

It is evident that further experimental work must be done before conclusions any more definite than the above can be drawn.

Intensities in $^2\Pi - {}^2\Sigma$ Transitions in Diatomic Molecules

LESTER T. EARLS, *College of the Ozarks, Clarksville, Arkansas*

(Received June 3, 1935)

Simple intensity expressions for $^2\Pi - {}^2\Sigma$ and $^2\Sigma - {}^2\Pi$ transitions in diatomic molecules have been developed for cases in which the $^2\Pi$ state is intermediate between Hund's case (a) and case (b), by specializing the general formulas given by Hill and Van Vleck. Numerical values have been worked out for all branches in typical $^2\Pi$ cases, for low values of J.

SEVERAL years ago Hill and Van Vleck[1] developed formulas based on the new quantum mechanics giving the amplitudes necessary for finding the intensities of electronic transitions in diatomic molecules. These formulas are applicable to transitions in which either initial or final state, or both, is intermediate between case (a) and case (b) as classified by Hund.[2] The amplitudes are functions of the rotational quantum number J and of a parameter $\lambda = A/B$ for each state. $\lambda = \pm\infty$ in case (a), 0 in case (b). The present work involves the application of these general formulas to $^2\Pi \rightarrow {}^2\Sigma$ transitions, the reduction of the resulting expressions to surprisingly simple forms, and the substitution of numerical values to facilitate comparison with experimental data. Hill and Van Vleck gave formulas for these transitions, but did not put them in as simple explicit algebraic form as in the present paper. It is found experimentally that the $^2\Sigma$ state is nearly always case (b), but that the $^2\Pi$ state lies intermediate between case (a) and case (b). Accordingly the amplitude expressions were developed for arbitrary λ in the $^2\Pi$ state but $\lambda = 0$ in the $^2\Sigma$ state, squared to give intensities, and simplified; the resulting expressions for the intensities of the twelve possible branches become the following functions of λ (in the $^2\Pi$ state) and J:

$^2\Pi \rightarrow {}^2\Sigma$	$^2\Sigma \rightarrow {}^2\Pi$	*Intensity*
P_2 $^{PP}P_{12}$	R_2 $^{RR}R_{21}$	$\dfrac{(2J+1)^2 \pm (2J+1)\,U(4J^2+4J+1-2\lambda)}{32(J+1)}$
$^{Q}P_{21}$ P_1	$^{Q}R_{12}$ R_1	$\dfrac{(2J+1)^2 \mp (2J+1)\,U(4J^2+4J-7+2\lambda)}{32(J+1)}$
Q_2 $^{P}Q_{12}$	Q_2 $^{R}Q_{21}$	$\dfrac{(2J+1)[(4J^2+4J-1) \pm U(8J^3+12J^2-2J+1-2\lambda)]}{32J(J+1)}$
$^{R}Q_{21}$ Q_1	$^{P}Q_{12}$ Q_1	$\dfrac{(2J+1)[(4J^2+4J-1) \mp U(8J^3+12J^2-2J-7+2\lambda)]}{32J(J+1)}$
R_2 $^{Q}R_{12}$	P_2 $^{Q}P_{21}$	$\dfrac{(2J+1)^2 \pm (2J+1)\,U(4J^2+4J-7+2\lambda)}{32J}$
$^{RR}R_{21}$ R_1	$^{PP}P_{12}$ P_1	$\dfrac{(2J+1)^2 \mp (2J+1)\,U[4J^2+4J+1-2\lambda]}{32J}$

where[3]

$$U = [\lambda^2 - 4\lambda + (2J+1)^2]^{-\frac{1}{2}}.$$

The designation of the branches for both $^2\Pi \rightarrow {}^2\Sigma$ and $^2\Sigma \rightarrow {}^2\Pi$ transitions is in the notation of Mulliken;[4] however, in any case the value of J is that in the $^2\Pi$ state. The level before the arrow is the upper state in emission. The intensity expressions as written include the statistical weight factor $2J+1$, but do not include an arbitrary factor which is independent of J. They are valid for all positive and negative values of λ (normal and inverted doublets), and for all values of $J > \frac{1}{2}$. For the case $J = \frac{1}{2}$, due to an anomalous correlation discussed by Hill and Van Vleck,[1, 5] the formulas must be specially considered and give the values shown in the curves and tabulated as follows:

$J = \frac{1}{2}$	$^2\Pi \rightarrow {}^2\Sigma$	$^2\Sigma \rightarrow {}^2\Pi$
$\lambda > 0$	$^{PP}P_{12} = P_1 = \frac{1}{6}$ $^{P}Q_{12} = Q_1 = \frac{1}{3}$	$^{RR}R_{21} = R_1 = \frac{1}{6}$ $^{R}Q_{21} = Q_1 = \frac{1}{3}$
$\lambda < 0$	$P_2 = {}^{Q}P_{21} = \frac{1}{6}$ $Q_2 = {}^{R}Q_{21} = \frac{1}{3}$	$R_2 = {}^{Q}R_{12} = \frac{1}{6}$ $Q_2 = {}^{P}Q_{12} = \frac{1}{3}$.

The intensities of the other branches are identically zero for $J = \frac{1}{2}$.

[1] Hill and Van Vleck, Phys. Rev. **32**, 250 (1928).
[2] Hund, Zeits. f. Physik **36**, 657 (1926).
[3] The positive square root is to be used.
[4] Mulliken, Phys. Rev. **30**, 785 (1927).
[5] The standard Mulliken notation, which we use, is really a misnomer when $J = \frac{1}{2}$, $\lambda > 0$ as the superscript no longer always gives the K behavior correctly in this exceptional case.

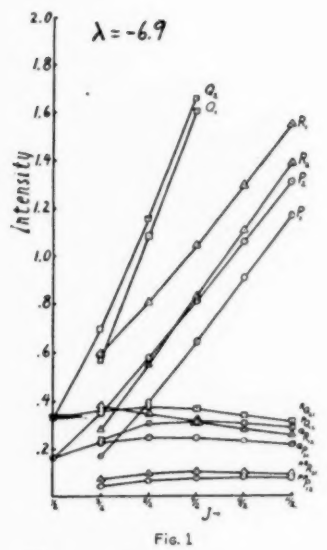

Fig. 1

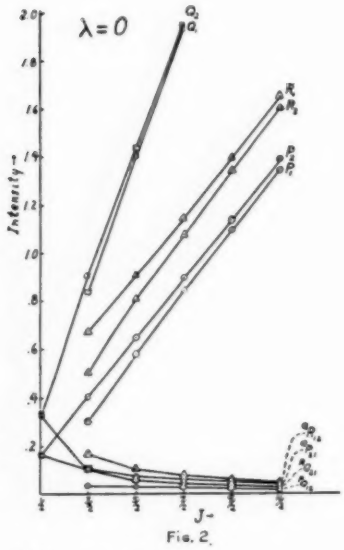

Fig. 2

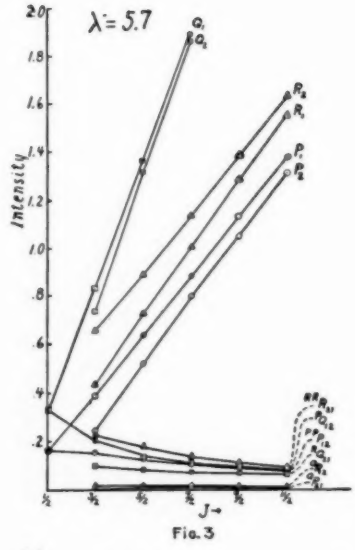

Fig. 3

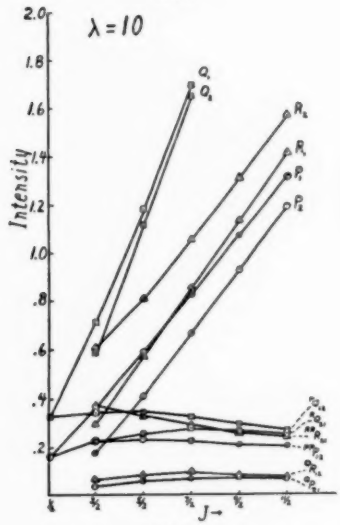

Fig. 3a

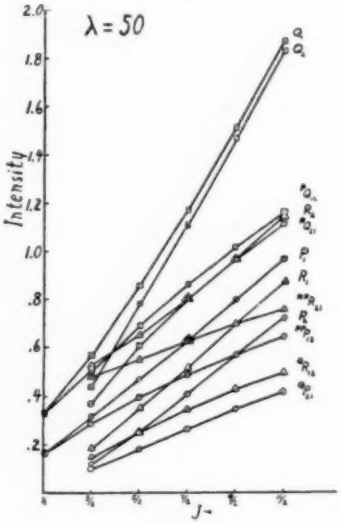

Fig. 4

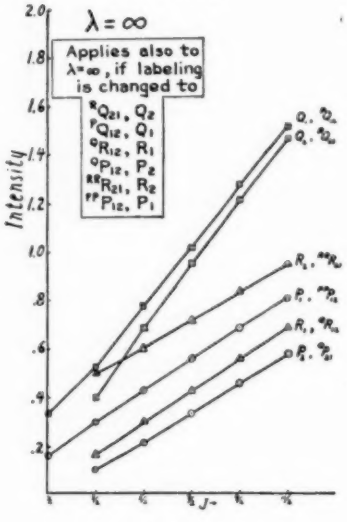

Fig. 5

Errata to Fig. 5: The following corrections should be made in the legend in the box: $\lambda = -\infty$; in the third line from the bottom, ${}^{Q}P_{21}$.

The accompanying curves show the rise of the two branches ${}^{PP}P_{12}$ and ${}^{RR}R_{21}$ (forbidden in case (b)) and the four satellite branches ${}^{Q}R_{12}$, ${}^{P}Q_{12}$, ${}^{R}Q_{21}$, ${}^{Q}P_{21}$ to intensities equivalent to those of the strong branches P_1, Q_1, R_1, P_2, Q_2, R_2, as λ increases. The notation on the curves is that appropriate to ${}^2\Pi \rightarrow {}^2\Sigma$ transitions. The relative position of the various branches varies fairly smoothly with λ in the regions intermediate between the various figures. The expressions given above are in agreement with the numerical values for the intensities in HgH ($\lambda = 560$) as calculated by Kapuscinski and Eymers.[6]

Appreciation is due and gladly given to Professor J. H. Van Vleck for his suggestion of this topic and his guidance in the work, which was done at the University of Wisconsin.

[6] Kapuscinski and Eymers, Zeits. f. Physik **54**, 246 (1929).

Magnetic Reversal Nuclei

Part V.[1] Propagation of Large Barkhausen Discontinuities

K. J. SIXTUS, *Research Laboratory, General Electric Company, Schenectady*

(Received May 3, 1935)

In a Ni-Fe wire in which a preferred direction of magnetization is created by application of tension, stable regions of antisaturated magnetization can be produced by short application of high local fields. These nucleus regions will not grow after removal of the local field, although the direction and magnitude of the uniform external field favors growth. This is explained by the fact that their demagnetizing field lowers the total field in the neighborhood below the value H_0, which in former papers was recognized to be the minimum field value at which propagation would proceed spontaneously. Propagation will start from a nucleus region if the external field is raised to a value H_S', where H_S' has to fulfill the condition: $H_S' = H_0 + H_d$. H_d, the demagnetizing field of the nucleus, was calculated from its dimensions. The approximate size of a natural nucleus in a stressed wire was determined from the starting field H_S of that wire; it had a length of a few mm and a diameter of several μ.

1. INTRODUCTION

ACCORDING to present views a ferromagnetic body is subdivided in small regions, each region being distinguished by having a uniform direction of magnetization which is different from the direction in its neighbors. Crystal orientation, local strain and external and internal fields determine the orientation of any region. There is evidence that its linear dimension is of the order of 10^{-3} cm. This small size, as well as the other factors just mentioned, make a detailed study of the process of magnetization in a region practically impossible.

The discovery of Preisach,[2] however, that uniform strain, such as tension, applied to a suitable material, such as, for example, ten percent nickel-iron wire, produces a uniformity in the direction of magnetization enables us to study the magnetic processes on a much larger scale. Thus the progress of magnetization was studied as a large magnetic discontinuity which traveled along wires.[1] It is probable that the results obtained apply also, with some modifications, to the case of magnetic reversal in unstrained material. The present investigation thus has possible significance along two lines. In the first place, it shows the conditions which have to be fulfilled in order to *start* a large discontinuity. Besides, it serves as a large scale model for the starting of a reversal in a small region.

The problem treated in this paper developed during the study of the propagation of large Barkhausen discontinuities. Some of the experiments were first carried out about four years ago. The major results were reported at the Physical Society meeting in Washington in April, 1934.

2. THE STARTING OF A LARGE DISCONTINUITY

In studying the propagation of magnetization along stressed Ni-Fe wires, a local adding field was employed to initiate the propagating reversal in a uniform field H where $H_S > H > H_0$ (Fig. 1). The total local field at a point has to exceed the local starting field, H_{Sl}, before the propagation can proceed spontaneously. The starting condition for a uniform wire is therefore:

$$H + H_a \geqq H_{Sl}. \qquad (1)$$

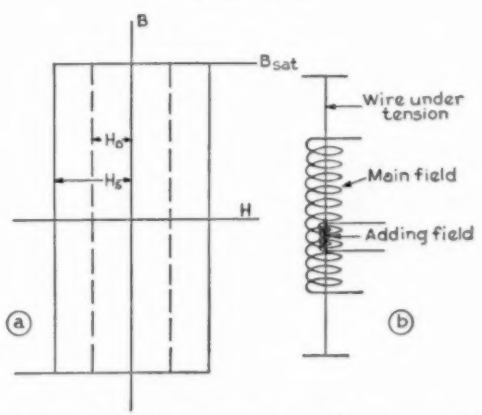

FIG. 1. a: Schematic hysteresis loop of a 15 percent Ni-Fe wire under high tension; b: schematic diagram of the experimental set-up.

[1] Part I: K. J. Sixtus and L. Tonks, Phys. Rev. **37**, 930 (1931); II: Phys. Rev. **42**, 419 (1932); III: L. Tonks and K. J. Sixtus, Phys. Rev. **43**, 70 (1933); IV: Phys. Rev. **43**, 931 (1933).

[2] F. Preisach, Ann. d. Physik **3**, 737 (1929).

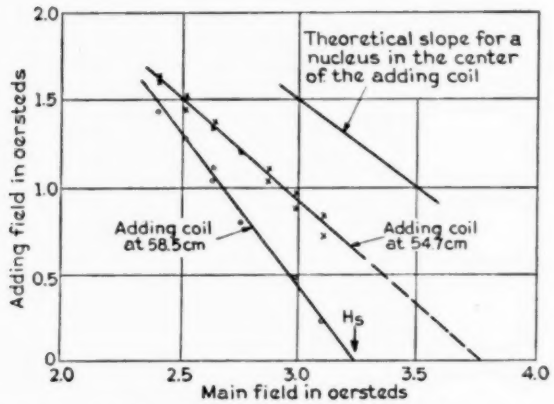

FIG. 2. The adding field necessary to start propagation as function of the main field in a 15 percent Ni-Fe wire.

The magnetic field symbols used here and in the following sections have the following meaning: H, main field; H_0, critical field; H_S, starting field; H_{Sl}, local starting field, H_S being the minimum value of H_{Sl} along the wire; H_a, adding field; H_{a0}, minimum adding field at a point necessary to start propagation at a given H.

In order to test Eq. (1) we have plotted in Fig. 2 both the straight line relation satisfying Eq. (1) and the experimental results at two different points along a cold drawn, 15 percent Ni, 85 percent Fe wire. If the adding coil is placed at 58.5 cm., it obviously controls the starting of the weakest nucleus on the wire since the curve intercepts the axis of abscissas at $H=H_S$. The deviation in slope from the theoretical one can be explained by assuming that the weakest nucleus was not situated in the center of the coil for which H_a was calculated from the coil constants but lay near the end of the coil where the field was smaller than in the center. At another place (54.7 cm) a higher adding field had to be applied, but the nucleus in this case was closer to the center of the adding coil; hence the close agreement between the experimental and the theoretical slope.

We thus find that for every value of main field a minimum value of adding field, H_{a0}, which will vary along the wire, is necessary to start propagation.[3] If, however, the adding field was not applied continuously, but only for a short time interval, fields in excess of the minimum value could be used without initiating propagation. It became apparent in several ways that the short field pulse caused local magnetic reversals in the coil region. These local changes will be discussed after describing the surge circuit used.

3. SURGE CIRCUIT

The problem of producing flat-crested current pulses of a duration between 0.0001 and 1 sec. can be solved with the help of a Helmholtz pendulum. Contact troubles, however, developed when this method was tried, and the suitability of two different tube circuits was tested. A. J. Maddock[4] used a circuit containing two Thyratrons which can furnish large currents, but it was found that the minimum time interval was 0.0005 sec. and that it was impossible to produce sufficiently rectangular shapes. Therefore a high vacuum tube arrangement was chosen finally which supplied perfectly rectangular surges with a maximum current of 50 ma and of a minimum duration below 0.0001 sec. Fig. 3 shows the circuit used. At the beginning current is flowing in tube B only. By throwing switch S a damped oscillation is initiated in the timing circuit, making grid B negative and positive in short succession. The current accordingly will shift from B to A and back to B again, a process described in I, p. 934. The grid bias of tube B has to be adjusted to such a value that only the first negative and positive crest voltage on C will be effective in shifting the current. UX-245 tubes were selected because, besides giving a high plate current, their high filament current reduced the effect of plate current on filament temperature.

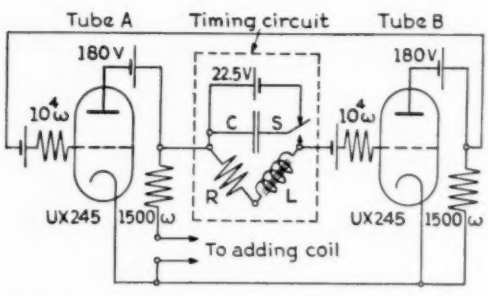

FIG. 3. Tube circuit for the production of short, square current impulses.

[3] Cf. K. J. Sixtus and L. Tonks, Phys. Rev. **39**, 357 (1932).

[4] A. J. Maddock, Proc. Phys. Soc. (4) **43**, 371 (1931).

4. Experiments on Nucleus Growth

Although experiments have been performed on a large number of different wires, only the results on three of them will be given, since they appear to be representative of the rest. Wire No. I was a cold drawn wire with 15 percent Ni and 85 percent Fe; No. II had the same composition but had undergone a heat treatment (1 min. at 930°C, cooled to room temperature, 1 hr. at 400°C), which made it more uniform and reduced its critical field considerably (see footnote 1, II); No. III was a permalloy (78.5 percent Ni, 21.5 percent Fe) wire which had been annealed at ~1100°C for 3 hr., at ~700°C for 2 hr., and was cooled rapidly to room temperature from 700°C.

The main field coil was 80 cm long and had a constant of 23.0 oersteds/amp. The adding field coil was, in most cases, wound directly on the wire. It consisted, in the case of Figs. 5 and 6, of 64 turns of 5-mil wire, with a coil constant of 80 oersteds/amp.

Two types of tests were performed with the surge circuit. At a given main field a time-adding field relation could be found by taking either time or field as independent variable and adjusting the other one, so that one surge would *just* start propagation. Incidentally, the start of propagation was indicated by a search coil, some distance away from the adding coil and connected to a galvanometer. The alternative method consisted in taking H_a as independent variable and applying a series of surges of short duration until propagation started. Both methods gave identical results, indicating that the *total* time during which the field was applied was of importance. One also can conclude from this observation that changes in the magnetic structure of the material proceeded only as long as the field was applied and that no readjustment took place between the periods of application of short pulses. Fig. 4 gives the experimental results for wire No. I under a tension of 75 kg/mm² and also the product $(t\times(H_a-H_{a0}))$ derived from them. The fact that this product, at a given main field, was constant made it appear as if an antisaturated region or nucleus had to grow to a certain size before it could initiate self-propagating reversal, the size, presumably, depending on the value of main field. Similar results, shown in Fig. 5, were found for wire No. III, although the main field had a value of only three percent of its value for wire No. I.

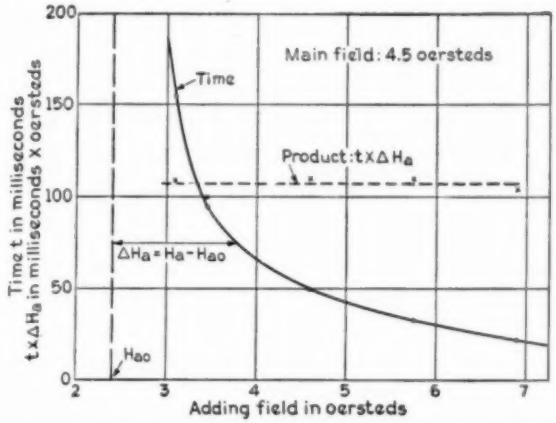

Fig. 4. Time intervals for which the adding field has to be applied in order to start propagation. Wire No. I, 15 percent Ni-Fe, unannealed.

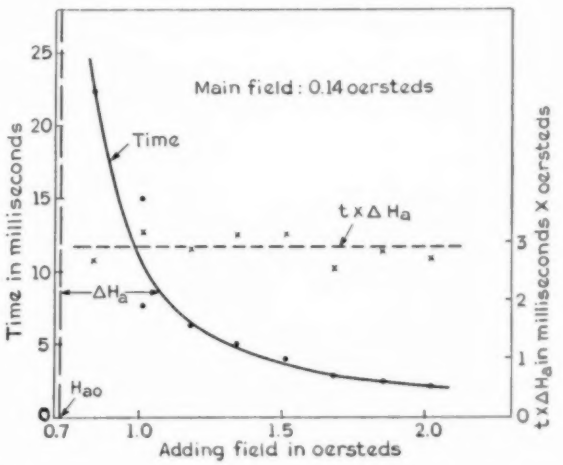

Fig. 5. The same relation as in Fig. 4, for wire No. III, 78.5 percent Ni-Fe, annealed.

This conjecture could be verified by direct measurement. By moving a search coil of 0.6-cm length connected to a ballistic galvanometer along that section of the wire where the antisaturated region had been developed, the flux leaving the wire could be measured accurately, at least in the case of the larger nuclei. In Fig. 6 three stages during the growth of a nucleus are shown. These nuclei were created by successive applications of field surges and the flux curves measured by rapid movement of the search coil from different places within the nucleus region to a place beyond it. Wire No. II under a tension of 65 kg/mm² was used in this experiment.

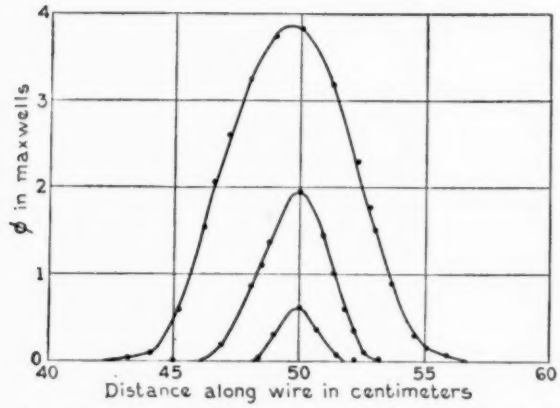

FIG. 6. The flux passing through the wire surface in a nucleus region as measured by a search coil for three nuclei of different size.

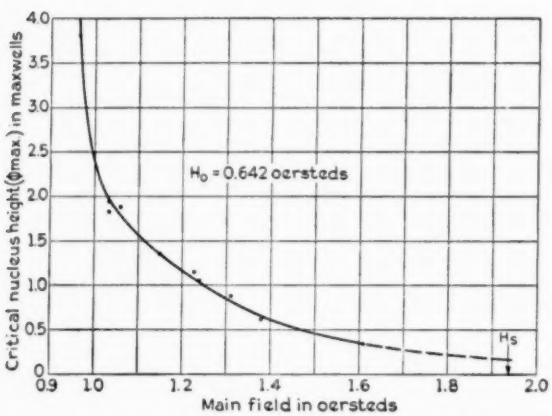

FIG. 7. Relation between nucleus height and the main field in which a given size nucleus would start propagation. Wire No. II, 15 percent Ni-Fe, annealed.

A nucleus once produced would not change its shape if the *main* field was increased until a certain value of main field was reached when it would start propagation. There was a definite, reproducible relation between nucleus shape, as measured by the height of its flux curve, and the main field in which a nucleus would initiate spontaneous propagation (Fig. 7).

5. Discussion of Results

Our experiments have shown that a nucleus may be stable in a surrounding antisaturated phase. If, however, the main field exceeds a certain value, the equilibrium becomes unstable and a spontaneous growth takes place. We shall call this value H_S' because it is closely related to the starting field H_S in a wire which does not contain "artificial" nuclei.

At this point it appears worth while to recall briefly the theory of condensation in supersaturated vapors, which offers a very close parallel to our magnetic two-phase problem. A drop of liquid can be in equilibrium with its supersaturated vapor because of the fact that it exhibits a surface tension as long as its size does not exceed a critical value. This critical size is for a given material determined by the degree of supersaturation, i.e., the ratio between the vapor pressures of the supersaturated to the saturated phase. If a critical size droplet is present, an infinitesimal amount of work will suffice to transform the vapor phase into the liquid phase.

If we want to apply these considerations to the case of a magnetic nucleus surrounded by an antisaturated phase, we find that instead of a surface energy we have to deal with a volume energy arising from the demagnetizing field H_d, caused by the nucleus itself and by the surrounding phase. In analogy to the vapor case we may assume that an amount of work

$$E = H_d \times I_s \tag{2}$$

equal to this energy has to be supplied to the wire in order to make the nucleus self-propagating—in addition to the energy $H_0 \times I_s$ necessary to sustain propagation (see next section). Preisach[5] has expressed the same idea in more general terms in his discussion of the natural starting field H_S. It appears plausible to postulate that the critical size nucleus is determined by the condition

$$H_s' - H_0 = H_d, \tag{3}$$

which infers that the field inside the nucleus has to have at least the value H_0 before that nucleus can grow spontaneously.

Experimental evidence speaks for the basic correctness of our assumptions (2) and (3). This conclusion was reached in the following way. From the measured flux curves of different size nuclei we calculated, with certain simplifications, the demagnetizing field, H_d, and compared it with the value of $H_s' - H_0$ for these cases. These simplifying assumptions were:

(1) The observed flux curve is caused by a coherent, saturated region with a definite boundary.

[5] F. Preisach, Physik. Zeits. **33**, 913 (1932).

(2) This region has the shape of an ellipsoid of rotational symmetry whose two axes can be derived from the flux curve.

The demagnetizing field for an ellipsoid surrounded by a medium of permeability 1 is NI_s, N being the demagnetizing factor. We are here concerned with ellipsoids whose ratio k of long to short axis is large, for which N has the value:[6]

$$N=(4\pi/k^2)(\ln 2k-1). \quad (4)$$

It can be shown that the surrounding anti-saturated phase contributes an equal amount NI_s to the field in the nucleus, and it follows that

$$II_d=(8\pi I_s/k^2)(\ln 2k-1). \quad (5)$$

The long axis was taken to be equal to the length of a flux curve such as are given in Fig. 6, whereas the short axis was determined from the height of the flux curve by assuming that the ratio of maximum nucleus cross section to wire cross section was the same as that of maximum nucleus flux to flux at saturation.

This procedure could be expected to give correct values for nuclei whose length was large compared with the coil dimensions, but to become, for two reasons, less and less accurate if this condition was not fulfilled. Firstly, there is a considerable leakage flux not intercepted by the coil if the nucleus length is of the same order or smaller than the coil diameter. Secondly, the fact that the search coil has a finite length will have the effect that instead of measuring the flux at one point we obtain a flux average over the length of the coil. The latter cause will make the measured flux curve longer than the actual one, and both causes will result in too low a maximum of the measured flux curve. If no corrections are applied, we obtain an apparent k larger than the actual value. It appears difficult to determine the error due to the first effect, whereas the second one could be compensated roughly by assuming the long axis to be equal to the difference between length of flux curve and coil length.

The check of Eq. (3) is contained in Fig. 8. The curve is a plot of Eq. (5) relating II_d to k, and the dots refer to four nuclei, created in wire No. II with different values of k, the ordinates giving the value of $H_s'-H_0$. The dots at both ends of an arrow refer to one and the same nucleus, the one on the right being plotted using the apparent k, the dot at the arrow point using the corrected k. The experimental points lie sufficiently close to the theoretical curve to furnish proof for the validity of Eq. (3).

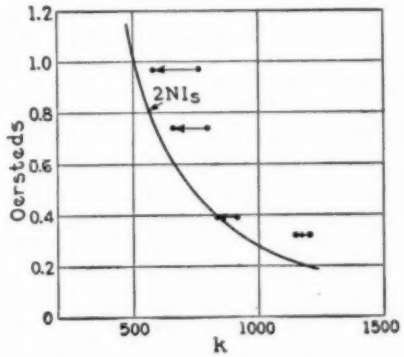

FIG. 8. Solid curve: Relation between demagnetizing field 2 NI_S of a nucleus and the length to thickness ratio k; Dots: H_S-H_0 for four nuclei with different values of k.

A similar test was performed with the permalloy wire No. III ($H_0=0.058$ oersted) in a field of 0.138 oersted, only one-tenth the field necessary for wire No. II. The critical size nucleus at this field had a diameter of 0.0156 cm and the remarkable length of 20 cm, resulting (with $I_s=950$ e. m. u.) in a demagnetizing field $2NI_s=0.057$ oersted. Although the agreement obtained here ($H_s'-H_0=0.080$ oersted and $2NI_s=0.057$ oersted) is not so close as with wire No. II, the discrepancy is not so large as to force one to abandon Eq. (3). It may be that nuclei of this extreme length no longer have the shape of an ellipsoid and that our method of field calculation becomes quite inaccurate for this reason.

Incidentally, these measurements have thrown some light on the rate of nucleus growth in axial and radial directions. They are not sufficiently complete to warrant the actual determination of these rates, but they show qualitatively that the rate of axial growth is larger than that for radial growth as could be expected from the propagation experiments. This accounts for the decrease in demagnetizing field connected with the growth of the nucleus.

Thus by comparatively crude considerations we have obtained an almost quantitative check for the condition expressed in Eq. (3). This equation, however, only describes the field in

[6] L. Graetz, *Handbuch d. Elektrizität u. des Magnetisms*, (1920), p. 151.

that part of the wire which contains the middle portion of the ellipsoid, and the field in the neighborhood of the ends may be quite different from it. A detailed study of local field distribution seems quite impossible at present, particularly on account of the unknown contribution of boundary effects, forcing us to content ourselves at present with energy considerations as given above.

6. The Starting Field H_S

Preisach has expressed the idea[5] that H_S formed a measure for the surface energy which has to be supplied to a natural nucleus in order to make it self-propagating. From our findings on artifical nuclei we must conclude that $H_S - H_0$ rather than H_S is the important quantity determining this energy.

H_0, according to the theory developed by Bloch[7] and Preisach is made up of two parts, H_{0R} and H_{0Z} (see the schematic diagram, Fig. 9). H_{0R} is a measure of the energy necessary to shift a boundary when the preferred orientation has been made axial by high tension; it is probably due to local variations in atomic distances. H_{0Z} measures the energy which has to be supplied to move the boundary through regions where the magnetization is not lined up in the direction of the field H due to insufficient applied stress. H_{0Z} vanishes when the applied tension exceeds the internal stresses σ_i. If the discontinuity is traveling in a field $H > H_0$, the additional energy $(H - H_0)\, I_s$ is converted mainly into eddy currents, which is shown by the correctness of the penetration formula (footnote 1, II) derived on that basis.

We want to consider H_S in a wire free of all "accidental" starting nuclei which are due to large scale distortions in the wire, such as bends, or which are formed by regions which have not been lined up with the rest because of the use of insufficient fields. Bloch has shown that there is a certain probability for the formation of small antisaturated regions, which we shall call "natural" nuclei, where the energy is supplied thermally. These "spontaneous reversal nuclei" will grow in a small applied field until stopped by a lattice distortion for whose overcoming a field H_0 is needed.

In the preceding section we have found a relation between nucleus size and starting field. It would be possible, therefore, to take the field $H_S - H_0$ as a measure of the nucleus size if we could be sure that the conditions remain fundamentally the same for the much smaller natural nuclei. The increase in $H_S - H_0$ with increasing tension would, in that case, be an indication of the accompanying reduction in nucleus size. Two influences have to be considered in a more rigorous treatment. The first is the interaction of different nuclei, the second is the role of the molecular field. Disregarding these complications, we have derived the approximate size of a natural nucleus as follows.

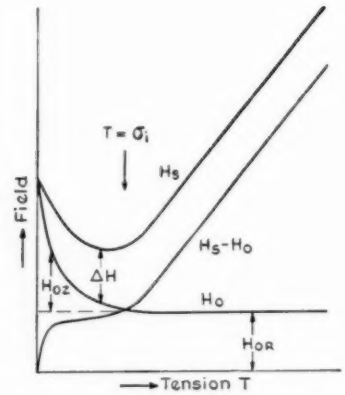

Fig. 9. Schematic relation between H_0, H_S and $H_S - H_0$ and tension for a well-annealed wire.

For the well-annealed 15 percent Ni-Fe wire No. II under a tension of 77 kg/mm², which, presumably, did not contain any accidental nuclei, the curve relating maximum flux of nucleus region to H_S' was extrapolated to the natural value of H_S for this wire (Fig. 7). The same was done for the curve showing the dependence of H_S on nucleus length. In this manner a rough value for the size of the natural nucleus which caused propagation in the wire at H_S was obtained: its diameter lay between 10^{-4} and 10^{-3} cm, and its length was of the order of a few mm. Its volume thus agrees with the average volume (10^{-8} cm³) of the Barkhausen regions,[8] which are responsible for the Barkhausen effect.

The author is greatly indebted to Dr. L. Tonks for valuable advice and for many stimulating discussions on the subject.

[7] F. Bloch, Zeits. f. Physik **74**, 333 (1932).

[8] R. M. Bozorth and J. F. Dillinger, Phys. Rev. **35**, 733 (1930).

A Theorem Connecting the Energy Momentum Tensor with the Velocity of Propagation of Waves

O. HALPERN, *New York University, University Heights*

(Received June 6, 1935)

It is shown that every wave phenomenon which is described by a symmetrical energy momentum tensor of the second order, propagates with the velocity of light, provided that the four dimensional divergence and the diagonal sum of the energy momentum vanish. This theorem is applied to the two different expressions given for the energy momentum tensor of electromagnetic phenomena in material bodies by Minkowski and Abraham.

I. INTRODUCTION

IT is well known that the energy momentum tensor T_{ik} of the electromagnetic field in vacuum possesses the following characteristic properties[1]

$$T_{ik} \equiv F_{ir}F_{kr} - \tfrac{1}{4}F_{rs}F_{rs}\delta_{ik}, \tag{1}$$

$$T_{ik} = T_{ki}, \tag{2}$$

$$T_{11}+T_{22}+T_{33}+T_{44}=0, \tag{3}$$

$$\partial T_{ik}/\partial x_k = 0. \tag{4}$$

In (1), F_{ik} stands for the antisymmetric tensor of the electromagnetic field. The symmetry of the energy momentum tensor[2] is essential for the conservation of angular momentum while (4) expresses the fact that the propagation can go on without any force being exerted by the outside system, a condition obviously necessary for vacuum. (3) has not received any direct physical interpretation except for special cases, as for that of the Hohlraum-radiation, for which (on the average) the relations

$$T_{11} = T_{22} = T_{33} = -\tfrac{1}{3}T_{44} \tag{5}$$

hold.

Starting from Eq. (4) a four dimensional vector I_k can be constructed which represents the total energy and momentum of the system. I_k is given by the relation

$$I_k = \int T_{k4}\,dx_1 dx_2 dx_3. \tag{6}$$

A *general* proof of its vector character is given, e.g., by Pauli.*

As is well known, every electromagnetic phenomenon in vacuum propagates itself with the velocity of light. We intend to show that this is not an isolated fact but a necessary consequence of the structure of the energy momentum tensor which would have to hold true for any system, the energy momentum tensor of which shows analogous properties to the tensor of the electromagnetic field in vacuum. This will be proved in paragraph II. Paragraph III contains a discussion of two energy momentum tensors which were proposed by Minkowski and Abraham to describe the mechanical effects of electromagnetic processes in material media.

II. A THEOREM ON THE VELOCITY OF PROPAGATION

Consider a system characterized by an energy momentum tensor S_{ik} satisfying the relations given above for Maxwell's energy momentum tensor

$$S_{ik} = S_{ki}, \quad (2a) \qquad S_i{}^i = 0, \quad (3a)$$

$$\partial S_{ik}/\partial x_k = 0. \quad (4a)$$

Any disturbance spreading in a system described by an energy momentum tensor which satisfies the relations (2a–4a) has the velocity of propagation of light.

To prove this theorem we show that we obtain a contradiction by assuming it to be wrong. If any disturbance, let us say, in the x direction should move with a velocity smaller than c we could always introduce a frame of reference such *that in it there is no flow of energy*. This is possible because, according to our assumption, the new frame of reference would have to move with a velocity smaller than c relative to the old one. In the new system the three quantities

$$S_{41},\ S_{42},\ S_{43},$$

[1] W. Pauli, *Relativitaetstheorie*, §30.
[2] Pauli, Reference 1, §42.
* Reference 1, §21.

representing the flow of energy per unit of area vanish and therefore, by symmetry, S_{14}, S_{24}, S_{34} also. In virtue of the fourth equation of (4a)

$$\frac{\partial S_{41}}{\partial x_1}+\frac{\partial S_{42}}{\partial x_2}+\frac{\partial S_{43}}{\partial x_3}+\frac{\partial S_{44}}{\partial x_4}=0$$

S_{44} becomes a function of the coordinates x_1 to x_3 only.

The other three equations of (4a) do not contain any more derivatives with respect to the time because all S_{4k} ($k=1, 2, 3$) are zero. The x component, for example, of (4a) takes, therefore, the form

$$\frac{\partial S_{11}}{\partial x_1}+\frac{\partial S_{12}}{\partial x_2}+\frac{\partial S_{13}}{\partial x_3}=0. \tag{7}$$

Integrate (7) over a domain which is bounded by a part of the $y-z$ plane and a surface which completely lies outside of the range which is occupied by the disturbance. This is possible since there is no spreading of the disturbance in the new frame of reference. Now (7), being a divergence, takes on the form

$$\int S_{1n}df=0; \tag{8}$$

the second index in (8) denotes the direction perpendicular to the surface over which we integrate. Since S_{1n} vanishes on the surface outside the domain of the disturbance (8) reduces to

$$\int S_{11}dydz=0. \tag{9}$$

The x coordinate of the $y-z$ plane over which we integrated was quite arbitrary; we can therefore integrate (9) with respect to x and thereby obtain

$$\int S_{11}dx_1dx_2dx_3=0. \tag{10}$$

A similar consideration can be carried out for every S_{ik} ($ik=1, 2, 3$) so that we finally obtain

$$\int S_{ik}dx_1dx_2dx_3=0 \ (i, k=1, 2, 3). \tag{11}$$

In obtaining (11) we have followed closely a method presented by Laue[3] in deriving the properties of so-called "complete static systems" in the mechanics of relativity.

Having derived (11) only one more step is necessary to obtain the contradiction which we are looking for. By integrating (3a) over the volume of the disturbance, we obtain on account of (11)

$$\int S_{44}dx_1dx_2dx_3=0. \tag{12}$$

We previously had found that all S_{4k} ($h=1, 2, 3$) are zero. Combining these statements we have

$$I_k\equiv 0. \tag{13}$$

In the frame of reference chosen all components of the vector I_k vanish identically. This vector, therefore, must vanish in every system of coordinates, which is only another way of saying that no disturbance exists. We thereby have established the contradiction and proved the theorem that the disturbance must spread with the velocity of light. If such is the case we could no longer introduce a frame of reference in which the components of the flux of energy vanish and could no more establish a contradiction.

III. The Minkowski and Abraham Tensor for the Electromagnetic Phenomena in Material Bodies[4]

It is customary to describe the electromagnetic phenomena in material bodies with the help of two sets of field vectors $\vec{E}$, $\vec{B}$ and $\vec{D}$, $\vec{H}$ which can be considered as the components of two antisymmetrical field tensors F_{ik} and H_{ik}. While there is no controversy about the form which Maxwell's equations for electromagnetic processes in material media assume in a relativistically invariant theory, two different expressions have been proposed for the energy momentum tensor of the electromagnetic field in material bodies. They are defined by the relations

$$M_i{}^k=F_{ir}H^{kr}-\tfrac{1}{4}F^{rs}H_{rs}\delta_i{}^k \tag{14}$$

and

$$A_i{}^k=\tfrac{1}{2}\{(M_i{}^k+M_k{}^i)-(\epsilon\mu-1)(v_i\Omega^k+v_k\Omega^i)\}, \tag{15}$$

$$\Omega^i=v_kF_{lr}v^r(H^{ik}v^l+H^{kl}v^i+H^{li}v^k). \tag{15a}$$

v^i stands for the four-vector of the velocity of the moving matter. Both tensors are presented as natural generalizations of Maxwell's tensor T_{ik} which is also the energy momentum tensor of the electron theory. Both tensors have retained certain properties of Maxwell's tensor but differ from it in others.

[3] v. Laue, *Relativitaetstheorie*, Vol. I. §33.

[4] Pauli, Reference 1, §35.

(a) Minkowski's tensor M_{ik}. Here we have

$$M_{ik} \neq M_{ki}, \quad (2b) \qquad M_i^i = 0, \quad (3b)$$

$$(\partial M_i^k / \partial x^k) = 0. \quad (4b)$$

(b) Abraham's tensor A_i^k,

$$A_{ik} = A_{ki}, \quad (2c) \qquad A_i^i = 0, \quad (3c)$$

$$(\partial A_i^k / \partial x^k \neq 0). \quad (4c)$$

Remembering the theorem proved in paragraph II, we can easily understand that neither of the two tensors can satisfy all three relations (2–4), since this would lead to the consequence that the waves in material media propagate with the velocity c. We can now easily see how, according to the two assumptions, this consequence is avoided. As we know from Maxwell's equation for material media the velocity of propagation of a wave equals $c/(\epsilon\mu)^{\frac{1}{2}}$. Introducing a frame of reference which moves relative to the matter with the velocity $c/(\epsilon\mu)^{\frac{1}{2}}$ we can therefore make the whole process stationary and make the components of the energy flux S_{4k} $(k=1, 2, 3)$ vanish, as was done in paragraph II. But, in the case of Minkowski's tensor, we can now no longer conclude that the components of the density of momentum vanish because M_{4k} is no longer symmetrical. Actual calculation leads, for example, for the case of a wave propagating in the x direction, to the following expression for the components

$$\begin{aligned} &\vec{E} = \vec{H} \equiv 0, \\ &M_{ik} = 0 \quad (ik = 1, 2, 3), \\ &M_{4k} = 0 \quad (l = 1, 2, 3 \textit{ and } 4!), \\ &M_{14} = \text{const}, \\ &M_{24} = M_{34} = M_{44} = 0. \end{aligned} \quad (16)$$

It is remarkable that, according to Minkowski's theory, we could introduce a frame of reference, namely, the one mentioned above, in which the *energy density* M_{44} vanishes. This follows easily from Maxwell's equation and the transformation formulae for the tensors F_{ik} and H_{ik}. That the principle of conservation of angular momentum is not true for Minkowski's tensor because $M_{ik} \neq M_{ki}$ has been noted already by other authors. Keeping this fact together with the properties of Minkowski's tensor discussed above, we feel justified in saying that it does not constitute a satisfactory way of overcoming the restrictions as imposed by the theorem of §2.

(b) Abraham's tensor A_{ik}. Here the relation (4a) is no longer maintained while the principle of angular momentum is conserved. That (4a) is now invalid means physically that a wave propagated in a transparent material medium exerts a force on this medium. The magnitude of this force per unit of volume is equal to

$$(\epsilon\mu - 1)/c^2(\partial \vec{s}/\partial t),$$

where $\vec{s}$ denotes the Poynting vector. This can easily be proved by forming the four dimensional divergence of A_{ik}. Since there is little hope of establishing the existence of this force experimentally, one can, for the moment, only discuss its theoretical aspects. From the theorem proved in paragraph II it follows that, maintaining the symmetry of the energy momentum tensor i.e. conservation of angular momentum, we must give up either the relation (3a) or assume the existence of a force, i.e., give up the relation (4a). Abraham maintained (2a) and (3a) by claiming that the energy of the field in material bodies is an average of the momentum tensor of the electron theory and that the relations (2a) and (3a) are not destroyed by the averaging process.

To appreciate this argument one has to remember that A_{ik} constitutes an average not only of the energy momentum tensor of the microscopic electromagnetic field but also of the matter which is not electromagnetically constituted. It therefore remains a somewhat arbitrary procedure to maintain (3a) and give up (4a). (2a) on the other hand which is necessary for the conservation of angular momentum seems to us to stand on a different footing.

The theorem of paragraph II might prove useful in the discussion of electromagnetic phenomena in the "Dirac Vacuum" and of correlated questions. It also imposes certain limits on theoretical views presented by various authors according to which, for example, light quanta in empty space travel with a velocity somewhat smaller than c. We hope to report on these applications at a later time.

On the Dirac Electron in a Gravitational Field

O. HALPERN, *New York University, University Heights* AND G. HELLER, *Columbia University*

(Received June 6, 1935)

In this paper the behavior of Dirac's electron in gravitational fields is discussed for several special cases. In paragraph II a general derivation of the red shift in a gravitational field is given without reference to the special atomic system concerned. Paragraph III contains a treatment of the gyromagnetic effect.

I. INTRODUCTION

SEVERAL authors[1] have lately given a formulation of the theory of Dirac's spinning electron in a gravitational field. To obtain full covariance it was necessary to remove the restriction

$$\pi_k\gamma_i-\gamma_i\pi_k=0$$

(π_k = generalized momentum vector) (1)

previously imposed on Dirac's matrices which made them independent of the coordinates x^l. The commutation relations

$$\mathring{\gamma}_i\mathring{\gamma}_k+\mathring{\gamma}_k\mathring{\gamma}_i=2\delta_{ik} \tag{2}$$

now take on the form

$$\gamma_i\gamma_k+\gamma_k\gamma_i=2g_{ik} \quad (g_{ik}=\text{metrical tensor}) \tag{3}$$

and by differentiation of (3) one easily obtains the fundamental relation

$$\partial\gamma_i/\partial x^k=\Gamma_{ik}{}^\mu\gamma_\mu+\Gamma_k\gamma_i-\gamma_i\Gamma_k. \tag{4}$$

$\Gamma_{ik}{}^\mu$ are the Christoffel symbols, Γ_k represent an infinitesimal contact transformation. Naturally, the conditions of integrability, $\partial^2\gamma_i/\partial x^k\partial x^l=\partial^2\gamma_i/\partial x^l\partial x^k$, or more explicitly

$$\Phi_{kl}\gamma_i-\gamma_i\Phi_{kl}=\tfrac{1}{2}(R_{kl,\ i\mu}-R_{kl,\ \mu i})\gamma^\mu, \tag{5a}$$

$$\Phi_{kl}\equiv\partial\Gamma_l/\partial x^k-\partial\Gamma_k/\partial x^l+\Gamma_l\Gamma_k-\Gamma_k\Gamma_l \tag{5b}$$

($R_{kl,\ \mu\nu}$ = Riemann's curvature tensor)

must be satisfied. (4) can now be brought into the form

$$\gamma_i\Gamma_k-\Gamma_k\gamma_i=(b_{k,\ i\mu}-b_{k,\ \mu i})\gamma^\mu, \tag{4a}$$

which is solved by

$$\Gamma_k=\tfrac{1}{2}b_{k,\ \mu\nu}\gamma^\mu\gamma^\nu+\varphi_k\cdot 1, \tag{4b}$$

where φ_k is arbitrary.

Dirac's equation written in its general form is

$$\gamma^k(\partial/\partial x^k-\Gamma_k)\psi=mc\psi/\hbar r, \tag{6}$$

where γ^k and Γ_k satisfy (3) and (4). It transforms covariantly both under point transformations, $x'^k=x'^k(x^i)$ (where it behaves like a scalar), and also under contact transformations (S transformations, spin transformations). For if we multiply (6) by S^{-1} matrices (det $S\neq 0$) from the left we are led to an equation of the same form (6) on using the substitutions

$$\psi\to S^{-1}\psi, \quad \gamma^k\to S^{-1}\gamma^kS, \quad \partial/\partial x^k\to\partial/\partial x^k,$$
$$\Gamma_k\to S^{-1}\Gamma_kS-S^{-1}\partial S/\partial x^k, \tag{7}$$
$$\varphi_k\equiv\tfrac{1}{4}tr\Gamma_k\to\varphi_k-\tfrac{1}{4}\partial\log\det S/\partial x^k.$$

From (6) we infer that the matrix vector Γ_k/i reduces to the covariant vector potential of Dirac's theory for the case of a Galilean metric, $g_{ik}=\delta_{ik}$, if the spinframe (as represented by the γ^k matrices) is selected independent of the coordinates.* Similarly, it can also be shown that Eq. (6) and its Hermitian conjugate lead to the general relativistic extensions of familiar conservation theorems.

In this paper we shall consider the application of the generalized theory to two important physical phenomena. Paragraph II gives a derivation of Einstein's red shift as a direct consequence of the principles of Dirac's equation. In paragraph III the equation is applied to the

[1] The most complete report on the subject is contained in a paper by W. Pauli, Ann. d. Physik **18**, 337 (1933). We follow in our notation the paper by E. Schrödinger, Berl. Ber. 105, 1932. Compare also V. Bargmann, Berl. Ber. 345, 1932.

*One always can select "natural" frames of reference in which the γ's depend only on coordinates explicitly appearing in the g_{ik}. Examples of this are Eq. (25) and the ordinary Dirac equation.

treatment of the Dirac electron in an "artificial" gravitational field; namely, to the gyromagnetic effect.

II. The Red Shift in a Gravitational Field

According to the original line of argument given by Einstein for the red shift of light coming from heavy celestial bodies, the mechanism of this process has to be understood in the following way: The emitting atom sets up a train of waves of definite frequency which transport this frequency with them to the observer. This statement is correct only if the system of coordinates is a so-called "static" system as given by the Schwarzschild metric. The shift in frequency in this system of coordinates is due to the slowing down of the atomic vibrations in the source which shares this retardation with any type of "clock." Since the theory did not possess a model of an atomic clock, this statement had to be taken, according to Einstein, as a postulate which would have to be supplanted by proofs showing that the atoms actually satisfy the condition imposed by the general theory.[2]

Quantitatively the red shift in the approximation always used is given by the relation

$$\nu = \nu_0 g_{44}^{\frac{1}{2}}, \tag{8}$$

in which ν_0 stands for the frequency at zero gravitational potential. It is remarkable that the red shift is determined by one component g_{44} of the metrical tensor only. It was, of course, a tacit assumption in the derivation of (8) that the gravitational field should have no other effect on the atomic clock apart from slowing it down.

From the point of view of the generalized Dirac theory the question presents itself in the following form: Since the frequencies of the emitted light are determined by the eigenvalues of the Dirac equation, it is necessary, in order to obtain conformity with (8), that all eigenvalues in a static gravitational field shall be connected with those at a zero gravitational potential by the relation

$$E = E_0 g_{44}^{\frac{1}{2}}. \tag{9}$$

This relation should hold true independent of the electromagnetic fields of force in which the electron is moving, and only to the approximation mentioned above, that is, to the first order in the gravitational potentials. That this is actually the case shall be proved in what follows.

The Schwarzschild metric for a static gravitational field with the origin of the system of coordinates in the center of the heavy mass is given by the expression

$$ds^2 = (1/g_{44})[(dx^1)^2 + (dx^2)^2 + (dx^3)^2] - g_{44}(dx^4)^2, \tag{10}$$

in which the actual value of

$$g_{44} = 1 - 2m/((x^1)^2 + (x^2)^2 + (x^3)^2)^{\frac{1}{2}} \tag{10a}$$

need not concern us. *If we neglect the change of the gravitational field over atomic dimensions*, and put the center of the system of coordinates into the nucleus around which the electron is moving, (10) takes on the form

$$ds^2 = (1/g'_{44})[(dx^1)^2 + (dx^2)^2 + (dx^3)^2] - g'_{44}(dx^4)^2, \tag{11}$$

in which g_{44}' is now a constant depending on the distance of the nucleus from the center of the heavy mass, i.e., on the average position of the electron. To the same approximation we are justified in neglecting the nondiagonal terms of the Γ_k and the Γ_{ik}^{μ}. The γ^k also become constants on account of (3),

$$\gamma^4 = \mathring{\gamma}^4 (g'_{44})^{\frac{1}{2}}, \quad \gamma^k = \mathring{\gamma}^k / (g'_{44})^{\frac{1}{2}}. \tag{12}$$

The Dirac equation therefore takes on the form (omitting the primes):

$$\left[(g^{44})^{\frac{1}{2}} \mathring{\gamma}^4 \left(\frac{\partial}{\partial x^4} - \Gamma_4\right) + \frac{1}{(g^{44})^{\frac{1}{2}}} \sum_1^3 \mathring{\gamma}^k \left(\frac{\partial}{\partial x^k} - \Gamma_k\right)\right] \psi = \frac{mc}{\hbar} \psi. \tag{13}$$

In (13) the quantities $\partial/\partial x^k$ are connected with their respective values in the zero gravitational field by the tensor transformations

$$\partial/\partial \mathring{x}^k = (\partial x^i / \partial \mathring{x}^k)(\partial/\partial x^i), \tag{14a}$$

$$\Gamma_k = (\partial \mathring{x}^i / \partial x^k) \mathring{\Gamma}_i. \tag{14b}$$

[2] Cf. W. Pauli, *Relativitätstheorie*, §53, b.

But here, on account of the constancy of the g_{ik} in the neighborhood of the nucleus, (14) becomes equivalent to

$$\partial/\partial\mathring{x}^k=(1/(g^{44})^{\frac{1}{2}})(\partial/\partial x^k) \quad (k=1, 2, 3), \tag{15a}$$

$$\Gamma_4=(g^{44})^{\frac{1}{2}}\Gamma_4, \quad \mathring{\Gamma}_k=(1/(g^{44})^{\frac{1}{2}})\Gamma_k. \tag{15b}$$

Correspondingly we have the relation

$$\partial/\partial x^4=E. \tag{15c}$$

E in (15c) stands for the new energy of the electron in the gravitational field. With these simplifications (13) reduces to

$$\mathring{\gamma}^4E(g^{44})^{\frac{1}{2}}\psi=\left[\frac{mc}{\hbar}+\mathring{\gamma}^4\mathring{\Gamma}_4-\sum_1^3\mathring{\gamma}^k\left(\frac{\partial}{\partial\mathring{x}^k}-\mathring{\Gamma}_k\right)\right]\psi. \tag{16}$$

In (16) the right side obviously is the same as it was in the absence of the gravitational field, namely

$$\mathring{E}\mathring{\gamma}^4\psi. \tag{17}$$

The factor of $\mathring{\gamma}^4\psi$ on the left side of (16) determines the eigenvalue for the system which must be equal to the value $\mathring{E}$ in the absence of a gravitational field. We therefore have the relation

$$E(g^{44})^{\frac{1}{2}}=\mathring{E} \tag{18}$$

or correspondingly

$$E=\mathring{E}(g_{44})^{\frac{1}{2}} \quad (g_{44}=1/g^{44}). \tag{9}$$

(9) constitutes the expression for the red shift as derived from the Dirac equation for the electron in a gravitational field. (8) and (9) are, of course, in agreement. This concludes the proof that the Dirac electron constitutes an atomic clock in the sense used by Einstein.

III. The Gyromagnetic Effect[3]

While in the derivation of the red shift a non-Euclidean metric was essential for the result obtained, we shall here treat a problem of rotating axes for which, obviously, the metric remains Euclidean though the g_{ik} differ from their Galilean values.

The gyromagnetic effect, as is well known, consists in the magnetization of substances containing spinning electrons and is due to a rotation of the matter in bulk. The Coriolis force set up by the rotation acts on the electrons like a magnetic field. The frequency of the rotation is connected with the intensity of the equivalent magnetic field by the relation

$$\omega/II=e/mc. \tag{19}$$

In (19) we have written down the relation for the case of interaction between spin and rotation. For orbital motion and rotation the ratio is given by

$$\omega/II=e/2mc. \tag{20}$$

The difference between (19) and (20) is known as the gyromagnetic anomaly of the spinning electron. The experiment leads to a factor which, though slightly smaller, lies close to (19).

The theoretical treatment of this problem is straightforward on the basis of the general theory of the Dirac electron. We introduce a frame of reference given by the relations:

$$\begin{aligned} x^1&=\mathring{x}^1\cos\omega t+\mathring{x}^2\sin\omega t,\\ x^2&=-\mathring{x}^1\sin\omega t+\mathring{x}^2\cos\omega t,\\ x^3&=\mathring{x}^3,\\ x^4&\equiv ict=\mathring{x}^4, \end{aligned} \tag{21}$$

from which we obtain for the g_{ik} the following scheme:

$$g_{ik}=\begin{Vmatrix} 1 & 0 & 0 & i\omega' x^2 \\ 0 & 1 & 0 & -i\omega' x^1 \\ 0 & 0 & 1 & 0 \\ i\omega' x^2 & -i\omega' x^1 & 01 & -\omega'^2[(x^1)^2+(x^2)^2] \end{Vmatrix} \cdot(\omega'=\omega/c). \tag{22}$$

Limiting ourselves to a first approximation, i.e., taking the quantity ω as small compared with all atomic frequencies, we can, with the help of (3) and (22) easily determine the quantities

$$\begin{aligned} \gamma_1&=\mathring{\gamma}_1+i\omega' x^2\mathring{\gamma}_4, \quad \gamma_3=\mathring{\gamma}'^3\\ \gamma_2&=\mathring{\gamma}_2-i\omega' x^1\mathring{\gamma}_4, \quad \gamma_4=\mathring{\gamma}_4. \end{aligned} \tag{23}$$

[3] Cf. the comprehensive report by L. T. Barnett, Rev. Mod. Phys. **7**, 129 (1935).

With the help of (22), (23) and (4) we can then calculate the explicit expressions for $\Gamma_{ik}{}^{\mu}$ and Γ_k. The matrix terms in Γ_k are given by

$$\begin{aligned}\Gamma_1&=(i\omega'/4)(\gamma^2\gamma^4-\gamma^4\gamma^2)=-\omega'\alpha_y/2,\\ \Gamma_2&=(i\omega'/4)(\gamma^4\gamma^1-\gamma^1\gamma^4)=\omega'\alpha_x/2,\\ \Gamma_3&=0,\\ \Gamma_4&=-(i\omega'/4)(\gamma^1\gamma^2-\gamma^2\gamma^1)=\omega'\sigma_z/2,\end{aligned}\tag{24}$$

and we arrive at the new form of the Dirac equation, which is accurate to the first power in ω':

$$H\psi\equiv[H_0\psi+\omega'(\alpha_x y-\alpha_y x)\pi_t+\tfrac{1}{2}\hbar\omega'\sigma_z]\psi=0. \tag{25}$$

H_0 stands for the Hamiltonian in a nonrotating system of coordinates, $H_0=-\pi_t+\alpha\cdot\pi+mc\beta$. The other symbols have their conventional meaning. H differs from H_0 by the terms

$$(\omega/c)(\alpha_x y-\alpha_y x)\pi_t+(\hbar\omega/2c)\sigma_z. \tag{26}$$

If the electron moved in a homogeneous magnetic field given by the vector potential

$$A_x=\tfrac{1}{2}Hy,\quad A_y=-\tfrac{1}{2}Hx, \tag{27}$$

and in a system of coordinates with a Galilean metric, the terms due to the vector potential would be equal to

$$(\bar{\omega}/c)(\alpha_x y-\alpha_y x)mc,\quad (\bar{\omega}=eH/2mc). \tag{28}$$

Comparing (26) and (28) we notice that the magnetic field which would produce the same additional terms as the rotating system of coordinates depends on the state of the electron. In other words, there does not exist a universal gyromagnetic relation between frequencies of rotation and intensity of the magnetic field.

It is justified in our approximation to write in (26)

$$\pi_t=mc,$$

because the difference between π_t and mc is of relativistic order of magnitude and can therefore be omitted *in the small correction term*. Noting furthermore, that

$$H\pi_t-\pi_t H=0, \tag{29}$$

i.e., $\pi_t=\text{const.}=E$,

and that

$$H_0\sigma_z-\sigma_z H_0\backsimeq 0 \tag{30}$$

except for terms of relativistic order of magnitude, we can form a second order equation out of (25)

$$H_0{}^2\psi-2m\omega(L_z+\tfrac{1}{2}\hbar\sigma_z)\psi=0. \tag{31}$$

Here L_z stands for the z component of the orbital angular momentum. $L_z+\frac{1}{2}\hbar\sigma_z$ is an integral of the equations of motion. In the case of a magnetic field given by the vector-potential (27) the equation analogous to (31) would take the form

$$H_0{}^2\psi-2m\bar{\omega}(L_z+\hbar\sigma_z)\psi=0. \tag{32}$$

(31) and (32) permit us to verify (19) and (20). For $L_z=0$ we would obtain equivalence of (31) and (32) for

$$\omega=2\bar{\omega},$$

while for $L_z\gg\hbar\sigma_z$ one obtains

$$\omega=\bar{\omega}.$$

Intermediate stages are given by the formula analogous to Landé's:

$$\omega/\bar{\omega}=(L_z+\hbar\sigma_z)/(L_z+\tfrac{1}{2}\hbar\sigma_z). \tag{33}$$

An alternative way of treating the problem[4] goes as follows: Starting from the original form of Dirac's equation and transforming the momentum operators to rotating coordinates with the help of the relations

$$\partial/\partial\bar{t}=\partial/\partial t+\omega y\partial/\partial x-\omega x\partial/\partial y,\quad \text{etc.}, \tag{34}$$

one arrives at the following (exact) Dirac equation

$$\bar{H}\Psi=[-\pi_t-\omega' L_z+\bar{\alpha}\cdot\pi+mc\beta]\Psi=0, \tag{35}$$

where

$$\begin{aligned}\bar{\alpha}_x&=\alpha_x\cos\omega t+\alpha_y\sin\omega t,\\ \bar{\alpha}_y&=-\alpha_x\sin\omega t+\alpha_y\cos\omega t,\\ \bar{\alpha}_z&=\alpha_z.\end{aligned}\tag{36}$$

This equation permits of an interpretation similar

[4] O. Halpern, Phys. Rev. **37**, 1719 (1931).

to that which we have given to (25) except for the ambiguity in (35). π_t *is no longer an integral of the equation of motion* since it does not commute with $\bar{H}$. This constitutes a special case illustrating a general feature of the covariant form of Dirac's equation. It is due to the fact that the α's and γ's are now functions of the coordinates. Two equations which are equivalent to each other are not interpretable with equal ease because, as a result of the special choice of γ^i, one does not admit the same integrals as the other one. Since (35) and (25) are equivalent, there must exist, of course, a spin transformation which connects the two equations with each other. The transformation is given by the matrices (accurate to first order terms in ω)

$$S=\cos\frac{\omega t}{2}\cdot 1-i\sin\frac{\omega t}{2}\cdot\sigma_z-\frac{\omega'}{2}\left(y\cos\frac{\omega t}{2}+x\sin\frac{\omega t}{2}\right)\alpha_x+\frac{\omega'}{2}\left(x\cos\frac{\omega t}{2}-y\sin\frac{\omega t}{2}\right)\alpha_y,$$
$$S^{-1}=\cos\frac{\omega t}{2}\cdot 1+i\sin\frac{\omega t}{2}\cdot\sigma_z+\frac{\omega'}{2}\left(y\cos\frac{\omega t}{2}+x\sin\frac{\omega t}{2}\right)\alpha_x-\frac{\omega'}{2}\left(x\cos\frac{\omega t}{2}-y\sin\frac{\omega t}{2}\right)\alpha_y. \quad (37)$$

The Hamiltonians are connected by the relation $H=S^{-1}\bar{H}S$ (7a)

and the eigenfunctions by $\psi=S^{-1}\Psi$. (7b)

SEPTEMBER 1, 1935 PHYSICAL REVIEW VOLUME 48

The Efficiency of the Tube Counter

SELBY M. SKINNER, *Columbia University*

(Received April 5, 1935)

The efficiency of counting ionizing particles by the tube counter is investigated, taking account of the electrical behavior of the counter and the random nature of the arrival of the particles. Expressions are obtained for the efficiency of counting, average recovery time, average voltage impulse delivered to the amplifier, and the average number of particles counted per unit time, N, in terms of the number of particles arriving per unit time, N_0, the time constant of the counter, and one other parameter, d, which is constant for a given counter. Methods for measuring d (which for most counters will lie between 1.3 and five) are indicated. The efficiency of counting decreases with an increase of N_0, rapidly at first, then more slowly, so as to have the asymptotic value $1/d$. The determination of N_0 from N, and the general question of counter efficiency are discussed.

THE behavior of Geiger-Müller and similar types of counters has been studied experimentally by various investigators.[1] As the negative potential on the tube, V_T, is increased from zero, the average number of counts per unit time, the source being constant, behaves as in Fig. 1. Counting begins at the "threshold voltage," V_S, rises rapidly to a value N, and remains nearly constant for a range of voltage which depends on the individual counter. In a well-built counter, the flat region of the curve extends over a considerable range of voltage. The counter is operated in this region, since any slight variation of supply voltage will then have negligible effect on the rate of counting. At higher voltages, the

[1] (The first two references give a good bibliography of the previous work.) Burger Scheidlin, Ann. d. Physik **12**, 283 (1932); Schulze, Zeits. f. Physik **78**, 92 (1932); Medicus, Zeits. f. Physik **74**, 350 (1932); Curtis, Bur. Standards J. Research **10**, 229 (1933); Brunetti and Ollano, Nuovo Cimento **10**, 92 (1933); Greiner, Zeits. f. Physik **81**, 543 (1933); Hummel, Zeits. f. Physik **76**, 483 (1932); Physik. Zeits. **34**, 331 (1933); Kuhn, Zeits. f. Instrumentenk. **54**, 415 (1934); Danforth, Phys. Rev. **46**, 1026 (1934); J. Frank. Inst. **219**, 108 (1935); Wernow, Trav. de l'Inst. d'Etat de Radium **2**, 30 (1933) (abstracted in Physik. Berichte **15**, 1448 (1934)); H. Teichmann, Physik. Zeits. **35**, 637 (1934); Bosch, Ann. d. Physik **19**, 65 (1934); Janossy, Zeits. f. Physik **88**, 372 (1934); Henning and Schade, Zeits. f. Physik **90**, 597 (1934); A relevant article on photon counters is Werner, Zeits. f. Physik **90**, 384 (1934); **92**, 705 (1934).

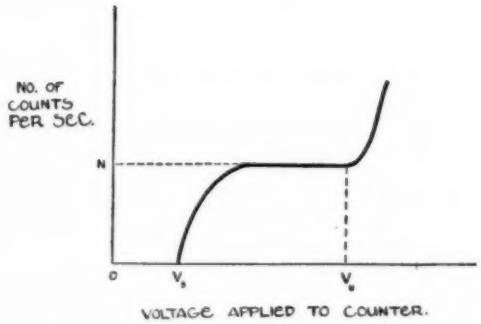

FIG. 1. Sensitivity curve for a tube counter.

curve begins to rise steeply, the conditions for breakdown are rapidly reached, and conditions are no longer suitable for counting.

When an ionizing particle passes through the counter, held at a potential in the region $V_S \rightarrow V_U$, the ions formed cause a discharge during which a certain amount of charge is transferred to the wire. In general, three types of behavior have been found. In the first, there is a small change in the wire potential, considerably less than that required to reduce the potential across the tube to V_S. The voltage impulse given the amplifier in this case is small compared to that in the other two, which we shall call types I and II. Fig. 2 shows the general behavior of these types of discharge, whose characteristics are beautifully shown in the photographs of Danforth.[1] The negative potential of the wire, v, is plotted against time. When $v = V_T - V_S$, the potential across the counter is the threshold potential. Thus, if $v > V_T - V_S$, no discharge is possible. In type I, there will then be no further discharge until v has fallen to $V_T - V_S$. The recovery time, τ, is the time necessary for this to take place. τ depends on the discharge which preceded it. The greater v is at the moment the discharge occurs, the less will be the initial potential of the wire, v_0, and the smaller will be the recovery time following the discharge. In type II, the counter will register no further particle until after the time T corresponding to the straight portion of the curve, Fig. 2b. The value of T can also depend on the value of v at the moment the last discharge occurred. In either case, there is a statistical distribution of τ's, but not a completely random distribution. The problem is a particular case of chain statistics. The efficiency of counting particles under such circumstances will be investigated below. The question has been considered under the assumption of a constant τ.[2] For a counter in actual operation, τ is not constant; the statistical distribution of τ's will be different in the two cases, type I and type II, hence they will be treated separately.

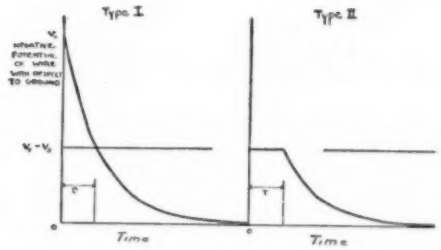

FIG. 2. Recovery time of counters.

Consider a situation in which, on the average, N_0 ionizing particles arrive per unit time. The chance of arrival of the particles is the same at any moment, i.e., the arrivals are distributed at random. The probability that the interval between the arrival of two particles lies between t_1 and $t_1 + dt_1$ is $N_0 \exp(-N_0 t_1) \cdot dt_1$. The probability that t_1 is more than any definite t_0 is $\int_{t_0}^{\infty} N_0 \exp(-N_0 t_1) \cdot dt_1 = \exp(-N_0 t_0)$. Let $\omega(\tau) d\tau$ be the probability that after a count the recovery time of the counter lies between τ and $\tau + d\tau$ when counting such a distribution of particles. Any particular τ_0 depends both on the recovery time for the previous discharge, and on the interval which elapsed after the last discharge, before the next particle arrived. If $t_1 < \tau_0$, the particle was not counted. Thus, in a great many discharges for which $\tau = \tau_0$, the fraction of the next particles to arrive which will be counted will be $\exp(-N_0 \tau_0)$. Those which arrive after an interval $t_1 > \tau_0$, thus being counted, cause a new discharge, whose recovery time $\tau' = \tau'(\tau_0; t_1)$. The relation $\tau' = \tau'(\tau_0; t_1)$ may be determined from the mechanism of the discharge. The probability that

[2] Johnson and Street, J. Frank. Inst. **215**, 239 (1933); Locher, J. Frank. Inst. **216**, 553 (1933); Volz, Zeits. f. Physik **93**, 539 (1935). If the counter be regarded as a mechanism which is not affected at all by any particle traversing it during its recovery time, its efficiency for constant τ is $(1 + N_0 \tau)^{-1}$, which is equivalent to the expression given in the first reference. The expression in the second reference gives too high an efficiency for particles arriving at random. The expression used by Volz allows for the ionization produced by the particle traversing the counter during its recovery time, and has the advantage of being mathematically tractable.

the new recovery time will lie between τ' and $\tau'+d\tau'$, is then: the product of the probability of the occurrence of a τ, by the probability the succeeding interval before the arrival of the next particle *counted* is such that $\tau'=\tau'(\tau;\ t_1)$, or $t_1=t_1(\tau;\ \tau')$ summed over all τ. Since for a particular τ only the fraction $\exp(-N_0\tau)$ are counted, the latter probability is

$$\frac{N_0 \exp(-N_0 t_1)\cdot dt_1}{\exp(-N_0\tau)}, \quad t_1 \geqslant \tau; \quad 0, \quad t_1 < \tau.$$

Therefore,

$$\omega(\tau')d\tau' = \int_{\text{all } \tau} \omega(\tau)d\tau \frac{N_0 \exp(-N_0 t_1)\cdot dt_1}{\exp(-N_0\tau)}, \qquad t_1 \geqslant \tau. \quad (1)$$

The range dt_1 must be that range, which, for any definite τ, corresponds to the range $d\tau'$.

$$\omega(\tau')d\tau' = \int_{\text{all } \tau} \omega(\tau)d\tau \frac{N_0 \exp(-N_0 t_1)}{\exp(-N_0\tau)}\left(\frac{\partial t_1}{\partial \tau'}\right)d\tau', \qquad t_1 \geqslant \tau. \quad (2)$$

The existence of a probability distribution of the τ's requires $\omega(\tau')$ to be the same function of τ', which $\omega(\tau)$ is of τ. (2) is an homogeneous integral equation for $\omega(\tau)$, with the kernel

$$K(\tau',\ \tau) = \left[\frac{N_0 \exp(-N_0 t_1)}{\exp(-N_0\tau)}\cdot\frac{\partial t_1}{\partial \tau'}\right], \quad (3)$$

in which t_1 is a function depending on the type of discharge. In both of the cases to be considered $K(\tau',\ \tau)$ is of the form $f(\tau')$. Therefore,

$$\omega(\tau') = \int_0^{\tau_{\max.}} \omega(\tau)d\tau f(\tau') \quad (4)$$

$$= If(\tau') \qquad (\partial I/\partial\tau' = 0). \quad (4')$$

Substituting (4') in (4), we see that a necessary condition for the existence of a solution, is

$$1 = \int_0^{\tau_{\max.}} f(\tau')d\tau'. \quad (5)$$

When (5) is true, (4') is the solution of (4). Evidently

$$\int_0^{\tau_{\max.}} \omega(\tau)d\tau = 1.$$

$$\therefore \quad I = 1, \quad \text{and} \quad \omega(\tau) = f(\tau). \quad (6)$$

The total number of counts that occur when N_0 particles per unit time arrive at the counter, is the number whose intervals equal or exceed the (variable) recovery time.

$$N = \int_0^{\tau_{\max.}} \omega(\tau) N_0 \exp(-N_0\tau)\cdot d\tau \quad (7)$$

and the fraction of incident particles counted is then

$$N/N_0 = \int_0^{\tau_{\max.}} f(\tau) \exp(-N_0\tau)\cdot d\tau. \quad (8)$$

The average and mean square recovery times are

$$\bar{\tau} = \int_0^{\tau_{\max.}} \tau f(\tau)d\tau, \quad \overline{\tau^2} = \int_0^{\tau_{\max.}} \tau^2 f(\tau)d\tau. \quad (9)$$

The average voltage impulse delivered to the amplifier, namely, the average rise of voltage of the wire during a discharge, is

$$v_A = \int_0^{\tau_{\max.}} (v_0' - v_1) f(\tau)d\tau. \quad (10)$$

The quantities "v" are defined below.

Discharges of Type I

The maximum potential to which the wire rises during a discharge is v_0. The decay through the system, R and C,[3] takes place according to the usual relation

$$v = v_0 \exp(-t/RC). \quad (11)$$

When $v \leq V_T - V_S$, a new discharge may occur. That is,

$$V_T - V_S = v_0 \exp(-\tau/RC). \quad (12)$$

The statistical variation of the v_0's conditions that of the τ's. If every discharge were to result in the raising of the wire to the same potential v_0, the τ's would have a value (constant so long as N_0 were constant) $\tau = RC \ln(v_0/[V_T - V_S])$ (where, in general, v_0, and therefore τ, depend on the value of N_0), and

[3] R and C will mean the total resistance and capacity from wire to ground, respectively.

$$N/N_0=\exp(-N_0\tau)=[v_0/(V_T-V_S)]^{-N_0RC}. \quad (13)$$

Danforth[1] has found in discharges of type I, the following:[4]

i. $v_0'-(V_T-V_S)$ increases with V_T;
ii. for the same V_T, v_0' decreases with increase of C; (from the examples given, $v_0'-(V_T-V_S)\propto 1/C$);
iii. v_0' is smaller if the discharge occurs before v from the previous discharge has become zero.

To these considerations, we add the fact that below the threshold voltage, the yield of new ions to continue the discharge decreases greatly. Thus, when the previous v has become zero, the relation will be

$$\begin{aligned} v_0'-(V_T-V_S)&=(A/C)(V_T-V_S), \\ A&=A(V_T) \\ v_0'&=((A+C)/C)(V_T-V_S) \\ &=(C_1/C)(V_T-V_S), \quad C_1>C. \end{aligned} \quad (14)$$

If C_1 be considered as the effective capacity of the system during discharge, this would correspond to a discharge which ceases when $V=V_S$, the quantity $q=C_1(V_T-V_S)$ being the amount carried over to the wire. This charge would be stored on C (which includes the capacity of the wire) and in the space between the wire and the tube. When the discharge ceases, the ions in the latter region are driven across by the remaining field, leaving only the small sheath about the wire, raising v from V_T-V_S to v_0, and decreasing C_1 to C. The actual relations during discharge, of course, may be quite different, and the relation above still hold.

If the discharge occurs at a time t_1 after the last pulse, when the previous $v=v_1\neq 0$, the voltage across the tube would be V_T-v_1, and the expression for v_0' would be

$$v_0'=v_1+q/C=v_1+(C_1/C)[(V_T-v_1)-V_S], \quad (14')$$

where

$$v_1=v_0\exp(-t_1/RC). \quad (11')$$

v_0 is the maximum voltage on the wire in the last impulse. Let the recovery times of the two discharges be τ' and τ, respectively; then

$$\begin{aligned} V_T-V_S&=v_0\exp(-\tau/RC) \\ &=v_0'\exp(-\tau'/RC). \end{aligned} \quad (15)$$

By (15), (11'), and (14'), the relation between τ', τ and t_1, is

$$\begin{aligned} &(V_T-V_S)\exp(\tau'/RC) \\ &\quad=(V_T-V_S)\exp[(\tau-t_1)/RC] \\ &\quad+(C_1/C)(V_T-V_S)\{1-\exp[(\tau-t_1)/RC]\} \end{aligned}$$

$$e^{-t_1/RC}=e^{-\tau/RC}\frac{d-e^{\tau'/RC}}{d-1}; \quad d=C_1/C>1. \quad (16)$$

Since $d>1$, the maximum τ' occurs when $v_1=0$, i.e., $t_1=\infty$. In that case (14) holds, and comparison with (15) shows

$$d=\exp(\tau_{\max.}/RC) \quad (17)$$

and therefore, (16) incorporates in itself the fact that $t_1\geqslant\tau$.

$$\begin{aligned} K(\tau',\tau)&=N_0\exp[-N_0t_1(\tau;\tau')+N_0\tau]\cdot\partial t_1/\partial\tau' \\ &=N_0\exp(N_0\tau) \\ &\quad\cdot\left[e^{-\tau/RC}\left(\frac{d-e^{\tau'/RC}}{d-1}\right)\right]^{N_0RC}\left[\frac{e^{\tau'/RC}}{d-e^{\tau'/RC}}\right] \\ &=f(\tau'), \end{aligned}$$

$$f(\tau')=N_0\left[\frac{d-e^{\tau'/RC}}{d-1}\right]^b\left[\frac{e^{\tau'/RC}}{d-e^{\tau'/RC}}\right]$$

$$[b=N_0RC]. \quad (18)$$

The condition (5) is satisfied, as may be seen by the substitution

$$w=\left[\frac{d-\exp(\tau'/RC)}{d-1}\right] \quad (19)$$

in the integrand. By this same substitution, and the substitution

$$x=[\exp(-\tau'/RC)]\cdot w,$$

we have,

$$N/N_0=\int_0^1 bx^{b-1}dx/(1+(d-1)x), \quad (20)$$

[4] Primed quantities refer to the following discharge, unprimed to the preceding one.

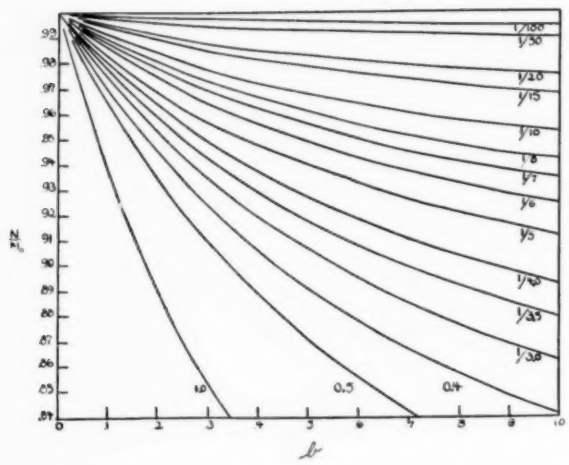

FIG. 3a.

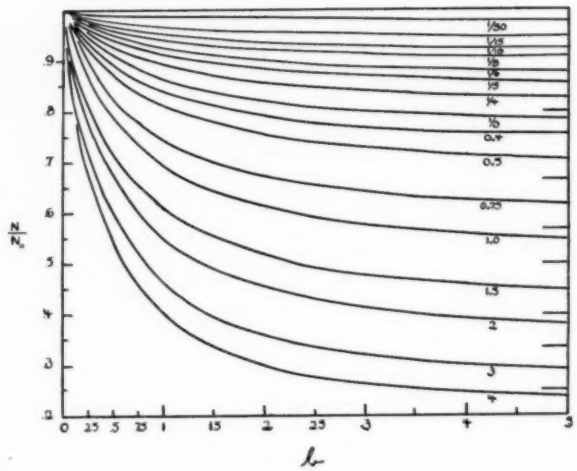

FIG. 3b.

FIG. 3. Efficiency of counting for discharges of type I. The abscissa is $b(=NRC)$. The value of "$d-1$" appears directly below each curve.

$$\bar{\tau}=bRC\ln d\int_0^1 \ln\left[1-(d-1)/d)w\right]w^{b-1}dw, \quad (21)$$

$$\bar{\tau}^2=b(RC)^2(\ln d)^2\int_0^1\{\ln\left[1-((d-1)/d)w\right]\}^2 \times w^{b-1}dw. \quad (21')$$

In order to evaluate (10) we have

$$(v_0'-v_1)=q/C=d[(V_T-V_S)-v_1] =d(V_T-V_S)[1-\exp(\tau-t_1)/RC],$$

which by (19), gives as the expression for the average voltage impulse delivered to the amplifier,

$$v_A=d(V_T-V_S)/(b+1) =(v_0)_{\max.}/(N_0RC+1). \quad (21'')$$

For the experimentalist, the important quantity is N/N_0. The integral in (20) is not a standard form, and, except for special values of the constants, recourse must be had to series expansion. The series below are convenient.

$$\frac{N}{N_0}=b\sum_0^\infty\frac{(-1)^n(d-1)^n}{n+b}$$

$$=1-b\sum_1^\infty\frac{(-1)^n(d-1)^n}{(n+b)}, \qquad 2>d\geq 1 \quad (22)$$

$$=\frac{b}{2}\left[Z'\left(\frac{b+1}{2}\right)-Z'\left(\frac{b}{2}\right)\right], \quad d=2;$$

where $Z'(a)=\dfrac{d}{da}\ln\Gamma(a)$

$$=\frac{b}{d}\sum_0^\infty\frac{(d-1)^n}{d^n}\frac{n!}{(b+n)(b+n-1)\cdots(b+1)b}. \quad (22')$$

For small values of d, the computation of (22) is more convenient, and it has the advantage of being an oscillating series. However, for $d\geq 2$, the expansion of the denominator in the integrand as $\Sigma(-1)^n(d-1)^nx^n$ is no longer uniformly convergent, and integration term by term is not possible. The formal series (22), it will be noted, is not convergent in this case. To obtain (22') we set

$$b\int_0^1\frac{x^{b-1}dx}{1+(d-1)x}=\frac{b}{d}\int_0^1\frac{x^{b-1}dx}{1+((d-1)/d)(x-1)} =\frac{b}{d}\sum_0^\infty\left(\frac{d-1}{d}\right)^n\int_0^1(1-u)^{b-1}u^ndu.$$

The series follows immediately.

The rapidity of convergence of the series (22) may be increased by a transformation of the Kummer type. Applied once, for instance, the series becomes

$$\frac{N}{N_0}=\frac{1}{d}+\frac{b(d-1)}{d}\sum_0^\infty\frac{(-1)^n(d-1)^n}{(b+n)(b+n+1)}.$$

Fig. 3 shows the behavior of the function N/N_0 as b is increased, for different values of the parameter d. Fig. 5 is a plot of NRC $(=bN/N_0)$ against b, showing the variation in the number of particles counted, with the number arriving, for different values of d. For the larger values of b, the curves are practically linear due to the approximate constancy of N/N_0 in this region. As the number of ionizing particles to be counted increases from zero, the efficiency of counting decreases steadily. In the limit, for a very large number of particles arriving per unit time, the ratio approaches the value $1/d$.

$$\frac{N}{N_0}=b\int_0^1 \frac{x^{b-1}dx}{1+(d-1)x}=\frac{1}{d}\int_0^b \frac{(1-v/b)^{b-1}dv}{1-((d-1)/d)v/b},$$

$$\operatorname*{Lim}_{b\to\infty}\left(\frac{N}{N_0}\right)=\frac{1}{d}\int_0^\infty e^{-v}dv=\frac{1}{d}.$$

In Fig. 3, the asymptotes are indicated by short lines directly under the curves. If, by some curious chance, the particles should arrive at equal intervals, the recovery time would be the same for each discharge.[5] However, it may easily be seen by Eq. (16), that τ would be constant only so long as the number of particles arriving per unit time remained the same. An increase of N_0 (the particles still coming at equal intervals) would decrease τ. Thus N/N_0 would not decrease exponentially to zero, as predicted by the assumption of a constant τ.

For a given system, RC ln d is equal to $\tau_{\max.}$, i.e., the value τ takes when the potential of the wire drops to zero before the arrival of the next particle. Therefore d does not vary with the rate of arrival of the particles. Both b and d are of dimensions zero. Any change in the unit of time used is immaterial, as it should be.

The trend of N/N_0 has experimental significance, but the limit is not closely approached in practice, since b will not usually take large values. (A possible exception occurs in the case of showers, where, for a short time, b may become large.) As the number of incident particles per second (and hence b) increases, the amount of charge available in each discharge, and the maximum potential of the wire, decrease to the point where the amplifier does not supply the mechanical recorder with sufficient impulse to register the counts. For example, the voltage impulse delivered to the amplifier decreases to one-fifth of the value for slow rates of counting, when N_0RC has become equal to four. The values of b for which the mechanical recorder fails to respond, in general, will correspond to values of N_0 of such order that the tube counter is not the logical detector for the incident particles. With a counter of the usual construction, RC will be of the order of 0.1 to 0.001 sec. A value of $b=5$ would mean the arrival of at least fifty ionizing particles per second. For the detection of such a stream, an electrometer or electroscope would profitably be used. For this reason, values of b greater than $b=5$ are not included in the figures.

[5] Eq. (13) referred to the case where τ is assumed constant, the particles arriving at random. In the case of particles coming at equal intervals, it is not permissible to assume the expression exp $(-N_0\tau)$.

Discharges of Type II

The discharge in this case is of the form in Fig. 2. This takes place at higher tube voltages, and with larger C. The charge involved raises the wire to V_T-V_S, and keeps it there for a time T, after which v falls exponentially to zero. τ is given by T. During the time T, a current $I=(V_T-V_S)/R$ is passing through the tube. The mechanism is less certain. The fact that the process occurs at higher voltages suggests a temporarily self-sustaining discharge. The treatment below will be quite general, however. The following assumptions will be made:

1. There exists a maximum potential to which the wire can rise, $\bar{v}$. For the present the only assumption that will be made in regard to $\bar{v}$ is that $\bar{v}\geqslant V_T-V_S$. This is logical, since if $\bar{v}$ were less than V_T-V_S, the next incident particle would be registered even if it were to arrive immediately afterwards. τ' would be zero, which, of course, is not true.
2. The total quantity of electricity which passes in the discharge is of the form $q=C_1(V_T-V_S-v_1)$. C_1 depends on V_T, R and C, but not on v_1. C_1 must be greater than C in order to have the straight line portion of the discharge occur. The dependence of C_1 on R may be expected since R affects the value of the current through

the tube in the steady state. If the counter is operated on the flat portion of its sensitivity curve, the variation of C_1 with V will be negligible. Thus, for a given counter, C_1 will have a definite value. We define $A=C_1-C$.

The relation between t_1, τ and τ', is obtained as follows: The particle arrives when $v=v_1$. Since it is not registered if $t_1<T$, the value of v_1 will be less than $\bar{v}$. In raising the wire to $\bar{v}$, an amount of electricity $C(\bar{v}-v_1)$ is used. During the rest of the discharge, an amount $q_1=C_1(V_T-V_S-v_1)-C(\bar{v}-v_1)$ will pass. This will flow to ground through R as a current $I=\bar{v}/R$, and in time T an amount $(\bar{v}/R)T$ flows to ground. This is equal to q_1, since the exponential decrease of wire potential is due to the loss of the charge on the wire and condenser, which has held them at $\bar{v}$.

$$T=\frac{q_1}{I}=C_1R\frac{V_T-V_S-v_1}{\bar{v}}-CR\left(1-\frac{v_1}{\bar{v}}\right). \quad (23)$$

The recovery time is $\tau=T+\tau_1$, where $\tau_1=RC\ln(\bar{v}/(V_T-V_S))$ is the time required for $\bar{v}$ to decay to V_T-V_S. The potential of the wire when $t>T$, is

$$v=\bar{v}\exp[-(t-T)/RC]$$

and we have

$$V_T-V_S=\bar{v}\exp[-\tau_1/RC]$$

so that

$$v=(V_T-V_S)\exp[(\tau_1+T-t)/RC].$$

The new recovery time is then, by (23)

$$\tau'=\tau_1'+T'=RC\ln[\bar{v}/(V_T-V_S)]$$
$$-((V_T-V_S)/\bar{v})R(C_1-C)\exp[(\tau-t_1)/RC]$$
$$+C_1R((V_T-V_S)/\bar{v})-CR \quad (24)$$

so that the relation between τ', τ, and t_1 is

$$\exp(-t_1/RC)=[\exp(-\tau/RC)]$$
$$\times\left[\frac{RC(\ln x)+(RC_1/x)-RC-\tau'}{R(C_1-C)/x}\right], \quad (25)$$

where

$$x=\bar{v}/(V_T-V_S).$$

The kernel of the integral equation for $\omega(\tau)$ is then,

$$N_0\left[\frac{RC\{(\ln x)-1\}+(RC_1/x)-\tau'}{R(C_1-C)/x}\right]^{N_0RC-1}$$
$$\cdot\left[\frac{RC}{R(C_1-C)/x}\right]=\frac{b}{g}\left[\frac{e-\tau'}{g}\right]^{b-1}, \quad (26)$$

the two equations being a definition of e and g.

For the existence of a solution, by (5),

$$\int_0^{\tau_{\max.}}\frac{b}{g}\left[\frac{e-\tau}{g}\right]^{b-1}d\tau=1,$$

where $\tau_{\max.}$ is the τ corresponding to an infinite t_1; by (25), $\tau_{\max.}=e$. The condition becomes

$$b\int_0^e\left[\frac{e-\tau}{g}\right]^{b-1}\frac{d\tau}{g}=[u^b]_0^{e/g}=1$$

so that for a solution to exist, e/g must be equal to one, which reduces to the equation

$$\phi(x)=\ln x+1/x=1; \quad (x=\bar{v}/(V_T-V_S)). \quad (27)$$

The function $\phi(x)$ has a minimum for $x=1$, at which its value is one. For all other values of x more than zero, the value of the function is more than one. The condition (27) therefore requires that

$$\bar{v}=V_T-V_S. \quad (28)$$

This is exactly what is found by Schulze, and by Danforth.

When $\bar{v}=V_T-V_S$;

$$\tau_1=0; \quad \tau=T, \quad e=g=R(C_1-C).$$

With these values of the constants,

$$\frac{N}{N_0}=\int_0^e\frac{b}{e}\left[1-\frac{\tau}{e}\right]^{b-1}\exp(-N_0\tau)\cdot d\tau$$
$$=\int_0^1 b[1-u]^{b-1}\exp(-fu)\cdot du \quad (29)$$
$$f=b(d-1),$$

where b and d are the same as before.

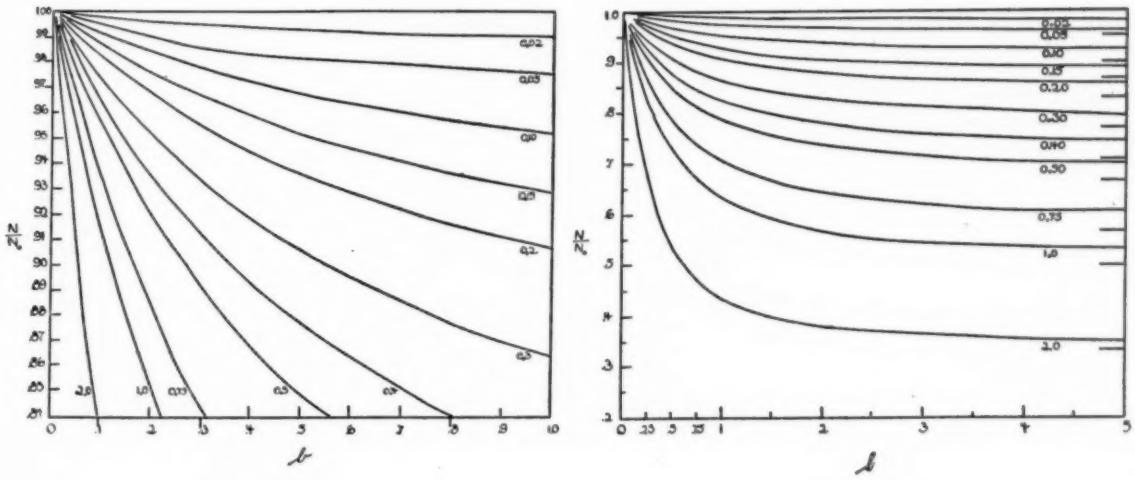

FIG. 4a. FIG. 4b.

FIG. 4. Efficiency of counting for discharges of type II. The abscissa is $b(=NRC)$. The value of "$d-1$" appears directly below each curve.

$$\bar{\tau}=\frac{b}{e}\int_0^e\left[1-\frac{\tau}{e}\right]^{b-1}\tau d\tau=\frac{e}{b+1}$$

$$=\frac{R(C_1-C)}{N_0RC+1}=\frac{RA}{N_0RC+1}, \qquad (30)$$

$$\bar{\tau}^2=\frac{e^2}{(b+1)(b+2)}. \qquad (30')$$

The average voltage impulse applied to the grid of the amplifier is obtained as follows:

$$v_0'-v_1=\bar{v}[1-\exp\,((T-t_1)/RC)]$$

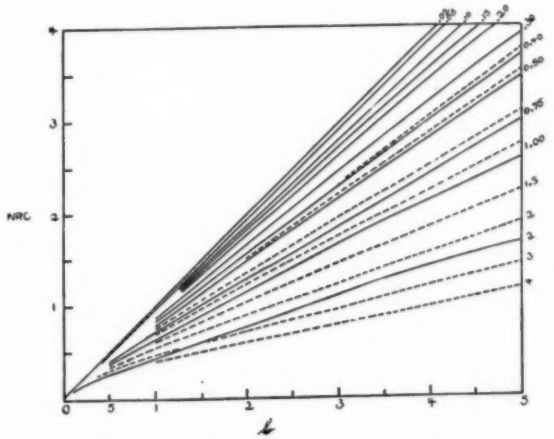

FIG. 5. The number of particles counted in relation to the number arriving. (The unit of time is RC.) The dashed lines refer to discharges of type I, the solid lines to those of type II. For small values of "$d-1$," the two cannot be drawn separately to this scale. The value of "$d-1$" is given at the right of each curve.

$$=(V_T-V_S)[1-(1-\tau'/e)],$$

$$v_A=(V_T-V_S)/(b+1) \qquad (30'')$$

$$=(v_0)_{\max.}/(N_0RC+1) \text{ as before.}$$

The behavior of the function N/N_0 and the function NRC are given in Figs. 4 and 5. Again the integral for N/N_0 is not a standard form, and must be evaluated by series expansion. Expanding the exponential, the expression below is obtained:

$$\frac{N}{N_0}=b\sum_0^\infty\frac{(-f)^n}{n!}\,\frac{\Gamma(b)\Gamma(n+1)}{\Gamma(n+b+1)}$$

$$=1-\sum_1^\infty\frac{(-1)^nb^n(d-1)^n}{(b+n)(b+n-1)\cdots(b+1)}. \qquad (29')$$

This series converges rapidly, and is in convenient form. The values of N/N_0 lie lower than in the previous case, which means physically that the excess charge, q_1 takes longer to leak off through R, due to the lower potential of the wire during the recovery period; thus on the average, the τ's are longer, resulting in more lost counts. By a limiting process exactly analogous to that used in the previous case, it may be shown that N/N_0 again approaches the value $1/d$ as a limit when b becomes large.

The average recovery time, of course, decreases with increase of N_0. Its behavior with regard to

C and R depends upon how A varies with C and R. If A varies according to some such relation as $A=KC/R$ where K varies very slowly with change of C or R, the expression becomes

$$\bar{\tau}=KC/(N_0RC+1).$$

Such a relation would be in accord with the experimental results in this type of discharge, namely, that $\bar{\tau}$ increases with decrease of R, or increase of C. A general behavior of this nature would be expected if the straight line portion of Fig. 2b is regarded as a temporarily self-sustaining discharge, which ceases when the potential applied to the tube of the counter happens to fall below the value V_T due to natural fluctuations in the source of supply, or some similar accident. A knowledge of the exact mechanism is not necessary, though, as in actual practice, for a given counter, C and R are constant, and the variation of A with V_T is negligible.

The Determination of the Number of Incident Ionizing Particles

In order to determine N_0 from the registered value N, the values of d and of the product RC must be obtained for the particular counter. Using the product of RC and the registered number of particles per unit time as ordinate, the value of b may be read from the curve with the correct value of d, in Fig. 6. Division by RC then gives the true value, N_0. If the unit of time is taken to be RC, N gives N_0 directly.

If it is possible to obtain a trace of some actual discharges, as, for example, by a Braun tube, both constants may be obtained directly from the trace. RC is of course obtained from the rate of decay, and the parameter d may be obtained from either of the relations

$$d=\exp\,(\tau_{\max.}/RC)=[v_0/(V_T-V_S)]_{v_1=0}.$$

If a trace is not obtainable, R and C may be measured directly. In that case, d can be obtained as follows:[6] A source of ionizing particles is brought to different distances from the counter, and values of N obtained. If the radiation at any one position is continued long enough, the inverse square law may be assumed to hold for the number of incident particles per unit time. This will give the ratio of the true number of incident particles, and the measured values will give the ratio of the N's. Knowing RC and the approximate number of incident particles, the value of d which gives a curve with the correct ratio of the N's for the chosen value of the ratio of the N_0's may be determined. (If desired, the more accurate value of one N_0 may be obtained from this curve, and the determination of d repeated, to increase accuracy.)

Discussion

The efficiency of counting depends only on b and d. A change in the potential which the experimenter applies to the counter affects only the quantity A and therefore d. From the sensitivity curve of the counter, Fig. 1, it is evident that a counter operated on the flat portion of its sensitivity curve will show no variation of efficiency with change of applied voltage. Therefore d is to be regarded as constant for a given counter.

The value of N/N_0 decreases rapidly at first, and then more slowly, approaching asymptotically the value $1/d$ in both cases above. Thus the number counted always increases with the number arriving. This behavior would be expected physically, since the potential of the wire varies between narrower and narrower limits as N_0 increases, and therefore the recovery time becomes smaller and smaller. In the limit the ratio of $\bar{\tau}$ to the average period between the arrival of particles, namely $(1/N_0)$, approaches the value $(d-1)$ for both cases. Now, for a large number of particles, the ratio of $\bar{\tau}$ to $1/N$ (that is, the ratio of the average recovery period to the average period between counts) should be equal to the number of lost counts divided by the total number to be counted. Since, in the limit, $N/N_0=1/d$,

$$\frac{d-1}{d}=\frac{N_0-N}{N_0}=\frac{\bar{\tau}}{1/N}=\frac{\bar{\tau}}{d(1/N_0)};$$

so that $N_0\bar{\tau}$ should actually have the limiting value which it does.

[6] The use of an electrometer to determine the average charge passing per count suggests itself. Then $d=C_1/C$, where C is measured, and $C_1=q/(V_T-V_S)$. If this is done, care must be taken that the number of counts per second is small, as q depends on the number of discharges per second, and the formula for C_1 is only valid when a long interval occurs between discharges.

In the actual counter, the registered number of counts will sometimes decrease as N_0 is increased. This is due to the smallness of the charge involved in each discharge, when N_0 becomes large. Thus the effect is to be traced to amplifier and mechanical registering device performance. For example, with a telephone message counter, five or six counts per second is very near the maximum obtainable, and a relatively large amount of charge must pass through it on each impulse to cause it to register. Commercial counters are on the market which will give somewhat over a hundred counts per second. Various laboratories have designed and are using counters using cheap watch mechanisms, capable of counting up to fifty or sixty evenly spaced impulses per second, accurately and conveniently. One such, designed in this laboratory, resolves impulses less than 0.01 sec. apart, and is accurate over the whole range up to its maximum count. This more than covers any experimental region which would be desired, and reduces the question of efficiency to amplifier and tube counter performance.[7]

In any counter there are a certain number of background counts (natural, cosmic, and radioactive contamination in the laboratory). With proper design and care, these may be reduced to as low as from one to five per minute. The correction in the case of a small number of background counts would consist, to sufficient accuracy, in the subtraction of this number from the number of registered counts. If much radioactive contamination is present in the laboratory, or, for any reason, the background radiation N' is of the same order as N, a better procedure would be to determine the true N's for the background, and the count separately, and then subtract. If the background becomes of the same order as the count, the usefulness of the counter decreases greatly.[8]

Throughout the above, the term, "ionizing particle" has been used. The number of particles which actually produce ionization in the counter is determined both by the actual number of particles, and by the ionization efficiency. The latter quantity will vary with the nature and velocity of the particles.[9] For the theoretical explanation of natural phenomena, however, the value of N, and the nature of the source are important. Corrections are then possible. If only the registered number is known, the true number of incident particles cannot, in general, be determined, since the counter of each investigator will have a different efficiency, and a different variation of efficiency with the rate of counting. Only for high rates of counting will the efficiency be sensibly constant, as may be seen from the curves given.

[7] For a good discussion of this, see the article by Locher, reference 2.

[8] The useful sensitivity is given by the expression $(N-N')/(N+N')^{\frac{1}{2}}$. Evans and Mugele, Phys. Rev. **47**, 427 (1935).

[9] In this connection, see Chase, Phys. Rev. **36**, 984 (1930).

Some Physical Properties of Compressed Gases

V. The Joule-Thomson Coefficient for Nitrogen

W. EDWARDS DEMING AND LOLA S. DEMING, *Bureau of Chemistry and Soils, U. S. Department of Agriculture, Washington, D. C.*

(Received May 6, 1935)

Corrected values of the Joule-Thomson coefficient μ for nitrogen are tabulated between -70 and 600°C, and to 1200 atmospheres. μ=const. contours are exhibited on a p–t diagram. The inversion temperature for zero pressure is found to be about 326°C.

IN previous papers[1] values of certain physical properties of nitrogen, carbon monoxide, and hydrogen have been presented, the calculations having been made by mechanical methods from compressibility data. The purpose of the present paper is to correct an error in the published values of the Joule-Thomson coefficient for nitrogen,[1a] also to exhibit the family of μ=const. contours (Fig. 28 ahead)—a form of presentation that in the case of other gases has proved to be useful in thermodynamic calculations.

In computing the Joule-Thomson coefficient μ for nitrogen from the equation[2]

$$\mu\rho C_p=(T/v)(dv/dT)_p-1, \qquad (14)$$

the factor for converting cc atmos./g into cal./mole was inadvertently omitted from the calculation. The published values of μ are on this account too high numerically by the factor 1.474. We are indebted to Dr. J. R. Roebuck for advising us that he had discovered a serious discrepancy between these published values of μ and the results of his own work on nitrogen.[3]

The corrected values of μ appear in Table V. They were obtained by dividing the source of the entries in column 9 of Table I by 1.474. The agreement over that portion of the pressure and temperature range covered by Roebuck and Osterberg's work is now entirely satisfactory. This substantiation gives support to the hope previously expressed that the calculations of physical properties of gases from compressibility

TABLE V. *The Joule-Thomson coefficient μ for nitrogen.*

p in atmospheres, t in degrees centigrade, μ in degrees per atmosphere.

p	$t=-70$	−50	−25	0	20	50	100	200	300	400	500*	600*
0*	0.443	0.408	0.346	0.285	0.242	0.181	0.118	0.058	0.012	−0.025	−0.043	−0.054
20	.425	.379	.319	.262	.220	.168	.110	.051	.007	−.029	−.046	−.056
40	.402	.347	.288	.233	.197	.155	.101	.043	.001	−.032	−.049	−.059
60	.366	.314	.260	.209	.178	.141	.093	.036	−.004	−.035	−.052	−.061
80	.319	.275	.230	.188	.160	.128	.085	.030	−.008	−.037	−.054	−.063
100	.276	.241	.202	.168	.143	.115	.078	.024	−.012	−.039	−.056	−.064
200	.087	.092	.091	.085	.077	.064	.040	.001	−.028	−.050	−.063	−.068
300	.019	.024	.027	.029	.029	.026	.014	−.015	−.039	−.055	−.066	−.072
400	−.009	−.008	−.005	−.003	−.001	−.001	−.007	−.028	−.048	−.060	−.068	−.075
500	−.022	−.024	−.024	−.022	−.021	−.020	−.024	−.038	−.052	−.064	−.071	−.077
600	−.030	−.034	−.035	−.035	−.035	−.034	−.035	−.046	−.057	−.066	−.073	−.079
800	−.039	−.043	−.047	−.048	−.048	−.048	−.049	−.056	−.065	−.071	−.076	−.079
1000	−.044	−.049	−.053	−.054	−.054	−.054	−.055	−.062	−.070	−.075	−.078	−.081
1100*	−.047	−.052	−.055	−.056	−.056	−.055	−.056	−.064	−.071	−.076	−.079	−.081
1200*	−.051	−.055	−.058	−.057	−.057	−.056	−.058	−.067	−.073	−.077	−.079	−.081

* Extrapolated

[1] W. Edwards Deming and Lola E. Shupe, (*a*) Phys. Rev. **37**, 638–654 (1931); (*b*) **38**, 2245–2264 (1931); (*c*) **40**, 848–859 (1932); (*d*) **45**, 109–113 (1934).

[2] The equations and tables have been numbered consecutively throughout the series; those that reappear from previous papers will be given their original numbers.

[3] J. R. Roebuck and H. Osterberg. Phys. Rev. **48**, 450–457 (1935).

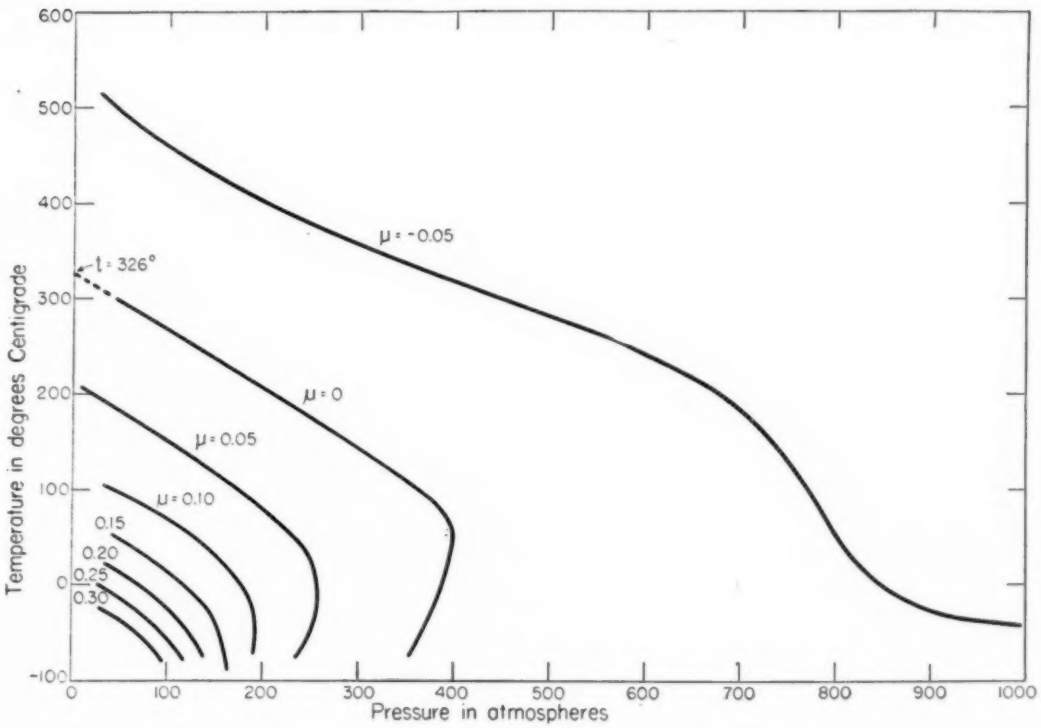

FIG. 28. The μ contours on the pressure-temperature diagram for nitrogen.

data may be of practical and theoretical importance until more direct experimental work is carried out.

Fig. 28 shows the family of μ contours on the p–t diagram. These were obtained by plotting the data of Table V in the form of μ against p in isotherms, and reading off values of μ at $p=20$, 40, 60, $\cdots$, 1000, with an extrapolation to $p=0$. The starred values in Table V for $p=1100$ and 1200 atmos., and for $t=500$ and 600°C are based on extrapolations of the Δ curves, as described on page 647 of reference 1*a*.

It is evident from the spacing between contours that the variation of μ with both pressure and temperature increases as μ increases. The contour $\mu=0$ in Fig. 28 is the inversion curve. It crosses the axis $p=0$ at about 326°, which is therefore the inversion temperature for zero pressure.

The Joule-Thomson Effect in Nitrogen

J. R. ROEBUCK AND H. OSTERBERG, *Department of Physics, University of Wisconsin*

(Received May 6, 1935)

The measurements were made with the same apparatus and procedure as in the case of argon. The effect of the known impurities in the nitrogen, namely argon and oxygen, can be safely neglected. The data for the isenthalpic curves are given in detail and are plotted. The values of the Joule-Thomson coefficient, μ, over the field (-150 to 300°C and 1 to 200 atmos.) are calculated, plotted and tabulated as functions of pressure and temperature. Both upper and lower branches of the inversion curve are measured and the whole inversion curve plotted. The isenthalpic curves, the Joule-Thomson coefficient, and the inversion curve in nitrogen are exceedingly like the corresponding phenomenon in air and in argon. C_p is spread over the pressure range and agrees well with the values of Deming and Shupe, and of Mackey and Krase.

THE measurements on the Joule-Thomson effect in air,[1, 2] in helium[3, 4] and in argon[5] are here extended to nitrogen. They cover the now customary range of pressure (1 to 200 atmos.) and of temperature (-150°C to 300°C). The apparatus is the same as that used for measuring argon. Reference is made to the argon and earlier articles for details of both apparatus and methods.

NITROGEN SUPPLY

Air Reduction Company commercial nitrogen was purchased for these measurements. It was stated to contain 0.1–0.2 percent of oxygen and 0.25–0.5 percent of argon, as well as traces of hydrocarbon vapors from their compressor oil. Analysis made by bringing samples of the gas in contact with hot metallic calcium, showed the argon present to be below 0.2 percent.

To determine the effect of these small argon impurities on the nitrogen data, pure argon was added to the nitrogen in small measured amounts, and runs made with these mixtures at 25, 50 and 75°C. Extrapolation of these data to low percentages of argon showed that the percentage change in the drop in temperature for a drop in pressure of 120 atmos. was approximately equal to the percent of argon in the mixture. As the analyses showed 0.13 percent of argon impurity, the error from this impurity falls well below the 0.5 percent error estimated for these Joule-Thomson measurements.

There is less difference between the critical temperatures of oxygen and nitrogen than of argon and nitrogen so that it seems safe to assume that the effect of the smaller percent of oxygen present as impurity will also fall below the 0.5 percent.

The preparation of very pure nitrogen by cracking of ammonia was considered carefully but was not attempted since: (1) Such freedom from impurity, as indicated above, was hardly necessary; (2) the time and labor involved were considerable; and (3) the risk of handling the required quantities of hydrogen in our location was not desirable.

We hope soon to make comprehensive measurements on the Joule-Thomson effect in mixtures of nitrogen and argon. Experimental evidence bearing on the effect of this neglect of argon impurity in the nitrogen will be available in the report on the mixture work.

APPARATUS

In the work on air, serious difficulty was experienced in obtaining zero temperature drop across a plug permeable enough to give a negligible pressure drop. The observed result is a shift of the initial point off the isenthalpic curve. As suggested,[1] a heater coil was wound around the thermostat tank to increase the homogeneity of the bath temperature.

For the work above room temperature with helium, argon and nitrogen, use was made of a flat heater coil which was placed directly below the plug support. The current through this heater was adjusted to maintain zero reading of a thermocouple having one junction against the

[1] Roebuck, Proc. Am. Acad. **60**, 537 (1925).
[2] Roebuck, Proc. Am. Acad. **64**, 287 (1930).
[3] Roebuck and Osterberg, Phys. Rev. **43**, 60 (1933).
[4] Roebuck and Osterberg, Phys. Rev. **45**, 332 (1934).
[5] Roebuck and Osterberg, Phys. Rev. **46**, 785 (1934).

plug support and the other in the bath liquid. These two heaters appear to have lessened materially the number of instances in which the initial point falls seriously off the isenthalp.

This situation is often complicated by uncertainty in the next two or three points down the isenthalp. If the same plug is to be used for the whole curve, the flow at these points may not be large enough to submerge the effect of heat leaks. It is often necessary to use a more permeable plug to duplicate the high pressure section of the isenthalp. In the present work this was required near both extremes of temperature.

It is noteworthy that the life of the fiber packing in the compressor is greatly prolonged by changing the lubricating water frequently to avoid alkali accumulation.

Experimental Results

The data are given in Table I. The individual experimental runs are referred to by their approximate bath temperatures. The last temperature and pressure readings in a run are, respectively, the bath temperature and the inlet high pressure. The temperatures are in the hydrogen centigrade scale, and the pressures in atmospheres absolute.

About half of the runs were completely repeated at least once with a different plug, and most of the runs were repeated over part of their range. Out of 75 runs actually made, 46 have been selected for publication.

Isenthalpic Curves

The data from Table I are plotted in Fig. 1. The curves below that at $-50°$C are plotted to half the temperature scale of those above. In the upper group the temperature scale is broken and the curves crowded together. Confusion has been avoided by not attempting to show every point from Table I. They were all used, however, in the working drawing from which Fig. 1 was traced.

The data for the vapor pressure curve, shown dashed in Fig. 1, are taken from the International Critical Tables. The points for an isenthalp which has intersected the vapor pressure curve follow along the vapor pressure curve. Since many runs were continued below this intersection, the resulting mass of points is not plotted in Fig. 1. The points fall into a narrow band whose width is such as might be expected from experimental errors.

The points which belong to the isenthalps entering the vapor pressure curve from below show a tendency to fall below the vapor pressure curve whereas the corresponding points of the isenthalps entering from above do not. A volatile impurity of lower critical temperature than that of nitrogen can be expected to produce this tendency. This explanation appears reasonable in the case of the larger tendency in argon[5] in which nitrogen was the known volatile impurity. It fits also in the case of carbon dioxide[6] where air acted as the known volatile impurity.

With air this observed tendency was rather large but there was no known suitable volatile impurity. With nitrogen the tendency is much smaller though still observable and a suitable known impurity is likewise lacking. Failing this explanation, it would seem that there are either instrumental or systematic (i.e., whether the two methods measure in all particulars the same phenomenon) differences between the two methods of obtaining the vapor pressure curve. A thorough study of carbon dioxide containing various impurities is expected to lead to a better understanding of the situation.

Theory[7] requires that the isenthalp through the critical point shall be tangent to the vapor pressure curve at the critical point. The $-120°$ isenthalp falls very close to this particular isenthalp.

The curves intersecting the vapor pressure curve from the left, starting at T_c, meet it at a small and decreasing angle, till finally a particular isenthalp grazes the vapor pressure curve. Below this point of tangency and between the grazing isenthalp and the vapor pressure curve the isenthalps must come out of the vapor pressure curve, as in the case of the $-97°$ isenthalp, Fig. 1. This situation is well known in throttling calorimetric work with steam[8] and is indicated for carbon dioxide by Burnett.[6]

The maximum observed drop in temperature

[6] E. S. Burnett, Bull. of Univ. of Wis. **9**, No. 6 (1926).
[7] A. G. Worthing, Phys. Rev. **33**, 256 (1911).
[8] H. N. Davis, Proc. Am. Acad. **45**, 241 (1910).

TABLE I. *Experimental data on isenthalpic curves.*

#	p	t
300°	CURVE	PLUG 65
1	4.1	300.93
2	22.1	301.16
3	45.7	301.22
4	69.2	301.24
5	89.9	301.17
6	114.2	300.97
7	137.4	300.79
8	161.7	300.40
9	201.2	300.02
250°	CURVE	PLUG 52
1	4.8	249.37
2	18.9	249.79
3	42.1	250.30
4	65.7	250.72
5	87.9	250.97
6	113.8	251.17
7	134.8	251.19
8	158.4	251.21
9	181.0	250.95
10	201.8	251.02
250°	CURVE	PLUG 65
1	3.3	249.13
2	21.7	249.70
3	45.4	250.21
4	69.2	250.60
5	89.9	250.83
6	113.9	251.02
7	137.5	251.14
8	160.8	251.13
9	201.2	251.02
200°	CURVE	PLUG 52
1	4.8	195.47
2	18.1	196.16
3	41.7	197.22
4	66.2	198.14
5	88.2	198.89
6	112.6	199.50
7	134.5	199.98
8	158.5	200.30
9	181.4	200.44
10	201.8	200.69
200°	CURVE	PLUG 43
1	4.2	194.66
2	20.8	195.56
3	44.1	196.61
4	67.0	197.50
5	88.1	198.20
6	112.5	198.84
7	135.6	199.32
8	158.9	199.48
9	181.8	199.99
10	201.2	200.46
200°	CURVE	PLUG 26
1	58.4	197.18
2	80.3	197.95
3	103.1	198.60
4	125.3	199.14
5	155.3	199.59
6	177.9	199.87
7	196.7	200.06
8	221.3	200.27
150°	CURVE	PLUG 52
1	6.4	139.97
2	18.5	141.18
3	45.7	143.07
4	67.3	144.64
5	90.9	146.00
6	114.0	147.09
7	136.8	148.04
8	158.0	148.93
9	175.5	149.36
10	201.6	150.22
150°	CURVE	PLUG 65
1	5.1	139.84
2	20.4	141.17
3	45.3	142.98
4	67.2	144.53
5	88.0	145.76
6	112.2	146.97
7	135.8	147.89
8	158.9	148.72
9	182.0	149.39
10	201.2	150.19
150°	CURVE	PLUG 26
1	57.5	143.65
2	77.5	144.92
3	100.4	146.12
4	112.2	146.68
5	135.3	147.72
6	157.8	148.48
7	182.1	149.15
8	221.3	150.11
125°	CURVE	PLUG 57
1	3.6	111.31
2	20.5	113.21
3	44.3	115.54
4	67.6	117.56
5	90.0	119.22
6	114.1	120.81
7	135.6	122.02
8	160.4	123.19
9	201.5	124.97
125°	CURVE	PLUG 65
1	4.7	111.78
2	20.1	113.40
3	44.1	115.71
4	67.6	117.80
5	88.0	119.34
6	112.3	120.91
7	135.8	122.19
8	159.2	123.22
9	181.8	124.08
10	201.2	124.96
125°	CURVE	PLUG 26
1	58.4	197.18
2	80.3	197.95
3	103.1	198.60
4	125.3	199.14
5	155.3	199.59
6	177.9	199.87
7	196.7	200.06
8	221.3	200.27
100°	CURVE	PLUG 26
1	4.6	83.11
2	21.4	85.33
3	45.0	88.18
4	67.0	90.53
5	89.1	92.64
6	113.7	94.63
7	135.2	96.11
8	157.9	97.44
9	182.7	98.42
10	201.3	99.62
100°	CURVE	PLUG 52
1	5.2	83.21
2	18.7	84.97
3	44.5	87.94
4	68.3	90.38
5	89.4	92.46
6	112.7	94.27
7	136.5	95.91
8	159.2	97.27
9	176.1	98.10
10	201.6	99.45
100°	CURVE	PLUG 65
1	4.7	83.28
2	20.4	85.28
3	44.0	88.18
4	67.2	90.66
5	88.4	92.62
6	112.9	94.61
7	136.1	96.19
8	158.4	97.50
9	182.0	98.63
10	201.2	99.62
75°	CURVE	PLUG 52
1	6.4	55.30
2	19.3	57.41
3	48.3	61.46
4	70.5	64.41
5	92.8	66.93
6	117.4	69.30
7	140.4	71.10
8	177.6	73.62
9	201.6	75.16
75°	CURVE	PLUG 57
1	3.5	54.30
2	20.5	57.14
3	44.1	60.62
4	67.6	63.73
5	89.7	66.28
6	114.8	68.74
7	138.1	70.73
8	158.7	72.36
9	176.0	73.45
10	201.5	75.06
75°	CURVE	PLUG 65
1	5.4	55.26
2	20.8	57.67
3	44.1	61.06
4	67.6	64.09
5	90.2	66.63
6	114.5	69.01
7	133.6	71.47
8	158.8	72.46
9	175.9	73.57
10	201.5	75.06
50°	CURVE	PLUG 59
1	2.7	24.04
2	19.0	27.36
3	42.8	31.76
4	65.5	35.57
5	89.7	38.96
6	111.1	41.46
7	135.0	44.27
8	157.9	46.33
9	201.6	49.78
50°	CURVE	PLUG 57
1	4.2	24.49
2	20.8	27.92
3	43.7	32.15
4	67.5	35.95
5	90.0	39.15
6	114.7	42.19
7	137.5	44.61
8	158.7	46.50
9	175.9	47.89
10	201.5	49.82
25°	CURVE	PLUG 59
1	3.3	−6.80
2	19.0	−2.70
3	43.8	3.02
4	67.3	7.81
5	91.0	11.97
6	112.4	15.23
7	136.2	18.27
8	158.5	20.85
9	201.6	24.62
25°	CURVE	PLUG 52
1	6.8	−5.54
2	19.3	−2.42
3	42.8	3.14
4	67.6	8.00
5	92.3	12.32
6	114.8	15.65
7	139.5	18.67
8	159.3	20.91
9	177.0	22.47
10	201.6	24.62
25°	CURVE	PLUG 57
1	3.8	−6.46
2	22.0	−2.10
3	44.6	3.23
4	67.6	7.91
5	89.9	11.78
6	114.7	15.47
7	137.8	18.43
8	159.0	20.76
9	181.7	22.95
10	201.5	24.71
0°	CURVE	PLUG 43
1	1.6	−38.58
2	18.9	−33.00
3	41.1	−26.44
4	65.4	−20.25
5	88.4	−15.36
6	112.5	−11.04
7	136.5	−7.39
8	159.0	−4.46
9	180.5	+2.10
10	201.8	+0.134
0°	CURVE	PLUG 57
1	4.5	38.24
2	20.8	32.92
3	43.7	26.29
4	67.6	20.36
5	89.9	15.61
6	114.2	11.22
7	137.7	7.65
8	160.3	4.70
9	181.5	2.35
10	201.5	0.44
−25°	CURVE	PLUG 43
1	2.5	73.94
2	17.2	67.52
3	43.0	57.96
4	74.6	48.36
5	97.6	42.63
6	121.5	37.72
7	160.7	31.60
8	181.7	29.03
9	201.8	27.09
−25°	CURVE	PLUG 57
1	3.6	74.65
2	21.1	66.93
3	44.0	58.25
4	68.2	50.67
5	90.2	44.77
6	113.9	39.56
7	137.8	35.25
8	159.0	32.07
9	182.9	29.08
10	201.5	27.07
−50°	CURVE	PLUG 43
1	1.5	108.91
2	14.6	100.53
3	40.5	87.53
4	65.1	78.35
5	88.6	70.76
6	112.5	64.62
7	136.8	59.68
8	158.4	56.12
9	179.7	53.24
10	201.8	50.94
−75°	CURVE	PLUG 43
1	2.5	146.27
2	17.9	132.43
3	44.2	113.95
4	70.1	101.43
5	91.2	93.68
6	115.7	87.13
7	136.8	82.84
8	160.0	79.23
9	181.7	76.42
10	201.8	75.06
−91°	CURVE	PLUG 43
1	1.5	173.46
2	16.5	150.00
3	44.6	128.32
4	68.2	115.62
5	91.8	107.25
6	116.0	101.22
7	136.8	97.47
8	159.5	94.49
9	181.4	91.63
10	201.8	91.09
−97°	CURVE	PLUG 43
1	1.6	186.18
2	12.9	165.87
3	20.8	155.62
4	26.5	149.06
5	32.4	143.17
6	45.3	133.00
7	68.1	120.77
8	92.9	112.28
9	114.3	107.15
10	137.5	103.25
11	201.6	97.37
−99°	CURVE	PLUG 43
1	1.7	189.81
2	13.2	165.13
3	20.8	157.03
4	25.8	151.16
5	31.9	144.82
6	44.5	134.43
7	68.9	121.50
8	91.5	113.72
9	115.2	108.39
10	138.2	104.70
11	201.6	99.06
−100°	CURVE	PLUG 43
1	1.5	191.76
2	19.4	158.55
3	40.1	138.49
4	70.4	121.74
5	99.8	112.40
6	119.6	108.74
7	141.3	105.56
8	168.7	102.64
9	201.8	100.51
−100°	CURVE	PLUG 43
1	12.8	165.86
2	26.6	150.77
3	29.5	147.77
4	33.8	143.86
5	58.4	127.19
6	201.6	100.70
−110°	CURVE	PLUG 43
1	18.2	159.42
2	21.4	156.48
3	29.9	149.92
4	34.7	146.17
5	40.1	142.03
6	46.8	137.66
7	52.0	134.76
8	59.0	131.57
9	65.3	129.05
10	75.9	125.40
11	88.7	121.95
12	112.5	117.41
13	135.9	114.32
14	157.1	112.19
15	182.3	110.32
16	201.8	110.06
−100°	CURVE	PLUG 52
1	158.9	112.31
2	181.3	110.83
3	201.6	110.06
−120°	CURVE	PLUG 43
1	47.2	140.60
2	68.3	132.69
3	91.9	127.71
4	117.0	124.51
5	136.5	122.98
6	159.7	121.20
7	182.1	119.02
8	201.8	120.25
−120°	CURVE	PLUG 43
1	0.6	198.24
2	1.2	193.49
3	12.4	166.50
4	20.4	157.67
5	25.2	153.52
6	31.8	148.78
7	43.1	141.86
8	55.1	136.89
9	78.7	130.07
10	104.3	125.99
11	201.8	120.25
−120°	CURVE	PLUG 52
1	141.9	122.58
2	159.2	121.60
3	181.8	120.68
4	201.6	120.25
−126°	CURVE	PLUG 43
1	3.6	183.13
2	10.8	170.35
3	18.8	160.17
4	24.6	154.57
5	28.9	151.39
6	33.5	147.89
7	39.3	144.45
8	52.3	138.91
9	64.8	135.31
10	89.0	130.90
11	112.5	128.32
12	135.4	126.57
13	157.8	125.46
14	179.5	124.34
15	201.8	126.04
−130°	CURVE	PLUG 43
1	45.9	142.45
2	69.1	137.04
3	91.9	133.98
4	115.4	131.88
5	137.3	130.68
6	160.3	129.57
7	181.1	128.73
8	201.8	130.23
−130°	CURVE	PLUG 43
1	25.6	152.78
2	30.5	149.58
3	43.3	143.03
4	65.6	137.20
5	92.2	133.75
6	114.7	131.88
7	137.1	130.64
8	160.0	129.63
9	181.4	129.00
10	201.8	130.23
−130°	CURVE	PLUG 52
1	147.4	131.07
2	164.2	130.52
3	181.6	130.14
4	201.6	130.23
−141°	CURVE	PLUG 43
1	28.9	150.90
2	32.0	149.41
3	38.9	148.10
4	45.6	147.06
5	68.1	144.50
6	97.7	142.68
7	136.0	141.52
8	159.1	141.30
9	175.1	141.08
10	201.6	141.79
−141°	CURVE	PLUG 52
1	144.5	141.54
2	164.7	141.45
3	181.9	141.42
4	201.6	141.79
−151°	CURVE	PLUG 43
1	15.2	163.17
2	21.1	157.21
3	25.9	153.82
4	32.2	153.24
5	44.5	152.07
6	68.0	150.74
7	91.3	149.97
8	114.3	149.54
9	136.3	149.52
10	201.6	150.61
−141°	CURVE	PLUG 52
1	136.0	149.69
2	160.2	149.83
3	181.6	150.06
4	201.6	150.61
−163°	CURVE	PLUG 43
1	20.3	161.20
2	33.2	160.74
3	44.2	160.53
4	67.7	160.29
5	90.9	160.23
6	114.2	160.31
7	135.7	160.61
8	201.6	162.71
−163°	CURVE	PLUG 52
1	136.0	160.80
2	160.5	161.26
3	181.6	161.74
4	201.6	162.71

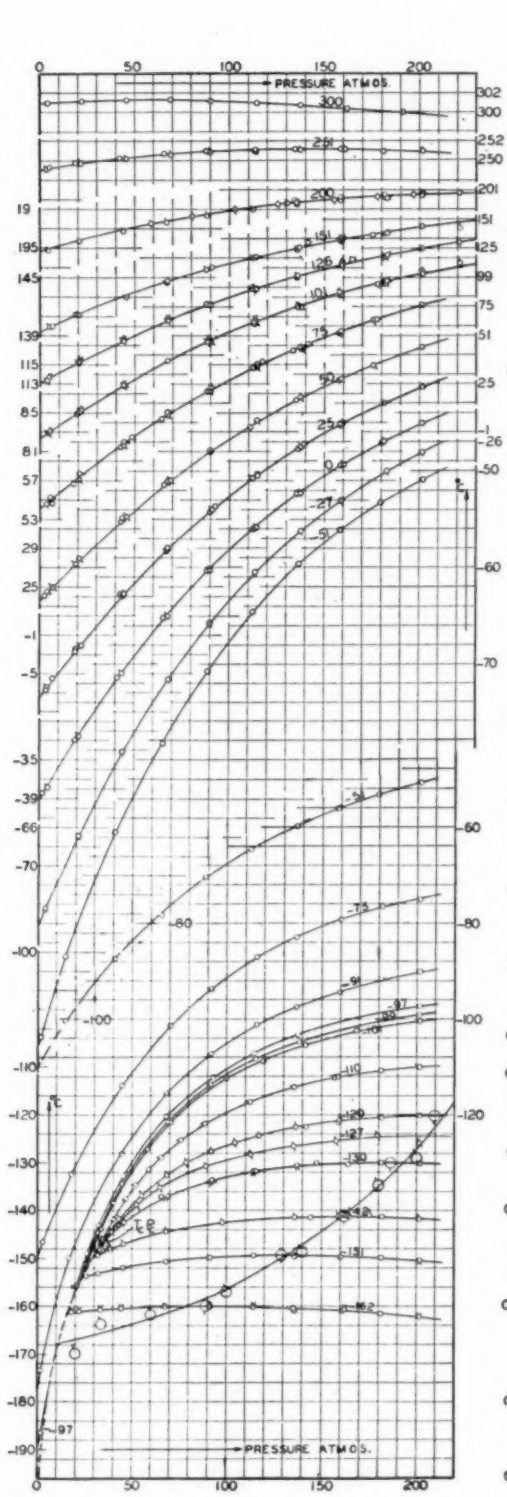

FIG. 1. t as a function of p at constant enthalpy.

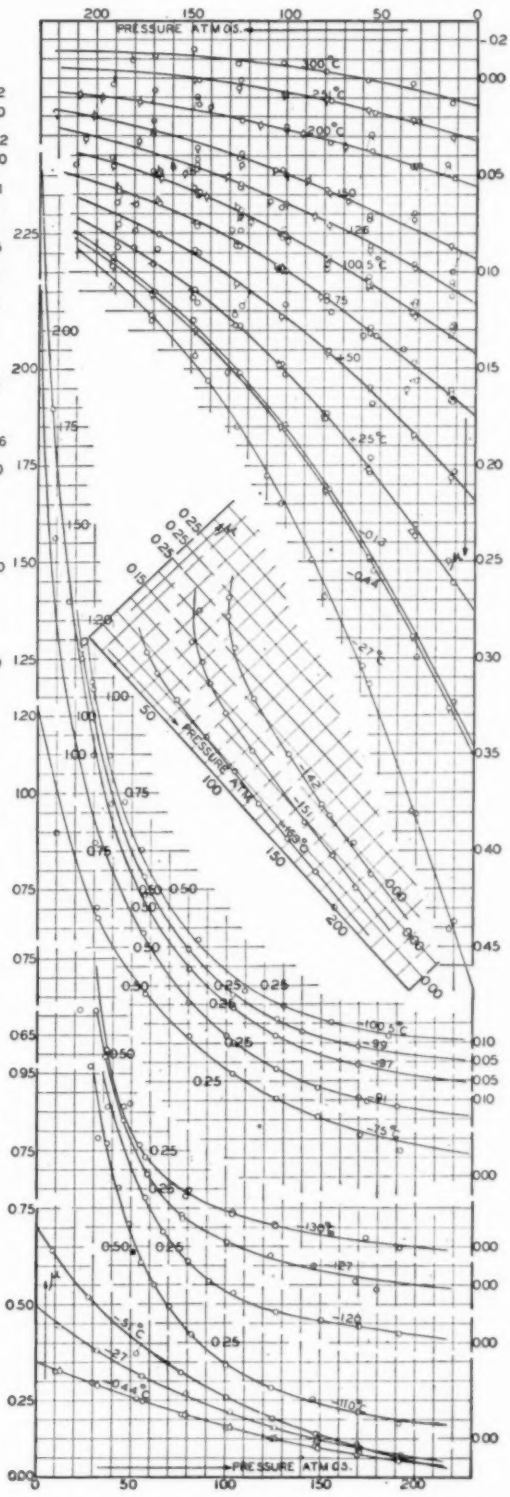

FIG. 2. μ as a function of p at constant enthalpy.

across the plug is 87°C and the maximum value of μ 2.32°C/atmos. These values are smaller than the corresponding values (120° and 3.0°C/atmos.) for argon.[5]

The same precautions as those taken with argon again proved sufficient to prevent the plug clogging from introducing uncertainty except in the lower ends of the $-50°$, $-75°$ and $-91°$ isenthalps.

Comparison of this whole group of isenthalps (Fig. 1) for nitrogen with the corresponding groups for air[1, 2] and for argon,[5] shows remarkable similarity between them. The comparison immediately suggests that the theorem of corresponding states will fit at least approximately. Scattered numerical examples from these measurements show that this theorem may be applied to the Joule-Thomson effect with approximately the same precision as to pv data. A systematic application of this theorem to our data is in progress.

Joule-Thomson Coefficient, $\mu \equiv (dt/dp)_h$

As in previous papers,[1, 5] the numerical values of μ are obtained by taking the ratio of the successive and corresponding differences of temperature and of pressure for each experimental run. These values of μ are plotted against the corresponding average pressure to give the isenthalpic curves of Fig. 2. To avoid confusion these curves are plotted in groups and, occasionally, to shifted scales. This family of isenthalpic curves is more complex than the corresponding family for argon. Each curve was obtained from the data of the original isenthalp (Fig. 1) designated by the same approximate bath temperature.

From the curves of Fig. 2 the values of μ for a series of selected pressures were picked off and the corresponding temperatures obtained from the isenthalpic curves of Fig. 1. These values of μ and t are plotted in Fig. 3 as isopiestics. It was necessary to shift these isopiestics apart since μ shifts very slowly in a part of the field. The ordinate scale is indicated for each isopiestic. As in the case of air, the critical isopiestic (33.5 atmos.) has been plotted.

As indicated by the work of Burnett,[6] the critical isopiestic is tangent to the "Limit Curve" at the critical point. Thus the slope of the vapor pressure curve at the critical point[7] ($T_c\mu_c$, Fig. 3) is common to the critical isopiestic and to the limit curve. The slope of the vapor pressure curve as a function of temperature is the curve plotted with square points. The limit curve (long dashed line in Fig. 3) enters at the lower left-hand edge of the diagram, bends upward so as to pass vertically through the critical point, and leaves at the point $\mu = 2.20$.

The points for locating the limit curve were obtained by determining the slopes of the isenthalps of Fig. 1 at the points at which they strike the vapor pressure curve. The p and t of each intersection was read from Fig. 1. The corresponding isenthalp of Fig. 2 was then extrapolated to the value of p as read from Fig. 1, and μ for this pressure picked off. These values of μ are plotted against the corresponding temperatures as the triangles in Fig. 3. In the resulting limit curve, the upper branch, rising from the critical point, is associated with the steep isenthalps intersecting the vapor pressure curve from above. The lower branch, descending from the critical point, is associated with the flat isenthalps intersecting the vapor pressure curve from below.

The discontinuity in μ when a point moves along an isopiestic across the vapor pressure curve in Fig. 1, e.g., along the 20 atmosphere isopiestic is represented in Fig. 3 by the vertical dotted line between the upper and lower branches of the limit curve. As the chosen isopiestic moves to lower pressures in Fig. 1, the dotted line in Fig. 3 moves to the left. Presently a pressure is reached at which a particular one of the upper isenthalps of Fig. 1 is tangent to the vapor pressure curve. At this pressure the corresponding isopiestic, the upper branch of the limit curve, and the curve of the slopes of the vapor pressure curve intersect (Fig. 3, point P). The upper branch of the limit curve will probably rise continually to the triple point pressure.

Final values of μ for the range of these experiments were read from the curves of Fig. 3 before it was inked and are listed in Table II.

Deming and Shupe[9] have calculated the values of μ for nitrogen from the pv measurements of Bartlett and co-workers. Their corrected values

[9] Deming and Shupe, Phys. Rev. **37**, 638 (1931).

NITROGEN
INVERSION CURVE
ROEBUCK & OSTERBERG
DEMING & SHUPE
M
PRESSURE ATMOS.
0 40 80 120 160 200 240 280 300 340 380
300 250 200 150 100 50 0 -50 -100 -150

FIG. 4. t as a function of p where $\mu=0$.

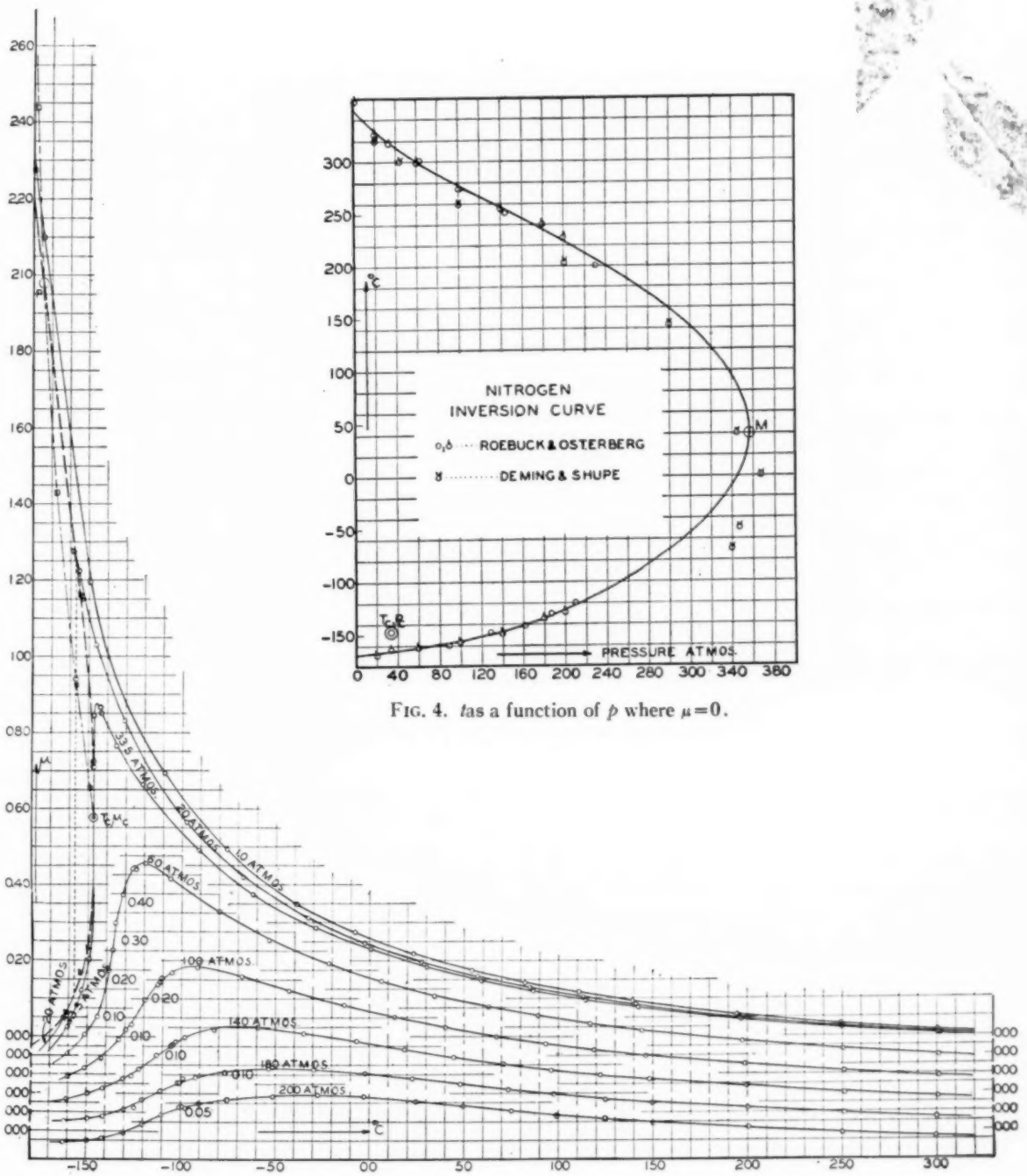

FIG. 3. μ as a function of t at constant pressure.

are given in the article which just precedes this. Comparison of these values with ours shows that when the high percentage divergences where μ is small are omitted, the average numerical percentage divergence and the average percentage difference are, respectively, 5.2 and 2.4 percent. The numerical divergences between the μ's where μ is small average only 0.007°C/atmos. Their values of μ are greater than ours at low temperatures, but become slightly smaller at the highest temperatures. These differences show no clearly marked trend with pressure. Con-

TABLE II. *Final values of μ from Fig. 3.*

t \ p	1	20	33.5	60	100	140	180	200
300°C	0.0135	0.0095	0.0050	−0.0010	−0.0070	−0.0120	−0.0150	−0.0160
250	0.0320	0.0250	0.0225	+0.0160	+0.0075	+0.0015	−0.0030	−0.0050
200	.0540	.0460	.0420	0.0365	.0260	.0170	+0.0100	+0.0075
150	.0840	.0755	.0715	.0615	.0480	.0350	.0250	.0225
125	.1035	.0945	.0880	.0770	.0615	0460	.0345	.0320
100	.1250	.1140	.1070	.0955	.0760	.0580	.0460	.0415
75	.1505	.1380	.1300	.1165	.0930	.0735	.0580	.0535
50	.1795	.1660	.1575	.1415	.1150	.0910	.0730	.0660
25	.2145	.2000	.1905	.1690	.1380	.1100	.0875	.0780
0	.2570	.2420	.2310	.2040	.1660	.1310	.1020	.0900
−25	.3120	.2925	.2775	.2475	.1975	.1510	.1120	.0950
−50	.3840	.3625	.3370	.2995	.2315	.1695	.1155	.0940
−75	.4870	.4535	.4200	.3640	.2680	.1770	.1090	.0840
−87.5	.5525	.5095	.4730	.4020	.2825	.1675	.0980	.0760
−100	.6280	.5785	.5355	.4430	.2810	.1425	.0800	.0620
−112.5	.7190	.6645	.6050	.4880	.2375	.0980	.0515	.0375
−125	.8280	.7725	.6870	.4945	.1475	.0530	.0200	.0070
−137.5	.9650	.9100	.7910	.2500	.0685	.0210	−0.0040	−0.0140
−150	1.225	1.097	.1775	.0620	.0215	−0.0025	−0.0180	−0.0255
−160	1.580	0.0730	.0330	.0075	−0.0075	−0.0160	−0.0235	−0.0295
−170	1.940	−0.0075	−0.0360					
−180	2.315							

sidering the precision required in Bartlett's work and the difficulties in Deming and Shupe's calculation, the above agreement must be considered remarkable.

INVERSION CURVE $\mu=0$

The data for plotting the inversion curve for nitrogen are obtained from: (a) the estimated points of zero slope on the isenthalpic curves of Fig. 1; (b) the points of zero μ on the isenthalpic curves of Fig. 2; and (c) the points of zero μ on the isopiestics of Fig. 3. These data are plotted in Fig. 4. The three groups of data are mutually consistent.

To this are added data from the work of Deming and Shupe[9] to serve as a guide in connecting the upper and lower branches of the inversion curve. This carries the meeting point M of the two branches to a higher pressure than our data alone had suggested. This is in agreement also with the results of Porter's[10] analysis of the experimental data of Amagat on nitrogen.

Along the upper branch the data of Deming and Shupe[9] fall consistently near our curve, but below M their data diverge from it.

The data from this smooth curve have been picked off and are assembled in Table III. The maximum pressure is 376 atmospheres falling at 40°C.

The data for the low pressure end of the upper branch were obtained by a moderate extrapolation, and lead quite definitely to the indicated turn upward. Ignoring the upward turn shifts the 1 atmosphere reading to 334°C. In some of our unpublished inversion curves for nitrogen-helium mixtures the low pressure ends of the upper branches have been determined with greater certainty than in nitrogen, but show no upward turn at low pressure. This casts doubt upon the reality of the upward turn in nitrogen.

TABLE III. *Data from the inversion curve, $\mu=0$.*

t°C Upper	p (atmos.)	t°C Lower	t°C Upper	p (atmos.)	t°C Lower
348.0	1		212.5	220	−117.2
330.0	20	−167.0	187.0	260	−96.4
299.6	60	−162.4	158.7	300	−68.7
277.2	100	−156.5	121.3	340	−35.3
256.5	140	−148.0	93.7	360	−10.0
235.0	180	−134.7	40.0	376	+40.0

The low temperature branch is shown also in Fig. 1 since the isenthalps in this part of the field are plotted without relative displacement. This part of the nitrogen curve resembles that for air[2] more closely than the straighter curve for argon.[5] Nitrogen and air are the only substances for which parts of both branches of the inversion have been measured. These two inversion curves resemble each other strongly.

In the group of substances (air, O_2, A, CH_4, CO) whose critical temperatures are above that of N_2 the upper branch of the inversion curve falls largely or completely above our temperature range. In the group of substances (Ne, H_2, He) whose T_c's fall below that of N_2, the lower branch of the inversion curves falls completely below our temperature range. The fall in p_c accompanying that in T_c, is estimated to bring

[10] A. W. Porter, Phil. Mag. (6) **19**, 891 (1910).

the whole upper branch of H_2 within our temperature and pressure range.

Specific Heat C_p

The data on the specific heat of nitrogen are much more satisfactory than those for argon.

Deming and Shupe[9] select a series of values of C_p at one atmosphere to cover the range -70 to 600°C. For the sake of ready comparison we have used their values to spread C_p over our pressure range by the method described in the air articles.[1, 2] These values were plotted in Fig. 5, and the data of Table IV were read from the smooth curves of the working drawing. C_p at 1 atmos. cannot be spread at low temperatures because of the conditions set up by the critical state as explained earlier in detail.[1, 2]

The values of C_p calculated by Deming and Shupe[9] and those measured by Mackey and Krase[11] are compared with ours in Table V which contains a representative group of values selected to cover the common field. The data of Deming and Shupe are in italics, of Mackey and Krase in black face, and of the writers in ordinary type. The two former have been reduced to cal./g°C by the divisor 28.025 given by Deming and Shupe.

Examination of Table V shows agreement within the expected error. Our variations from Deming and Shupe show no regular trend, averaging only 0.2 percent with a maximum of 2.8 percent. These are about the same as the differences shown on the plot between the curves and the unsmoothed values. Our values of C_p are uniformly larger than those of Mackey and Krase by an average of 0.6 percent with a maximum of 1.1 percent.

Such agreement between data obtained by three radically different methods justifies considerable confidence in the results. It adds also to the confidence with which the values of Deming and Shupe at higher temperatures and pressures may be used.

It is a pleasure to acknowledge our indebtedness to the Wisconsin Alumni Research Foundation for financial aid providing for relief from teaching and for adequate assistance.

Acknowledgment should also be made of grants from the Rumford Fund of the American Academy, some of which were used for this work.

We plan to measure next mixtures of argon with helium and of argon with nitrogen, and to make a thorough study of carbon dioxide.

Table IV. *C_p in cal./g°C as a function of pressure and temperature.*

p \ t°C	−100	−50	0	50	100	150	200	300
1	.2473	.2466	.2466	.2469	.2476	.2484	.2490	.2501
20	.2813	.2636	.2557	.2522	.2510	.2507	.2510	.2523
33.5	.3010	.2748	.2626	.2569	.2543	.2533	.2530	.2538
60	.3345	.2967	.2769	.2658	.2601	.2573	.2560	.2556
100		.3233	.2942	.2775	.2680	.2627	.2602	.2581
140		.3438	.3071	.2865	.2754	.2687	.2648	.2605
180		.3577	.3179	.2943	.2810	.2735	.2688	.2629
200			.3243	.2986	.2841	.2759	.2706	.2690

Table V. *Comparison of C_p for nitrogen, data from Deming and Shupe[9] (italics) Mackey and Krase[11] (black face) and authors (ordinary).*

p \ t°C	−50	0°C	50	100	150	200	300
1	0.2466	0.2466	0.2469	0.2476	0.2484	0.2490	0.2501
	.2466	*.2466*	*.2469*	*.2476*	*.2483*	*.2490*	*.2501*
			.2469	**.2476**	**.2483**		
20	.2636	.2557	.2522	.2510	.2507	.2510	.2523
	.2629	*.2569*	*.2537*	*.2519*		*.2516*	*.2519*
50				**.2573**		**.2566**	
60	.2967	.2769	.2658	.2601	.2573	.2560	.2556
	.2976	*.2794*	*.2662*	*.2601*		*.2568*	*.2551*
100	.3233	.2942	.2775	.2680	.2627	.2602	.2581
	.3326	*.3012*	*.2776*	*.2676*		*.2608*	*.2580*
			.2755	**.2669**	**.2626**		
200		.3243	.2986	.2841	.2759	.2706	.2690
	.3807	*.3301*	*.2990*	*.2837*		*.2701*	*.2640*
			.2969	**.2826**	**.2733**		

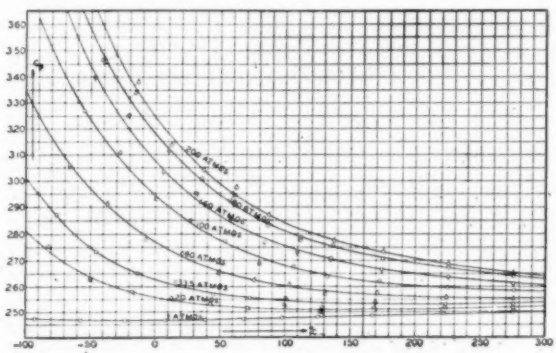

Fig. 5. C_p as a function of t at constant pressure.

[11] Mackey and Krase, J. Ind. and Eng. Chem. **22**, 1060 (1930).

The Temperature Scales of Columbium, Thorium, Rhodium and Molybdenum at 0.667μ

L. V. WHITNEY, *Department of Physics, University of Wisconsin*

(Received June 18, 1935)

To establish temperature scales for columbium, thorium, rhodium and molybdenum spectral emissivities were measured for these metals at $\lambda=0.667\mu$. The Mendenhall V wedge was used for columbium and rolled cylinders were used for the other metals. Rolled cylinders were more satisfactory for measuring emissivities than specimens in other forms. Rigorous heat treatment was found necessary for accurate results. Emissivities for all four metals were constant with temperatures. Results are:

	Emissivity $\lambda=0.667\mu$	*Temperature range covered*
Columbium	0.374	1300°–2200°K
Thorium	.380	1300°–1700°
Rhodium	.242	1300°–2000°
Molybdenum	.382	1300°–2100°

A CONVENIENT method of establishing the temperature scale for a substance at incandescent temperatures is to measure its spectral emissivity as a function of the apparent temperature. By Wien's law:

$$1/T=1/T_s+(\lambda/C_2)\log_e \epsilon_\lambda.$$

Hence if we measure the brightness temperature T_s by means of an optical pyrometer, and know the spectral emissivity, ϵ_λ, as a function of the brightness temperature, we can calculate the true temperature.

PREVIOUS METHODS OF MEASURING SPECTRAL EMISSIVITY

For emissivity measurements it is necessary to have a black body and the surface of the material being studied at the same temperature. Readings of each can then be taken. For a molten metal one of the earliest ways of doing this was to sight an optical pyrometer directly on the liquid surface to get the brightness temperature and to sight down a small cavity in a carbon rod partly immersed in the metal for the true temperature. Another early method was to insert a small specimen of solid metal into a cavity in a carbon rod allowing it to project out from the surface of the rod. When heated, apparent temperatures were read from the metal surface and true temperatures from a nearby cavity in the carbon.

Dr. C. E. Mendenhall was the first to use the metal being studied as its own black body.[1] He took a thin strip of metal, bent it into a V wedge 3 cm or more long by 4 to 8 mm wide on a side, and measured the apparent temperatures from the outer surface and the true temperatures from the wedge cavity. For a metal with a spectral emitting surface having an angular opening of ten degrees or less, he showed that the radiation coming from the wedge was practically black body. With thin metal specimens there is no problem of temperature difference between inner and outer surfaces of the wedge. However, unless mounted so as to allow for expansion and contraction, there is some tendency for the wedge to warp out of shape upon heating and so make a poorer black body. Two separate pieces of tungsten were used by Mendenhall to form a wedge and there was some trouble with their separating along the line of contact. However, if the wedge does maintain its shape, results are quite reliable. Many experimenters have used the V wedge among them being Forsythe, Edgerton and Milford, Spence and others.

Burgess and Waltenburg used a secondary standard method of measuring emissivities.[2] They took a minute speck of metal, placed it on a strip filament of platinum or iridium, and measured the radiation from both the speck and the filament. The metals were heated to their melting points and readings taken above and below these temperatures. Three objections can be cited to this method. First, there is the danger of the specimen alloying with the filament thus invalidating results. Next, most of this work was done in an atmosphere of hydrogen. Work done with rhodium by the writer indicates that such results might be questionable if applied to metals being

[1] C. E. Mendenhall, Astrophys. J. **33**, 91 (1911).

[2] Burgess and Waltenburg, Bur. Stan. Bull. **11**, 591 (1914).

worked in a high vacuum. In any case, emissivity values should be obtained under conditions similar to those for which they are to be applied. Lastly, the method depends on the emissivity of platinum which was taken as 0.33 at 0.650μ. Judging by later work, this value is somewhat high. Worthing gives 0.30 for the emissivity of platinum at 1425°K and 0.31 at 1800°K.

A. G. Worthing used two types of tubular filaments for measuring emissivities.[3, 4] For tungsten he made up a squirted tube about 1.5 mm O.D. and 0.8 mm I.D. Fine holes were punctured through the sides of the tube for measuring true temperatures. The thickness of the walls made it necessary to correct for temperature differences through the walls. For molybdenum he used tubular filaments formed by winding molybdenum ribbon into closed helices. There was a tendency for hot spots to develop where windings touched and readings had to be taken at a distance from such places. He also used two other methods of measuring molybdenum emissivities. At room temperatures and at 1080°K he used reflectivity data. At 2000°K he took readings on a compound molybdenum-tungsten filament. This was formed by mounting a tungsten filament and a molybdenum filament end to end and heating carefully until the molybdenum just melted. Readings were taken above and below the junction. However, neither of these latter methods were as satisfactory as the tubular filament method. In the reflectivity work the data taken at 1080°K were obtained under unfavorable conditions, and with the compound filament the spread of alloying action at high temperatures prevented their long use.

Present Methods Used in Emissivity Measurements

In the present work the Mendenhall V wedge was used for columbium and rolled cylinders described below were used for thorium, rhodium and molybdenum. The V wedge was about 5.5 cm long and 4 mm wide. The opening was about ten degrees and good black-body conditions were obtained. The method of mounting was such as to minimize strain and distortion of the wedge, the method being similar to that used for the rolled cylinders.

The rolled cylinders were about 5.5 cm long and $2\frac{3}{4}$ mm in diameter. For soft metals these were easy to make. After taking a strip of the metal to be measured and giving it a slight lengthwise curl around a small metal rod, all that was necessary was to run it through smaller and smaller holes in an ordinary drill gauge. However, for more brittle metals such as thorium, cracks would develop in the edges of the specimen and ruin the cylinder. This difficulty was eventually met in a simple way. A thin flexible sheet of copper was soldered to a small diameter rod in such a way as to allow winding the copper sheet around the rod. Before winding, the specimen to be measured was laid on the copper sheet and rolled with it to practically a butt joint. The rolled copper was then loosened and the cylinder slipped out. Another rolling was sometimes needed to make the butt joint more perfect. A hole drilled in the side of the cylinder was used for measuring the true temperatures. Metals too brittle to fold into a wedge can be made into such cylinders.

Such rolled cylinders have many advantages for emissivity work. They are easy to make, and, because of their shape, are stronger than any other form. When mounted carefully there is no tendency for the butt joint to open up. They can be made quite long (6 cm or more) thus giving a region of uniform temperature at the center. It was not uncommon to have a region 2 cm in length along which temperature differences could not be detected. An advantage over the V wedge is that only one pyrometer is needed for readings instead of two. There is no need to correct for temperature difference through the walls as they are but 0.04 mm thick. The large inside diameter makes for excellent black-body conditions. In these respects the rolled cylinder is more satisfactory than the squirted tube with its thick walls and small inside diameter. The cylinders were mounted vertically, the return lead being a molybdenum strip rolled thin enough to expand about the same amount as the cylinder upon heating. Thus there was very little strain on the cylinder at any time.

[3] A. G. Worthing, Phys. Rev. **10**, 377 (1917).
[4] A. G. Worthing, Phys. Rev. **25**, 846 (1925).

Pyrometers and Their Calibration

All readings were taken with Holborn-Kurlbaum pyrometers with entrance and exit aperatures arranged as described by Fairchild and Hoover.[5] Readings were taken through flat Pyrex windows sealed to the experimental tube. The pyrometers were calibrated through these windows.

In the course of the work three pyrometers were used. The gold point of each, 1063°K, was determined in the usual way by matching with a black-body furnace in which gold had been melted. By the use of sectors a calibration curve for each pyrometer was then obtained for temperatures from 1150°K to 1850°K. As a check on the accuracy of the calibrations, all three pyrometers were sighted simultaneously on a common source and compared throughout this range. Finally, palladium was melted in the black-body furnace and readings taken. It was found that the palladium point, as determined by calibration from the gold point, was within a half of a degree of the point as determined by the actual melt for all three pyrometers. This fact was not only good evidence of the accuracy of calibration of the pyrometers, but also constituted a convincing check on the palladium point itself, 1828°K, as determined by Roeser, Caldwell and Wenzel.[6]

Results

The emissivities of all four metals were found to be constant over the temperatures measured. (See Fig. 1.) Whether there is any significance to this result or not, the writer is not prepared to say. However, it does make one feel that if measurements of emissivity change with temperature, one should take special precautions to make sure the effect is genuine and not due to changing surface conditions.

Columbium

Between the temperatures 1300°K and 2200°K an emissivity of 0.374 was found. The specimen was heat treated for over 500 hours and measurements made under pressure conditions of 10^{-6} mm or better as indicated by a McLeod gauge. This value is much lower than Burgess and Waltenburg's, which is 0.49.

Thorium

Readings on thorium were made after 600 hours of heat treatment and an emissivity of 0.38 was found over the temperature range 1300°K to 1700°K. The cylinder was somewhat shorter than those used for rhodium and molybdenum being about 3.5 cm long instead of 5.5 cm but conditions inside the cylinder appeared uniform. Burgess and Waltenburg's value for thorium is 0.36.

Rhodium

Work with rhodium showed that reliable results could not be obtained unless heat treatment were thorough. Preliminary work on this metal was done in a water-cooled brass chamber with a vacuum of $1\text{–}2\times10^{-6}$ mm. For temperatures between 1700°K and 2200°K emissivities increased from 0.24 to 0.29. Below 1700°K there was a sudden change of surface conditions which led to emissivities in the neighborhood of 0.60. Later work in an all Pyrex system showed that these results were completely untrustworthy. It was found that the temperature at which this sudden change of surface conditions took place was a function of the partial oxygen pressure. Vacuum conditions inside the brass container apparently were never satisfactory.

With the all Pyrex system (similar to that used for all the other metals) heat treatment was continued for over 700 hours and pressures as measured with an ion gauge were better than 4×10^{-8} mm. All traces of sudden surface changes disappeared as far as the eye could tell. However, in the early stages of heat treatment, values of 0.24 were found for lower temperatures and 0.26 to 0.28 for higher temperatures. Eventually after the 700-hour heat treatment, the constant value of 0.242 was found as the average over the entire temperature range. This value is low compared to the Burgess and Waltenburg value of 0.29.

Molybdenum

After over 100 hours of baking and 400 hours of outgassing an average value of 0.382 for emissivity was found in the entire temperature range 1300°K to 2100°K. As with rhodium, the pressures were about 4×10^{-8} mm. Although this

[5] Fairchild and Hoover, J. Opt. Soc. Am. **7**, 543 (1923).
[6] Roeser, Caldwell and Wenzel, Bur. Standards J. Research **6**, 1119 (1931).

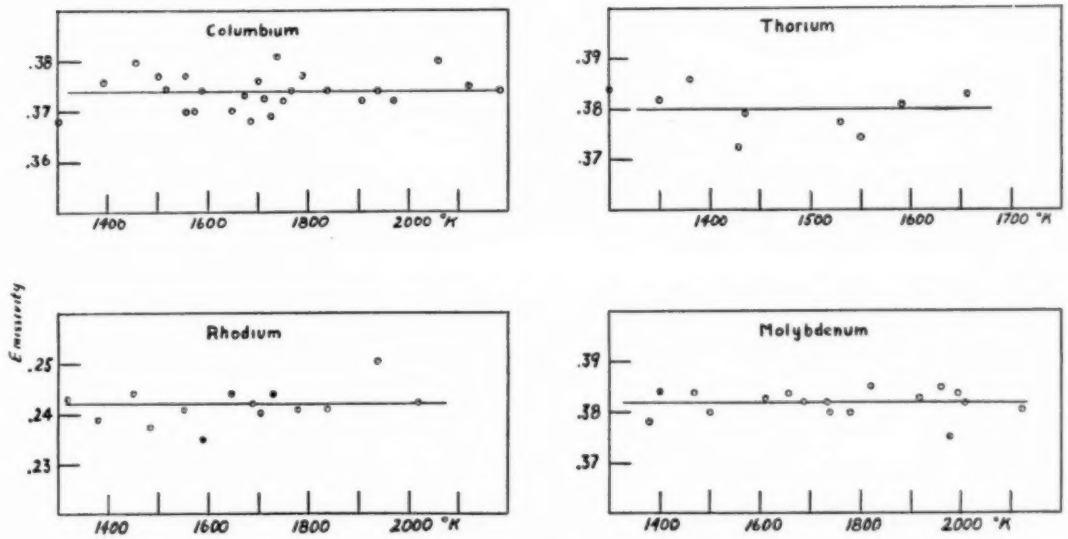

FIG. 1. Spectral emissivities at $\lambda = 0.667\mu$.

value is lower than Burgess and Waltenburg's who give 0.43, and lower than Mendenhall's who gives 0.44 to 0.39 over the range, it is definitely higher than Worthing's value at the high temperatures. Worthing obtained 0.354 at 2000°K. While it is true that almost every error one can make tends to give too high an emissivity, the following experimental evidence warns against assuming such a conclusion for all cases.

For several days readings were taken between 1300°K and 1800°K after heat treating at about 1950°K. Then the temperature was raised to over 2100°K and readings taken. The emissivity immediately dropped from the constant value 0.382, characteristic of the lower temperatures, to 0.369. The writer first believed this to be due to a cleaning up of the metal and expected the lower temperature points to fall in line after further heat treatment. This did not take place. Instead, the emissivity at the high temperatures gradually climbed to 0.382. It seemed that conditions were unsteady immediately after going to a high temperature and that the low emissivity was really characteristic of this unsteady condition.

The molybdenum used was the best grade obtainable from the Fansteel Company. To eliminate the possibility of differences due to different sources, a rolled cylinder was made up from molybdenum kindly furnished by Professor Wahlin by Dr. Forsythe. This molybdenum was similar to that used in A. G. Worthing's work. Measurements made on this sample checked the value 0.382.

This work was done under the direction of Dr. Mendenhall and Dr. Wahlin. The writer wishes to express his indebtedness to them for assistance in the course of the work and also to Mr. John Reynolds who aided in taking and checking many of the readings.

LETTERS TO THE EDITOR

Prompt publication of brief reports of important discoveries in physics may be secured by addressing them to this department. Closing dates for this department are, for the first issue of the month, the twentieth of the preceding month; for the second issue, the fifth of the month. The Board of Editors does not hold itself responsible for the opinions expressed by the correspondents.

Diffuse Scattering of X-Rays from Piezoelectrically Oscillating Quartz

Using a photographic method, Fox and Fraser[1] have recently found that when a crystal is piezoelectrically oscillating the increased intensity of the Laue spots is accompanied by an increased intensity of the undeviated beam penetrating the crystal. Obviously it is of interest to determine whether piezoelectric oscillations affect the intensity of the diffusely scattered x-rays. We used an unetched "Y cut" quartz plate of thickness 0.105 cm and the ionization chamber technique described by Jauncey and Claus.[2] A typical result is shown in Fig. 1. This curve is corrected for scattering from the aluminum electrodes placed in contact with the quartz plate. The ratio of "oscillating" to "not oscillating" reaches its maximum value of 2.0 at the center of each component of the double Laue spot. The curve shows evidence of the doubleness of the spot. Beyond the Laue spot on either side where there is only diffuse scattering the ratio drops to 1.00 ± 0.01, indicating no change in the diffuse scattering. Numerous readings showed that the S values for quartz are changed, if at all, by no more than one percent. This lack of effect of piezoelectric oscillations on the diffuse scattering supports the view that the effect on the Laue spots is due to a change in the extinction coefficient, since the value of this coefficient has no effect on the diffusely scattered x-rays.

Our ionization chamber method showed no change in the intensity of the undeviated beam penetrating the crystal greater than one percent. This is at variance with the increased area and blackness of the central spot as reported by Fox and Fraser.

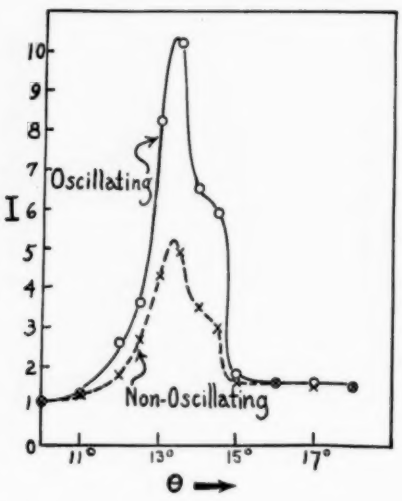

FIG. 1. Curve for the ionization chamber set at a scattering angle of 30°. θ is the angle between the normal to the crystal plate and the primary beam. The flat portions of the curve are due to diffuse scattering.

G. E. M. JAUNCEY
J. H. DEMING
Wayman Crow Laboratory of Physics,
Washington University,
St. Louis, Missouri,
July 30, 1935.

[1] Fox and Fraser, Phys. Rev. **47**, 899 (1935).
[2] Jauncey and Claus, Phys. Rev. **46**, 941 (1934).

The Velocity of Light Within a Massive Enclosure

D. C. Miller explains in his report,[1] that the difference between his results and those of other experimenters in the field[2] may be due to entrapping of the ether in the heavily enclosed apparatus of the other investigators, while his own apparatus is quite open to the outside atmosphere. If this explanation be correct, it should be possible to detect a differential light velocity between a light beam in a heavily walled tube with stopped ends held in the direction of the earth's velocity and a light beam just outside and parallel to the tube.

An apparatus was therefore constructed in which an unpolarized beam of white light was divided by means of a half-silvered mirror into two beams of approximately equal intensities. One beam, entered transversely a heavy walled steel tube with lead plugged ends through a small hole near one end, was reflected by means of a fully silvered mirror a distance of 89.4 centimeters along the axis of the tube, then encountered another fully silvered mirror which reflected the beam out through a small lateral hole near the other end of the tube. Outside the second hole was another fully silvered mirror which projected the beam parallel to the tube toward the originally encountered half-silvered mirror through which a portion of the half-beam passed a second time, but now at right angles to its original direction. The second of the original half-beams traversed the same path indicated above but in the opposite direction from the half-beam first considered. Since the two half-beams partly reunited after passing through the half-silvered mirror for the second time, a pattern of interference fringes was seen in the field of the half-silvered mirror. If any differential velocity existed between the light inside the tube and that outside, the position of the interference pattern should depend on this differential velocity. The velocity difference should yield an apparent path difference of $2VD/C$, where V is the difference in the ether drifts outside and inside the tube, C

is the velocity of light in air, and D is the length of the light path along the axis of the tube.

In my apparatus D has a value of 89.4 cm, and a shift in the position of the interference pattern of 1/10 of a fringe can be detected. It should then be possible to detect a difference in an ether drift between the inside of the tube and the outside of 1 km/sec.

On September 1, 1934, the apparatus was set up on the top of a high hill about two miles south of Moscow, and many observations were made in all azimuths during the daylight hours of September 1, 2 and 3. No shift of the interference fringes was observed, although conditions were very favorable, and a shift of 1/10 fringe would easily have been seen.

I conclude that Professor Miller's explanation of the difference between his results and those of the other investigators is not correct.

G. W. HAMMAR

University of Idaho,
Moscow, Idaho,
July 27, 1935.

[1] D. C. Miller, Rev. Mod. Phys. **5**, 203–242 (1935).
[2] R. J. Kennedy, Astrophys. J. **68**, 367 (1928); A. Piccard and E. Stabel, Comptes rendus **183**, 420 (1926); Naturwiss. **16**, 25 (1928); A. A. Michelson, F. G. Pease and F. Pearson, J. Opt. Soc. Am. **18**, 181 (1929); G. Joos, Ann. d. Physik (5) **7**, 385 (1930).

Heavy Particles from Lead

During an investigation of cosmic-ray showers with a large cloud chamber,[1] one photograph was obtained showing a dense track originating in a lead plate supported in the center of the chamber. The particle traveled a distance equivalent to a path of 10 cm in air at which point it passed out of the illuminated region. This event in conjunction with the recent ionization chamber results of Clay[2] led us to investigate the phenomenon more fully. An estimate from Clay's data indicates that if such particles exist, they should be expected in the ratio of one heavy particle to every 100 to 200 penetrating electrons. In the ordinary operation of the cloud chamber the time interval during which the chamber is sensitive is approximately a tenth of a second. A calculation, based on our knowledge of the frequency of occurrence of cosmic-ray electrons, shows that, on the average, one penetrating electron through the lead (area 280 cm^2) should be observed on a photograph taken at random. If we assume that both upper and lower surfaces of the lead are effective, we should expect one heavy track in 75 photographs. In order to increase the probability of observing these particles we adjusted the apparatus so that the sweeping field was removed about 0.3 sec. before the expansion. With this adjustment three of 38 photographs showed heavy particles. They had air equivalent ranges as follows: 9 cm ending in the illuminated space, 12.9 cm passing out of the lighted field, 12.6 cm ending in the gas. The latter is reproduced in Fig. 1. In the 38 photographs three short range heavy tracks (presumably alpha-particles) were observed leaving the lead. Thus it seems impossible to ascribe the long range particles to any ordinary radioactive contamination because of the relatively small number of shorter tracks observed. The heavy particle observed on the shower photograph was definitely not coincident in time with the cosmic-ray shower.

J. C. STREET
E. G. SCHNEIDER
E. C. STEVENSON

Research Laboratory of Physics,
Harvard University,
August 2, 1935.

[1] E. C. Stevenson and J. C. Street, Phys. Rev. (this issue).
[2] J. Clay, Physica **2**, 111 (1935).

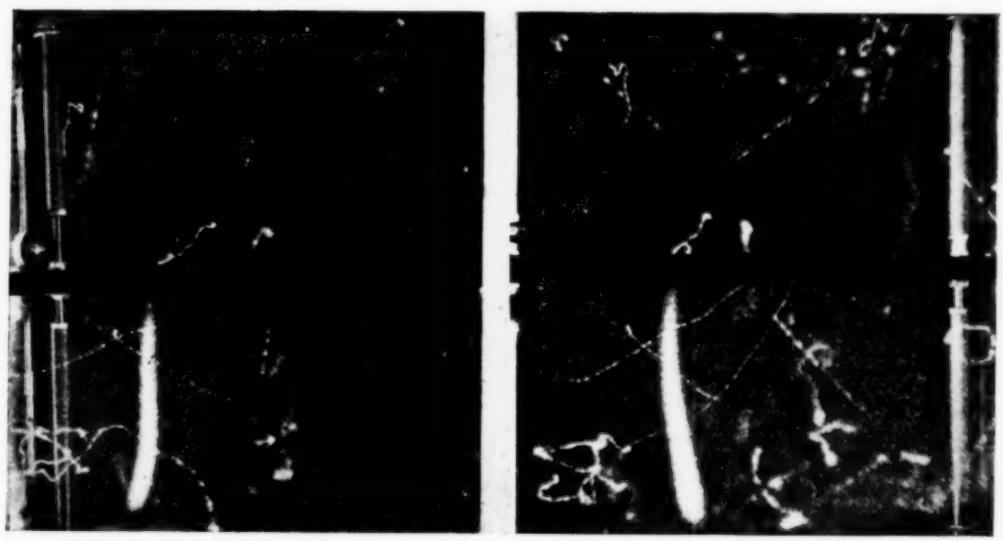

A B

FIG. 1. The heavy particle emerging from the lower side of the lead plate is quite evidently old, occurring one or two tenths second before the expansion.

Cosmic-Ray Showers Produced by Electrons

The cloud chamber observations of Anderson *et al.*,[1] Blackett,[2] and others have shown frequent examples of electron showers directly produced by some non-ionizing radiation, presumably of the γ type. However, the observations obtained with certain counter arrangements[3, 4] indicate the presence of an ionizing radiation above the scattering material coincident with a shower below. We have now made cloud chamber observations of showers selected by such an arrangement of counters. Three points in technique were found to be important in making observations of this type: (1) It is essential that the cloud photographs show the space above as well as below the scattering material. (2) Heavy material other than the scattering block must be reduced to a minimum. (3) The apparatus must be sufficiently large to give showers with reasonable frequency. To meet these requirements we have constructed a cloud chamber with a wooden frame (7/8-inch wall thickness) made gas tight with a 0.005-inch copper lining. The sensitive illuminated volume is 35 cm×30 cm×8 cm. The scattering lead block, 1.3 cm thick, is supported in the center of this space on insulated posts and acts as the sweeping electrode. The low expansion ratio 1.09 obtained by using ethyl alcohol vapor in argon makes the operation of such a chamber feasible. Fig. 1 shows schematically the arrangement of counters, chamber, and scattering block.

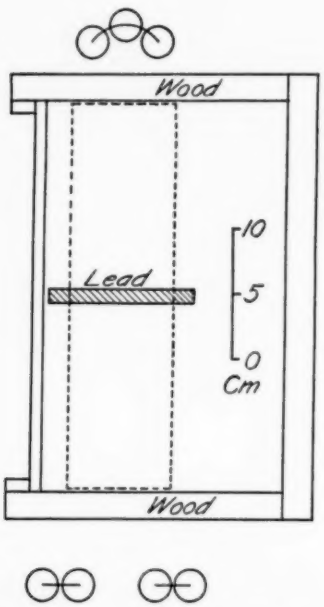

FIG. 1. Geometrical arrangement of counting tubes, cloud chamber and lead scattering block. The section between the dotted lines is illuminated. The three tubes above are connected in parallel as one unit. Below the chamber are two units each with two tubes in parallel. A triple coincidence of the three units sets off the expansion.

Photographs showing at least three classes of phenomena have been obtained. (1) The simplest type is illustrated in Fig. 2 where a single ionizing ray passes through the top counter and the upper half of the chamber and produces a shower in the lead. (2) A second type shown in Fig. 3 consists of a shower from the lead which actuates the two lower counters. No ray is visible above. Possibly the top counter is discharged by a photon scattered backward or by an associated ionizing ray not visible in the chamber. (The chance of an accidental coincidence is too small to account for the number of this type observed.) Occasionally very complex effects are observed combining both of the above types (Fig. 4). (3) In a third type only a single ray suffering a large deflection in passing through the lead is observed. Here, one or both of the lower counters may

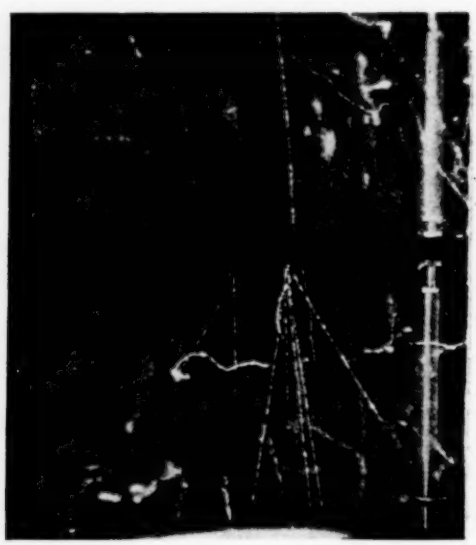

FIG. 2.

FIG. 3.

FIG. 2. A shower produced by an electron. A companion stereoscopic photograph (not reproduced here) checks the position of the ray above the lead. The slight displacement of the ray above the lead is due to an irregularity in the expansion, a fact which has been verified by stereoscopic photographs of several straight rays.
FIG. 3. A shower produced by a non-ionizing ray.

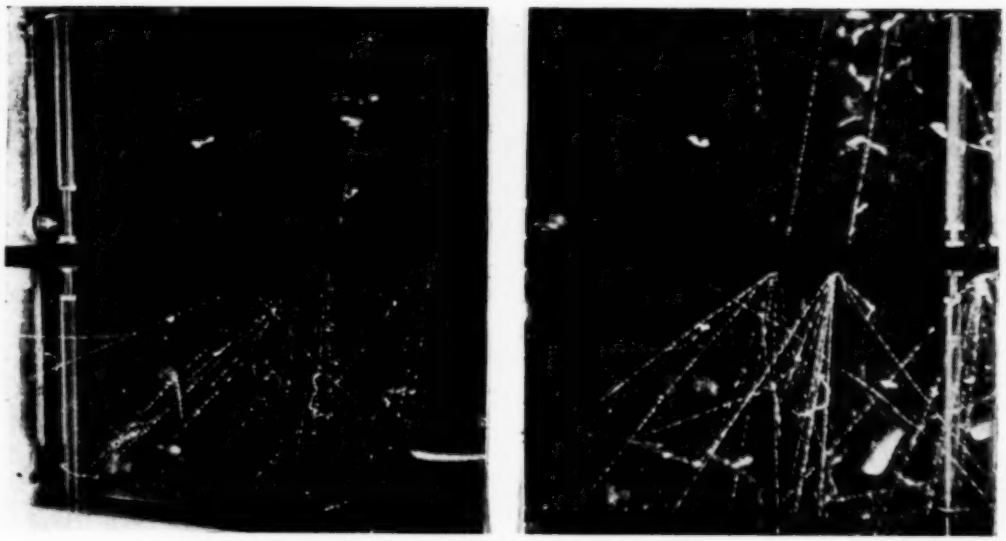

A. B.

FIG. 4. Stereoscopic pair (each at 30° with the normal) showing complex shower phenomena. In this remarkable event three showers emerge from the lead with every appearance of simultaneity. Two are produced by electrons with very closely parallel paths and the third by a non-ionizing ray.

be excited by secondaries from scattered photons which arise at a nuclear collision in the lead. Although the number of photographs taken is too small to make a reliable estimate of the relative frequencies of these three types it is of interest to note that out of 35 successful photographs 13 may be definitely classified as type (1).

E. C. STEVENSON
J. C. STREET

Research Laboratory of Physics,
Harvard University,
July 27, 1935.

[1] Anderson, Millikan, Neddermeyer and Pickering, Phys. Rev. **45**, 352 (1934).
[2] Blackett and Occhialini, Proc. Roy. Soc. **A139**, 699 (1933).
[3] Street and Johnson, Phys. Rev. **42**, 142 (1932).
[4] J. H. Sawyer, Jr., Phys. Rev. **47**, 515 (1935).

Additional First Negative Oxygen Bands

To five bands of the first negative system, those at λλ5295, 5631, 6026, 6419 and 6856A, the quantum numbers (2,0), (1,0), (0,0), (0,1) and (0,2) were early assigned. The measurement of three further bands at λλ5005, 7334 and 7891A, with the numbering (3,0), (0,3) and (0,4) was given some time ago.[1] An additional band, joining on the high frequency side of the 6026A band at about 5900A was reported by Steubing,[2] but the later investigators, e.g., Cario[3] and Frerichs[4] assigned no quantum numbers to this band. This is not surprising if one considers that on the pictures of these authors,* because of the high effective temperatures of their strong hollow-cathode light sources, the very complicated rotational structure of the main band overlaps that place completely.

The high frequency discharge which proved successful in Zeeman effect work (see above), being rather cooler and at the same time not much less intense, allows the various vibrational bands to appear at the expense of the rotational development of each. About nine additional bands could be recognized fairly well, not only by their heads, but by several other typical parts too. The present status of experimentally identified heads (long wavelength side "most obvious" heads) is given in Table I. Steubing's

TABLE I. *First negative oxygen bandheads.*

v' \ v''	0	1	2	3	4
0	16,589	15,575	14,581	13,606	12,669
1	17,751	16,736	15,741		
2	18,878	17,860	16,871		
3	19,972	18,953	17,959	16,992	
4				18,043	17,097

band, with proper head measurement of course, represents the (2,2) band. Since the recognition of the interlacing higher vibrational bands renders the appearance of the main bands ($v''=0$ and $v'=0$ progressions) somewhat less complicated, the prospects of a rotational analysis seem to be increased by the present work.

L. BOZÓKY
R. SCHMID

Physical Institute of the Royal Hungarian University for Technical and Economic Sciences, Budapest,
August 9, 1935.

[1] R. S. Mulliken and D. S. Stevens, Phys. Rev. **44**, 720 (1933).
[2] W. Steubing, Ann. d. Physik **33**, 553 (1910).
[3] His pictures have been measured by F. Holland, Zeits. f. wiss. Phot. **23**, 342 (1925).
[4] R. Frerichs, Zeits. f. Physik **35**, 683 (1926).
* Thanks should be expressed to Dr. Frerichs for letting us have his and Dr. Cario's old plates.

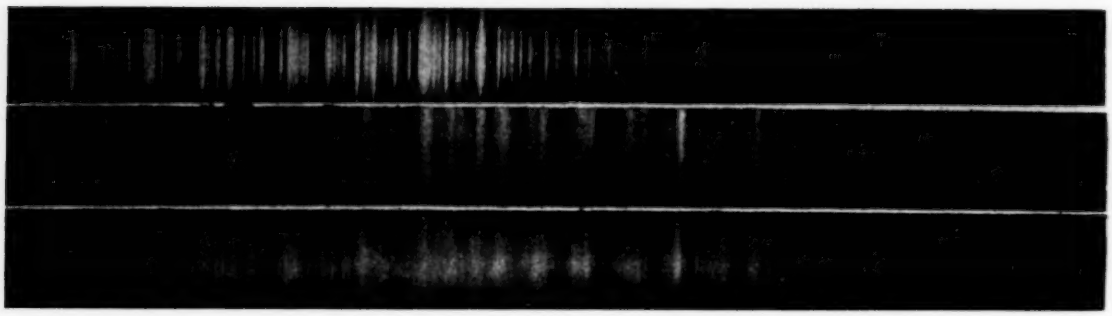

FIG. 1. Zeeman effect in the first negative oxygen bands, $\lambda = 5631$A. Upper, no field; center, $2\Delta\nu_{\text{norm.}}$ $H = 15{,}300$ gauss; lower, $2\Delta\nu_{\text{norm.}}$ $H = 23{,}300$ gauss.

Zeeman Effect in the First Negative Oxygen Bands

As light sources for the first negative oxygen bands the admixing of small amounts of oxygen in a Geissler-discharge in a rare gas, the hollow cathode and the constricted d.c. arc[1] in pure oxygen have been used by previous workers. All these sources have now been tried by us between magnet poles, but none of them gave light enough to photograph a Zeeman effect with a large grating. An apparatus, however, which originally had been built for Zeeman effect work in rare gases by us,[2]—consisting chiefly of a radio circuit, the high frequency voltage being transmitted by oil-cooled outer electrodes on the special-shaped quartz discharge tube,—was able to keep a bright and constant discharge in a capillary placed transversely between the magnet poles.

The bands were photographed with the 21-foot, 15,000 line per inch grating of the Institute, mounted in parallel light of a collimator lens (stigmatic projection), the dispersion being about 4.74A/mm in the first order of the visible spectrum, on Ilford Hyperpan films. The reproduction shows an enlarged photograph of the O_2^+ band at $\lambda = 5631$A with and without fields. The corresponding widths of $2\Delta\nu_{\text{normal}}$ are marked in Fig. 1 also. Although the structure of the bands is unknown as yet, a doublet or quartet structure is probable. The observed effects,—shifts or splittings of the order of magnitude of $2\Delta\nu_{\text{normal}}$,—are consistent with this expectation. A detailed report with probable explanations will be given later.

L. BOZÓKY
R. SCHMID
Physical Institute of Royal Hungarian University for Technical and Economic Sciences, Budapest,
August 9, 1935.

[1] See especially D. S. Stevens, Rev. Sci. Inst. **6**, 40 (1935).
[2] See recent papers of B. Pogány, Zeits. f. Physik **86**, 729 (1933); **93**, 364 (1935); also Zeeman volume of Physica, 336 (1935).

Is the Quantum-Mechanical Description of Physical Reality Complete?

In a recent paper Einstein, Podolsky and Rosen[1] conclude that the description of reality given by wave functions is not complete. This conclusion is directly opposed to the view held by many theoreticians, that a physical property of a given system has reality only when it is actually measured, and that wave mechanics gives a faithful and complete description of all that we can learn from measurements. The purpose of this note is to examine the reason for this divergence of conclusion. The reason is that the authors adopt a criterion of reality different from the one just mentioned; they say, that if, without in any way disturbing a system, we can predict with certainty the value of a physical quantity, there exists a corresponding element of physical reality. They consider two systems, I and II, which interact up to a certain time, after which there is no interaction. They show that by measuring the quantities belonging to certain operators A and B, characteristic of system I, it is in general possible, without disturbing system II, to predict with certainty *either* the value of a quantity P, *or* the value of a quantity Q; where P and Q belong to system II, and do not commute. However, there is no question of actually measuring *both* A and B; indeed, we can show that if P and Q do not commute, A and B in general do not, so that the corresponding physical quantities cannot be measured simultaneously. (Doubtless it is possible to extend the scheme to three systems, so that in the sense discussed by Einstein, Podolsky and Rosen either A or B could be predicted by studying the third system; and so on, until an indefinite number of systems is employed; but this does not help matters, nor is it necessary for the purposes of this discussion.)

The conclusion drawn by Einstein, Podolsky and Rosen is, that in accordance with their criterion of reality, the quantities corresponding to both P and Q possess reality; so that the wave description, failing to yield both of them, is incomplete.

This conclusion can be attacked by anyone who prefers to say that P and Q could possess reality only if *both* A and B (not merely one or the other) could be simultaneously measured. Indeed, this is clearly stated in the paper under discussion. Whereas, Einstein, Podolsky and Rosen say it is not reasonable to suppose the reality of P and Q can depend on the process of measurement carried out on system I, an opponent could reply: (1) that it makes no difference whether the measurements are direct or indirect; (2) that system I is nothing more than an instrument, and the measurement of A makes this instrument unfit for the measurement of B. Such an opponent will feel that the ingenious method of measurement discussed by Einstein, Podolsky and Rosen suffers from all the essential difficulties common to measurements which result in disturbing system II.

It seems to the writer that in the present state of our knowledge the question cannot be decided by reasoning based on accepted physical principles. The arguments which can be advanced on either side seem to be far from conclusive, and the issue involved appears to be a matter of personal choice or of definition.

ARTHUR E. RUARK

University of North Carolina,
Chapel Hill, North Carolina,
July 2, 1935.

[1] Einstein, Podolsky and Rosen, Phys. Rev. **47**, 777 (1935).

Some Investigations of Neutrons from Different Sources

The neutrons were produced by bombarding different targets with deuterons accelerated by a 400,000-volt transformer-rectifier outfit. The ions came from a canal-ray discharge similar to that used by Oliphant and Rutherford,[1] the ion current being between 20 and 120 microamperes (μA) measured in a Faraday cage with retarding potentials for trapping the secondary electrons, but without magnetic separation. Besides compounds of heavy hydrogen (phosphoric acid and sodium deuteroxide) we used as targets pieces of metallic beryllium and an artificial LiF-crystal. The voltage was measured with the electrostatic generating voltmeter constructed by Harnwell and Van Voorhis.[2] For measuring the yield of the neutrons we allowed them to activate different substances and compared their radioactivity—similarly to Bjerge and Westcott[3]—with that produced under the same conditions by neutrons from beryllium bombarded by alpha-rays of radium. As alpha-ray source we did not use radon, but 15 millicuries (mc) of $RaBr_2$ mixed thoroughly with finely powdered beryllium.[4] This source has the obvious advantage over the usual radon source of being constant. In some of the experiments we surrounded the targets with different amounts of paraffin or water for slowing down the neutrons and for comparing the effect of different amounts of substances rich in hydrogen on the neutrons from the different sources, which have widely different energy distributions. Our investigations do not yet allow us to give quantitative results of this effect.

With Ag activated in a beaker containing 675 cc of water, the neutrons from the D–D reactions produced at 100 kv and 100μA total ion current about the same effect as 400 mc of our Ra-Be source, increasing slowly with increase of the voltage. At such low voltages the deuterium targets are obviously much more effective for producing neutrons than Be or Li targets, but the D targets which we used did not last long.

The yield of the neutrons from the Be target (a flat piece of 2 mm thickness), investigated also by activation of Ag, but in a large paraffin block of 9000 cc, corresponded at 200 kv and 100μA to about 215 mc, showing fluctuations of 25 percent or more, due probably to changing amounts of deuterium adsorbed at the target and to the consequently changing effect of the neutrons from the D–D reaction.

The neutrons from the LiF target gave more constant results especially when we measured their yield by activating quartz. The radioactivity of Si is due to fast neutrons only and is, according to Bjerge and Westcott,[3] not produced by the neutrons from the D–D reaction, as their energy ($\sim$2 MV) is probably not high enough. When slowing down the neutrons from the LiF target by paraffin wax and activating silver (in the same way as with the neutrons from the Be target) we again found fluctuations of the yield,[5] probably due to changing amounts of the D–D neutrons. A corresponding difference appeared in the excitation-function of the neutrons activating quartz and silver, respectively, as shown in Table I. The relative yield of the neutrons is given by the activity of the two substances, their value being put arbitrarily equal to 100 at 150 kv.

TABLE I.

VOLTAGE (kv)	RADIOACTIVITY OF QUARTZ	RADIOACTIVITY OF SILVER
75		20
150	100	100
250	1200	350
275	1900	

The logarithm of the effect in quartz is a linear function of $(1/E^z)^{\frac{1}{2}}$, where E^z, the "effective" voltage, $= E\,M/(M+m)$, E is the applied voltage, M the mass of the disintegrated nucleus and m the mass of the bombarding particle, in agreement with the quantum-mechanical chance of penetrating the nuclear barrier.[6]

The effect is very much larger in silver than in quartz, as well with the neutrons from the LiF target as from our Ra-Be source. In units of this source the effect in silver corresponded at 100 kv and 100 μA to 57 mc and at 200 kv to 260 mc, with an uncertainty of nearly 20 percent due to the fluctuations of the neutron yield in bombarding the LiF target. The effect in quartz corresponded at 200 kv to about 130 mc, but our Ra-Be source was not strong enough to allow accurate measurements of the quartz activity. In these experiments with the LiF target the effect in silver surrounded by paraffin is partly due to the neutrons from the D–D reaction, whereas the effect in quartz is probably entirely due to the reaction

$$_1D^2 + {}_3Li^7 \rightarrow 2\ {}_2He^4 + {}_0n^1.$$

As the necessary completion and improvements of our investigations will take many more months this preliminary report seemed advisable.

We wish to express our appreciation to the Rockefeller Foundation for a special grant and to the Department of Chemistry for the preparation and the supply of heavy hydrogen.

R. LADENBURG
R. ROBERTS
M. B. SAMPSON

Palmer Physical Laboratory,
Princeton, New Jersey,
August 2, 1935.

[1] M. L. E. Oliphant and Lord Rutherford, Proc. Roy. Soc. **A141**, 259 (1933).
[2] G. P. Harnwell and S. N. Van Voorhis, Rev. Sci. Inst. **4**, 540 (1930).
[3] T. Bjerge and C. H. Westcott, Nature **134**, 177 (1934).
[4] J. C. McLennan, L. G. Grimmett and J. Read (Nature **135**, 147 ff (1935)) used also radium itself instead of radon.
[5] As these fluctuations do not appear in the activity of quartz they are not due to a change in the ratio of atomic and molecular ions.
[6] Compare, for example, J. D. Cockcroft, International Congress of Physics (London 1934), Vol. I, p. 127.

The Probability of K Shell Ionizaton of Silver by Cathode Rays

In a very interesting paper[1] recently published, J. C. Clark describes the measurement of the absolute probability of K shell ionization of silver by cathode rays of different energies. The observed values are compared with certain theoretical values. In particular, in Fig. 5 comparison is made with three so-called wave-mechanical theories, one due to Wetzel, one to Soden, and the other is attributed to us. Unfortunately because of an oversight the wrong absolute values of our calculated probabilities were forwarded by us in our correspondence with Dr. Clark and the true values agree very closely with the observed—as shown in Fig. 1. and certainly better than do the other curves given in Clark's paper. This is to be expected, as the results of Wetzel and Soden do not represent wave-mechanical theories different from ours, but simply different and less accurate approximations to the integrals which arise in the wave-mechanical theory of collisions when applied in the first approximation. These integrals involve the average of the interaction energy between the ionizing electron and the atom over the wave functions of the initial and final states of the two electrons concerned (the incident and atomic electrons, respectively).

Wetzel[2] uses plane waves to represent the final wave function of the ejected electron and difficulties arise because of the lack of orthogonality between such a function and that representing the K shell states. We use final ejected electron wave functions which are exactly orthogonal to the K shell function, and must be quite accurate in the region of importance (screened hydrogenic functions being actually used). Soden[3] also uses orthogonal functions but does not evaluate the integrals involved exactly (an approximate method due to Bethe[4] being used)—and introduces a somewhat doubtful relativity correction.

It is of interest to point out that closer agreement is obtained between experiment and the first approximation of the wave-mechanical theory for the K ionization of silver than for the ionization of helium at corresponding energies (up to six times the ionization potential). This is to be expected, partly because the screened hydrogenic wave functions used are more accurate for silver than for helium and also because one would expect the second approximation of the theory (which allows of double collisions in which the excited atom is deactivated before the impinging electron passes out of the atomic field and so results in a reduction of probability) to be less important, the inelastic scattering from the K shell being small compared with the elastic scattering by the nucleus.

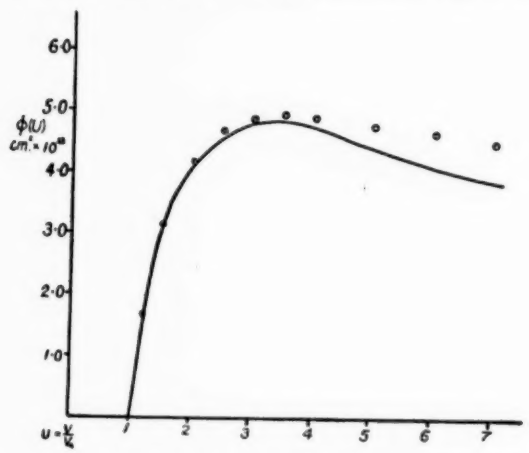

FIG. 1. Cross section $\phi(u)$ for k shell ionization *vs.* energy in case of silver. The circles represent Clark's experimental cross section. The full line is that calculated theoretically by the authors.

A more complete account will be published later and a correct relativistic treatment of the ionization probability is also being carried through.

H. S. W. MASSEY
E. H. S. BURHOP

Cavendish Laboratory,
Cambridge, England,
July 27, 1935.

[1] J. C. Clark, Phys. Rev. **48**, 30 (1935).
[2] W. W. Wetzel, Phys. Rev. **44**, 25 (1933).
[3] D. Graf Soden, Ann. d. Physik **19**, 409 (1934).
[4] H. Bethe, Ann. d. Physik **5**, 325 (1930).

On the Stability of $_4Be^8$

Evidence for the formation of $_4Be^8$ in nuclear reactions has been obtained by various authors.[1, 2, 3] Since this isotope is spectroscopically as yet unknown, it was proposed that it is an unstable isotope of beryllium. From the gamma-ray spectrum resulting from the bombardment of Li by H, Crane and Lauritsen[1] come to the same conclusion; they deduce that Be has an excess of 0.0016 mass units and splits up therefore instantaneously into two alpha-particles of 3.5 mm range. These conclusions do not depend upon the assumed spectroscopic values of mass and are compatible with Bethe's[4] or Oliphant and others'[3] corrected values of mass.

Bonner and Brubaker[2] from the reaction $_1H^2+{}_3Li^7 \rightarrow {}_4Be^8+{}_0n^1$ obtain for $_4Be^8$ a mass 0.3 ± 0.75 MEV greater than that of two alpha-particles. Recently Oliphant, Kempton and Rutherford[3] in a general revision of mass of light atoms assume that $_4Be^8$ is probably just stable.

It is known[5] that beryllium, when bombarded with gamma-rays, emits neutrons and it is probable that $_4Be^8$ is formed in this reaction.* We have therefore attempted, by using a linear amplifier, to detect alpha-particles, which can be perhaps ejected from Be bombarded with gamma-rays. One of the electrodes of the ionization chamber was covered with a layer of Be. Photographic oscillographic records were taken every 10 minutes alternately in absence and in presence of gamma-rays; a source of about 45 mc in equilibrium was used. In spite of the very strong gamma-radiation we are able to detect a single particle which produces in the chamber 4000 ion pairs.

From some experiments on activation by slow neutrons it results that our source produces in a second 1000 neutrons per gram of Be at 1 cm distance. This datum has been kindly communicated to us from Professor E. Fermi and Dr. B. Pontecorvo. We want here to express our gratitude to them.

If we take into account geometrical conditions, on the hypothesis that the initial range of the particles is, re-

spectively, 4, 3.5, 3, 2.5 mm we find that every 60, 80, 120, 240 seconds one alpha-particle, on an average, must traverse the chamber with at least 2 mm residual range (4000 ion pairs). The first results are as follows: 16 particles in 68 minutes without gamma-rays, 2 particles in 63 minutes with gamma-rays.

From foregoing data we may calculate, for the different initial ranges, the probability that the number of particles really observed can be attributed to statistical fluctuations.

Table I is of significance. The first column contains the

TABLE I.

RANGE (mm)	$n°$ TO BE EXPECTED	PROBABILITY RATIO
4	77	1.13×10^{-19}
3.5	61	7.95×10^{-14}
3	45	1.87×10^{-8}
2.5	30	5.63×10^{-4}

supposed initial ranges in mm of air. The second column gives the average number of particles to be expected. A null effect of 14 particles per hour, resulting from prolonged visual counts, is, of course, contained in it. The third column contains the ratio of the probability of observing 2 particles (number really observed) to that of observing the average number which is reported in the second column.

In our opinion this ratio permits one to decide whether alpha-particles of various range are generated in Be, or not. We are, therefore, able to conclude that, if ${}_4Be^8$ is formed in the reaction, it is stable or it has an excess of mass less than 0.56 MEV. This latter corresponds to the energy of two alpha-particles of 2.5 mm range. This value has been obtained by extrapolating the Briggs curve and it is in fair accord with Blackett's and Curie's data.[6]

The foregoing result excludes therefore the production of particles of 3.5 mm range, as has been proposed by Crane and Lauritsen, while it agrees with Bonner and Brubaker and with Oliphant, Kempton and Rutherford. We must remark that our result is truly an upper limit. It is, however, the only one deduced by a direct experiment and without using spectroscopic mass data. More details will appear in *La Ricerca Scientifica* (to be published soon).

In conclusion we wish to thank Professor L. Tieri for his valuable advice and helpful discussions. Our thanks are also due to the "Soc. An. Cappelli-Ferrania" (Milano), which has kindly put at our disposal the necessary film.

G. BERNARDINI
M. MANDO

Arcetri,
July 29, 1935.

* See also references 1 and 2.

[1] Crane and Lauritsen, Phys. Rev. **47**, 420 (1935).
[2] Bonner and Brubaker, Phys. Rev. **47**, 973 (1935).
[3] Oliphant, Kempton and Rutherford, Proc. Roy. Soc. **A150**, 241 (1935).
[4] Bethe, Phys. Rev. **47**, 633 (1935).
[5] Szilard and Chalmers, Nature **134**, 494 (1934); Gentner, Comptes rendus **199**, 1211 (1934); Ridenour, Shinohara and Yost, Phys. Rev. **47**, 318 (1935); Arzimowitch and Palibin, Physik. Zeits. d. Sowjetunion **7**, 244 (1935); Brasch, Lange, Waly, Banks, Chalmers, Szilard and Hopwood, Naturwiss. **22**, 839 (1934).
[6] Rutherford, Chadwick and Ellis, *Radiation from Radioactive Substances*, p. 106.

The Disintegration of Nitrogen by Slow Neutrons

Nitrogen was one of the first elements to be disintegrated by fast neutrons.[1] The nuclear reaction that takes place is

$$ {}_7N^{14}+{}_0n^1\rightarrow{}_5B^{11}+{}_2He^4. $$

From Bethe's values for the masses, the reaction is exothermic by 1.5 mev, and hence should be expected to take place for slow neutrons in a manner similar to that of lithium and boron. In fact, Chadwick and Goldhaber[2] reported a small but definite increase in the number of counts from a nitrogen filled ionization chamber when the source of neutrons and the chamber were surrounded by paraffin.

We have observed the disintegration of nitrogen by slow neutrons in a cloud chamber. When the incident neutrons have nearly zero energy, the ${}_5B^{11}$ and ${}_2He^4$ particles recoil in opposite directions and appear as a single straight track. These tracks should all be the same length, as the energy contributed by the neutrons is negligible.

Our source of neutrons was a beryllium target which we bombarded with 0.85 mev deuterons. The neutrons were slowed down by a paraffin sphere 7.5 cm in diameter which we placed around the target, and by blocks of paraffin which we placed around the chamber. Because the Pyrex glass ring of the chamber contained boron which would stop the slow neutrons, we replaced it by a thin brass one for this work.

We have taken 2600 stereoscopic pairs of photographs with our cloud chamber when it was filled with nitrogen and saturated water vapor, and operated at an expanded pressure of 0.6 atmosphere. From these pictures we have measured the lengths of 152 straight tracks that begin and end in the chamber. Numerous disintegration forks which were due to the fast neutrons were observed, and an analysis of them will be given later. The 152 track lengths have been converted to cm of air equivalent range by the use of the stopping power (0.592) which was accurately determined from the mean range of polonium alpha-particles.

The range distribution of these tracks is given in Fig. 1. There are three different types of tracks represented: those due to recoil nitrogen nuclei, recoil protons, and those due to the disintegration of nitrogen. Neutrons with 4.42 mev maximum energy[3] should project nitrogen nuclei with a maximum range of 0.28 cm in excellent agreement with the curve of Fig. 1. A small number of recoil protons from the water vapor with all ranges up to 28 cm should be observed. These appear as the background above 0.28 cm. The single

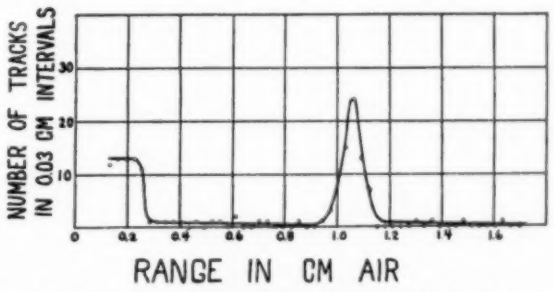

FIG. 1. Range distribution of the tracks observed in the cloud chamber.

line with a mean range of 1.06 ± 0.02 cm is due to the combined tracks of the alpha-particles and B^{11} nuclei produced in the disintegration of nitrogen by slow neutrons. The energy of disintegration, Q, was computed and found to be 2.57 mev if Duncanson's range-velocity curve[4] for alpha-particles was used, and 2.06 mev if we used Briggs' curve.[5] At present, it is not clear which of these curves is better, so we may tentatively say that the value of Q is 2.31 ± 0.35 mev. As Bethe's masses[6] give 1.5 mev for Q, this indicates that the value for the mass of $_7N^{14}$ should be raised slightly or that of $_5B^{11}$ lowered, or the masses of both should be altered.

T. W. BONNER*
W. M. BRUBAKER

Kellogg Radiation Laboratory,
California Institute of Technology,
August 12, 1935.

[1] N. Feather, Proc. Roy. Soc. **A136**, 709 (1932).
[2] J. Chadwick and M. Goldhaber, Nature **135**, 65 (1935).
[3] T. W. Bonner and W. M. Brubaker, Phys. Rev. **47**, 910 (1935).
[4] W. E. Duncanson, Proc. Camb. Phil. Soc. **30**, 102 (1934).
[5] G. H. Briggs, Proc. Roy. Soc. **A114**, 341 (1927).
[6] H. Bethe, Phys. Rev. **47**, 633 (1935).
* National Research Fellow.

Slow Neutrons

As the upper energy limit for the neutrons which show anomalous absorption in such elements as cadmium and silver has not been determined, we have performed experiments with a cloud chamber in an attempt to find such a limit.

We have used a Wilson chamber filled with hydrogen and saturated water vapor at an expanded pressure of $\frac{1}{2}$ atmosphere so that we could measure the tracks of the short range recoil protons which are projected by neutrons in the energy interval of 0.03 to 0.6 mev. We have done two separate experiments, both of which indicate that there is no anomalous absorption in the interval investigated.

The first of these experiments was to determine the effect produced on the number of neutrons in this energy interval by surrounding our lithium deuteron source with a paraffin sphere 7.5 cm in radius. Alternate runs of 200 pictures each were taken with and without the sphere in place. The results of this experiment are given in Table I. It is apparent that there is no very great change in the distribution of the neutrons in this energy interval when the paraffin sphere is placed around the source. This means that approximately the same number of neutrons are removed from these intervals into ones of lower energy as are brought into this region from higher energies by passing through the paraffin.

TABLE I.

NEUTRONS FROM	NO. RECOIL PROTONS IN ENERGY INTERVALS 0.03–0.19 mev	0.20–0.39	0.40–0.59	NO. EXPANSIONS
Lithium deuterons	14	21	10	2200
Same, surrounded with paraffin sphere	16	16	14	2200

TABLE II.

ABSORBER	NO. TRACKS IN A GIVEN ENERGY INTERVAL (MEV) 0.03–0.19	0.2–0.39	0.4–0.59	NO. PICTURES
None	17	20	10	1000
LiCl 2.7 g/cm²	15	11	16	1000
Cd 5.1 g/cm²	18	17	16	1000
Ag 6.8 g/cm²	15	11	13	1000
Average	16	15	14	

To make certain that such a sphere actually did increase the number of slow neutrons, we have measured the increase in activity produced in a sheet of indium which was placed just outside this paraffin sphere. The increase of activity obtained after an hour's bombardment with the sphere around the target to that obtained in a similar instance without the sphere was thirty-fold, showing that the paraffin sphere increases the number of slow neutrons to a marked extent.

The second experiment was to find the energy distribution of the neutrons with and without absorbers of LiCl, Cd and Ag placed between the source and the chamber. The results are given in Table II.

We see that there appears to be no very large absorption by the elements tested. The thickness of the absorbers was such that a large absorption would have been obtained even if the target areas were considerably smaller than they are known to be for slow neutrons.

W. M. BRUBAKER
T. W. BONNER*

Kellogg Radiation Laboratory,
California Institute of Technology,
August 12, 1935.

* National Research Fellow.

Increased Frequency of Cosmic-Ray Bursts with Reduced Shielding

It is well known that the frequency of cosmic-ray showers increases with the thickness of absorbing material up to about 2 cm in the case of lead and then falls off rather rapidly for greater thicknesses. The decrease is due to the short range of the shower particles as well as the absorption of the shower producing radiation. That a somewhat similar situation exists in the case of "bursts" occurring in ionization chambers has not been so well recognized. It is the purpose of the present communication to describe some preliminary observations bearing on this point, which indicate that the effect is one of considerable magnitude.

The Compton-Bennett recording meter, used in the tests, consists of a 20-liter spherical ionization chamber filled with 50 atmospheres of highly purified argon and completely surrounded by 17 cm of lead shot contained in an outer steel shell. With a full shield the frequency of bursts larger than $15(10)^6$ ions ranges from 0.14 to 0.24 per hour at sea level. Of seven meters tested over a period of several months, one or two gave a burst frequency smaller than the others. Having in mind the situation in regard to showers, the

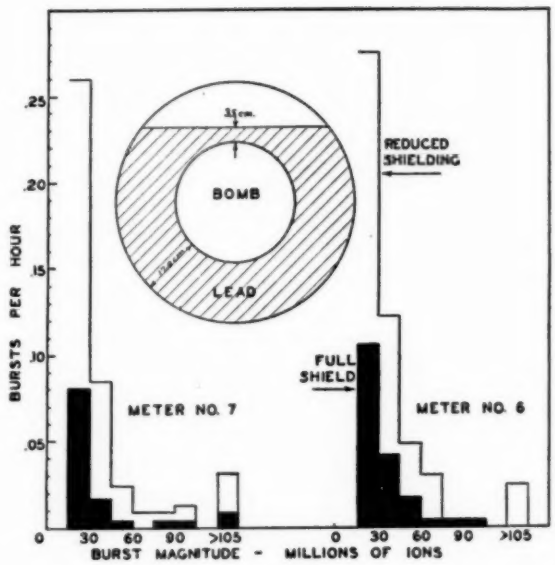

FIG. 1.

writer decided to remove about 250 lbs. of lead shot from Meter No. 7, leaving a minimum thickness of from 3 to 4 cm above the top of the bomb (see Fig. 1). The burst frequency at once jumped from the lowest in the group to approximately twice that of the highest in the group. After a few days an equal amount of shot was removed from Meter No. 6 as a check and a similar large increase of burst frequency was noted. The results for a period of approximately 250 hours before reducing the shielding and an equal period afterwards are shown in Fig. 1.

The observed increase of burst frequency with reduced shielding indicates that the burst-producing radiation is absorbed rather strongly in the lead. With the reduced shield it seems likely that some of the bursts are due to tertiaries produced by air secondaries whereas with the full shield the air secondaries can hardly be effective and all of the bursts are presumably due to tertiaries produced by lead secondaries.

RICHARD L. DOAN

Ryerson Physical Laboratory,
University of Chicago,
August 14, 1935.

Direct Detection of the Angular Momentum of Light

It has been known for some time that, on the basis of either the wave theory[1] or the quantum theory (by assigning an angular momentum of $\pm h/2\pi$ to a photon), a beam of circularly polarized light should exert a torque on a doubly refracting plate which changes the state of polarization of the light beam. The result can be extended to elliptically polarized light and it is quantitatively the same on the basis of both theories.

The purpose of this note is to announce the direct mechanical detection of this effect.

The apparatus used involves a torsional pendulum with about a ten-minute period consisting of a round quartz half-wave plate (for a wavelength of 1.2 mu) one inch in diameter suspended with its plane horizontal from a quartz fiber about 25 centimeters long. About 4 millimeters above this is mounted a fixed quartz quarter-wave plate (for the same wavelength) with its axes turned 90 degrees from those of the hanging plate. The *top* side of the upper plate was coated by evaporation with a reflecting layer of aluminum. This whole system is mounted in a heavy copper vacuum chamber with a fused quartz window at the bottom for the light beam. The rotation of the pendulum is observed by a telescope and scale.

Just below the bottom window is mounted a second quarter-wave plate for 1.2 mu in a ring which may be rotated in a horizontal plane from a position in which its axes are at 90 degrees to those of the hanging half-wave plate (i.e., the same direction as the top plate) to a position in which its axes are parallel to those of the hanging plate and back again.

Light from a 3-millimeter tungsten ribbon filament lamp passes up through a fused quartz condensing lens and a large Nicol prism and enters this plate system from the bottom. With the plane of polarization of the Nicol at 45 degrees to the plate axes, the change in light torque caused by rotating the lower plate through 90 degrees was measured by a resonance method, the plate being turned at the end points of the pendulum swing first so as to decrease the amplitude for two full cycles and then so as to increase the amplitude for two full cycles. Preliminary values for the torques obtained at various filament temperatures are as follows:

Filament temperature, degrees absolute		
2400	2600	2800
Torque change, dyne-cm		
2×10^{-9}	3×10^{-9}	4×10^{-9}

Blank runs made by removing the lower plate from the ring holding it, but otherwise turning the ring in the same way with the light on showed no trace of the effect.

At present the largest uncertainty in predicting the exact magnitude of the effect on the basis of the theory is the lack of knowledge of the spectral transmission characteristic of the optical train. With this uncertainty all that can be said at present is that the order of magnitude of the effect found is correct.

More exact measurements of the effect are now being made and will be considered in connection with a more detailed theoretical treatment of the effect in a complete paper to be submitted later.

RICHARD A. BETH*

Palmer Physical Laboratory,
Princeton University,
August 3, 1935.

[1] A. Sadowsky, Acta et Commentationes Imp. Universitatis Jurievensis **7**, No. 1–3 (1899); **8**, No. 1–2 (1900). P. S. Epstein, Ann. d. Physik **44**, 593 (1914).

* On leave-of-absence from the Physics Department of the Worcester Polytechnic Institute.

Proceedings of the American Physical Society

MINUTES OF THE MINNEAPOLIS MEETING, JUNE 21–22, 1935

THE 199th regular meeting of the American Physical Society was held in Minneapolis, Minnesota at the University of Minnesota on Friday and Saturday, June 21 and 22, 1935. There were two parallel sessions for the reading of ten-minute contributed papers on Friday morning. The presiding officers were H. A. Erikson and Anthony Zeleny of the University of Minnesota. The attendance was about one hundred.

The Society held a dinner on Friday evening, June 21st, at the Minneapolis Automobile Club on the Minnesota River twelve miles from the city. F. K. Richtmyer, Vice President of the Society, presided at the dinner and introduced as speakers Professor H. A. Erikson, Chairman of the Department of Physics of the University of Minnesota, and Professor G. E. Uhlenbeck of the University of Michigan. There were ninety-two guests present at the dinner, who were entertained afterwards by a program of chamber music by a trio consisting of Messrs. Leslie Atkins, William P. Dunn, and Abe Pepinsky.

On Saturday morning, June 22, a symposium of invited papers on Nuclear Physics was held. G. E. Uhlenbeck presided and the papers were as follows:

Some Current Nuclear-Physics Problems in the Region Below 1000 Kilovolts. L. R. HAFSTAD, *Carnegie Institution of Washington.*

Rates of Nuclear Reactions Due to Bombardment with Charged Particles. G. BREIT, *University of Wisconsin.*

Gamma-Rays and Electrons from the Transmutation of Some Light Elements. C. C. LAURITSEN, *California Institute of Technology.*

Nuclear Structure and Stability. H. BETHE, *Cornell University.*

On Saturday afternoon eighty-five members and guests attended a picnic with opportunity for golf, tennis, and water sports at Old Orchard on Lake Minnetonka and returned after dining at the Inn.

Meeting of the Council. At its meeting held on Friday, June 21, 1935 the deaths of two fellows (William Duane and Charles E. St. John) and two members (John C. Deagan and George M. Read) were reported. Two candidates were elected to fellowship and thirteen were transferred from membership to fellowship. Twenty-eight candidates were elected to membership. *Elected to Fellowship:* Enrique Gaviola and Ernest C. Pollard. *Transferred from Membership to Fellowship:* Arthur J. Ahearn, Robert F. Bacher, F. H. Crawford, John R. Dunning, Malcolm C. Henderson, Walter S. Huxford, Roy J. Kennedy, Franz N. D. Kurie, Edwin C. McMillan, Harry R. Mimno, Raymond J. Seeger, Lewis K. Sillcox, and Clinton L. Utterback. *Elected to Membership:* Carl J. Christensen, C. H. Dix, G. M. B. Dobson, Coleman Dodd, Bourne G. Eaton, Rebecca S. Fiske, J. W. Flowers, Robert C. Gore, Eugene W. Greenfield, Ernest J. Handley, John Harty, Hirosi Hasunuma, George A. Hawkins, Emil J. Konopinski, Rose S. Marx, W. D. McElroy, Masahumi Nagase, Koreiti Ogata, Robert S. Prescott, Jacob R. Risser, Louis A. Rohret, Ryokichi Sagane, George L. Shue, Akira Sogawa, Asao Sugimoto, Ryozi Uyeda, James H. Wayland, and Robert M. Whitmer.

The regular scientific program of the Society consisted of thirty-seven papers of which numbers 3, 4, 6, 9, 15, 18, 27, and 32 were read by title. The abstracts of the contributed papers are given in the following pages. An *Author Index* will be found at the end.

GEORGE B. PEGRAM, *Secretary pro tempore*

ABSTRACTS

1. X-Ray Ionization Chamber Materials. J. N. SAYLER, *University of Iowa.* (Introduced by G. W. Stewart.)—The rate of discharge of alpha-particles from materials of possible use in ionization chamber construction has been made by counting the number of particles (having energy in excess of a predetermined minimum) per hour per hundred square centimeters of surface exposed. The following results were found: cold rolled steel 12, electroplated

copper (CuCN) 37, commercially electroplated chromium 48, commercially electroplated nickel 31, commercial brass 15, commercial aluminum foil 34, commercial tin foil 47, commercial platinum foil 29, commercial molybdenum 195, Pyrex glass 16. The data confirm and supplement work of Bearden (Johns Hopkins) in 1932. Measurements were made by photographically recording alpha-particle currents in an ionization chamber, amplified by FP-54 vacuum tube system.

2. The Effect of the Spectrometer on the Width of Spectral Lines. ROY C. SPENCER, *University of Nebraska.*—The energy distribution of a spectral line is represented by a function $\phi(x)$. Each ordinate of $\phi(x)$ is spread out by the spectrometer into a curve $F(x)$. Let $\phi(O)=1$ and let the area under the curve $F(x)$ be unity. Then the experimental curve is

$$G(\beta)=\int_{-\infty}^{\infty}\phi(\beta-x)F(x)dx. \quad (1)$$

The fractional drop at the peak is

$$\phi(O)-G(O)=\int_{-\infty}^{\infty}[1-\phi(-x)]F(x)dx. \quad (2)$$

This approximates the increase in width at half-maximum divided by the width of $G(\beta)$. The factor $[1-\phi(-x)]$ causes the contribution of $F(x)$ to be negligible for small values of x but proportional to the area under $F(x)$ for large values of x. *Application to the Correction of X-Ray Line Widths.* If $\phi(x)$ is a witch of width a, Eq. (2) becomes

$$\phi(O)-G(O)=\int_{-\infty}^{\infty}[x^2/(a^2+x^2)]F(x)dx. \quad (3)$$

If $x=a\tan\theta$

$$\phi(O)-G(O)=\int_{-\pi/2}^{\pi/2}x^2F(x)d\theta. \quad (4)$$

Eq. (4) is in a form adapted to graphical integration. If $F(x)$ is also a witch of width b, Eq. (3) or (4) gives $b/(a+b)$. Over half of the contribution of the integral comes from beyond the point $x=a$. Crystal curves in the (1, −1) position should therefore be measured out as far as possible.

3. Computations Related to Liquid Structure by the Methods of Trial and of Fourier Series Analysis. G. A. BOYD, *University of Iowa.* (Introduced by G. W. Stewart.)—The suggestion has been made that one may obtain useful comparisons with experimental x-ray diffraction in liquids by using a structure consisting of an adjacent organized layer and at a larger distance a uniform distribution of scattering units. This method is found quite unsatisfactory and even misleading in some respects. At any rate it seems that even when extended to other layers this method is not as satisfactory as the Fourier's series method exemplified by the recent work of Pierce with heptane.

4. Effect of Chlorine Ions on X-Ray Diffraction in Aqueous Solution. G. W. STEWART, *University of Iowa.*—This is a record of quantitative measurements of the effect of chlorine ions on the x-ray diffraction of an aqueous solution. In using NH_4Cl, observation was made of the x-ray diffraction for angles less than that of maximum intensity, 12.5°, to 1° using Mo $K\alpha$ radiation. The increase in number of scattering electrons per cm³ by the addition of NH_4Cl was 17.7 percent or 12 percent for the Cl^- alone. The diffraction curve showed a fairly constant increase of about 11 percent over the selected range. If the radius of the Cl^- is as usually 1.81×10^{-8} cm and if it occupies a total volume corresponding to a closely packed liquid, the mean density of its electrons in this volume is approximately twice that in the water molecule. With 12 percent of the total scattering units occurring in the regions of a doubled density, an effect of gaseous scattering would be discernible at the small angles. But there is no such effect. Either there is a superstructure or the ion occupies a greater volume than assumed. If Cl^- is as loosely packed as the water molecules a detectable effect would still be expected.

5. The Influence of Chemical Combination on X-Ray Emission Spectra. JOSEPH VALASEK, *University of Minnesota.*—The study of the effect of chemical combination on the K beta lines of sulphur, chlorine and potassium which has been reported in the June 15th issue of *The Physical Review* has been extended to other compounds with the following preliminary results:

COMPOUND	LINE	WAVELENGTH
Na_2S	S $K\beta_1$	5018.06 X.U.
CdS	S $K\beta_1$	5015.87
AgCl	Cl $K\beta_1$	4393.57

Coupled with Stelling's data on the absorption edges, these measurements give information in regard to some of the electronic energy levels in the solid state. The case of AgCl is of interest because of its use in photography. Although the electron affinity of Cl^- as obtained from x-ray data is lower than in any other halide observed as yet, yielding a value of 4.6 electron volts, the value is larger than is to be expected from the photoelectric threshold indicating the presence of a lower energy state which does not enter into the processes observed here.

6. General Theory of Radioactive Fluctuations. ARTHUR E. RUARK, *University of North Carolina.*—*Generalization of Bateman's equation.* Let $f_n(t)$ be the probability that an event occurs in dt at t, when n have occurred in the interval O, t. Let W_n be the probability of n events in this interval. Then $dW_n/dt=f_{n-1}W_{n-1}-f_nW_n$. (1) For a source containing N atoms initially, $f_n=(N-n)\lambda$; $W_n=C_n^N(e^{\lambda t}-1)^ne^{-N\lambda t}$. (2) Suppose f depends on t, but not explicitly on n. Then $W_n=x^ne^{-x}/n!$ where $x=\int_0^t f(t)dt$. *Effect of solid angle subtended by detecting device.* Statements in the literature that the use of small solid angle prevents us from testing the random character of radioactive decay are wrong. There is a unique connection between W_n and the probability P_m for ejection of m particles into solid angle ω in time t. Let $\omega/4\pi=g$. For a source containing N atoms

$$P_m=W_mg^m[1+(e^{\lambda t}-1)(1-g)]^{N-m}.$$

For a "constant" source giving f particles/sec., P_m is given by Bateman's formula with fg substituted for f. These facts necessitate reconsideration of data on decay constants of artificially radioactive substances.

7. The Desorptive Action of Radon. E. L. HARRINGTON AND H. H. PENLEY, *University of Saskatchewan.*—Observations made in the course of the routine operation of a radon

plant pointed to the conclusion that when radon is admitted to a vacuum system adsorbed gases, not readily removable by vacuum pumps, are released (or else are formed) by the action of the radon. An experimental investigation of the problem has yielded results supporting the conclusion.

8. A Multiple-Column Mercury Manometer. J. R. ROEBUCK AND WINSTON CRAM, *University of Wisconsin.*—An open-tube multiple-column mercury manometer has been constructed. It consists of nine U tubes, approximately 17.5 meters long, connected in series. Toluene is used to transmit the pressure from one mercury surface to the next. A level reading device is placed at the top and the bottom of each U tube. It consists of a contact point moved in a one-inch diameter tube by a nut running on a micrometer screw driven from the outside through a packed joint. The connecting tubes of $\frac{1}{16}$ inch I.D., $\frac{1}{4}$ inch O.D. steel tubing are each enclosed in a larger pipe which forms part of a circulating oil bath for the control of the temperature. The temperatures of the liquids are read by seven mercury thermometers placed in different parts of the system. A Société Génevoise invar tape is used to measure the distance between contacting devices. The system has been connected so that any pressure below 192 atmospheres can be measured. The accuracy of pressure measurements depends on (1) the measurement of the length of the mercury columns, (2) the determination of the densities of the two liquids as a function of room temperatures and (3) the control of the temperature. The instrument is being tested by measuring the vapor pressure of carbon dioxide at the ice point.

9. The Principal Expansion Coefficients of Single Crystals of Mercury. DONALD M. HILL, *Rutgers University.*—The expansion coefficients were measured at 5° intervals from −115°C to −160°C, where the pentane bath became too viscous to use, and mean values found from −160°C to −190°C. The upper limit of the measurements was set by a recrystallization process which set in between −115°C and −110°C. $\alpha_{||}$ was found to be larger and to increase more rapidly with the temperature than $\alpha_{\perp}$. Carpenter and Oakley[1] measured the volume coefficient near the melting point and interpreted their data as a linear relation with the temperature. The present measurements at lower temperatures show that the relation is not linear and, when plotted in conjunction with Carpenter and Oakley's values, give values of the volume coefficient from the melting point to −160°C where the coefficient apparently begins to decrease rapidly with the temperature. Several crystals were found which had lower specific resistances than the values for $\rho_{||}$ given by Grüneisen and Sckell.[2] The experimental data and curves are ready for publication.

[1] L. G. Carpenter and F. H. Oakley, Phil. Mag. **12**, 511 (1931).
[2] E. Grüneisen and O. Sckell, Ann. d. Physik **19**, 387 (1934).

10. Thermal Equilibrium of the Gas in the d.c. Carbon Arc. W. T. GRAY, *Northwestern University.* (Introduced by W. S. Huxford.)—The rotational temperature of the cyanogen molecules has been determined in d.c. carbon arcs, using a standard projector carbon. A 10-foot concave grating in a Rowland mounting was used for the band exposures and a quartz spectrograph with an 8-step diaphragm for the density marks. The relative intensities of the rotational lines show a Maxwell-Boltzmann distribution of rotational energies in the (0,0) λ3883 and (0,1) λ4216 CN bands. The temperature corresponding to this distribution is 5300°±300°K over the current range from 7 to 21 amperes. By reflecting the arc light through the hot gas, it was found that self-absorption had no effect upon the relative intensities. The range of rotational lines in the (0,1) band was extended by using several lines beyond the head of the (1,2) band. Independent measurements of the temperature in the outer flame of the arc, using the method of line reversal, have been extrapolated to include the central region. The mean temperature of the violet kernel obtained from the curve which gives the radial reversal temperature distribution is in good agreement with the rotational temperature of the CN molecules, which are excited only within this region.

11. An Inexpensive d.c. Amplifier. R. D. HUNTOON, *University of Iowa.* (Introduced by A. Ellett.)—A circuit using a commercial type 2A6 vacuum tube to measure currents of the order of 10^{-13} ampere with a wall galvanometer is discussed. Modifications necessary to construct a portable amplifier with a sensitivity of 10^{-11} amp. which may be operated directly from a.c. mains are shown. A simplified balancing procedure is outlined.

12. Statistical Distribution Curves in the Radio Tube Industry. WALTER DEHLINGER, *Hygrade Sylvania Corporation, Emporium, Pa.*—Statistical considerations have played an important part in physics during the last ten years. Many industries have taken advantage of this development. For a long time, the theory of small samples has been the focus of interest. Economical considerations would naturally encourage this trend for this application of statistics. The trend is now in the direction of establishing standard distribution curves for the characteristics of the various types of tubes. This means a slight increase in inspection but a great saving of losses due to shrinkage and a considerable improvement in quality. The standard curves, which are prepared from samples of several thousand tubes per type by means of a Hollerith machine, are discussed. A daily check for distribution type is made from samples of about 200 tubes. A variation of the shape of the distribution curve indicates the approach of trouble before the shrinkage has increased. The cause of the trouble may be found and eliminated before a serious loss due to shrinkage takes place. The character of the distribution curves was designated in the beginning of the development as Maxwellian and Fermian, corresponding to their shapes. Practical application soon indicated the way to three types of distribution curves connected with the main characteristics of a radio tube: (1) Plate Current Type, (2) Emission Type, (3) Mixed or Gauss Type. The operation of the system is described and further developments of the method and its applications are discussed.

13. Λ-Type Doubling Widths in $^3\Pi$ States of Molecules Intermediate between Hund's Cases (a) and (b). M. H. HEBB, *Harvard University.*—The theoretical work of Van Vleck on Λ-type doubling has been extended to molecules in $^3\Pi$ states, making no assumption about the magnitude of the ratio B/A. With unperturbed representation appropriate to Hund's case (a), general formulas for the doubling widths have been set up, which are valid through the entire range from Hund's case (a) to case (b). It is shown that the rotational distortion causes a gradual transition away from case (a) for small J toward case (b) as J increases. This means a mixing of the $^3\Pi_2$, $^3\Pi_1$ and $^3\Pi_0$ states of case (a) with consequent sharing of the Λ-type doubling widths. The theory has been applied to the experimental data of Naudé on N_2 with good agreement.

14. Isotope Relations in the Spectra of LiH and LiD. F. H. CRAWFORD AND T. JORGENSEN, JR., *Harvard University.*—The authors have called attention (Phys. Rev. June 15, 1935) to the fact that the failure of the simple isotope theory in hydride and deuteride molecules is in part due to the neglect of the effect of certain correction terms predicted by Dunham (Phys. Rev. **41**, 721 (1932)). Thus the constants determined from an *empirical* analysis of a band spectrum differ from the ordinary mechanically significant molecular constants by terms in $(B_e/\omega_e)^2$. In general, $Y_{lj}=f(\omega_e B_e)[\alpha_{lj}+\beta_{lj}(B_e/\omega_e)^2+\cdots]$ where the correction coefficients β_{lj} involve the coefficients a_1, a_2, $a_3\cdots$ in the potential energy function of the usual Kratzer form. Provided sufficiently extensive and precise data are available it is possible to compute these coefficients with considerable accuracy. Unfortunately these data are available only for a few states of H_2 and for LiH (and LiD). We have accordingly determined these coefficients from a_1 to a_5 and find for the *ground* state of LiH that the corrections are appreciable. Thus the ratios $[B_e^i/B_e]^{\frac{1}{2}}$ and ω_e^i/ω_e are respectively $(\rho+0.000184)$ and $(\rho+0.000217)$, where ρ is the isotope ratio determined from mass-spectrograph values $(\rho=0.750486)$, where the differences are now presumably direct measures of the effect of the "nuclear wobbling" caused by electronic motions [discussed by Kronig, Physica **1**, 617 (1934)].

15. The Application of Integral Equations to Eigenvalue Problems in Quantum Mechanics. A. F. STEVENSON, *University of Toronto.*—It is shown that the wave function for the discrete spectrum in a one-electron problem satisfies an integral equation which is analogous to that occurring in Born's theory of scattering by a static field, the energy occurring (nonlinearly) as an unknown parameter. The solution of the equation by successive approximations, starting from assumed initial approximations to energy and wave function, is discussed. In the case of perturbations, the first approximation to the energy leads to a result which is identical, to the first order in the perturbation, with that obtained from the ordinary theory, while the second approximation should yield a result comparable in accuracy with that obtained from the second-order perturbation in the usual theory. The calculation of the integrals involved is discussed and a simple example where the correct solution is known is considered in order to test the efficacy of the method. The extension of the integral equation to the general case is also given.

16. The Scattering of Slow Neutrons by Heavy Atoms. J. H. VAN VLECK, *Harvard University.* Bethe has shown that the anomalously large scattering or absorption reported by Fermi, Dunning and Pegram is to be expected whenever the integral $I=2\int_0^R[2M(W-V)/h^2]dr$ is a half integer, where R is the nuclear radius. The value of I has been computed with the Thomas-Fermi statistical model of the nucleus and the Majorana form of the neutron-proton interaction. The constants for this interaction have been taken from the work of Feenberg. The values of I turn out too small to permit the interpretation of the anomalous scattering in Hg, for instance, as due to an additional node as compared with Cd.

17. Photoelectric Properties of Pure and Gas Contaminated Magnesium. R. J. CASHMAN AND W. S. HUXFORD, *Northwestern University.*—Specially purified samples of magnesium metal were freed from gas by successive distillations and very slow sublimation in a high vacuum. The photoelectric threshold was found to lie at 3430 ± 20A, both for layers deposited on molybdenum and tantalum plates and for those deposited on the glass walls of the tube. A threshold characteristic of hydrogen contaminated surfaces lies at 5100A. Minute amounts of oxygen sensitize pure magnesium, causing a shift in the threshold to about 6000A. Further exposure of this sensitized surface to small amounts of oxygen results in deactivation, and a recession of the threshold to a value below 2000A. Air and hydrogen, or mixtures of oxygen and hydrogen, cause a marked increase in emission, with excursions of the long wave limit to 7000A and beyond. Magnesium surfaces are sensitized by nitrogen only when a glow discharge is set up in the gas. These changes in work-function are explained on the hypothesis that surface films of polar non-homonuclear molecules are formed by the action of the various gases. Fowler's theory is found to hold accurately for magnesium surfaces activated by hydrogen, the apparent threshold at 5100A being changed to the true value 5040A.

18. Scattering Intensity of Electrons as a Function of Voltage. H. J. YEARIAN AND J. D. HOWE. (Introduced by K. Lark-Horovitz, Purdue University.*)—Electrons of 10 to 80 kv are diffracted by gold and silver films in the way described previously.[1] The diffracted intensity is determined photographically and the coherent scattering plotted as a function of angle. It has been found that the scattered intensity at voltages below the K absorption limit of the element investigated cannot be accounted for by the usual first approximation of Born and Mott.[2] Instead of a smooth curve for the amplitude of scattering as a function of angle, maxima are observed of the type predicted by the further approximation of Henneberg which takes into account the distortion of the electron waves by the diffracting atom.[3]

* Grateful acknowledgment is made to the American Philosophical Society for a grant-in-aid of this research. (K. L.-H.)

[1] K. Lark-Horovitz, H. J. Yearian and J. D. Howe, Phys. Rev. **47**, 331 (1935).

[2] Born, Zeits. f. Physik **38**, 803 (1926); Mott, Proc. Roy. Soc. **A127**, 658 (1930).

[3] Henneberg, Zeits. f. Physik **83**, 555 (1933).

19. The Scattering of Potassium Ions by Mercury Vapor. ARTHUR G. ROUSE, *University of Iowa.* (Introduced by John A. Eldridge.)—An apparatus has been designed to measure the scattering at large angles of potassium ions by mercury vapor. Neglecting effects at small angles, both the classical kinetic theory or wave mechanics lead to a uniform scattering function for a rigid sphere model; for "softer" molecules they lead to a predominance in the forward direction; and for a Coulomb law force to the familiar Rutherford relation. Zabel has shown that for uncharged heavy atoms, moving with thermal velocities, the rigid sphere model is satisfactory. In the present work it is found that with K^+ ions with energies between 20 and 300 e-volts the scattering is predominately in the forward direction.

20. Electron Diffraction by Gas Molecules; (I) Structure of Phosphorus, (II) Valence Angle of Oxygen. LOUIS R. MAXWELL, V. M. MOSLEY AND STERLING B. HENDRICKS, *Bureau of Chemistry and Soils, Washington, D. C.*—(I) Electron diffraction photographs have been obtained from gas molecules of phosphorus (P_4) for de Broglie wavelengths ranging from 0.080A to 0.055A. Four different methods were used for analyzing the photographs obtained, as follows: (1) visual measurements, (2) measurements of densitometer records, (3) conversion of densitometer records into relative intensity curves by the use of plate calibrations for electrons, (4) use of a comparison between experimental and complete theoretical intensity curves in which each value of the intensity is multiplied by $[(1/\lambda)\sin\theta/2]^2$ in order to produce real maxima for measurement in all cases. By considering the results obtained from these different methods of treatment the most probable form of the P_4 molecule was found to be a regular tetrahedron with a P–P distance of 2.21 ± 0.02A. This distance is in agreement with recent x-ray studies on black amorphous and crystalline phosphorus (Gingrich and Hultgren; Hultgren and Warren, Washington meeting 1935). (II) The valence angle of oxygen α was measured by electron diffraction in a similar manner for the molecule 4,4′ diiododiphenyl ether $(C_6H_4I)_2O$. Complete theoretical intensity curves were computed for $\alpha=90°$, 110°, 120° and 180°. The model $\alpha=120°$ gave the best fit with the experimental results. By interpolation, it is estimated that the most probable value for the valence angle of oxygen in this molecule is $118°\pm3°$.

21. A Study of the First Spark Spectrum of Caesium as Excited by Electron Impact. ROY R. SULLIVAN, *University of Minnesota.*—An apparatus with which one may study the controlled excitation of spectra of volatile metals is described. Certain aspects of the optical excitation functions for several Cs II lines have been determined. A comparison of onset potentials found experimentally with those predicted by existing energy level schemes is made. Possible transitions are suggested for the two unclassified lines λλ4264.7 and 4763.6. Of the two groups into which the Cs II spectrum divides itself, the lines coming from terms built upon the $^3P_1$ state of Cs III show very broad excitation function maxima, while the lines coming from those terms built upon the $^3P_{1\frac{1}{2}}$ state of Cs III show relatively sharp maxima.

22. Optical Excitation of HgH and CN Bands. LEONARD O. OLSEN, *University of Iowa.* (Introduced by A. Ellett.)—Hg Vapor in the presence of 0.01 mm H_2 and about 3 mm N_2 was irradiated with the light from either an Hg+H_2 or Hg+He discharge. In both cases there occurred a weak excitation of the $^2\Pi-{}^2\Sigma$ HgH bands. There was no evidence of optical excitation of the HgH bands, such as occurs with CdH and ZnH. Evidently the HgH molecule in its normal state dissociates very quickly, as Wood and Gaviola have supposed. The HgH bands are evidently excited by collision and were obtained when only the 6^3P states of the Hg were excited, but the precise mechanism is not clear.

$$H_2+Hg(6^3P)\rightarrow HgH(^2\Pi)+H$$
$$H+Hg(6^3P)\rightarrow HgH(^2\Pi)$$

appear to be excluded by energy considerations. At one time there was observed strong emission of the λ3383A CN bands, evidently due to cyanogen formed from organic vapors (stop-cock grease) and excited by collisions of the second kind.

23. Effect of a Magnetic Field Upon the Polarization of Impact Radiation. W. H. MCCORKLE, *University of Iowa.* (Now at Agricultural and Mechanical College, College Station, Texas.) (Introduced by A. Ellett.)—Sodium *D*-line radiation excited by electrons moving parallel to a magnetic field of 300 gauss or more shows about 16 percent polarization, the major electric vibration being parallel to the direction of the exciting electron beam. In fields below 300 gauss the polarization is less, decreasing to zero in the absence of a field. That the polarization changes in a magnetic field must be due to the fact that the $3^2P_{\frac{1}{2}}$ level is a hyperfine multiplet which undergoes Paschen-Back effect.

24. Dissociation of NO and HCl by Electron Impact. ELMO E. HANSON, *University of Minnesota.*—By means of an apparatus of the type used by Lozier a study has been made of ionization with dissociation in NO and HCl. Ions possessing a considerable amount of kinetic energy were found in each of these gases and their distribution in energy was measured as a function of the electron energy. From determinations of the least electron energy necessary to form an ion having a specific kinetic energy it was possible to calculate the heat of dissociation of the molecular ion and of the normal molecule. The following is a summary of the results and the assumed processes. Unless specified the products are in their normal states.

PROCESS	KINETIC ENERGIES	HEAT OF DISSOCIATION
$NO\rightarrow N+O$		5.3 ±.2 volts
$NO^+\rightarrow N^++O(^1D_2)$	0 to 6 volts	
$NO^+\rightarrow N+O^+$		9.37±.2
$NO+e\rightarrow N+O^-$	1 to 2.5	ELECTRON AFFINITY OF O = 2.0 ±.5
$HCl\rightarrow H+Cl$		4.7 ±.2
$HCl^+\rightarrow H^++Cl$	0 to 10	
$HCl^+\rightarrow H+Cl^+$		4.7 ±.2
$HCl+e\rightarrow H+Cl^-$	LESS THAN 0.5	

The kinetic energy distribution curves for ions formed in HCl showed a peculiar three-peaked structure for electron energies above 40 volts.

25. The Ionization of Hydrogen Chloride under Electron Impact. ALFRED O. NIER AND ELMO E. HANSON, *University of Minnesota.*—A mass spectroscopic investigation has been made of the ions produced in HCl under electron impact. The following ions were observed: HCl^+, HCl^{2+}, H^+, Cl^+, Cl^{2+}, Cl^{3+}, Cl^{4+}, Cl^{5+} and Cl^-. Using He and Ne as calibrating gases the following appearance potentials were observed: HCl^+, 12.9 ± 0.2 volts; HCl^{2+}, 35.7 ± 1.0; H^+, 18.6 ± 0.3 and 28.4 ± 0.3; Cl^+, 17.2 ± 0.5 and 21.2 ± 0.5; Cl^{2+}, 45.7 ± 0.3; Cl^{3+}, approximately 160; Cl^-, approximately 1.6 volts. The Cl^{4+} and Cl^{5+} peaks were too small for the determination of their appearance potentials. No H_2^+ or Cl_2^+ ions were observed. The efficiency of ionization curves were of the usual form. Special precautions were taken to reduce to a minimum the amount of water vapor present in the tube and it can be stated with certainty that the H^+ ions found were not caused by the presence of water vapor. From the ratio of the peak heights of HCl^{35} to HCl^{37} the abundance ratio of Cl^{35} to Cl^{37} was found to be 3.07 ± 0.03. Cl^{39} if present was less than 1/20,000 of Cl^{35}.

26. Spectral Emissivities of Columbium, Thorium, Rhodium and Molybdenum. L. V. WHITNEY, *University of Wisconsin.*—To establish an accurate temperature scale spectral emissivities for columbium, thorium, rhodium, and molybdenum were measured at $\lambda=0.667\mu$. The Mendenhall V wedge was used for columbium and rolled cylinders were used for the other metals. The rolled cylinders used to measure black body and brightness temperatures proved superior to other forms of specimens and results should be more reliable. Rigorous outgassing treatment was found necessary for accurate results. Emissivities for all four metals were constant with temperatures over the ranges measured. Results are:

	EMISSIVITY $\lambda=.667\mu$	TEMPERATURE RANGE COVERED
Columbium	0.374	1300°–2200°K
Thorium	0.380	1300°–1700°K
Rhodium	0.242	1300°–2000°K
Molybdenum	0.382	1300°–2100°K

27. A Rydberg Series in I(I). W. C. PRICE, *The Johns Hopkins University.*—A well developed series has been found in Turner's data on the far ultraviolet spectrum of I(I) (L. A. Turner, Phys. Rev. **27**, 397 (1926)). It conforms within the experimental error to the Rydberg-Ritz formula

$$=79{,}210-R/(n-4.129+(0.105/n^{*2}))^2 \qquad n=6,\ 7,\ 8.$$

The lower state is the $5p\ ^2P_{\frac{1}{2}}$ state of I(I) and the series probably goes to the $^3P_0$ state of the ion. The series arising from $5p\ ^2P_{\frac{3}{2}}$ is weaker and only a few terms are observed. If the doublet separation of 7600 cm^{-1} is added to the limit given above, we get 10.71 volts as an ionization potential of I(I). This is not the lowest ionization potential as the ground state of I(II) is probably $^3P_2$ (jj coupling is closely approached). The separation $^3P_0-{}^3P_2$ is estimated to be a few tenths of a volt. It must be subtracted from the value given above to get the lowest ionization potential of I(I).

28. Some Current Nuclear Physics Problems in the Region Below 1000 Kilovolts. L. R. HAFSTAD, *Carnegie Institution of Washington.*

29. Rates of Nuclear Reactions Due to Bombardment with Charged Particles. G. BREIT, *University of Wisconsin.*

30. Gamma-Rays and Electrons from the Transmutation of Some Light Elements. C. C. LAURITSEN, *California Institute of Technology.*

31. Nuclear Structure and Stability. H. BETHE, *Cornell University.*

32. Distribution of Counts in a Counter with Constant Recovery Time. ARTHUR E. RUARK, *University of North Carolina.*—Skinner (Bull. Am. Phys. Soc. **10**, No. 2, p. 12) has considered the efficiency of counters and the distribution of recovery times. The theory of the distribution of counts, taking variability of the recovery time into account, will be very complicated. To get an approximate theory, we assume a constant recovery time, τ. Let f be the average number of ionizing particles (not counts!) per sec. and $P_n(t)$ the probability of n counts in an interval t, after a count has occurred. The functions P_n can be obtained seriatim. We have: $P_0=1$ for $t\leqq\tau$; $P_0=e^{-f(t-\tau)}$ for $t\leqq\tau$. $P_1=0$ for $t\leqq\tau$; $P_1=1-e^{-f(t-\tau)}$ for $\tau\leqq t\leqq2\tau$;

$$P_1=e^{-f(t-2\tau)}[1+f(t-2\tau)]-e^{-f(t-\tau)}$$

for $t\leqq2\tau$; and so on. P_n obeys a difference-differential equation, which has so far proved intractable in the general case.

33. The Magnitude of the *K*-Absorption Discontinuity for Tin and for Silver. E. L. HARRINGTON AND G. A. WIENSHALL, *University of Saskatchewan.*—An experimental study of the variation of the mass absorption coefficient with wavelength has been made for tin and for silver and the magnitudes of the K-discontinuity for each metal determined on the basis of the results obtained. The apparatus employed included a Bragg x-ray spectrometer provided with rotating sectored disks and a twin ionization chamber.

34. The Low Frequency Electrodeless Ring Discharge. F. H. CRAWFORD AND C. G. SMITH, *Harvard University.*—Although the electrodeless discharge in low pressure gases has been studied extensively at radiofrequencies, no attempts seem to have been made to determine the conditions for successful operation at *low frequencies* (<6000 cycles). The possibility of using *iron* and relatively large powered generators both point to the possibility of greatly increased currents. Actually by using properly designed step-down transformers having a few turns of heavy wire in the primary, and a single "turn" of low pressure gas as a "secondary," it has been possible to obtain quite heavy discharges in various gases at pressures of 10^{-4} mm of mercury and frequencies of 5400 and 900∼. The magnetic circuit must be constructed with the best iron and have as little magnetic leakage as possible. Operation has been obtained

with Cs and Hg vapors when the ordinary and the first ionized spectra are strongly developed. Under the most favorable conditions currents of over 300 amperes have been obtained (with a 10 kw generator and Hg at 10^{-4} mm) without serious heating of the tube. The use of this type of discharge for the intense excitation of molecular spectra and as a possible rich source of positive ions is suggested.

35. Temperatures Generated by the Passage of High Frequency Alternating Currents Through Animal Tissue with Special Reference to Electro-Surgery. R. D. HUNTOON, *University of Iowa.* (Introduced by A. Ellett.)—The temperature rise caused by the flow of high frequency currents through tissue was measured by means of thermocouples. Various sources of error were investigated and means of elimination devised. Measurements in the close vicinity of cutting and coagulating electrodes, as normally used in electro-surgery, are compared with previous measurements and the large observed differences explained on the basis of the observed effects of high frequency currents on improperly protected thermocouples.

36. Sources of Asymmetry in X-Ray Diffraction Grating and Refraction Measurements. ROY C. SPENCER, *University of Nebraska.*—If the product of the x-ray line function and the asymmetrical function is $(a+2\theta)/(b^2+\theta^2)$, then the shift in the peak is b^2/a. The shifts in the following cases are, however, too small to affect present wavelength measurements. *Case 1.* X-ray diffraction grating at grazing angles. The variation in dispersion causes an asymmetry in the x-ray line (which consists of a range of wavelengths). *Case 2.* The ordinary grating formula for N slits indicates an asymmetry in the peak due to the single slit pattern. *Case 3.* Refraction through a prism placed between the crystals of a double crystal spectrometer. The angular width of the x-ray line reflected from the first crystal causes a variation in the angle of incidence which causes both a variation in the coefficient of transmission and a variation in dispersion. Both effects cause asymmetry. *Case 4.* The diffraction pattern for parallel light passing through an absorbing prism is derived. It is a witch for angles near the normal but is asymmetrical near grazing angles.

37. Relation Between the Half-Lifetimes and the Atomic Weights of the β-Ray Emitters. H. H. GOLDSMITH, *Columbia University.*—The recent work on induced radioactivity has added considerably to the data on the half-lifetimes of the β-radioactive nuclei. The analysis of these data reveals several regularities connecting the half-lifetime, the atomic number and the atomic weight of nuclei. Some of the regularities have not been noted previously. The others—based, till now, upon a few examples in the natural radioactive series—are confirmed and extended to lower atomic numbers. The rules are used in order to (a) resolve the doubt concerning the atomic weight of some of the induced β-rayers; (b) predict the half-lifetimes of a large number of nuclei not yet produced; (c) predict the existence of stable nuclei; (d) understand some of the negative results of Fermi; (e) confirm the existence of the various assumed interactions between nuclear particles. The attempts by Yeh[1] and by Kurtschatov[2] to use less complete data in order to support the hypothesis of nuclear shells are criticized.

[1] W. Yeh, Comptes rendus **199**, 1209 (1934).
[2] I. Kurtschatov, Comptes rendus de l'academie des sciences U.S.S.R. **4**, 202 (1934).

AUTHOR INDEX TO ABSTRACTS OF THE MINNEAPOLIS MEETING

Bethe, H.—No. 31
Boyd, G. A.—No. 3
Breit, G.—No. 29

Cashman, R. J. and W. S. Huxford—No. 17
Cram, Winston—see Roebuck
Crawford, F. H. and T. Jorgensen, Jr.—No. 14
—— **and C. G. Smith**—No. 34

Dehlinger, Walter—No. 12

Goldsmith, H. H.—No. 37
Gray, W. T.—No. 10

Hafstad, L. R.—No. 28
Hanson, Elmo E.—No. 24
—— see Nier
Harrington, E. L. and H. H. Penley—No. 7
—— **and G. A. Wienshall**—No. 33
Hebb, M. H.—No. 13
Hendricks, Sterling B.—see Maxwell
Hill, Donald M.—No. 9
Howe, J. D.—see Yearian
Huntoon, R. D.—Nos. 11, 35
Huxford, W. S.—see Cashman

Jorgensen, T., Jr.—see Crawford

Lauritsen, C. C.—No. 30

Maxwell, Louis R., V. M. Mosley and Sterling B. Hendricks—No. 20
McCorkle, W. H.—No. 23
Mosley, V. M.—see Maxwell

Nier, Alfred O. and Elmo E. Hanson—No. 25

Olsen, Leonard O.—No. 22

Penley, H. H.—see Harrington
Price, W. C.—No. 27

Roebuck, J. R. and Winston Cram—No. 8
Rouse, Arthur G.—No. 19
Ruark, Arthur E.—Nos. 6, 32

Sayler, J. N.—No. 1
Smith, C. G.—see Crawford
Spencer, Roy C.—Nos. 2, 36
Stevenson, A. F.—No. 15
Stewart, G. W.—No. 4
Sullivan, Roy R.—No. 21

Valasek, Joseph—No. 5
Van Vleck, J. H.—No. 16

Whitney, L. V.—No. 26
Wienshall, G. A.—see Harrington

Yearian, H. J. and J. D. Howe—No. 18

Proceedings of the American Physical Society

MINUTES OF THE LOS ANGELES MEETING, JUNE 26–29, 1935

THE 200th regular meeting of the American Physical Society was held in affiliation with the Pacific Division, American Association for the Advancement of Science, in the auditorium of the Physics-Biology Building of the University of California at Los Angeles during the period Wednesday morning, June 26, to Saturday morning, June 29, 1935.

On the first day there was a joint session with the Astronomical Society of the Pacific at which a symposium on the Geologic and Cosmic Age Scale was held, the following papers being presented by invitation:

1. **The Age of the Earth from Sedimentation.** GEORGE D. LOUDERBACK, *University of California, Berkeley.*
2. **The Age of the Earth from Radioactive Disintegration Products.** ROBLEY D. EVANS, *Massachusetts Institute of Technology.*
3. **The Age of the Earth from the Changes in its Temperature and Elastic Properties.** BENO GUTENBERG, *California Institute of Technology.*
4. **The Age of the Galaxy from the Disintegration of Galactic Star Clusters and Binary Star Systems.** G. P. KUIPER, *Lick Observatory.*
5. **The Age of the Universe from the Red Shift in the Spectra of Extragalactic Objects.** RICHARD C. TOLMAN, *California Institute of Technology.*
6. **On Attempts to Reconcile the Long and the Short Time Scales in Cosmogony.** PAUL S. EPSTEIN, *California Institute of Technology.*

On Thursday, June 27, a symposium on Nuclear Structure was held with the following five invitational papers. In addition, the President of the American Physical Society, Professor Robert W. Wood, presented a sixth paper on the Eccentricities of High Explosives.

1. **A Survey of Present Knowledge of the Nucleus.** CARL D. ANDERSON, *California Institute of Technology.*
2. **Recent Developments in Artificial Transmutation.** ERNEST O. LAWRENCE, *University of California.*
3. **Gamma-Rays from Nuclear Transmutations.** H. RICHARD CRANE, *California Institute of Technology.*
4. **A Mathematical Interpretation of Nuclear Phenomena.** PAUL S. EPSTEIN, *California Institute of Technology.*
5. **Absorption of High-Energy Electrons.** SETH H. NEDDERMEYER, *California Institute of Technology.*

On Friday and on Saturday there was a program of 39 contributed papers. By vote of the Society the program as printed in the following pages was rearranged at some points in order that papers on a common topic by several authors could be grouped, thus making small symposia.

The Physical Society met at luncheon on Wednesday, Thursday and Friday at Kerckhoff Hall on the Los Angeles campus. The meetings were well attended. The attendance at the symposia was in the neighborhood of three hundred while the contributed ten-minute-paper program had an attendance of about a hundred.

At the close of the regular sessions on Saturday morning, a short business meeting was held at which the Society voted to hold the 202nd meeting of the American Physical Society on the Pacific Coast at the University of California, Berkeley, California, on December 20 and 21. The Society expressed itself as of the opinion that it wished to meet with the Pacific Division in Seattle in June, 1936. The Secretary presented the situation as regards the proposed September meeting time to the Society. No formal vote was taken either on the matter of September meetings or on the question of meeting with the Pacific Division in Seattle, formal vote on this question being postponed until the December meeting.

LEONARD B. LOEB
Local Secretary for the Pacific Coast
University of California
Berkeley, California

ABSTRACTS

1. Structure of a Heavy Deposit of Solid Selenium Condensed from the Vapor, the Liquid Being at About 250°C. L. E. DODD, *University of California at Los Angeles.*—A condensation surface was provided by the hemispherical end of a glass tube kept cool by a steady flow of tap water through it. At a good vacuum in the outer tube, the vapor was fed to this cold surface through a platinum barrier pierced with apertures, the liquid being maintained at a temperature (about 250°C) well above the melting point, so that the condensation was relatively rapid. The

resulting deposit showed some striking structural features, described in this paper with photographs and photomicrographs. The nature of the deposit in general is microcrystalline, with a grosser structure of what appear to be crystal units. In this deposit has been found the nuclear "amorphous" layer corresponding to that found by Goetz[1] with bismuth deposited under somewhat similar conditions.

[1] Goetz, Nature **132**, 206 (1933).

2. A.C. Voltage Stabilizer Unit. H. J. WHITE AND M. E. GARDNER, *University of California.*—An iron core choke coil provided with an auxiliary winding for direct current can have its impedance changed by changing the direct current in the auxiliary winding. When a current is passed through the d.c. coil the flux magnetizes the iron and makes it less receptive for additional magnetic flux from the a.c. coils and hence the impedance is lowered. Thus the potential drop across the choke coil can be regulated by varying the magnitude of the current in the auxiliary winding. Such a device can therefore be employed to control the a.c. voltage applied to a load. This regulation can be made automatic by applying the load voltage to a rectifier and filter unit and balancing this against the potential from a battery. The resultant potential differences are amplified and applied to the grid of a small power tube. The plate current of this tube is used as the control current in the auxiliary winding of the choke coil. Any change in the applied voltage will thus be almost completely absorbed in the choke coil. The choke coil may be designed to carry very large load currents and the voltage drop across the coil can be made sufficiently large to compensate for line voltage fluctuations of considerable magnitude. An experimental model of the stabilizer, controlling about 10 amperes at 100 volts, maintained the load voltage constant to within 0.2 volt for a line voltage change of 20 volts.

3. Acoustical Absorption as a Function of Frequency and Angle of Incidence. F. A. OSBORN AND PAUL M. HIGGS, *University of Washington.*—A parallel beam of sound produced by a loudspeaker at the principal focus of a parabolic mirror of five feet aperture is directed against a plane surface of the material under investigation. The regularly reflected sound beam is received by a second parabolic mirror and focused upon a condenser microphone. The interference pattern formed at the focus of the receiving mirror is kept in motion by frequency-modulating the sound. The absorption coefficient of the material is given by: $a=1-(A/B)^2$, where A is proportional to the sound pressure indicated by the microphone when receiving the beam reflected from the material and B is proportional to the pressure indicated when the mirrors are placed coaxially and facing one another. The total length of air path traversed by the sound is the same for all measurements. Coefficients of three typical commercial materials have been determined for frequencies from 500 to 4000 cycles per second and at angles of incidence between fifteen and seventy degrees. The results obtained are in agreement with the known acoustical properties of the materials. This work is preliminary to further investigation of acoustical absorptions.

4. Polarization Bands. JOHN STRONG, *California Institute of Technology.*—I have used the name, polarization bands, to refer to the band phenomenon discovered by R. W. Wood[1] because the bands occur only for the polarization perpendicular to the grating ruling. The second conspicuous property of these bands is the fact that their position, λ, depends on the angle of incidence, i, of the light on the grating. Measurements of polarization bands have been made with the grating, exhibited at the Pacific Coast meeting last June, coated with water, gold, copper, silver, magnesium and aluminum. This grating is ruled on an aluminum film supported by a plate glass foundation. The grooves are 0.2μ wide and 1.67μ apart. The grating gives double bands, a bright band in juxtaposition to, and on the red side of, a dark band. The dark band exhibits a sharp edge on its blue side. No change in the position of the sharp edge of the dark band was observed for any of these coats. However, the different metals were observed to shift the bright band. This shift is measured by Δ in the equation $(n-\Delta)\lambda=1\pm\sin i$, where n is an integer. For any particular metal, silver for example, Δ is a function of λ only. Values of Δ for silver vary from 0.1 at $\lambda=6800$A to 0.54 at $\lambda=4500$A. Δ's corresponding to the sharp edge of the dark bands are zero, for all metals as well as for water, at all wavelengths observed. This phenomenon of the bands seems to be a general property of the diffraction grating. It is desirable to have a physical picture of its origin.

[1] R. W. Wood, Phil. Mag. **4**, 396 (1902).

5. Two Radioactivities Produced in Magnesium by Deuteron Bombardment and Their Excitation Functions. M. C. HENDERSON, *University of California.*—Under bombardment by 3.3 MEV deuterons, magnesium becomes radioactive with the emission of negative electrons and with two decay periods: $10\frac{1}{2}\pm\frac{1}{4}$ min. and 15 ± 1 hr. These periods are characteristic of Mg^{27} (Fermi) and Na^{24} (Lawrence). The reactions presumably are:

$$_{12}Mg^{26}+{}_1H^2={}_{12}Mg^{27}+{}_1H^1; \quad {}_{12}Mg^{27}={}_{13}Al^{27}+\text{beta}$$
$$_{12}Mg^{26}+{}_1H^2={}_{11}Na^{24}+{}_2He^4; \quad {}_{11}Na^{24}={}_{12}Mg^{24}+\text{beta}.$$

The alpha-particles and protons have not been looked for. The Mg^{27} beta-rays have 2.0 MEV maximum energy, determined by absorption in Al, and there is possibly a soft gamma-ray. The voltage excitation functions of these two activities have been studied by exposing a pile of thin magnesium foils (0.0024 cm or 1.5 cm air equivalent) to the deuteron beam and measuring the activities of the foils separately. After a two-hour exposure to about 0.4 microampere, the initial activities of the top foil were 19.5 for Mg^{27} and 0.18 for Na^{24}. The fifth foil, at 2.0 MEV deuterons, gave similarly 2.36 and 0.007. No Na^{24} could be detected at less energy. At 3.3 MEV one atom becomes Na^{24} for each ten Mg^{27}. Both activities increase nearly exponentially with voltage at low voltages but at 3 MEV show signs of reaching a maximum. The Na^{24} excitation function is a steeper function of the voltage than Mg^{27}. An excitation curve of

the Gamow type fits Na^{24} and it is hoped to fit one of the new Oppenheimer type[1] to Mg^{27}. The thick target yield of Mg^{27} atoms is about 5 per ten million 3.3 MEV deuterons. The nuclear cross section (Mg^{26}) for transmutation at 3.3 MEV is about 1.4×10^{-26} cm².

[1] Science **81**, 421 (1935).

6. The Spectrum of Ce IV. R. J. LANG, *University of Alberta.*—The spectrum of cerium has been photographed by means of a two-meter vacuum spectrograph and a vacuum spark source from 3200A to 250A. An analysis of the Ce IV spectrum has resulted in the location of the following multiplets: $6S-6P$, $6P-6D$, $6P-7S$, $5D-6P$ and $5D-5F$. Previous work by Badami on this spectrum is not correct.

7. Photo-Ionization in Gases. R. N. VARNEY AND L. B. LOEB, *University of California.*—The balanced space-charge, positive ion detector, used in the experiments on ionization by positive alkali ions[1] has been used in the study of photo-ionization in gases. The following experiments were performed: (1) A hydrogen discharge tube, operated by either a 1000 or an 8000 volt transformer, was set up so that the radiation emitted could pass through a fluorite window into one of the space-charge, ion detectors. The detector contained N_2 at 0.02 mm pressure. When the pressure in the discharge tube was lowered to about 5 mm or less, the character of the discharge changed noticeably and ionization of the N_2 was observed, but it was definitely shown that all ionization that occurred was of electrostatic origin, despite careful shielding, and was not caused by radiation. It is believed that this may explain to some extent the ionization of gases observed by Lenard,[2] for he used an intense, high frequency aluminum spark as a light source. (2) An apparatus similar to that used by Mohler[3] was used in which electrons of energies up to 150 volts were allowed to ionize the gas at one end of a tube and the resulting radiation to ionize the same gas in one of the balanced space-charge cylinders at the other end. As observed by Mohler, photo-ionization of argon by its own radiation was found, but this disappeared when a fluorite window was inserted. The same was true in xenon gas. Since xenon has a metastable level near 1500A, this experiment seems to eliminate the possibility of ionization being produced by absorption of two quanta, each having a fraction of the necessary energy. No ionization of N_2 by its own radiation was observed with or without fluorite window. This is analogous to Mohler's non-observance of ionization in H_2. Similar results were observed in air.

[1] Varney, Phys. Rev. **47**, 483 (1935).
[2] Lenard, Heidelberg. Akad. der Wiss. 1910–1911.
[3] Mohler, Phys. Rev. **28**, 46 (1926).

8. Field Current Emission at Small Currents. F. R. ABBOTT AND JOSEPH E. HENDERSON, *University of Washington.*—Field emission from a carefully shielded tungsten filament surrounded by coaxial copper electrodes was investigated over a wide range of applied potential. Currents down to the order of 10^{-17} ampere were measured by use of an FP54 Pliotron used in a balanced circuit with floating grid. The higher range of currents to 10^{-6} ampere were measured directly by a galvanometer. The pressure was maintained at about 10^{-8} mm Hg. The linear relation between the logarithm of the current and the reciprocal of field intensity, as given by the equation, $i=Ce^{-b/F}$, clearly exists throughout the entire range investigated. Previous tests with poorer vacuum conditions (10^{-7} mm Hg) had indicated a slight deviation from this linear relation. A preliminary investigation of the energy distribution of the emitted electrons has been made for a total current of about 10^{-14} ampere. The main features of the observed distribution for higher currents[1] were observed also throughout the lower range of currents.

[1] Henderson, Abbott, Dahlstrom, Phys. Rev. **41**, 261 (1932).

9. The Velocity of Sound in Free Air in the Frequency Range 3.5 to 15 kc as a Function of Humidity. LEO P. DELSASSO AND JOHN H. MUNIER, *University of California at Los Angeles.*—The experimental arrangement, previously reported to the Physical Society at the Los Angeles meeting in December, for accurately determining the velocity of sound in air has been used in a constant-temperature, acoustically treated room for the purpose of verifying experimentally the anomalous dispersion of sound predicted by the theory of H. O. Kneser and others.

10. The Scattering of High Energy Protons by Oxygen Nuclei. MILTON G. WHITE, *University of California.*—In view of the apparently anomalous scattering of high energy protons by hydrogen it is of some interest to examine the scattering by heavier nuclei. During the course of some cloud chamber experiments on the scattering of protons by hydrogen a number of impacts with oxygen were observed, the oxygen being supplied by the water vapor in the cloud chamber. Some 1045 stereoscopic photographs were examined in which about 28,000 protons of energy greater than 800 kv entered the chamber. Of these protons about 15 percent had an energy greater than 1000 kv. A total of 97 measurable collisions with oxygen were observed. Although such meager data cannot be regarded as conclusive the results do strongly suggest that Rutherford scattering is entirely adequate to explain the results. It was found that the scattering decreased rapidly with increasing angle of scattering and increasing energy of the incident proton. With the energies here available one would hardly expect to find any serious deviation from Coulomb's law. However, since several thousand more photographs will soon be available it will be possible to give a definite answer to this problem sometime in the near future.

11. Absorption of Cosmic Radiation in Matter. A. W. NYE, *University of California; University of Southern California.*—Absorption of cosmic radiation, near sea level, was measured for water, sand, coal, copper sulphate, iron sulphide and barium sulphate, with triple coincidence Geiger counters. The materials were contained in a hopper and the counters arranged in vertical alignment underneath. The hopper was open to the sky in the cases of water and sand, and covered with a light wood roof in the others. Runs were made for various absorbing thicknesses

up to 101.5 cm. Absorption coefficients were found to be nearly linear with density; the absorption per bound electron was nearly constant, decreasing somewhat for FeS and $BaSO_4$. Correspondence with Bloch's equation was very good, indicating that the absorption was largely a bound electron phenomenon with deep-lying electrons less effective. Shower effects were measured with the top tube out of line by varying amounts. The showers in some cases reached a maximum with increasing thickness of absorber and in others no maximum was reached, indicating greater penetration of shower producing radiation than usual. Tubes disposed in other geometrical modes gave evidence of the amount of the spread of the showers.

12. Anomalous Diffraction Gratings. R. W. Wood, *Johns Hopkins University.*—Gratings similar to those described and studied by the author in 1907 and 1912 have been more fully investigated. They show narrow bright and dark bands in the continuous spectrum of a white source. Classical theory has never accounted for these anomalies, though tentative efforts were made at the time by Lord Rayleigh. The present work was done with a chromium plated echelette grating of 7200 lines to the inch ruled on copper, and one of 15,000 lines ruled by Dr. Babcock on an aluminum film on glass. The behavior of the bands as the incidence angle is altered has been very completely recorded by photography and the energy missing in the grating spectra has been found in excess in the spectrum of the central image. The dark bands appear to be due to the circumstance that diffracted wavelets from the lines are inhibited by the collective effects from neighboring lines, i.e., there is a sort of destructive interference along the plane of the grating. This obtains, however, only when the grating space is equal to an integral multiple of λ (for normal incidence) which means that the dark bands correspond to λ values which are passing off the grating on both sides at grazing emergence. The spectra formed by the Al grating are completely plane polarized, because of the circumstance that the width of the scratches is considerably less than the wavelength of the light. The dynamical action of the gratings is discussed, and the anomalous behavior is shown to be due to the presence of exceedingly narrow diffracting elements, which may be present even in the case of rather coarse rulings.

13. Further Study of the Vegard-Kaplan Bands. Joseph Kaplan, *University of California at Los Angeles.*—By using the same tube in which the Vegard-Kaplan bands of N_2 were discovered by the author, but by greatly diminishing the current and interrupting the discharge so rapidly that it did not have time enough to come to a steady state, it has been possible to enhance greatly these bands relative to the strong second-positive bands and the Goldstein-Kaplan bands. This has made it possible to photograph several new members of this system and it makes highly probable the discovery of more new bands of this system when longer exposures are used. In spite of the large reduction of current in the tube the absolute intensity of the Vegard-Kaplan bands has not gone down correspondingly. Since these bands originate on the metastable $A^3\Sigma$ state of N_2 it is thought that this technique of excitation can be extended to the photography of radiation from other metastable atomic and molecular states.

14. The Variation of Sparking Potential with Intense Ultraviolet Illumination. Harry J. White, *University of California.*—The static sparking potential has been found to be lowered by illuminating the cathode of a spark gap with intense ultraviolet light, an auxiliary spark gap being used as the source of ultraviolet illumination. The photoelectric current released from the cathode of the illuminated gap was about 10^6 times larger with this source than with a quartz mercury arc for illumination. The amount of lowering of the sparking potential was found to increase as the intensity of the spark illumination was increased and reductions up to about 10 percent were noted in air. The reduced sparking potentials in air were found to be a function of gas pressure times gap length and therefore obey Paschen's law. The approximate law for the amount of lowering of the sparking potential can be expressed by the condition that a certain number remains constant. This number is the number of positive ions generated by electron collision in the gas as the result of a given number of photoelectrons being liberated at the cathode by one flash of the illuminating spark. One may interpret this as meaning that the breakdown is a space-charge phenomenon and that some fixed value of the field is necessary for breakdown to occur. Then if the distribution of the space charge does not change appreciably, the amount necessary to produce the given field will be constant.

15. The Radioactivity of Oxygen, Silicon and Phosphorus Under Deuteron Bombardment. Henry W. Newson, *University of California.*—It has been found that oxygen, silicon and phosphorus become radioactive after bombardment with 3.2 MV deuterons. The half-lives are 1.16 minutes, 170 minutes and 14.5 days, respectively. All of these periods are identical with those of known radioactive substances which are probably formed in these new reactions:

$$O^{16}+D^2\rightarrow F^{17}+n^1$$
$$Si^{30}+D^2\rightarrow Si^{31}+H^1$$
$$P^{31}+D^2\rightarrow P^{32}+H^1.$$

Chemical analysis confirms the last two reactions. The excitation function of the oxygen activity has been measured by allowing the beam to pass through a series of copper screens in an atmosphere of oxygen. The activities which are deposited on the screens by recoil, plotted against the residual ranges of the deuterons, give a fair approximation of the excitation curve. The activation shows a threshold at 2.0 MV; this is probably due to the loss of that amount of energy in the reaction. The absorption of the electrons from Si^{31} and P^{32} has been measured in aluminum. The maximum range for silicon is 0.616 gram per square centimeter, while that for phosphorus is 0.712; the corresponding energies, calculated from the empirical rule of Feather, are 1.38 and 1.57 MV, respectively. F^{17} emits positrons.

16. The Photoelectric Effect of Aluminum Films Deposited by the Vacuum Evaporating Process. E. GAVIOLA AND JOHN STRONG.—The effect has been studied using a carefully cleaned and partially outgassed glass cell provided with a quartz window and a charcoal-liquid air trap. The cell has the shape of a horn, so that absorption of the oncoming radiation is practically total. As light source a mercury lamp was used. The light was resolved by a Hilger quartz monochromator. We have found that the long wavelength limit of the sensitivity curve lies between 2800 and 2900A, and that it has a definite selective maximum around 2700A.

17. The Existence of Townsend's Coefficient β in Gaseous Breakdown at Higher Pressures. D. Q. POSIN, *University of California.*—If a sufficiently low pressure is chosen, the simple Townsend equation for electron current delivered to an anode as a function of plate separation (and constant *average field*) holds extremely well for N_2 throughout the range of investigation between X/p 20 and 215 (X in volts per cm and p in mm in Hg). If the pressure is high enough, the curves corresponding to X/p between 120 and 215 can all be *made* to deviate from the simple Townsend requirement; i.e., at some plate distance (the apparatus permits investigation between 1 and 7.5 cm) the current begins to rise sharply. This sharp increase has been attributed to date to the Townsend β or γ coefficients—i.e., (β) to gaseous ionization by positive ions or (γ) electron liberation from cathode either by positive ion bombardment or photoelectric liberation due to excitation radiation from the gas. A study at $X/p=120$ made for the pressures below gave a deviation from the normal curve at the distances noted.

p (mm)	d_t (APPARENT TURNING POINT IN CM)	APPROX. PRODUCT $p \times d_t$
1.4	4.2	5.88
1.33	4.4	5.85
1.015	5.4	5.48
0.93	5.7	5.3
0.735	7	5.15

In each case the value of α/p (α as taken from the "normal" part of the curve) is approximately 0.95, *a constant.* Calculations of β/p from the curves show that not only does β/p vary irregularly from curve to curve (all $X/p=120$) but it is not even constant for a given curve. Moreover, for a given X and p the rate of abnormal increase beyond the turning point is a function of the initial electron current density (liberated from the cathode by the external ultraviolet source). Calculation shows that the so-called "β" is a function of current density at a given X and p. Thus in N_2 and also probably in air[1] Townsend's original interpretation of the phenomenon in terms of a β is not tenable in this pressure range unless the current density is sufficiently low. The abnormal current increase appears to be due to a constantly increasing variable, α, resulting from a nonuniform field between the plates. Accordingly at sufficiently high X and p or large d, the positive ions build up a sufficiently large space charge to distotr the field between the plates, giving α on the average higher values than expected from the field $X=V/D$ applied. Hence in the high pressure range, the static spark is preceded by enormous field distortion due to positive ion space charge as the result of which ultimately processes occur at the cathode which lead to the breakdown.

[1] M. Paavola, Arch. f. Elektrotech. **22**, 443 (1929); F. H. Sanders, Phys. Rev. **44**, 1020 (1933).

18. Search for Interaction of Matter and Radiation as Explanation of Nebular Red-Shift. R. J. KENNEDY AND WALTER H. BARKAS, *University of Washington.*—The possibility of an effect of the free electrons in a highly ionized gas on the frequency of light traversing it has been investigated. Ions to a density exceeding 10^{12}/cc can be produced in a low voltage arc. The line Hg 5461A was caused to traverse the discharge of a battery of low voltage arcs in helium. By means of a fixed quartz interferometer in vacuum a frequency shift of about 1 part in 10^{10} could have been detected. Approximately two hundred photographs of the rings were taken. Alternate exposures were "controls." A very satisfactory null result was obtained. The sensitivity was such as to eliminate any probability that the observed red-shift of extra galactic nebulae has its origin in an interaction of the light and the thinly diffused, ionized, gaseous substratum of the Universe.

19. The Vapor Pressure of Hydrogen Deuteride. R. B. SCOTT AND F. G. BRICKWEDDE, *National Bureau of Standards.*—Hydrogen deuteride (HD) was separated by distillation from 4 liters of an equilibrium mixture of H_2, HD and D_2, containing equal parts of hydrogen and deuterium, by use of a still with a reflux rectification column, immersed in liquid hydrogen. There were obtained 500 cm³ of HD of purity 99.95 percent or better as estimated by a comparison of its vapor pressure with that of two fractions collected immediately before and after. The vapor pressure of this "pure" HD was compared with that of liquid normal H_2 in the range 13.92 to 20.38° K. The following empirical equations were obtained, expressing pressures in mm of Hg:

$$\log_{10} P(\text{HD liquid}) = -0.85411 + 1.27713 \log_{10} P(H_2) - 0.02212 \log^2_{10} P(H_2)$$

$$\log_{10} P(\text{HD solid}) = -1.11571 + 1.33969 \log_{10} P(H_2)$$

TEMPERATURE °K	VAPOR PRESSURE IN MM OF HG		LATENT HEAT OF HD IN CAL/MOLE	
	H_2	HD	VAPORIZATION	FUSION
22.13[1]	1230	760.0		
20.38	760.0	438.0	261	
16.60[2]	201.4	93.6	265 (liquid)	37
16.60	201.4	93.6	302 (solid)	
13.92	54.0	15.96	296	

[1] Obtained by extrapolating the vapor pressure equation to $P(\text{HD}) = 760$ mm.
[2] Triple Point.

By use of the Clapeyron equation and the equation of state of H_2 for HD, latent heats were calculated from the above equations for HD and the vapor pressure-temperature equation of normal hydrogen.

After 15 days there was no reversion to the equilibrium mixture of H_2, HD and D_2 that could be detected by a change in vapor pressure.

20. Short-Lived β-Radioactivity. H. R. CRANE, L. A. DELSASSO, W. A. FOWLER AND C. C. LAURITSEN, *California Institute of Technology.*—Cloud chamber investigations have been made of the half-lives and energy spectra of the short-lived β-active isotopes produced by bombarding various targets with deuterons. The disintegrations producing the radio elements are believed to be accompanied by proton emission. The results are tabulated below:

TARGET	ACTIVE ISOTOPE	E_{max}	HALF-LIFE
Boron	B^{12}	11.0 mev.	0.02 ± 0.01 sec.
Lithium	Li^8	9.5 mev.	0.5 ± 0.1 sec.
Carbon	No activity		
Fluorine	F^{20}	4.5	

The accuracy of the masses of the isotopes involved in the boron transmutation and the great spread in the energy spectrum indicates that B^{12}, in disintegrating, loses an amount of energy corresponding to the upper limit of the electron spectrum and not to the mean energy.

21. The Energy of Formation of Negative Ions in Oxygen. LEONARD B. LOEB, *University of California.*—A year ago preliminary results were obtained on the energy required to remove an electron from the O_2 ion, using negative ions formed by a 100 kilocycle arc in O_2 and freed of electrons by a high frequency transverse field (filter) by subjecting the ions to a more uniform transverse high frequency field (smasher) whose potential could be varied until the ions gained enough energy to lose their electrons in molecular impacts. The phenomenon was detected by an abrupt decrease in the ion current *through* the smasher (accompanied by an increase in the current *to* the smasher), due to capture of the electrons liberated. The phenomena observed from 25 mm to 2 mm were studied at 10^6, 3×10^6 and 10^7 cycles per second in the smasher field. Very complex curves were encountered under the different conditions. At 3×10^6 and 10^6 cycles between 2 and 13 mm pressure a phenomenon interpreted with some certainty as due to break up of the negative ion was observed to give a linear relation between field strength and pressure. This gives the value of X/p for negative ion break up as 90 (X volts/cm p in mm of mercury). As at just this range of values of X/p the free path and thus average energy of ions in a field in a gas is uncertain, we can only assert that this corresponds to an energy *not less than 0.12 volt and not more than 0.68 volt.* At best only half of this energy is available for detachment on impact. Thus the energy of formation of negative ions in O_2 lies between 0.06 and 0.34 volt, the higher value being the more probable.

22. The Total Energy Distribution for Field Current Electrons. R. K. DAHLSTROM, K. V. MACKENZIE AND JOSEPH E. HENDERSON, *The University of Washington.*—The total energy distributions for field current electrons have been measured by a method similar in principle to the one described previously.[1] This was done by using a tungsten point emitter placed at the center of two concentric spheres. The inner sphere was really a grid formed by drilling the sphere with a large number of holes. Field electrons emitted from the tungsten point were accelerated to the grid, and those that passed through were then decelerated by the same potential which liberated them, the outer sphere being connected through a small accelerating potential to the tungsten point. Analysis of the current to the outer sphere as a function of the small accelerating potential gave the distribution in energy of the field electrons. The distribution curves obtained earlier with coaxial cylinders gave the distribution for electrons emitted on a plane perpendicular to the axes of the cylinders, not the total energy distribution. The present method, since the point was almost completely surrounded, gave the total energy distribution. The distributions found in this manner exhibit the major characteristic obtained earlier,[1] i.e., a rapid rise to a maximum when the work done by the field was approximately 4.5 volts. The range of energies was not so great, extending over about 10 volts, instead of 15 to 20 volts as indicated by the coaxial cylinder method.

[1] Henderson, Abbott, Dahlstrom, Phys. Rev. **41**, 261 (1932).

23. Influence of the Temperature on the Plasticity of Crystals. POL E. DUWEZ, *California Institute of Technology.*—The theory of the plasticity of crystals recently published[1] has been extended in order to take into account the influence of the temperature on the stress strain curve. The model of the deformed crystal, deduced from Zwicky's secondary structure theory, shows that the two quantities G and τ_{max}, i.e., the modulus of elasticity and the stress producing rupture of the crystal, are dependent upon the temperature. Furthermore G and τ_{max} vary independently. Therefore the relation between stress and strain remains the same, with G and τ_{max} functions of T instead of constants. The variation of G is known for a number of metals over a wide range of temperatures. In general a linear function can be used, except in the neighborhood of crystallographic or magnetic transition points. Very few data are available concerning the temperature dependence of τ_{max} for single crystals. Many polycrystalline metals were studied up to the melting point. It seems probable that τ_{max} is a function of the ratio T/T_m, T_m being the melting temperature. The curve $\tau_{max}(T/T_m)$ is characteristic and is almost a straight line, except for values of the ratio T/T_m approaching 0 and 1. Simple theoretical calculations may explain the general form of the function $\tau_{max}(T/T_m)$.

[1] Duwez, Phys. Rev. **47**, 494 (1935).

24. The Local Variation of the Earth's Electric Field. JOSEPH G. BROWN, *Stanford University.*—Following a suggestion by Scrase[1] the mean local diurnal variation of the potential gradient has been obtained for 22 land stations assuming that the unitary variation at land stations, ΔF_1, is equal to the ocean variation, ΔF_0, times the ratio of the mean gradients, F_1/F_0. The resulting local variations are only slightly different from those obtained

previously[2] but presumably they are better approximations. Each local variation has been analyzed into a 24-hour component and a daytime depression as before. The local components at all stations have greater amplitudes than the unitary components. The 24-hour components fall into three groups according to latitude. The mean latitude curves are of two types, narrow maximum and broad maximum. The broad maximum type includes stations which are known to be affected by pollution, the narrow maximum type includes stations relatively free from pollution. The polar curves are of the narrow type and the tropical are a very broad type. It is quite evident that some lower atmosphere factors are the chief cause for the 24-hour component rather than a change in height of the conducting layer as previously inferred. Seasonal changes in the depression component indicate very strongly that it is caused by vertical convection.

[1] Scrase, Met. Office, *Geophys. Mem.* No. 60, 1934.
[2] Brown, Phys. Rev. **47**, 259 (1935).

25. A Study of the Farnsworth Cold Cathode Oscillator. MERLE STARR, *University of California.*—A cold cathode regenerative oscillator similar to that described by P. T. Farnsworth has been constructed to give self-maintained oscillations at a natural frequency near 5×10^7 sec.$^{-1}$ with 40 watts energy. The oscillator consists of a collecting ring and two symmetrically placed silver plates treated with oxygen and caesium in proportions to give high efficiency of secondary emission. In operation the two plates are connected to the negative of a potential source, the ring to the positive, and a uniform magnetic field applied parallel to the axis of the tube to prevent excess electron current to the ring. Measurements on a Lecher wire system show that the natural mode of oscillation is determined by the time required for an electron to travel from one plate to the other under the influence of the electric field due to the applied potential difference and the high frequency alternating potential arising from circuit constants. The energy acquired by an electron from the alternating potential is sufficient to produce several secondaries upon impact with the plate, multiplication increasing in this manner to space-charge limitation. Characteristic curves of electron current from the ring *versus* applied voltage are of a nature to make possible radio- or audiofrequency amplification.

26. The Primary Ionization of High Speed Electrons in Nitrogen. DONALD H. LOUGHRIDGE AND HAROLD K. SKRAMSTAD, *University of Washington and the Tumor Institute, Swedish Hospital, Seattle, Washington.*—A large expansion chamber in a magnetic field of about 400 gauss is used to study the tracks of high energy beta-rays produced by bombarding a lead screen inside the chamber by gamma-radiation from radon. Two photographs at right angles are taken, and the tracks examined by reprojection onto a screen in their original configuration. Measurements are made of the number of primary ions per centimeter path produced in nitrogen. The results can be expressed approximately by the equation: $I=19/\beta^{-1.15\pm.15}$. Measurements on a few tracks in oxygen agree within experimental error with the results of Williams and Terroux. The primary ionization of the positive electrons observed is indistinguishable from that of the negative electrons. Comparisons are made with the theoretical calculations of Bethe, Moller and Bloch, and the agreement is excellent over the range of velocities used. The magnitude obtained for the primary ionization corresponds to an average ionization potential of 16.6 for the 5 outer electrons in the nitrogen atom, which is very near its minimum ionization potential. The variation with velocity checks well for values of $\beta<0.97$ but the predicted increase for very high energies is not observed. Further work with neon and argon is now in progress.

27. The Photometry of Electric Furnace Absorption Multiplets. ROBERT B. KING AND ARTHUR S. KING, *Mount Wilson Observatory.*—The intensities of lines in multiplets of iron of temperature classes I and II between λ3650A and λ4500A have been measured in absorption spectra produced in the electric vacuum furnace. The relative intensities have been measured in that part of the "curve of growth" of an absorption line dominated by Döppler broadening, where the total absorption $\sim N\cdot f$. The equivalent breadth of lines in this part of the curve is less than 0.03A at furnace temperatures (about 2100°C) but with high contrast plates measures can be made on lines whose total absorption is less than 0.002A. By keeping the temperature constant and gradually increasing N, lines of the same multiplet and of different multiplets can be passed successively through this part of the curve and measures of their relative intensities made at various stages. Since the atoms are in thermal equilibrium the Boltzmann factor can be applied and the intensities compared with theoretical intensities. The whole "curve of growth" of an absorption line, from the region of Döppler broadening where $I\sim N\cdot f$ to the region of dominance of radiation damping where $I\sim(N\cdot f)^{\frac{1}{2}}$, can be traced. However, under present conditions the latter part of the curve may be influenced considerably by collision broadening.

28. A High Voltage Lenard Tube and Search for Radioactivity Induced by Electron Bombardment. J. J. LIVINGOOD AND A. H. SNELL, *University of California.*—A Sloan type resonance transformer high voltage generator has been adapted to accelerate electrons out into the room by mounting a filament on the high voltage end of the coil, which hangs from its grounded upper end inside a steel vacuum tank. One of the filament current leads is the copper coil itself, the other being the internal concentric copper water-cooling pipe. Electrons are accelerated during alternate half-cycles (6 megacycles) towards the grounded tank wall and emerge through a 0.001 inch copper window supported on a water-cooled copper grid. Space charge in the shield around the filament reduces the emission during the lower parts of the voltage waves. Absorption measurements indicate a maximum range of 0.048 inch of aluminum, corresponding to about 845 kilovolts. Fifty-one elements, including deuterium, lead and thorium, have been bombarded for several minutes each with 100

microamperes total current and examined with a Geiger counter for induced radioactivity. No counts above background were obtained, indicating that (a) the range of the radiation is less than 4 cm of air, or that the periods are either (b) a small fraction of a second or else (c) many hours, or (d) that the effect does not exist at the potential used.

29. Solved Example Illustrating a New Property of Least Squares. W. EDWARDS DEMING, *U. S. Bureau of Chemistry and Soils, Washington, D. C.*—In the February 1935 *Philosophical Magazine* it was shown that when a curve has been fitted by least squares, there is no correlation between the errors of the calculated points and the residuals in the observed points. In the case of a single sample this reduces to the independence of the mean and standard deviation, found by Student in 1908. Mathematically, the general property is expressed by the vanishing of $\Sigma(w_x U_x V_x + w_y U_y V_y)$, the summation to be taken over all points. w_x and V_x denote the weight and residual of the x coordinate of an observed point; U_x denotes the error of the calculated coordinate. w_y, V_y and U_y are similarly defined. The vanishing of this cross-product term is essential for the existence of a chi-square distribution; hence if either the chi-test or the analysis of variance (comparison of *internal* with *external* consistency, as Birge has called it) is to be used for testing the fit of an empirical formula it is necessary to do the fitting by least squares. As an illustration twelve points are fitted with a second degree curve and a numerical evaluation of the cross-product term made. The twelve points were obtained by taking observations with Tippett's *Random Sampling Numbers* on the x and y coordinates of twelve points known to lie on a curve of the form fitted.

30. The Dark Current from Barrier-Layer Photo-Cells. PAUL R. GLEASON, *Colgate University.*—The spontaneous current delivered by barrier-layer photo-cells from several manufacturers has been further investigated[1] when the cells are in complete darkness. This current persists under all conditions under which the cells have been placed, seems to diminish over long periods of time and otherwise appears to be a function only of the temperature. By placing a photronic cell without its glass window in an air tight chamber whose humidity could be varied, it was established that the dark currents are independent of the humidity over the normal range of humidities experienced in laboratory conditions down to zero percent relative humidity attained by desiccating for a period of two weeks. However, in an atmosphere approaching saturation, a much larger current appears, probably due to excessive absorption of moisture by the selenium. The dark current is in the same direction as the self-generated current produced by exposure to light. It varies from cell to cell approximately within the range from 10^{-10} amp. to 10^{-9} amp. Within a group of four Weston Photronic cells, the variation in the dark current bears no relation to their sensitivities for visible light, but seems to be roughly proportional to their sensitivities for x-rays.

[1] Gleason, J. O. S. A. **23**, 193A (1933).

31. Electron Optics of a 3000 kv X-Ray Tube. D. L. WEBSTER, W. W. HANSEN AND P. KIRKPATRICK, *Stanford University.*—The design of an x-ray tube to be operated at potentials up to 3000 kv involves special problems in electron control. Electrical and mechanical considerations necessitate electron paths about 50 feet long from cathode to target, with five intermediate accelerating electrodes. Each electrode unavoidably constitutes a converging electron lens. Students of electron optics have heretofore shown little interest in electrons energetic enough to show relativity effects. It is found that the focal length of an electron lens for fast electrons is less than that for slow electrons in the ratio $\frac{1}{4}((\epsilon+2)/(\epsilon+1))^2$ where ϵ = electron kinetic energy $/m_0c^2$. An expression for the focal length of an electrostatic electron lens consisting of two coaxial cylindrical electrodes is given which does not involve the usual laborious step by step computation of electron paths. In the present problem all practicable accelerating electrodes are undesirably powerful as lenses, and it is theoretically impossible to image the cathode upon the target without at least one intermediate focus.

32. Absorption of Electrons. SETH H. NEDDERMEYER AND CARL D. ANDERSON, *California Institute of Technology.*—From a new set of about 10,000 counter-tripped cosmic-ray photographs it was possible to make 166 direct measurements of the energy lost in a 0.35 cm Pb plate by electrons (+ and −) with energies in the range below 150 mev. Among these 166 cases there were 46 in which the particle was apparently stopped by the Pb. A division of these electrons into three groups according to initial energy, *viz.* (1) below 50 mev, (2) 50 to 100, (3) 100 to 150, has given the result that groups 1, 2, 3 with mean initial energies of 28, 71 and 124 mev showed mean specific energy losses of 51, 91 and 90 mev/cm, respectively. A comparison between these values and those obtained theoretically by Bethe and Heitler (in the limiting case of a very thin plate), *viz.* 62, 140, 250 mev/cm for electrons with energies equal to the above mean initial energies, shows approximate agreement with theory in the low energy range, but indicates a breakdown above 100 mev. The 166 electrons ejected 3 single (+) secondaries and 2 (+ −) pairs, with a mean energy (calling (+'s) pairs) of 10 mev. The observed number and energies of the positron-negatron pairs ejected and the observed losses of energy by the same group of electrons are roughly consistent with the assumption that the pairs arise from the absorption of photons given off in radiative collisions.

33. A Search for Temperature Changes Accompanying Field Current Emission. JOSEPH E. HENDERSON AND G. M. FLEMING, *University of Washington.*—Two platinum-gold thermocouples, one of which was sharpened at the junction to a fine point, the other being blunt, were mounted similarly and close together opposite the anode of a G.E. XP-DFW water-cooled x-ray tube. These thermocouples were mounted in opposition to each other so that any electromotive force generated in both because of general

temperature changes would cancel. During the application of the field only the sharp point emitted electrons so that any temperature effect which might accompany the emission would be indicated by a galvanometer connected in series with the two thermocouples. It was possible to detect a difference in temperature of the junctions of less than one degree centigrade. With emission currents ranging up to a few milliamperes, no change in temperature, either cooling or heating, was detected within the limits of experimental error.

34. The Dynamical Theory of Gratings. R. M. LANGER, *California Institute of Technology.* The original work of Wood on intensity anomalies of reflection gratings led Rayleigh to develop a theory which did not use the assumptions of ordinary diffraction theory. Rayleigh's theory explained very little of Wood's observations and much less of the more extended experiments recently made by Strong. Voigt has shown how it is possible to generalize Rayleigh's methods to take into account the finite number of diffracted orders and the finite conductivity of the grating surface. This theory breaks down just in the case where the intensity anomalies become important. Nevertheless it is possible to discuss qualitatively many of the phenomena observed by Strong and unexplained in Rayleigh's theory. These include the occurrence of dark as well as bright bands in various orders when a higher order almost satisfies the condition that its direction is parallel to the surface. The effects of groove form and conductivity of the metal surface are fairly clear and it turns out that only gratings with scratches narrow compared with the grating spacing should give pronounced bands. This situation was recognized by Strong from his experiments and he calls attention to the fact that gratings ruled for spectroscopic work in the visible do not often have these defects because this condition leads to weak diffracted beams. In the infrared the rulings are more often relatively fine and Ingersol has published observations on this effect. Another type of experiment where these anomalies may play a significant part is in the case of x-ray reflections from ruled surfaces. The rulings are light and few and incidence and emergence are almost grazing.

35. Density and Surface Tension by the Capillary Elevation Method. L. E. DODD, *University of California at Los Angeles.*—Measurement of surface tension by the capillary elevation method requires that the density be known. To avoid temperature difficulties in weighing, one may take a series of readings, on the same test sample, of capillary elevations under a relatively large range of gas pressures, thus obtaining a straight-line graph. The constants of this permit computation of both density and surface tension. By this method measurements have been made on different test liquids, such as methyl alcohol, ethyl alcohol and acetone, with 8 or 10 points graphed in each case. The capillary bore is of the order of 0.2 mm diam. Correlation coefficients indicate linearity of the graph to within about 0.01 percent. The assembled apparatus including manometer is immersed in the same water bath. A nonelectric thermostat has been found satisfactory, being adjustable within an ample temperature range.

36. A Theory of the Local Variation of the Earth's Electric Field. JOSEPH G. BROWN, *Stanford University.*—A theory of the local variation of the earth's electric field is proposed which shows the significance of the two components suggested in a previous paper. It is maintained that the chief factor in determining the conductivity is the number of condensation nuclei, and that the potential gradient at the surface varies almost inversely with the conductivity. While the seasonal variations in the gradient, in a given region, may be accounted for by the total number of nuclei, it is believed that the diurnal variations are a result of the daily cycle of turbulence, vertical convection and subsidence of the atmosphere which changes the vertical distribution of the nuclei and thereby the conductivity and the gradient. The 24-hour component is interpreted to represent the change in gradient which would result from turbulence and subsidence alone, and the daytime depression is the decrease in gradient produced by an inversion in the number of nuclei caused by the convection. Evidence for the theory is based on gradient, space-charge and wind records taken at Stanford University, on cumulus cloud observations by Clayton,[1] and on nuclei counts by Wigand[2] in balloon flights and by Landsberg[3] on mountains and adjoining planes.

[1] Clayton, Anns. Ast. Obs. Harvard, Vol. 30, Part 4.
[2] Wigand, Ann. d. Physik **59**, 689 (1919).
[3] Landsberg, Mo. Weath. Rev. **62**, 442 (1934).

37. Determination of the Variation of Carbon Content in Mild Steel by Magnetic Analysis. DAVID L. SOLTAU AND DONALD H. LOUGHRIDGE, *University of Washington.*—By means of a magnetic analysis method, the variations of carbon content in steel have been correlated with the currents induced in a secondary coil surrounding the steel specimen, when the latter is placed in an alternating magnetic field of known intensity. Two similar specimens are placed in identical magnetic fields and cause, by their presence, the induction of the measured currents in two identical secondary coils, one around each specimen. These coils are connected differentially to an electro-dynamometer, by which the magnitude and phase relationships of the various harmonic components of the resultant current are determined. One specimen, the standard, remains fixed in position, while successive points upon the other, the test specimen, are examined. Curves drawn from the data thus obtained provide a graphic "picture" of the relative magnetic homogeneity or inhomogeneity of the test specimen. The critical points of these curves—maxima and minima of the differential current output—determine those points of the test specimen at which sections are made and examined photomicrographically. From the photomicrographs, the carbon content is determined by finding the percentage of pearlite in the specimen. These data, when plotted to the same scale as that of the magnetic analysis, show the correlation between the carbon variation and the current output of the test specimen. This method provides a means of examining mild steel, in the form of small rods or bars, for carbon content variation without the time and labor of chemical analyses and at the same time leaves the specimen untouched and unimpaired in all its physical properties.

38. Raman Spectrum of Heavy Benzene C_6D_6. R. W. Wood, *Johns Hopkins University.*—The Raman spectrum of 1.5 cm³ of C_6D_6 supplied by Professor H. S. Taylor showed such a strong continuous background that only two Raman lines appeared. Having destroyed the fluorescent impurity in heavy water by exposure to ultraviolet light, the same technique was employed with the benzene, and spectrograms taken subsequently were excellent. The $\Delta\nu$ frequencies of C_6H_6 and C_6D_6 are given in the following table:

C_6H_6	C_6D_6	C_6H_6	C_6D_6
605	581	2947	
849	662	3042	2266
991	945	3062	2293
	1000 faint	3157	2575
1178	873	3176	2617 } doubtful
1584 }	1548		2663 } doubtful
1606 }		3573	3052
	2031 broad faint	3627	3108

The doublet 1584–1606 is fused to a single line 1548 as predicted by E. Bright Wilson. Corresponding lines are joined by dotted lines in the table. The lines 605 and 849, of very different intensities with ordinary benzene, are represented by lines of equal intensity in this case. Of special interest are the lines 3052–3108 found with heavy benzene, with excitation both by Hg 4046, and Hg 4358. The corresponding lines were searched for with ordinary benzene, and a green sensitive plate. With 4358 excitation two faint lines were found at wavelengths 5162 and 5177, giving $\Delta\nu$ values of 3573 and 3627, and as no mercury lines were found at this point I feel certain that the lines are real. The optical technique employed in the work will be found in a current number of the *Journal of Chemical Physics.*

39. The Role of Space-Charge in the Study of the Townsend Ionization Coefficients and the Mechanism of Static Spark Breakdown. R. N. Varney, H. J. White, L. B. Loeb and D. Q. Posin, *University of California.*—The mechanism of spark breakdown has been investigated largely by the study of the deviations of the prespark current from the simple electron ionization law $i = i_0 e^{\alpha d}$. The deviations indicate a greater current than this for large d. The customary explanation has been that ionization by positive ions occurs or that additional electrons are liberated from the cathode by photoelectric processes or by ion bombardment. We have studied the possibility of increased current being caused, not by a new process, but by a distortion of the field of the spark gap by space-charge, giving an apparent increase in the exponential coefficient α. The coefficient α is a function of the field strength in the gap, but the function consists of three distinct parts. When the field strength is in its lowest range of values, α increases exponentially with field strength; in the middle range, α increases as the square of the field strength; in the third region α increases more slowly than the first power of the field strength. It is shown by solution of Poisson's equation that space-charges can occur, that they *will* cause an increase in α in the first two regions but not in the third, that the deviation of α from a constant value in a particular case due to field distortion occurs very sharply as d increases, particularly so in the first region, and that a sparking condition occurs if the original, applied field strength is not so high that local distorted fields extend into the third region. The effect of space-charge is only difficultly separable from the other (Townsend) ionization phenomena which may occur, when the field strength is up in the second region, but it is probably the primary cause of spark breakdown in the first region. The Townsend processes are undoubtedly completely valid in the third region.

AUTHOR INDEX TO ABSTRACTS OF THE LOS ANGELES MEETING

Abbott, F. R. and Joseph E. Henderson—No. 8
Anderson, Carl D.—see Neddermeyer

Barkas, Walter H.—see Kennedy
Brickwedde, F. G.—see Scott
Brown, Joseph G.—Nos. 24, 36

Crane, H. R., L. A. Delsasso, W. A. Fowler and C. C. Lauritsen—No. 20

Dahlstrom, R. K., K. V. Mackenzie and Joseph E. Henderson—No. 22
Delsasso, Leo A.—see Crane
—— **and John H. Munier**—No. 9
Deming, W. Edwards—No. 29
Dodd, L. E.—Nos. 1, 35
Duwez, Pol E.—No. 23

Fleming, G. M.—see Henderson, Joseph E.
Fowler, W. A.—see Crane

Gardner, M. E.—see White, Harry J.
Gaviola, E. and John Strong—No. 16
Gleason, Paul R.—No. 30

Hansen, W. W.—see Webster
Henderson, Joseph E.—see Abbott
—— see Dahlstrom
—— **and G. M. Fleming**—No. 33
Henderson, M. C.—No. 5
Higgs, Paul M.—see Osborn

Kaplan, Joseph—No. 13
Kennedy, R. J. and Walter H. Barkas—No. 18
King, Arthur S.—see King, Robert B.
King, Robert B. and Arthur S. King—No. 27
Kirkpatrick, P.—see Webster

Lang, R. J.—No. 6
Langer, R. M.—No. 34
Lauritsen, C. C.—see Crane

Livingood, J. J. and A. H. Snell—No. 28
Loeb, Leonard B.—No. 21
—— see Varney
Loughridge, Donald H.—see Soltau
—— **and Harold K. Skramstad**—No 26

Mackenzie, K. V.—see Dahlstrom
Munier, John H.—see Delsasso

Neddermeyer, Seth H. and Carl D. Anderson—No. 32
Newson, Henry W.—No. 15
Nye, A. W.—No. 11

Osborn, F. A. and Paul M. Higgs—No. 3

Posin, D. Q.—No. 17
—— see Varney

Scott, R. B. and F. G. Brickwedde—No. 19
Skramstad, Harold K.—see Loughridge
Snell, A. H.—see Livingood
Soltau, David L. and Donald H. Loughridge—No. 37
Starr, Merle—No. 25
Strong, John—No. 4
—— see Gaviola

Varney, R. N. and L. B. Loeb—No. 7
——, **H. J. White, L. B. Loeb and D. Q. Posin**—No. 39

Webster, D. L., W. W. Hansen and P. Kirkpatrick—No. 31
White, Harry J.—No. 14
—— see Varney
—— **and M. E. Gardner**—No. 2
White, Milton G.—No. 10
Wood, R. W.—Nos. 12, 38

THE AMERICAN INSTITUTE OF PHYSICS

INCORPORATED

GOVERNING BOARD

For The American Physical Society:

KARL T. COMPTON, *Chairman*
Massachusetts Institute of Technology

GEORGE B. PEGRAM, *Secretary*
Columbia University

JOHN T. TATE
University of Minnesota

For The Optical Society of America:

E. C. CRITTENDEN
Bureau of Standards

PAUL D. FOOTE
The Gulf Companies

F. K. RICHTMYER
Cornell University

For The Acoustical Society of America:

HARVEY FLETCHER
Bell Telephone Laboratories

VERN O. KNUDSEN
University of California at Los Angeles

WALLACE WATERFALL
The Celotex Company

For The Society of Rheology:

E. C. BINGHAM
Lafayette College

A. STUART HUNTER
du Pont Rayon Company

S. E. SHEPPARD
Eastman Kodak Company

For The American Association of Physics Teachers:

HOMER L. DODGE
University of Oklahoma

PAUL E. KLOPSTEG
Central Scientific Company

FREDERIC PALMER
Haverford College

ADMINISTRATIVE STAFF

HENRY A. BARTON, *Director* JOHN T. TATE, *Adviser on Publications*

MADELINE M. MITCHELL, *Editorial Secretary*

Office: 11 East 38th Street, New York, New York

JOURNALS

THE PHYSICAL REVIEW

REVIEWS OF MODERN PHYSICS

PHYSICS

JOHN T. TATE, *Editor*
J. W. BUCHTA, *Assistant Editor*
E. C. BINGHAM, *Rheology Editor*

THE JOURNAL OF THE OPTICAL SOCIETY OF AMERICA

THE REVIEW OF SCIENTIFIC INSTRUMENTS WITH PHYSICS NEWS AND VIEWS

F. K. RICHTMYER, *Editor*

JOURNAL OF THE ACOUSTICAL SOCIETY OF AMERICA

F. R. WATSON, *Editor*

THE JOURNAL OF CHEMICAL PHYSICS

HAROLD C. UREY, *Editor*

THE AMERICAN PHYSICS TEACHER

DUANE ROLLER, *Editor*

The American Institute of Physics is a membership corporation of which five societies are the founding members. These five societies are the principal national societies devoted to pure and applied physics in America. Their names, and those of their representatives who form the Governing Board of the Institute, are given above. The principal work of the Institute is the publication of journals sponsored by the societies or by itself. The names and the editors of the journals are also listed above.

The broad purpose of the Institute is to represent, in all matters of wide or common interest, the five thousand or more members and subscribers associated with the Founder Societies and the journals. It aims to advance the science and profession of physics, and to promote cooperation between pure research, the applied sciences and the industries. To achieve these aims, it is greatly in need of an endowment and is empowered by law to administer grants and funds of any kind.

CONTENTS

PHYS. REV. 48 (1935) SEPTEMBER 1

Measurement of X-Ray Wavelengths by Large Ruled Gratings. J. A. BEARDEN 385

Energy Spectrum of the Beta-Rays of Radium E. . . . . F. A. SCOTT 391

Spectra of Argon in the Extreme Ultraviolet. . . . . J. C. BOYCE 396

Collisions of Alpha-Particles in Hydrogen. E. POLLARD AND H. MARGENAU 402

Relative Intensities in the Principal Doublet of Thallium Under Arc and Fluorescence Excitation . . . . . L. N. MORSCHER, JR. 406

Total Scattering of Electrons in Helium. . A. L. HUGHES AND W. HARRIS 408

Velocity Distributions for Elastically Colliding Electrons. . . . . PHILIP M. MORSE, W. P. ALLIS AND E. S. LAMAR 412

Ionization of Neon and Argon by Singly Charged Magnesium Ions. . . . . J. C. MOUZON AND N. H. SMITH 420

Intensities in $^2\Pi$–$^2\Sigma$ Transitions in Diatomic Molecules. . LESTER T. EARLS 423

Magnetic Reversal Nuclei. Part V. Propagation of Large Barkhausen Discontinuities. . . . . K. J. SIXTUS 425

Theorem Connecting the Energy Momentum Tensor with the Velocity of Propagation of Waves. . . . . O. HALPERN 431

On the Dirac Electron in a Gravitational Field . O. HALPERN AND G. HELLER 434

Efficiency of the Tube Counter. . . . . SELBY M. SKINNER 438

Some Physical Properties of Compressed Gases. V. The Joule-Thomson Coefficient for Nitrogen. W. EDWARDS DEMING AND LOLA S. DEMING 448

Joule-Thomson Effect in Nitrogen. . . J. R. ROEBUCK AND H. OSTERBERG 450

Temperature Scales of Columbium, Thorium, Rhodium and Molybdenum at 0.667μ. . . . . L. V. WHITNEY 458

Letters to the Editor:

Diffuse Scattering of X-Rays from Piezoelectrically Oscillating Quartz . . . . . G. E. M. JAUNCEY AND J. H. DEMING 462

Velocity of Light Within a Massive Enclosure . . . . . G. W. HAMMAR 462

Heavy Particles from Lead . . . . . J. C. STREET, E. G. SCHNEIDER AND E. C. STEVENSON 463

Cosmic-Ray Showers Produced by Electrons . . . . . E. C. STEVENSON AND J. C. STREET 464

Additional First Negative Oxygen Bands . . . . . L. BOZÓKY AND R. SCHMID 465

Zeeman Effect in the First Negative Oxygen Bands . . . . . L. BOZÓKY AND R. SCHMID 466

Is the Quantum-Mechanical Description of Physical Reality Complete? . . ARTHUR E. RUARK 466

Some Investigations of Neutrons from Different Sources . . . . . R. LADENBURG, R. ROBERTS AND M. B. SAMPSON 467

Probability of *K* Shell Ionization of Silver by Cathode Rays . . . . . H. S. W. MASSEY AND E. H. S. BURHOP 468

On the Stability of $^4Be^8$ . . . . . G. BERNARDINI AND M. MANDO 468

Disintegration of Nitrogen by Slow Neutrons . . . . T. W. BONNER AND W. M. BRUBAKER 469

Slow Neutrons . . . . . W. M. BRUBAKER AND T. W. BONNER 470

Increased Frequency of Cosmic-Ray Bursts with Reduced Shielding . . . RICHARD L. DOAN 470

Direct Detection of the Angular Momentum of Light . . . . . RICHARD A. BETH 471

Proceedings of the American Physical Society:

MINNEAPOLIS MEETING, June 21–22, 1935; Minutes and Abstracts 1–37; Author Index 472

LOS ANGELES MEETING, June 26–29, 1935; Minutes and Abstracts 1–39; Author Index 479

LANCASTER PRESS, INC., LANCASTER, PA.